PARACHUTE DYNAMICS AND STABILITY ANALYSIS

by

S. K. Ibrahim
R. A. Engdahl

February 1974

8-28601

Prepared under Contract No. NAS-[redacted] by

HONEYWELL INC.
Systems and Research Center
Minneapolis, Minnesota 55413

for

NATIONAL AERONAUTICS AND SPACE ADMINISTRATION
George C. Marshall Space Flight Center
Marshall Space Flight Center, Alabama 35812

PARACHUTE DYNAMICS AND STABILITY ANALYSIS

by

S. K. Ibrahim
R. A. Engdahl

February 1974

8-28607
Prepared under Contract No. NAS-~~82860~~7 by

HONEYWELL INC.
Systems and Research Center
Minneapolis, Minnesota 55413

for

NATIONAL AERONAUTICS AND SPACE ADMINISTRATION
George C. Marshall Space Flight Center
Marshall Space Flight Center, Alabama 35812

FOREWORD

This is the final report describing a study conducted for the National Aeronautics and Space Administration, George C. Marshall Space Flight Center under Contract Number NAS 8-28607. This study was a "Parachute Dynamics and Stability Analysis" as applied to the Solid Rocket Booster recovery system of the Space Shuttle. This report covers the period from 1 February 1973 through 1 February 1974. The Contract Technical Monitor is Mr. Gaines L. Watts

The authors wish to express their gratitude to Mr. M. Bazakos for his assistance with the computer simulation programs that were developed and to Dr. R. E. Rose, Program Manager, for his guidance and supervision.

CONTENTS

	Page
FOREWORD	iii
SUMMARY	1
INTRODUCTION	1
LIST OF SYMBOLS	2
SUBSCRIPTS	4
RECOVERY SYSTEM ANALYSIS	5
The Approach to the Problem	5
General Recovery Sequence	6
Simplifying Assumptions	6
SYSTEM MODELING	10
Development of a Nonlinear Dynamical Model of the Parachute/Riser/Payload System	10
DEVELOPMENT OF AN AERODYNAMIC FORCE AND MOMENT SYSTEM IN AN UNSTEADY AIRMASS	39
ANALYSIS OF THE SOLID ROCKET BOOSTER RECOVERY SYSTEM	56
CONCLUSIONS	96
RECOMMENDATIONS	96
REFERENCES	97
APPENDIX A - DOCUMENTATION OF THE PARACHUTE DYNAMICS AND STABILITY ANALYSIS PROGRAMMING SYSTEM	

LIST OF ILLUSTRATIONS

Figure		Page
1	Nominal SRB Recovery Sequence	7
2	SRB/Drogue Baseline Configuration	8
3	SRB/Main Baseline Configuration	9
4	Reference Frame Definition and Orientation for a 3-Body Parachute Riser Payload System	12
5	Euler Angle Rotations	13
6	Fully Inflated Conical Ribbon Canopy Shape as Calculated by Program CANO	29
7	Parachute and Riser Geometry	30
8	Suspension Line Geometry	33
9	Parachute Force and Moment System	40
10	Polynomial Curve Fit to Normal Force Coefficients for a 20° Conical Ribbon Parachute	41
11	Polynomial Curve Fit to Tangential Force Coefficients for a 20° Conical Ribbon Parachute	42
12	Polynomial Curve Fit to Moment Coefficients for a 20° Conical Ribbon Parachute	43
13	SRB Force and Moment System	44
14	Polynomial Curve Fit to Normal Force Coefficients for the SRB	45
15	Polynomial Curve Fit to the Tangent Force Coefficients for the SRB	46
16	Polynomial Curve Fit to the Moment Coefficients of the SRB	47
17	Mean Wind Profile and Gust Envelope	49

(LIST OF ILLUSTRATIONS (CONTINUED))

Figure		Page
18	Main Parachute SRB Response to a 20° Pendulum Disturbance	60
19	Main Parachute SRB Angle of Attack Response to a 20° Pendulum Disturbance	61
20	Recovery System Trajectory, Pendulum Initial Conditions	62
21	Main Parachute - SRB Response to a Scissors Displacement (θ_1 = -20 deg, θ_3 = +20 deg Initially)	63
22	Main Parachute - SRB Angle of Attack Response to Scissors Displacement (θ_1 = -20 deg, θ_3 = +20 deg Initially)	64
23	Recovery System Trajectory, Scissors Initial Conditions	65
24	Initial Deployment Conditions for SRB/Drogue Combination	66
25	SRB Coning Angle as Reduced by the A tion of the Drogue Parachute	68
26	Drogue Parachute/SRB Angle of Attack Response to Initial Conditions Illustrated in Figure 24	69
27	Airmass Velocity Profile	70
28	Main Parachute SRB Response to a Non Steady Air Mass; Vertical Descent Initial Conditions	71
29	Main Parachute SRB Angle of Attack Response to a Non Steady Air Mass	72
30	Main Parachute SRB Response to a Downwind Pendulum Initial Condition in a Non Steady Air Mass	73
31	Main Parachute SRB Angle of Attack Response to a Downwind Pendulum Initial Condition in a Non Steady Air Mass	74
32	Recovery System Trajectory in a Non Steady Air Mass	75

LIST OF ILLUSTRATIONS (CONTINUED)

Figure		Page
33	Main Parachute SRB Response to an Upwind Pendulum Initial Condition in a Non Steady Air Mass	76
34	Main Parachute SRB Angle of Attack Response to an Upwind Pendulum Initial Condition in a Non Steady Air Mass	77
35	Main Parachute SRB Response to Scissors Initial Conditions in a Non Steady Air Mass	79
36	Main Parachute SRB Angle of Attack Response to Scissors Initial Conditions in a Non Steady Air Mass	80
37	Main Parachute SRB Response to a 20° Pendulum Initial Condition, Elastic Suspension System	81
38	Main Parachute SRB Angle of Attack Response to a 20° Pendulum Initial Condition, Elastic Suspension System	82
39	Main Parachute - SRB Response to Scissors Initial Conditions, Elastic Suspension System (θ_1 = -20 deg, θ_3 = +20 deg Initially)	83
40	Main Parachute - SRB Angle of Attack Response to Scissors Initial Conditions, Elastic Suspension System (θ_1 = -20 deg, θ_3 = +20 deg Initially)	84
41	Short Period Eigenvalue Time Histories for the SRB/Main Parachute Configuration, Pendulum Initial Conditions, (θ_1 = +20 deg, θ_3 = +20 deg)	86
42	Long Period Eigenvalue Time-History for the SRB/Main Parachute Configuration, Pendulum Initial Conditions (θ_1 = 20 deg, θ_3 = 20 deg)	87
43	Short Period Eigenvalue, Time-Histories for the SRB/Main Parachute Configuration, Scissors Initial Conditions (θ_1 = -20 deg, θ_3 = +20 deg)	88
44	Long Period Eigenvalue Time History for the SRB/Main Parachute Configuration, Scissors Initial Conditions (θ_1 = -20 deg, θ_3 = +20 deg)	89

LIST OF ILLUSTRATIONS (CONCLUDED)

Figure		Page
45	Short Period Eigenvalue Time Histories fo.· the SRB/ Main Parachute Configuration, Vertical Descent Initial Conditions, Non Steady Air Mass	90
46	Long Period Eigenvalue Time History for the SRB/Main Parachute Configuration, Vertical Descent Initial Conditions, Non Steady Air Mass	91
47	Short Period Eigenvalue Time Histories for the SRB/ Main Parachute Configuration, Pendulum Initial Conditions, Non Steady Air Mass (θ_1 = 20 deg, θ_3 = 20 deg)	92
48	Long Period Eigenvalue Time History for the SRB/Main Parachute Configuration, Pendulum Initial Conditions Non Steady Air Mass (θ_1 = +20 deg, θ_3 = +20 deg)	93
49	Short Period Eigenvalue Time Histories for the SRB/ Main Parachute Combination, Pendulum Initial Conditions, Elastic Suspension System ($\theta_1 = \theta_3$ = +20 deg Initially)	94
50	Long Period Eigenvalue Time History for the SRB/Main Combination, Pendulum Initial Conditions, Elastic Suspension System ($\theta_1 = \theta_3$ = +20 deg Initially)	95

PARACHUTE DYNAMICS AND STABILITY ANALYSIS

By: S. K. Ibrahim and R. A. Engdahl

SUMMARY

The nonlinear differential equations of motion for a general parachute-riser-payload system are developed. The resulting math model is then applied for analyzing the descent dynamics and stability characteristics of both the drogue stabilization phase and the main descent phase of the Space Shuttle Solid Rocket Booster (SRB) recovery system.

The formulation of the problem is characterized by a minimum number of simplifying assumptions and full application of state-of-the-art parachute technology. The parachute suspension lines and the parachute risers can be modeled as elastic elements, and the whole system may be subjected to specified wind and gust profiles in order to assess their effects on the stability of the recovery system.

A numerical linearization technique is provided as an optional subroutine. It permits the linearization of the system's equations of motion at selected points of the descent trajectory and the calculation of the Eigenvalues describing the principal motions. Root locus plots may be obtained to study the variation in stability characteristics as a function of time. Computer simulations with the nonlinear system of equations were run for a wide range of initial conditions both with and without the elastic suspension system effects and the wind and gust models. For selected runs, the linearization procedure was applied at predetermined points, the Eigenvalues were calculated, and the stability characteristics were examined. It was determined that, for the range of anticipated initial conditions, the projected drogue configuration quickly stabilizes the SRB motions, the SRB/Main descent configuration is stable, and the motions of the system, with the specified wind and gust profiles, remain within acceptable limits at water impact.

INTRODUCTION

This is the final report of a one-year program of analytical and computational work. The program's primary objective was to formulate a realistic mathematical model for the descent dynamics of a parachute/vehicle system and to use that model as the basis for a computer simulation, stability analysis, and parametric optimization of the Space Shuttle Solid Rocket Booster (SRB) recovery system.

The recoverable weight of the SRB is at least three times that of any previously recovered payload. Full scale testing may not be feasible and large scale drop tests are very costly; hence, the need for realistic simulation models to permit detailed studies of optimum system parameters and stability characteristics and to minimize the number of drop tests.

The math model described in this report is more general than previously published models. Among other things, it permits 6 degrees-of-freedom motion for both the parachtue and the vehicle, it includes elastic representation for the risers and suspension line, the effect of deterministic winds and gusts on the system's performance and a more general representation of apparent mass effects. A separate computer program, using the elastic element approach, permits the calculation of more realistic canopy profile shapes.

LIST OF SYMBOLS

ALCM	Length from confluence point to plane of skirt
B^j_{ik}	Direction cosines matrix element, body j, row i, column k (i, j, k = 1, 2, 3)
B_{S1}-B_{S3}	Direction cosine scalar products, Parachute
B_{S4}-B_{S6}	Direction cosine scalar products, SRB
$\vec{C}_i$	Velocity vector of body i, i = 1, 2, 3
C_{Ni}	Normal force coefficient, body i, i = 1, 3
CM	Center of mass
C_{M_I}	Moment Coefficient, body i, i = 1, 3
C_{T_i}	Tangent force coefficient, body i, i = 1, 3
CP	Center of pressure
F_{1i}	Aerodynamic forces on body 1 in direction i(i=X, Y, Z), lb
F_{3i}	Aerodynamic forces on body 3 in direction i(i=X, Y, Z), lb
F_2	Riser force, lb
g	Gravitational acceleration, ft/sec^2
I_i	Principal moments of inertia matrix, body i, slug ft^2

I_{A1}	Principal apparent moments of inertia matrix, slug ft^2 body 1
K_{LS}	Suspension line spring constant, lb/ft
K_R	Riser spring constant, lb/ft
L	Length
L_1	Length from confluence point to parachute CP
L_2, L_R	Length of riser
L_3	Length from SRB attach point to SRB CM
L_{3T}	Length of SRB
L_4	ength from SRB CM to SRB CP, positive towards engine
L_{CM}	Length from confluence point to parachute CM
L_S	Length of suspension lines
m_i	Mass of body i
m_I	Included mass of the parachute
m_{1A}	Apparent mass tensor of parachute
m_C	Canopy mass
m_L	Suspension line mass
M_{1i}	Moments about axis i of body 1 i = X Y, Z
M_{3i}	Moments about axis i of body 3 i = X, Y, Z
N	Number of suspension lines, Normal force
P_i	Angular Velocity about X-axis, body i
Q_i	Angular Velocity along Y-axis, body i
R_i	Angular Velocity about Z-axis, body i
R_o	Skirt Radius
q_i	Dynamic pressure at CP of body i, lb/ft^2

S_{oi}	Nominal area, body i, ft^2
U_i	Linear velocity in X-direction, body i, ft/sec
V_i	Linear velocity in Y-direction, body i, ft/sec
W_i	Linear velocity in Z-direction, body i, ft/sec
X_i, Y_i, Z_i	Right-handed orthogonal axes of body fixed reference frame i
X_{Ei}, Y_{Ei}, Z_{Ei}	Earth fixed coordinates for body i, ft
α_i	Angle of attack, body i
β_i	$\mathrm{Tan}^{-1} \dfrac{V_i}{U_i}$, body i
ψ_i, θ_i, ϕ_i	Euler angles, body i
$\vec{\omega}$	Angular velocity vector
$(\dot{\ })$	Dot notation for time derivative, $\dfrac{d(\ )}{dt}$
ζ	Damping coefficient,lb sec/ft
ρ	Air density, slug/ft^3

SUBSCRIPTS

1	Parachute
2	Riser
3	Payload (SRB)
o	Nominal conditions

RECOVERY SYSTEM ANALYSIS

THE APPROACH TO THE PROBLEM

The technical approach is structured to assess the descent dynamics and stability characteristics of a general parachute-riser payload combination. The advantage to a general case study is the ability to study a wider range of possible configurations with a minimum number of simplifying assumptions. Three primary tasks describe the approach taken in the analysis of the problem.

- The parachute riser-payload configuration was arranged and then said to be nominal according to specifications provided by the contracting agency and particular requirements of the descent conditions. A mathematical model incorporating elastic risers and suspension lines, three bodies each with six degrees of freedom, and a non steady air mass was developed. A complete software package was written to perform the nonlinear simulation.

- Using the nonlinear software package, simulations of the nonlinear dynamics of the parachute-riser-payload were made for a variety of initial conditions both with and without the influence of the nonsteady air mass and the elasticity of the suspension lines and riser. Particular attention was paid to equilibrium trajectories and to the occurrence of limit cycle responses.

- Using numerical techniques, linearization of the state equations of motion was accomplished. The stability of the system to disturbances was then assessed using the Root Locus technique. Using the same linearization technique, stability analysis as a function of certain parameters can be assessed.

While the state of the art of parachute recovery of large payloads extrapolates to a successful recovery of the space shuttle solid rocket booster (SRB), the magnitude of the SRB recovery problem is at least three times the size of any previous successful recovery. The large suspended load (approximately 150,000 lb), the size of the parachutes (3-130 ft Conical Ribbon) and the overall length of the system (about 400 ft) demand highly sophistocated math modeling and simulation if accurate stability conclusions are to be rightfully drawn. The technical objective of this study then is to, as accurately as possible, analyze the descent dynamics, predict stability characteristics, and reduce the cost of the recovery by providing a better starting point for full scale testing and evaluation.

GENERAL RECOVERY SEQUENCE

A schematic representation of the space shuttle SRB recovery is shown as Figure 1. The recovery process begins with the disengagement of the space shuttle main body and the SRB by explosive charges. The SRB then continues on a ballistic trajectory modified by its own aerodynamics through the apogee of nearly 200,000 ft, descending to approximately 20,000 ft, at which point the drogue parachute (48 ft Conical Ribbon) is deployed. Stabilization through the next 6000 ft of the descent provides sufficient conditions for the deployment in reefed stages of a three-parachute cluster. The cluster of 130-ft conical ribbon parachutes is fully deployed and fully inflated at an altitude of approximately 6000 ft. A steady descent concludes with water impact.

The analysis of the descent dynamics is made during the final 6000 ft, during which the motion of the system is effected by a potentially non-steady air mass perturbed by gusts. The analysis begins at full inflation of the cluster and ends at water impact.

The recovery system components, the drogue parachute, the main parachutes, and the SRB were chosen to meet the requirements established by the contracting agency. The drogue was chosen as a 48-ft, 20-deg conical ribbon parachute (Ref. 1). A cluster of 3-130 ft, 20-deg conical ribbon parachutes provides the required 80 fps descent rate during the final 4000 ft (Ref. 2). The dimensions and mass of the SRB have continually changed during this study. The dimensions and mass used, however, are representative and provide an adequate model of the final configuration. The SRB/Drogue combination is shown in Figure 2, and the SRB/Main is shown in Figure 3.

SIMPLIFYING ASSUMPTIONS

Several simplifying assumptions are employed which reduce the computational magnitude without compromising the general nature of the problem. Others are made to improve the math models to the extent that the state of the art allows.

- The Parachute is assumed to be axisymmetric and to have a fixed-shape canopy with elastic suspension lines.
- The riser connecting the parachute and payload is elastic and transmits only axial forces to the attach points on the SRB and parachute axes of symmetry.
- The SRB is a rigid, axisymmetric body.

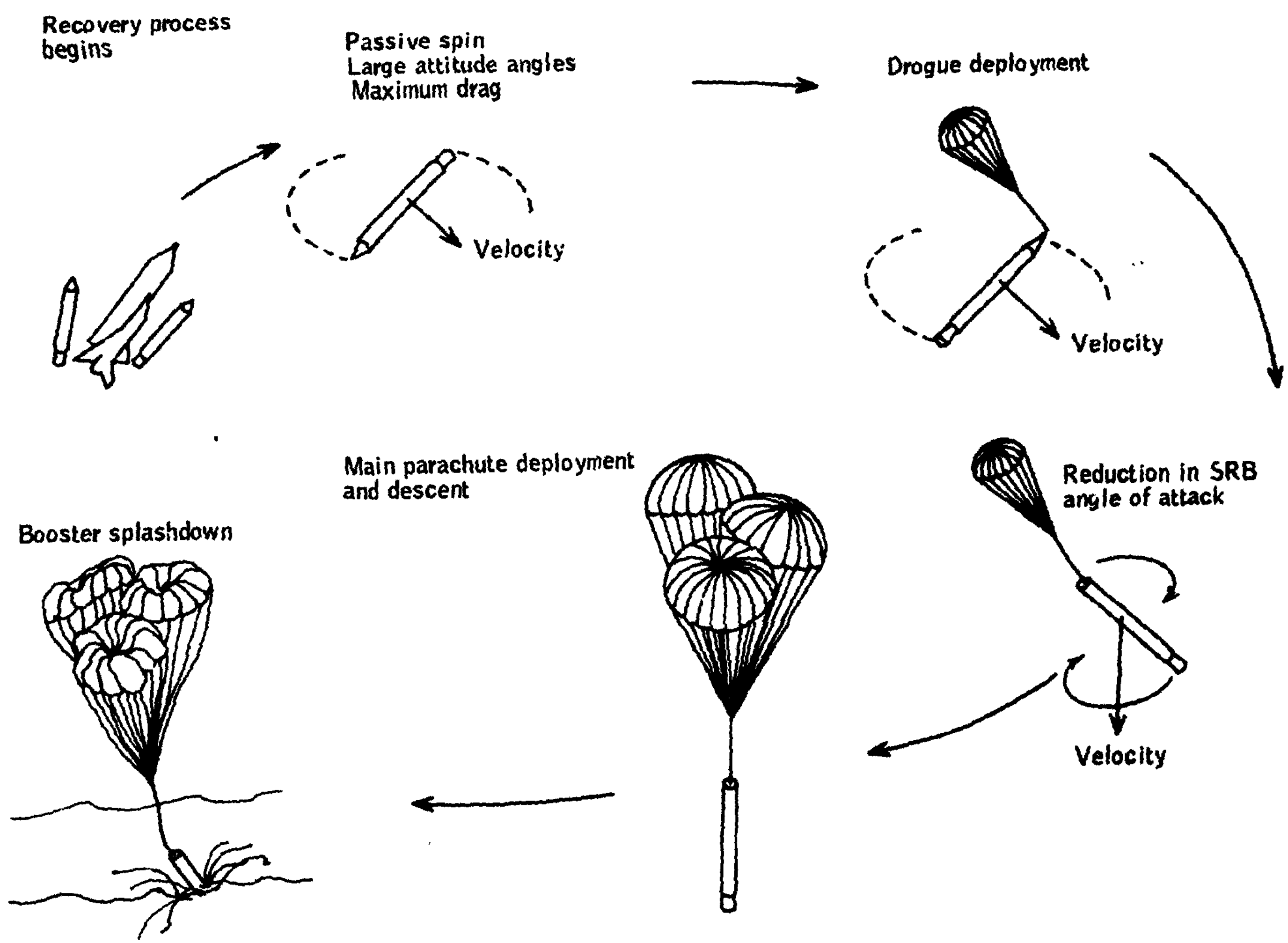

Figure 1. Nominal SRB Recovery Sequence

Drogue

D_0 = 48 ft

D_1 = 0.77 D_0 = 37 ft

l_S = 2.0 D_0 = 96 ft

L_1 = 103 ft

L_{CM} = 102 ft

L_{CP} = 0.163 D_o

L_S - 96 ft

SRB

D_3 = 11.8 ft

L_3 = 81 ft

L_{3T} = 157 ft

L_4 = 0.0 ft

System

L_2 = D_0 = 48 ft

L = 231 ft

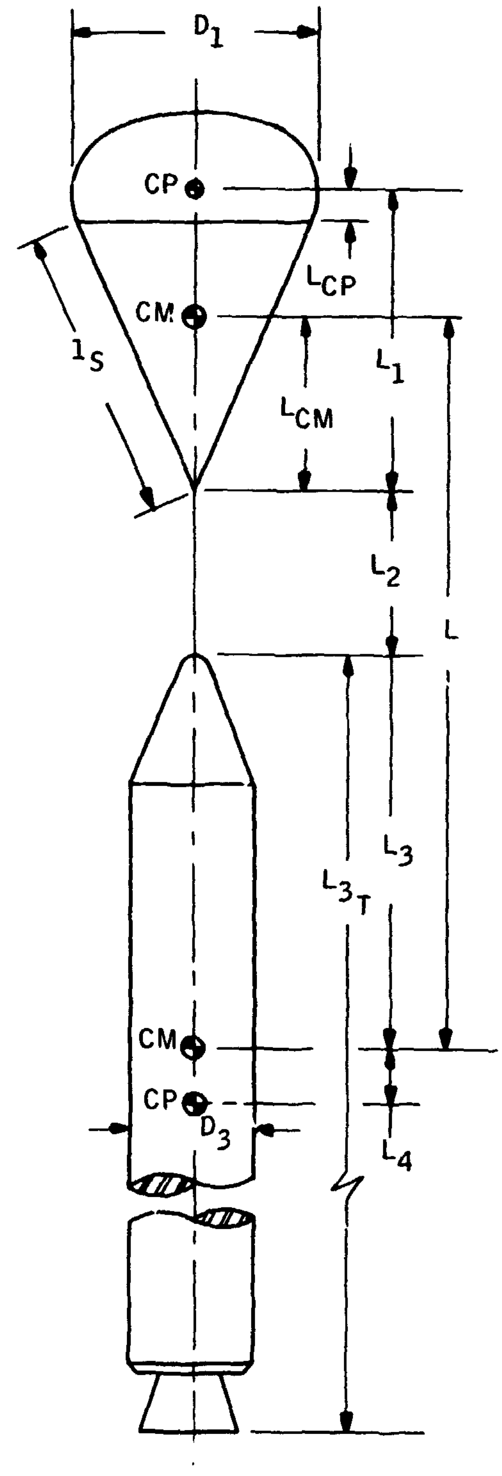

Figure 2. SRB/Drogue Baseline Configuration

Main

D_0 = 130 ft

L_1 = 292 ft

L_{CP} = 0.163 D_0

L_{CM} = 290 ft

D_1 = 0.75 D_0 = 94 ft

SRB

D_3 = 11.8 ft

L_{3T} = 145 ft

L_3 = 75 ft

L_4 = 0 ft

System

L_2 = 67 ft

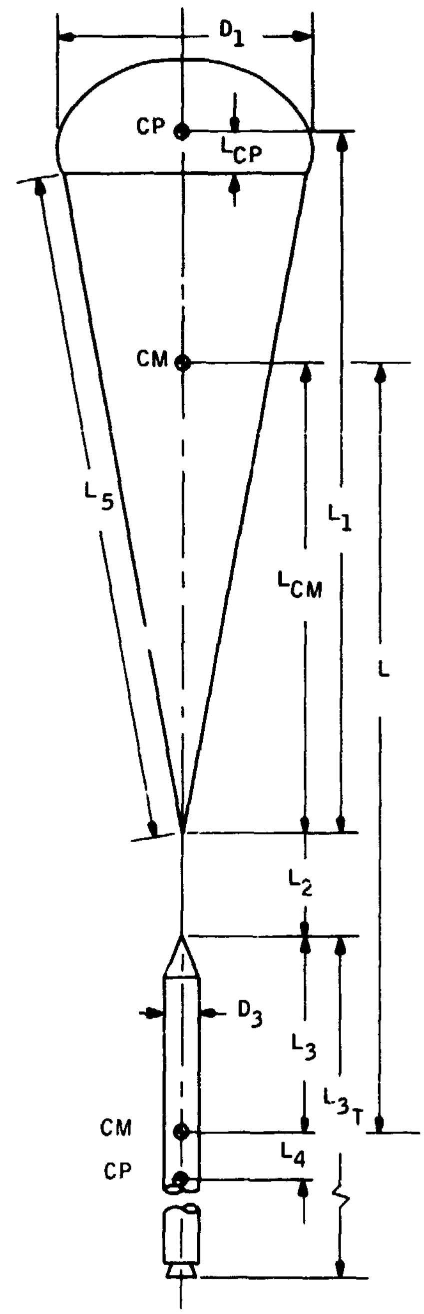

Figure 3. SRB/Main Baseline Configuration

- The aerodynamic centers of pressure are constrained to remain on the axes of symmetry of the SRB and the parachute but do not necessarily coincide with the centers of mass of those bodies.

- The energy modification of the air mass caused by the movement of the parachute through it is represented by tensors of apparent mass and apparent moments of inertia and not considered for the SRB motion.

- The separation distance between the SRB and the main parachutes is large enough to neglect forebody wake effects.

- The non steady air mass is represented by a wind velocity field and a gust velocity field perturbation.

- A flat earth is used for trajectory calculations.

SYSTEM MODELING

The mathematical modeling of the primary subsystems, the parachute, the riser, and the solid rocket booster is described in this section as used in the development of an analytical nonlinear simulation programming system. Modeling of the elastic elements and the non steady air mass is also described.

The equations of motion of the three body system are written relative to a flat earth. The forces and moments on the parachute and SRB result from aerodynamics and gravity. The application of the aerodynamics into the equations of motion is discussed.

Finally, in this section the techniques used to linearize the nonlinear motion and to perform a stability analysis are outlined.

DEVELOPMENT OF A NONLINEAR DYNAMICAL MODEL OF THE PARACHUTE/RISER/PAYLOAD SYSTEM

The parachute/riser/payload system is modeled as a three-body, six-degree-of-freedom-each problem. Since the parachute and SRB are connected by the riser, the constrained system finally reduces to a 15-degree-of-freedom problem.

<u>The differential equations of motion</u>. -- The equations of motion are developed in general terms first with no elasticity and a steady air mass. The effects of the inclusion of the elastic suspension lines is then included. The basic math model is adapted from Reference 3.

Reference frames: The reference frames and their initial orientation are shown in Figure 4.

Four right handed orthogonal reference frames are needed to specify the motions of the parachute (System 1), the riser (System 2), and the payload (System 3).

Earth fixed frame: Origin O_E is fixed on an assumed flat earth directly below the initial position of the SRB Center of Mass. Z_e is direct-downward, X_E is horizontal on the flat earth aligned in the vertical earth plane containing the initial SRB Center of Mass velocity vector, and Y_E is cross range to the right.

Body-fixed, moving frames 1, 2, and 3: The origins of the parachute and payload (SRB), body-fixed reference frames are at the respective centers of mass, O_1 and O_3. Z_i axes are aligned with the axes of symmetry with Z_1 directed toward the parachute confluence point, Z_2 directed from the parachute confluence point to the SRB attach point, and Z_3 directed toward the engine end of the SRB. X_i axes are aligned initially parallel to the vertical earth plane containing the payload center of mass initial velocity vector.

Euler angles: The Euler angles ϕ_i, θ_i, ψ_i describe the orientation of the body-fixed reference frames with respect to the earth fixed inertial frame. The ordered rotations are ψ_i about Z_i followed by θ_i about Y_i and then ϕ_i about X_i as illustrated in Figure 5.

The direction cosine matrix $[B^j]$ transforms a vector in earth fixed reference frame to the jth body fixed reference frame in the following manner:

$$\vec{V}_j = [B^j]\,\vec{V}_E \tag{1A}$$

Conversely, by premultiplying by $[B^j]^{-1}$

$$\vec{V}_E = [B^j]^{-1}\,\vec{V}_j \tag{1B}$$

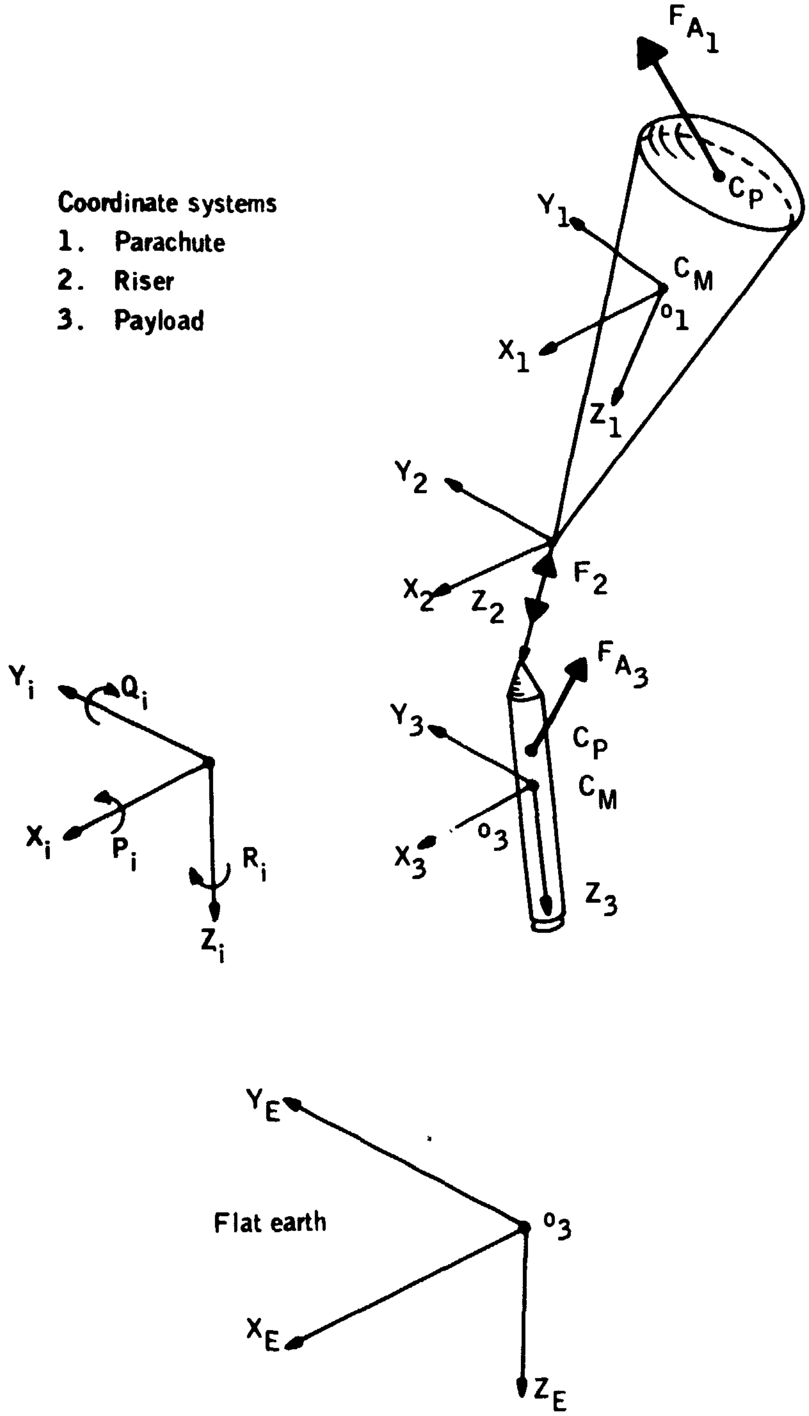

Figure 4. Reference Frame Definition and Orientation for a 3-Body Parachute Riser Payload System

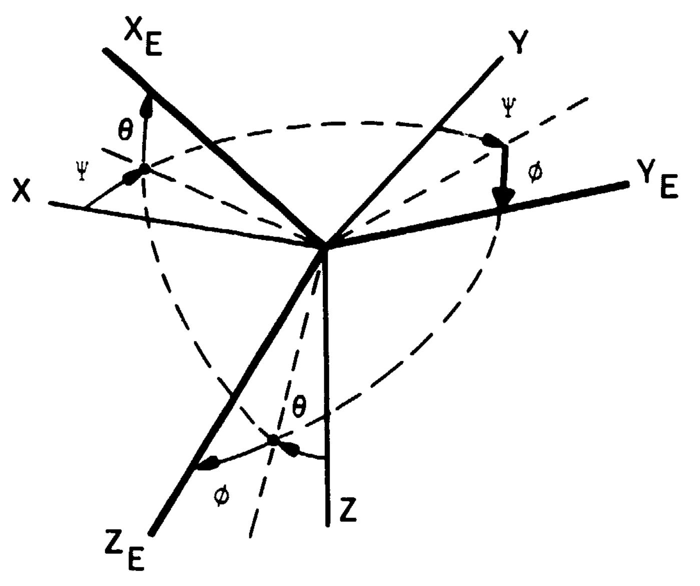

Figure 5. Euler Angle Rotations

The direction cosine matrix $[B^j]$ is such that its transpose is the same as its inverse; i. e.,

$$[B^j]^T = [B^j]^{-1}$$

Hence, Equation (1B) can also be written

$$\vec{V}_E = [B^j]^T \vec{V}_j \tag{1C}$$

In terms of the Euler angles and the sequence ψ, θ, ϕ, $[B^j]$ is as follows:

$$[B^j] = \begin{bmatrix} \cos\theta_j \cos\psi_j & \cos\theta_j \sin\psi_j & -\sin\theta_j \\ \sin\theta_j \cos\psi_j \sin\phi_j & \sin\phi_j \sin\theta_j \sin\psi_j & \sin\phi_j \cos\theta_j \\ -\cos\phi_j \sin\psi_j & +\cos\phi_j \cos\psi_j & \\ \cos\phi_j \sin\theta_j \cos\psi_j & \cos\phi_j \sin\theta_j \sin\psi_j & \cos\phi_j \cos\theta_j \\ +\sin\phi_j \sin\psi_j & -\sin\phi_j \cos\psi_j & \end{bmatrix}$$

Its elements are written B^j_{ik} where i is the row number and k is the column number.

The Euler angle rates are given by

$$\begin{aligned} \dot{\psi}_j &= (Q_j \sin\phi_j + R_j \cos\phi_j) \sec\theta_j \\ \dot{\theta}_j &= Q_j \cos\theta_j - R_j \sin\phi_j \\ \dot{\phi}_j &= P_j + (Q_j \sin\phi_j + R_j \cos\phi_j) \tan\theta_j \end{aligned} \tag{3}$$

The indices $j = 1, 2, 3$ correspond to the parachute, riser, and payload, respectively.

The dynamics of motion: force and moment equations. --

The parachute: The equations of motion for the parachute are divided into force and moment equations about the center of mass.

The force equations are written

$$\vec{F}_1 + m_1[B^1]\,\vec{g} + [B^1]\,[B^2]^T\,\vec{F}_2 = m_1(\dot{\vec{C}}_1 + \vec{\omega}_1 \times \vec{C}_1)$$

$$+[m_{1A}]\,(\dot{\vec{C}}_1 + \vec{\omega}_1 \times \vec{C}_1) \qquad \text{(4A)}$$

where $\vec{F}_2$ is the riser force, $\vec{F}_2 = \begin{bmatrix} 0 \\ 0 \\ F_2 \end{bmatrix}$

m_1 is the parachute mass (canopy + suspension lines)

and

$$m_{1A} = \begin{bmatrix} m_{1AX} & 0 & 0 \\ 0 & m_{1AY} & 0 \\ 0 & 0 & m_{1AZ} \end{bmatrix}$$

is the apparent mass tensor resulting from the air mass accelerations produced by the parachute motion.

$$F_1 = \begin{bmatrix} F_{1X} \\ F_{1Y} \\ F_{1Z} \end{bmatrix}, \qquad \vec{g} = \begin{bmatrix} 0 \\ 0 \\ g \end{bmatrix}$$

$$\vec{C}_1 = \begin{bmatrix} U_1 \\ V_1 \\ W_1 \end{bmatrix}, \qquad \vec{\omega}_1 = \begin{bmatrix} P_1 \\ Q_1 \\ R_1 \end{bmatrix}$$

Equation (4), when written in matrix form, becomes

$$\begin{bmatrix} F_{1X} \\ F_{1Y} \\ F_{1Z} \end{bmatrix} + m_1 \begin{bmatrix} B^1_{11} & B^1_{12} & B^1_{13} \\ B^1_{21} & B^1_{22} & B^1_{23} \\ B^1_{31} & B^1_{32} & B^1_{33} \end{bmatrix} \begin{bmatrix} 0 \\ 0 \\ g \end{bmatrix} + \begin{bmatrix} B^1_{11} & B^1_{12} & B^1_{13} \\ B^1_{21} & B^1_{22} & B^1_{23} \\ B^1_{31} & B^1_{32} & B^1_{33} \end{bmatrix}$$

$$\begin{bmatrix} B^2_{11} & B^2_{21} & B^2_{31} \\ B^2_{12} & B^2_{22} & B^2_{31} \\ B^2_{13} & B^2_{23} & B^2_{33} \end{bmatrix} \begin{bmatrix} 0 \\ 0 \\ F_2 \end{bmatrix}$$

$$= \left\{ m_1 + \begin{bmatrix} m_{1AX} & 0 & 0 \\ 0 & m_{1AY} & 0 \\ 0 & 0 & m_{1AZ} \end{bmatrix} \right\} \left\{ \begin{bmatrix} \dot{U}_1 \\ \dot{V}_1 \\ \dot{W}_1 \end{bmatrix} + \begin{bmatrix} 0 & -R_1 & Q_1 \\ R_1 & 0 & -P_1 \\ -Q_1 & P_1 & 0 \end{bmatrix} \begin{bmatrix} U_1 \\ V_1 \\ W_1 \end{bmatrix} \right\} \quad (4B)$$

Equation (4), in scalar form, is

$$F_{1X} + m_1 B^1_{13} g + B_{S1} F_2 = (m_1 + m_{1AX})(\dot{U}_1 + W_1 Q_1 - V_1 R_1)$$

$$F_{1Y} + m_1 B^1_{23} g + B_{S2} F_2 = (m_1 + m_{1AY})(\dot{V}_1 + U_1 R_1 - W_1 P_1) \quad (4C)$$

$$F_{1Z} + m_1 B^1_{33} g + B_{S3} F_2 = (m_1 + m_{1AZ})(\dot{W}_1 + V_1 P_1 - U_1 Q_1)$$

where $\begin{Bmatrix} B_{S1} \\ B_{S2} \\ B_{S3} \end{Bmatrix}$ are the elements of the third column of the matrix $[B^1]\,[B^2]^T$

The aerodynamic forces are given by

$$F_{1X} = C_{N1}\,(q_1\,S_{o1})\cos\beta_1$$

$$F_{1Y} = C_{N1}\,(q_1\,S_{o1})\sin\beta_1$$

$$F_{1Z} = -C_{T1}\,(q_1\,S_{o1})$$

where $\beta_1 = \tan^{-1}\left(\frac{V_1}{U_1}\right)$.

The moment equations about the parachute body axes fixed at the Center of Mass may be written

$$\vec{M}_1 = \dot{\vec{h}}_1 + \vec{\omega}_1 \times \vec{h}_1 \qquad (5A)$$

where $\vec{\omega}_1 = \begin{bmatrix} P_1 \\ Q1 \\ R_1 \end{bmatrix}$, the total angular velocity vector of body 1 and $\vec{h}_1$ is the angular momentum vector of body 1 which can be written

$$\vec{h}_1 = [I]\,\vec{\omega}_1 = \begin{bmatrix} I_{XX1} & 0 & 0 \\ 0 & I_{YY1} & 0 \\ 0 & 0 & I_{ZZ1} \end{bmatrix} \begin{bmatrix} P_1 \\ Q_1 \\ R_1 \end{bmatrix} = \begin{bmatrix} P_1\,I_{XX1} \\ Q_1\,I_{YY1} \\ R_1\,I_{ZZ1} \end{bmatrix}$$

The apparent moments of inertia resulting from the air mass accelerations generated by the parachute rotational motions may be written assuming principal axes

$$[I_A] = \begin{bmatrix} I_{XXA1} & 0 & 0 \\ 0 & I_{YYA1} & 0 \\ 0 & 0 & I_{ZZA1} \end{bmatrix}$$

A combined moment of inertia matrix may be calculated, using the parallel axis theorem, and is written

$$[I^*] = \begin{bmatrix} I^*_{XX1} & 0 & 0 \\ 0 & I^*_{YY1} & 0 \\ 0 & 0 & I^*_{ZZ1} \end{bmatrix}$$

Hence, the moment equation may be written

$$\begin{bmatrix} M_{1X} \\ M_{1Y} \\ M_{1Z} \end{bmatrix} = \begin{bmatrix} I^*_{XX1} & 0 & 0 \\ 0 & I^*_{YY1} & 0 \\ 0 & 0 & I^*_{ZZ1} \end{bmatrix} \begin{bmatrix} \dot{P}_1 \\ \dot{Q}_1 \\ \dot{R}_1 \end{bmatrix} \cdot \begin{bmatrix} 0 & -R_1 & Q_1 \\ R_1 & 0 & -P_1 \\ -Q_1 & P_1 & 0 \end{bmatrix}$$

$$\cdot \begin{bmatrix} I_{XX1} & 0 & 0 \\ 0 & I_{YY1} & 0 \\ 0 & 0 & I_{ZZ1} \end{bmatrix} \begin{bmatrix} P_1 \\ Q_1 \\ R_1 \end{bmatrix} \qquad (5B)$$

In scalar form, Equation (5B) becomes

$$\begin{aligned} M_{1X} &= I^*_{XX1} \; \dot{P}_1 + (I^*_{ZZ1} - I_{YY1}) \, Q_1 \, R_1 \\ M_{1Y} &= I^*_{YY1} \; \dot{Q}_1 + (I^*_{XX1} - I_{ZZ1}) \, R_1 \, P_1 \\ M_{1Z} &= I^*_{ZZ1} \; \dot{R}_1 + (I^*_{YY1} - I_{XX1}) \, P_1 \, Q_1 \end{aligned} \qquad (5C)$$

The moments acting about the CM location due to the external forces are in vector notation:

$$\vec{M}_1 = \vec{F}_1 \times \vec{L} + \{[B^1] \, [B^2]^T \, \vec{F}_2\} \times \vec{L}_{C_M} \qquad (6A)$$

where

$$\vec{L} = \begin{bmatrix} 0 \\ 0 \\ L_1 - L_{C_M} \end{bmatrix} , \qquad \vec{L}_{C_M} = \begin{bmatrix} 0 \\ 0 \\ L_{C_M} \end{bmatrix}$$

In matrix form

$$\begin{bmatrix} M_{1X} \\ M_{1Y} \\ M_{1Z} \end{bmatrix} = \begin{bmatrix} F_{1X} \\ F_{1Y} \\ F_{1Z} \end{bmatrix} \times \begin{bmatrix} 0 \\ 0 \\ L_1 - L_{C_M} \end{bmatrix} - \begin{bmatrix} F_2 B_{S1} \\ F_2 B_{S2} \\ F_2 B_{S3} \end{bmatrix} \times \begin{bmatrix} 0 \\ 0 \\ L_{C_M} \end{bmatrix} \qquad (6B)$$

or

$$\begin{bmatrix} M_{1X} \\ M_{1Y} \\ M_{1Z} \end{bmatrix} = \begin{bmatrix} 0 & -F_{1Z} & F_{1Y} \\ F_{1Z} & 0 & -F_{1X} \\ -F_{1Y} & F_{1X} & 0 \end{bmatrix} \begin{bmatrix} 0 \\ 0 \\ L_1 - L_{C_M} \end{bmatrix} -$$

$$\begin{bmatrix} 0 & -F_2 B_{S3} & F_2 B_{S2} \\ F_2 B_{S3} & 0 & -F_2 B_{S1} \\ -F_2 B_{S2} & F_2 B_{S1} & 0 \end{bmatrix} \begin{bmatrix} 0 \\ 0 \\ L_{C_M} \end{bmatrix}$$

In scalar form, Equation (6, becomes:

$$M_{1X} = F_{1Y}(L_1 - L_{C_M}) - F_2\, B_{S2}\, L_{C_M}$$

$$M_{1Y} = -F_{1X}(L_1 - L_{C_M}) + F_2\, B_{S1}\, L_{C_M} \qquad (6C)$$

$$M_{1Z} = 0$$

There are no external forces acting off the axis of symmetry, hence $M_{1Z} = 0$.

The moment equations can be written using moment coefficients for the contribution to the total external moment due to aerodynamic forces as in Equation (74).

The Payload (SRB) -- The equations of motion for the payload are written along the same lines as those for the parachute, with the exception that the apparent mass and moment of inertia effects are not included.

The force equations are written

$$\vec{F}_3 + m_3 \, [B^3] \, \vec{g} - [B^3] \, [B^2]^T \, \vec{F}_2 = m_3(\vec{C}_3 + \vec{\omega}_3 \times \vec{C}_3) \tag{7A}$$

where

$$\vec{C}_3 = \begin{bmatrix} U_3 \\ V_3 \\ W_3 \end{bmatrix} \quad \text{and} \quad \vec{\omega}_3 = \begin{bmatrix} P_3 \\ Q_3 \\ R_3 \end{bmatrix}$$

Equation (7), in scalar form, becomes

$$\begin{aligned}
F_{3X} + m_3 \, B^3_{13} \, g - B_{S4} \, F_2 &= m_3 \, (\dot{U}_3 + W_3 \, Q_3 - V_3 \, R_3) \\
F_{3Y} + m_3 \, B^3_{23} \, g - B_{S5} \, F_2 &= m_3 \, (\dot{V}_3 + U_3 \, R_3 - W_3 \, P_3) \\
F_{3Z} + m_3 \, B^3_{33} \, g - B_{S6} \, F_2 &= m_3 \, (\dot{W}_3 + V_3 \, P_3 - U_3 \, Q_3)
\end{aligned} \tag{7B}$$

where $\begin{Bmatrix} B_{S4} \\ B_{S5} \\ B_{S6} \end{Bmatrix}$ are the elements of the third column of the matrix operation $[B^3] \, [B^2]^T$

The aerodynamic forces are given by

$$F_{3X} = C_{N3}\, q_3\, S_{o3} \cos \beta_3$$

$$F_{3Y} = C_{N3}\, q_3\, S_{o3} \sin \beta_3$$

$$F_{3Z} = -C_{T3}\, q_3\, S_{o3}$$

where

$$\beta_3 = \tan^{-1} \left(\frac{V_3}{U_3}\right)$$

The moment equations for the SRB are written

$$M_{3X} = I_{XX3}\, \dot{P}_3 + (I_{ZZ3} - I_{YY3})\, Q_3\, R_3$$

$$M_{3Y} = I_{YY3}\, \dot{Q}_3 + (I_{XX3} - I_{ZZ3})\, R_3\, P_3 \qquad (8A)$$

$$M_{3Z} = I_{ZZ3}\, \dot{R}_3 + (I_{YY3} - I_{XX3}0\, P_3\, Q_3$$

The moments acting about the CM location due to the external forces are

$$M_{3X} = -F_{3Y}\, L_4 - F_2\, B_{S5}\, L_3$$

$$M_{3Y} = F_{3X}\, L_4 + F_2\, B_{S4}\, L_3$$

$$M_{3Z} = 0$$

where L_3 is the length from the SRB's attach point to its center of mass and L_4 is the length from the center of mass to the center of pressure of the SRB. L_4 is positive when measured from the center of mass in the direction of $+Z_3$.

The moment equations can be written using moment coefficients for the contribution to the total external moment due to aerodynamic forces as in Equation (75).

The Kinematics of Motion: The Riser Constraint

The riser, assumed for the time being to be of fixed length, provides a convenient method of interconnecting the equations of motion of the parachute and the payload. Consider the linear velocities at each end of the riser.

At the confluence point of the parachute suspension lines:

$$[B^2]^T \begin{bmatrix} U_2 \\ V_2 \\ W_2 \end{bmatrix} = [B^1]^T \left\{ \begin{bmatrix} U_1 \\ V_1 \\ W_1 \end{bmatrix} + \begin{bmatrix} Q_1 L_{C_M} \\ -P_1 L_{C_M} \\ 0 \end{bmatrix} \right\} \tag{9}$$

At the attach point on the payload:

$$[B^2]^T \left\{ \begin{bmatrix} U_2 \\ V_2 \\ W_2 \end{bmatrix} + \begin{bmatrix} Q_2 L_2 \\ -P_2 L_2 \\ 0 \end{bmatrix} \right\} = [B^3]^T \left\{ \begin{bmatrix} U_3 \\ V_3 \\ W_3 \end{bmatrix} + \begin{bmatrix} -Q_3 L_3 \\ P_3 L_3 \\ 0 \end{bmatrix} \right\} \tag{10}$$

Subtracting Equation (9) from Equation (10), the linear velocities in the riser coordinate systems are eliminated:

$$\begin{aligned} [B^2]^T \begin{bmatrix} Q_2 L_2 \\ -P_2 L_2 \\ 0 \end{bmatrix} &= [B^3]^T \left\{ \begin{bmatrix} U_3 \\ V_3 \\ W_3 \end{bmatrix} + \begin{bmatrix} -Q_3 L_3 \\ P_3 L_3 \\ 0 \end{bmatrix} \right\} \\ &\quad - [B^1]^T \left\{ \begin{bmatrix} U_1 \\ V_1 \\ W_1 \end{bmatrix} + \begin{bmatrix} Q_1 L_{C_M} \\ -P_1 L_{C_M} \\ 0 \end{bmatrix} \right\} \end{aligned} \tag{11}$$

Differentiation of Equation (11) yields equations for $\dot{Q}_2$, $\dot{P}_2$ and $\dot{W}_1$:

$$\frac{d}{dt}[B^2]^T \begin{bmatrix} Q_2 L_2 \\ -P_2 L_2 \\ 0 \end{bmatrix} + [B^2]^T \begin{bmatrix} \dot{Q}_2 L_2 \\ -\dot{P}_2 L_2 \\ 0 \end{bmatrix}$$

$$= \frac{d}{dt}[B^3]^T \left\{ \begin{bmatrix} U_3 \\ V_3 \\ W_3 \end{bmatrix} + \begin{bmatrix} -Q_3 L_3 \\ P_3 L_3 \\ 0 \end{bmatrix} \right\} + [B^3]^T \left\{ \begin{bmatrix} \dot{U}_3 \\ \dot{V}_3 \\ \dot{W}_3 \end{bmatrix} + \begin{bmatrix} -\dot{Q}_3 L_3 \\ \dot{P}_3 L_3 \\ 0 \end{bmatrix} \right\}$$

$$-\frac{d}{dt}[B_1]^T \left\{ \begin{bmatrix} U_1 \\ V_1 \\ W_1 \end{bmatrix} + \begin{bmatrix} Q_1 L_{C_M} \\ -P_1 L_{C_M} \\ 0 \end{bmatrix} \right\} - [B^1]^T \left\{ \begin{bmatrix} \dot{U}_1 \\ \dot{V}_1 \\ \dot{W}_1 \end{bmatrix} + \begin{bmatrix} \dot{Q}_1 L_{C_M} \\ -\dot{P}_1 L_{C_M} \\ 0 \end{bmatrix} \right\} \tag{12}$$

The third scalar equation of Equation (12) gives an expression for $\dot{W}_1$ as follows:

$$\begin{aligned}
\dot{W}_1 = \frac{1}{B^1_{33}} & - \Big[\dot{B}^2_{13} Q_2 L_2 + \dot{B}^2_{23} P_2 L_2 - B^2_{13} \dot{Q}_2 L_2 + B^2_{23} \dot{P}_2 L_2 \\
& + \dot{B}^3_{13} (U_3 - Q_3 L_3) + \dot{B}^3_{23} (V_3 + P_3 L_3) + \dot{B}^3_{33} W_3 \\
& + B^3_{13} (\dot{U}_3 - \dot{Q}_3 L_3) + B^3_{23} (\dot{V}_3 + \dot{P}_3 L_3) + B^3_{33} \dot{W}_3 \\
& - \dot{B}^1_{13} (U_1 + Q_1 L_{C_M}) - \dot{B}^1_{23} (V_1 - P_1 L_{C_M}) - \dot{B}^1_{33} W_1 \\
& - B^1_{13} (\dot{U}_1 + \dot{Q}_1 L_{C_M}) - B^1_{23} (\dot{V}_1 - \dot{P}_1 L_{C_M}) \Big]
\end{aligned} \tag{13}$$

Expressions for $\dot{B}^j_{13}$, $\dot{B}^j_{23}$, and $\dot{B}^j_{33}$ from Equations (2), (3), and their derivatives are as follows:

$$\begin{aligned}
\dot{B}^j_{13} &= -Q_j B^j_{33} + R_j B^j_{23} \\
\dot{B}^j_{23} &= P_j B^j_{33} - R_j B^j_{13} \\
\dot{B}^j_{33} &= -P_j B^j_{23} + Q_j B^j_{13}
\end{aligned} \tag{14}$$

Substitution from Equation (14) into Equation (13) yields expressions for $\dot{W}_1$ free of derivatives of $\dot{B}^j_{ik}$.

Similarly, we can obtain equations for $\dot{Q}_2$ and $\dot{P}_2$ from the first and second scalar equations of Equation (12).

The riser force F_2 can be obtained from the third equation of Equation (4C) in terms of $\dot{W}_1$ as given by Equation (13).

$$F_2 = \frac{1}{B_{S3}} \{(m_1+m_{1_{AZ}}) [\dot{W}_1+V_1 P_1-U_1Q_1] - F_{12} - m_1B^1_{33} g\} \tag{15}$$

The riser force, of course, is directed along the Z axis of the riser reference frame.

System State Differential Equations for the Non-Elastic, Steady Airmass Case

Equations (3) to (8), (12), and (13) can be written in the following form:

$$\dot{U}_1 = \frac{1}{m_1 + m_{1_{AX}}} \{F_{1X}+m_1B^1_{13} g + F_2B_{S1}\} - W_1Q_1 + V_1R_1 \tag{16}$$

$$\dot{V}_1 = \frac{1}{m_1 + m_{1_{AY}}} \{F_{1Y}+m_1B^1_{23} g + F_2B_{S2}\} - U_1R_1 + W_1P_1 \tag{17}$$

$$\begin{aligned}
\dot{W}_1 = \frac{1}{B^1_{33}} \{ & L_2 [Q_2(Q_2B^2_{33} - R_2B^2_{23}) + P_2(P_2B^2_{33} - R_2B^2_{13}) \\
& -B^2_{13} \dot{Q}_2 + B^2_{23}\dot{P}_2)] + (R_3B^3_{23} - Q_3B^3_{33}) (U_3 - Q_3 L_3) \\
& +B^3_{13} (\dot{U}_3 - \dot{Q}_3L_3) + (P_3 B^3_{33} - R_3 B^3_{13}) (V_3 + P_3 L_3) \\
& +B^3_{23} (\dot{V}_3 + \dot{P}_3L_3) + (Q_3 B^3_{13} - P_3 B^3_{23}) (W_3) + B^3_{33} (\dot{W}_3) \\
& -(R_1 B^1_{23} - Q_1 B^1_{33}) (U_1 + Q_1 L_{C_M}) - B^1_{13} (\dot{U}_1 + \dot{Q}_1 L_{C_M}) \qquad (18) \\
& -(P_1 B^1_{33} - R_1 B^1_{13}) (V_1 - P_1 L_{C_M}) - B^1_{23} (\dot{V}_1 - \dot{P}_1 L_{C_M}) \\
& -(Q_1 B^1_{13} - P_1 B^1_{23}) (W_1)\}
\end{aligned}$$

$$\dot{U}_3 = \frac{1}{m_3} \{F_{3X} + m_3 B^3_{13} g - F_2 B_{S4}\} - W_3 Q_3 + V_3 R_3 \tag{19}$$

$$\dot{V}_3 = \frac{1}{m_3} \{F_{3Y} + m_3 B^3_{23} g - F_2 B_{S5}\} - U_3 R_3 + W_3 P_3 \tag{20}$$

$$\dot{W}_3 = \frac{1}{m_3} \{F_{3Z} + m_3 B^3_{33} g - F_2 B_{S6}\} - V_3 P_3 + U_3 Q_3 \tag{21}$$

$$\dot{P}_1 = \frac{1}{I^*_{XX1}} \{M_{1X} - (I^*_{ZZ1} - I^*_{YY1}) Q_1 R_1\} \tag{22}$$

$$\dot{Q}_1 = \frac{1}{I^*_{YY1}} \{M_{1Y} - (I^*_{XX1} - I^*_{ZZ1}) R_1 P_1\} \tag{23}$$

$$\dot{R}_1 = \frac{1}{I^*_{ZZ1}} \{M_{1Z} - (I^*_{YY1} - I^*_{XX1}) P_1 Q_1\} \tag{24}$$

$$\dot{P}_3 = \frac{1}{I_{XX3}} \{M_{3X} - (I_{ZZ3} - I_{YY3}) Q_3 R_3\} \tag{25}$$

$$\dot{Q}_3 = \frac{1}{I_{YY3}} \{M_{3Y} - (I_{XX3} - I_{ZZ3}) R_3 P_3\} \tag{26}$$

$$\dot{R}_3 = \frac{1}{I_{ZZ3}} \{M_{3Z} - (I_{YY3} - I_{XX3}) P_3 Q_3\} \tag{27}$$

$$\dot{\psi}_j = (Q_j \sin \phi_j + R_j \cos \phi_j) \sec \theta_j, \quad j = 1,\ 2,\ 3 \qquad (28)\text{-}(30)$$

$$\dot{\theta}_j = Q_j \cos \phi_j - R_j \sin \phi_j, \quad j = 1,\ 2,\ 3 \qquad (31)\text{-}(33)$$

$$\dot{\phi}_j = P_j + (Q_j \sin \phi_j + R_j \cos \phi_j) \tan \theta_j, \quad j = 1,\ 2,\ 3 \qquad (34)\text{-}(36)$$

$$\dot{P}_2 = -\frac{1}{B^2_{22}} \{Q_2(Q_2 B^2_{32} - R_2 B^2_{22}) + P_2(P_2 B^2_{32} - R_2 B^2_{12}) - \dot{Q}_2 B^2_{12}$$

$$+ \frac{1}{L_2} [(R_3 B^3_{22} - Q_3 B^3_{32}) (U_3 - Q_3 L_3) + B^3_{12} (\dot{U}_3 - \dot{Q}_3 L_3)$$

$$+ (P_3 B^3_{32} - R_3 B^3_{12}) (V_3 + P_3 L_3) + B^3_{22} (\dot{V}_3 + \dot{P}_3 L_3)$$

$$+ (Q_3 B^3_{12} - P_3 B^3_{22}) W_3 + B^3_{32} (\dot{W}_3) \tag{37}$$

$$- (R_1 B^1_{22} - Q_1 B^1_{32}) (U_1 + Q_1 L_{C_M}) - B^1_{12} (\dot{U}_1 + \dot{Q}_1 L_{C_M})$$

$$- (P_1 B^1_{32} - R_1 B^1_{12}) (V_1 - P_1 L_{C_M}) - B^1_{22} (\dot{V}_1 - \dot{P}_1 L_{C_M})$$

$$- (Q_1 B^1_{12} - P_1 B^1_{22}) W_1 - B^1_{32} (\dot{W}_1)]\}$$

$$\dot{Q}_2 = + \frac{1}{B^2_{11}} \{Q_2(Q_2 B^2_{31} - R_2 B^2_{21}) + P_2(P_2 B^2_{31} - R_2 B^2_{11}) + \dot{P}_2 B^2_{21}$$

$$+ \frac{1}{L_2} [(R_3 B^3_{21} - Q_3 B^3_{31}) (U_3 - Q_3 L_3) + B^3_{11} (\dot{U}_3 - \dot{Q}_3 L_3)$$

$$+ (P_3 B^3_{31} - R_3 B^3_{11}) (V_3 + P_3 L_3) + B^3_{21} (\dot{V}_3 + \dot{P}_3 L_3)$$

$$+ (Q_3 B^3_{11} - P_3 B^3_{21}) W_3 + B^3_{31} (\dot{W}_3) \tag{38}$$

$$- (R_1 B^1_{21} - Q_1 B^1_{31}) (U_1 + Q_1 L_{C_M}) - B^1_{11} (\dot{U}_1 + \dot{Q}_1 L_{C_M})$$

$$- (P_1 B^1_{31} - R_1 B^1_{11}) (V_1 - P_1 L_{C_M}) - B^1_{21} (\dot{V}_1 - \dot{P}_1 L_{C_M})$$

$$- (Q_1 B^1_{11} - P_1 B^1_{21}) W_1 - B^1_{31} (\dot{W}_1)]\}$$

$$\dot{R}_2 = 0 \tag{39}$$

In the set of Equations (16) through (39), there are no terms involving the riser linear velocity components U_2, V_2, W_2 or their derivatives.

The velocity of the SRB Center of Mass relative to the earth can be determined from Equations (19), (20), (21), the direction cosine matrix $[B^3]$ given by Equation (2), and Equation (1C).

By integrating Equations (19), (20), and (21) and applying Equation (1C), the linear velocity components of the SRB Center of Mass in the Earth fixed reference frame will be:

$$\dot{X}_{E3} = U_3 B_{11}^3 + V_3 B_{21}^3 + W_3 B_{31}^3 \tag{40}$$

$$\dot{Y}_{E3} = U_3 B_{12}^3 + V_3 B_{22}^3 + W_3 B_{32}^3 \tag{41}$$

$$\dot{Z}_{E3} = U_3 B_{13}^3 + V_3 B_{23}^3 + W_3 B_{33}^3 \tag{42}$$

Elastic Models

The entire parachute is made of elastic material and is subject to deformation under load. The riser too elongates when loaded. To account for any additional dynamics caused by the continuous dynamic flexing of the parachute-riser system, two elastic models are employed.

The first is a canopy shape model which depends on the suspended load, the canopy pressure distribution, the inflation condition, and the construction of the canopy (Ref. 4). Its use is independent of the simulation program but its result is an input to the simulation program.

The second is a damped spring mass model of the suspension lines and riser. The application of this model is dynamic in the simulation program.

Program CANO -- An elastic canopy shape analysis is done by Program CANO (Ref. 4).

For an assumed pressure distribution and an initial gore geometry specification (which assumes the canopy to be made up of discrete horizontal and radial elements) and a specified suspension line length and riser load the program solves for the equilibrium shape and loads of the discrete members.

The method assumes an elastic deformable frame (the canopy) under a specific load (the pressure distribution) to determine the loaded (equilibrium) shape. The pressure distribution is nondimensionalized by the length along the canopy surface. The load elongation curves are set for types of materials and are generalized as percentage of breaking strength and unit strain. Thus, only the type of materials and geometry of the gore need be specified.

For specific loading conditions such as reefed, fully open. overinflation lines, etc., the program iterates across the canopy surface, adjusting the breaking strength of each member to equal the calculated load. This in turn adjusts the weight and then the equilibrium shape of the canopy. For the new breaking strengths of the members, a new equilibrium shape for the canopy and new loads for each element are calculated. The loads are compared to the most currently defined breaking strength, and when all elements have breaking strengths within a range of zero to five percent more than the calculated load, the parachute is said to be optimized.

Using the assumption that for a particular material type (e.g., web, tape, or cord) the weight of a material is proportional to its breaking strength, the optimized weight of the radial and horizontal members and the suspension lines are calculated, and thus the weight of the total canopy is determined. From an input table of available materials characterized by breaking strength and type, which implies a load-strain characteristic and a parametric weight, materials are chosen that are the lightest available which meet the strength requirements for the calculated loads in individual elements. The "buildable" parachute weights are calculated and compared as non-optimum factors to the optimized parachute weights.

The program CANO can be applied to consecutive steps in the process of deployment. It can be used to calculate the optimum parachute to meet up to 21 loading conditions which are combinations of partial inflation, reefed skirt, overinflation lines, and fully open. Thus, an accurate estimate of canopy weight can be made for a particular set of loading and inflation conditions.

The canopy profile generated by CANO for a fully inflated 130 ft conical ribbon parachute with a 200,000 lb suspended weight is shown in Figure 6.

Elastic Suspension Lines and Risers -- The suspension lines and risers generally used in parachute construction are quite elastic. The additional dynamics introduced by their elastic characteristics are to be included in the general equations of motion describing the parachute/riser/payload descent.

The geometry of the parachute and riser is shown in Figure 7. The elastic elements are the suspension lines (length L_s) and the riser (length L_2). Elongation of the suspension lines results in a change in the suspension line angle and hence the suspension line moments of inertia. There is also a change in the location of the center of mass of the parachute and a resulting change in the total moments of inertia of the parachute.

Two key assumptions are made:

- The canopy is fixed in shape and thus the skirt radius R_o is constant.
- The angle between the parachute axis of symmetry and the riser is always small. The riser force then is transmitted to the confluence point along the parachute axis of symmetry and thus the parachute remains axially symmetric. That is, the confluence point remains on the axis of symmetry and the suspension line cone remains right circular with variations in height only.

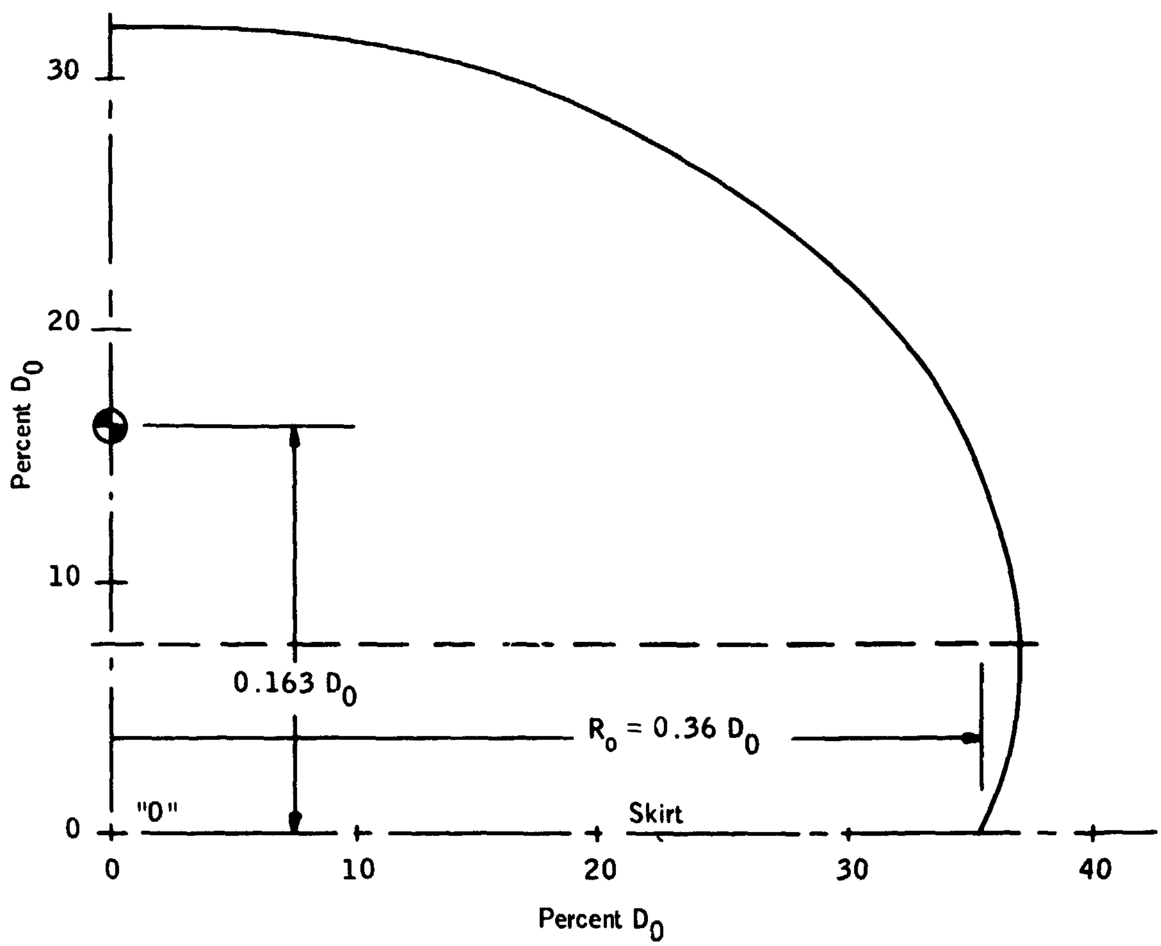

Figure 6. Fully Inflated Conical Ribbon Canopy Shape as Calculated by Program CANO (Ref. 4)

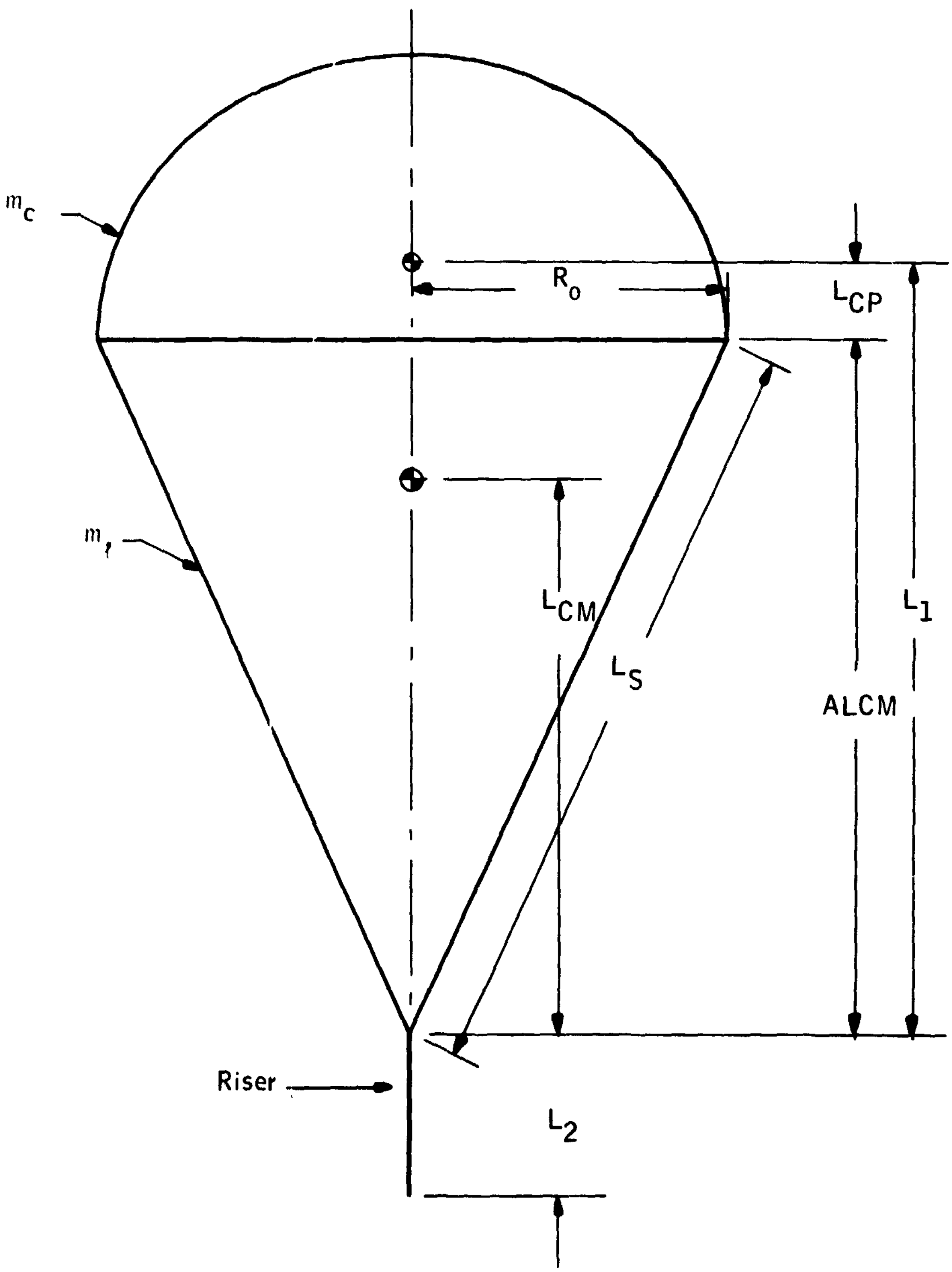

Figure 7. Parachute and Riser Geometry

The elastic elements are modeled as damped linearly elastic springs. The damping coefficient is taken as a representative value for dacron material (Ref. 5). Thus,

$$\zeta = 0.05 \text{ lb sec/ft} \tag{43}$$

The spring constants are determined as functions of the unstretched length, the elongation at break, the suspended load, and a safety factor of 3. Thus, for the riser,

$$K_R = \frac{3M_3 g}{1.2 L_{R_o}} \quad \text{lb/ft} \tag{44}$$

where $M_3 g$ is the suspended weight

L_{R_o} is the unstretched riser length

1.2 represents 20% elongation at break

and 3 is a safety factor

For the suspension lines the suspended load is the load carried by each line so that

$$K_{LS} = \frac{3M_3 g}{1.2 L_{So} N} \text{ lb/ft} \tag{45}$$

where L_{So} is the unstretched suspension line length and N is the number of suspension lines.

We can now model the dynamic length of the elastic elements for the suspension lines

$$L_S = L_{So} + \frac{(F_2 - \zeta \dot{L}_{CM})}{N K_{L_S} \cos\gamma}, \; \gamma = \tan^{-1}\left(\frac{Ro}{L_S}\right) \tag{46}$$

for the riser

$$L_R = L_{Ro} + \frac{(F_2 - \zeta \dot{L}_2)}{K_R} \tag{47}$$

In Equation (46) $\dot{L}_{CM}$ is used in place of $\dot{L}_S$. Differentiation of Equation (53) (yet to come) with respect to time validates this substitution provided that the suspension line angle is small and the included mass much greater than the canopy or suspension line mass.

The rate of change of lengths of the center of mass location and the riser are calculated using the central difference in average length divided by the change in time. Thus,

$$\left.\frac{dL_2}{dt}\right|_{t-\Delta t} = \frac{\left.\overline{L_2}\right|_{t-\Delta t \to t} - \left.\overline{L_2}\right|_{t-2\Delta t \to t-\Delta t}}{2\Delta t}$$

$$\left.\frac{dL_{C_M}}{dt}\right|_{t-\Delta t} = \frac{\left.\overline{L_{C_M}}\right|_{t-\Delta t \to t} - \left.\overline{L_{C_M}}\right|_{t-2\Delta t \to t-\Delta t}}{2\Delta t}$$

where for example $\left.\overline{L_2}\right|_{t-\Delta t \to t}$ is the averaged riser length during the interval $t - \Delta t$ to t and $\left.\frac{dL_2}{dt}\right|_t$ is the time derivative of L_2 at time t

$$\left.\frac{d^2L_2}{dt^2}\right|_{t-\Delta t} = \frac{\left.\frac{dL_2}{dt}\right|_{t-\Delta t} - \left.\frac{dL_2}{dt}\right|_{t-2\Delta t}}{\Delta t}$$

$$\left.\frac{d^2 L_{C_M}}{dt^2}\right|_{t-\Delta t} = \frac{\left.\frac{dL_{C_M}}{dt}\right|_{t-\Delta t} - \left.\frac{dL_2}{dt}\right|_{t-2\Delta t}}{\Delta t} \tag{48}$$

Parachute Center of Mass Location -- The canopy is modeled as a semi-oblate spheroid whose height is 32.5% of the nominal diameter, D_o and whose radius is 36% of the nominal diameter.

The canopy volume is

$$V_c = \frac{2}{3}\pi(0.325\, D_o)\ (0.36\, D_o)^2. \tag{49}$$

The included air mass is given by

$$m_I = V_c\, \rho \tag{50}$$

where ρ is the air density.

The center of pressure and the center of mass of the canopy are both assumed to be located at the centroid of the canopy volume.

The suspension lines are modeled as thin rods having uniform mass distribution as shown in Figure 8.

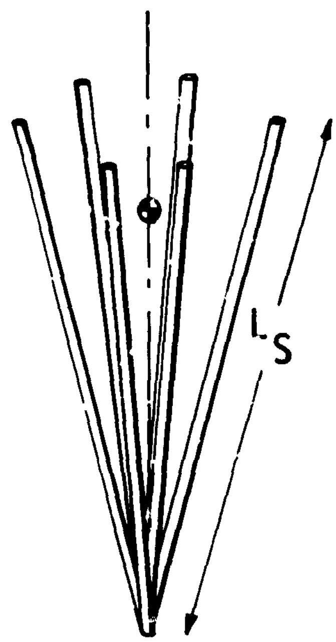

Figure 8. Suspe[illegible]e Geometry

The suspension line angle is given by

$$\gamma = \tan^{-1}\left(\frac{R_o}{L_S}\right) \tag{51}$$

The center of mass of all the suspension lines is

$$\frac{ALCM}{2} = \frac{L_S}{2}\cos\gamma \tag{52}$$

The center of mass location for the entire canopy then is given by the following relation

$$L_{C_M} = \frac{\dfrac{ALCM \times m_c}{2} + L_1 \times m_c + L_1 \times m_l}{m_1 + m_c + m_l} \tag{53}$$

Parachute moments of inertia: Canopy moments of inertia written about the point "o" in Figure 6 in the plane of the skirt are

$$
\begin{aligned}
I_{ZZ} &= \frac{2}{3} M_c \,(0.36\ D_o)^2 \\
I_{XX} &= I_{YY} = \frac{1}{3} M_c \,[(0.325\ D_o)^2 + (0.36\ D_o)^2]
\end{aligned}
\tag{54}
$$

Suspension line moments of inertia about the suspension line cone center of mass location are

$$
\begin{aligned}
I_{ZZ} &= \frac{M_\ell L_S^2}{12} \sin^2\gamma \\
I_{XX} &= I_{YY} = \frac{M_\ell L_S^2}{12} \cos^2\gamma
\end{aligned}
\tag{55}
$$

The apparent moments of inertia of the canopy written about the total parachute center of mass location are according to Reference 6:

$$
\begin{aligned}
I_{ZZ_{A_1}} &= 0.063\ \rho (R_o)^5 \\
I_{XX_{A_1}} &= I_{YY_{A_1}} = 0.042\ \rho\,(R_o)^5 + M_{1A}\,(L_1 - L_{C_M})^2
\end{aligned}
\tag{56}
$$

The total Parachute moments of inertia about the total parachute center of mass location then are given by

$$
\begin{aligned}
I_{XX_1}^{\,*} = I_{YY_1}^{\,*} &= \frac{M_\ell L_S^2}{12} \cos^2\gamma + M_c \left(L_{C_M} - \frac{ALCM}{2}\right)^2 \\
&\quad + \frac{M_c}{3} [(0.325^2 + 0.36^2)\ D_o^{\,2}] \\
&\quad + M_c\,(ALCM - L_{C_M})^2 + 0.042\ \rho\,(R_o)^5 \\
&\quad + M_{1A}\,(L_1 - L_{C_M})^2 \\
I_{ZZ_1}^{\,*} &= \frac{M_\ell L_S^2}{12} \sin^2\gamma + \frac{2}{3} M_c\,(0.36\ D_o)^2 \\
&\quad + 0.063\ \rho (R_o)^5
\end{aligned}
\tag{57}
$$

Additions to the nonlinear differential equations of motion. -- The inclusion of elasticity adds several terms to the differential equations of motion.

When writing the constraint equations which allow coupling of the motions of the parachute and SRB, the velocity of the confluence point relative to the center of mass location is amended to read

$$\left\{ \begin{bmatrix} U_1 \\ V_1 \\ W_1 + \dot{L}_{C_M} \end{bmatrix} + \begin{bmatrix} Q_1 L_{C_M} \\ -P_1 L_{C_M} \\ 0 \end{bmatrix} \right\} \tag{58}$$

The velocity of the end of the riser at the payload attach point is rewritten

$$\left\{ \begin{bmatrix} U_2 \\ V_2 \\ W_2 + \dot{L}_2 \end{bmatrix} + \begin{bmatrix} Q_2 L_2 \\ -P_2 L_2 \\ 0 \end{bmatrix} \right\} \tag{59}$$

Thus, with the addition of elasticity, the final constraint equation, corresponding to Equation (11) is:

$$\begin{aligned} [B^2]^T \begin{bmatrix} Q_2 L_2 \\ -P_2 L_2 \\ \dot{L}_2 \end{bmatrix} = {} & [B^3]^T \left\{ \begin{bmatrix} U_3 \\ V_3 \\ W_3 \end{bmatrix} + \begin{bmatrix} -Q_3 L_3 \\ P_3 L_3 \\ 0 \end{bmatrix} \right\} \\ & - [B^1]^T \left\{ \begin{bmatrix} U_1 \\ V_1 \\ W_1 + \dot{L}_{C_M} \end{bmatrix} + \begin{bmatrix} Q_1 L_{C_M} \\ -P_1 L_{C_M} \\ 0 \end{bmatrix} \right\} \end{aligned} \tag{60}$$

Differentiating the constraint equation above results in

$$\frac{d}{dt}\,[B^2]^T \begin{bmatrix} Q_2L_2 \\ -P_2L_2 \\ \dot{L}_2 \end{bmatrix} + [B^2]^T \left\{ \begin{bmatrix} \dot{Q}_2L_2 + \dot{L}_2Q_2 \\ -\dot{P}_2L_2 - \dot{L}_2P_2 \\ \ddot{L}_2 \end{bmatrix} \right\}$$

$$= \frac{d}{dt}\,[B^3]^T \left\{ \begin{bmatrix} U_3 \\ V_3 \\ W_3 \end{bmatrix} + \begin{bmatrix} -Q_3L_3 \\ P_3L_3 \\ 0 \end{bmatrix} \right\}$$

$$+ [B^3]^T \left\{ \begin{bmatrix} \dot{U}_3 \\ \dot{V}_3 \\ \dot{W}_3 \end{bmatrix} + \begin{bmatrix} -\dot{Q}_3L_3 \\ \dot{P}_3L_3 \\ 0 \end{bmatrix} \right\} \qquad (61)$$

$$- \frac{d}{dt}\,[B^1]^T \left\{ \begin{bmatrix} U_1 \\ V_1 \\ W_1 + \dot{L}_{C_M} \end{bmatrix} + \begin{bmatrix} Q_1L_{C_M} \\ -P_1L_{C_M} \\ 0 \end{bmatrix} \right\}$$

$$- [B^1]^T \left\{ \begin{bmatrix} \dot{U}_1 \\ \dot{V}_1 \\ \dot{W}_1 + \ddot{L}_{C_M} \end{bmatrix} + \begin{bmatrix} \dot{Q}_1L_{C_M} + \dot{L}_{C_M}Q_1 \\ -\dot{P}_1L_{C_M} - \dot{L}_{C_M}P_1 \\ 0 \end{bmatrix} \right\}$$

From Equation (61) we can obtain expressions for $\dot{W}_1$, $\dot{P}_2$, $\dot{Q}_2$.

Equations (16) to (39) describe the nonelastic differential equations of motion. Equations for $\dot{W}_1$, $\dot{P}_2$, and $\dot{Q}_2$ [(18), (37), and (38)] are rewritten here to incorporate the changes due to the inclusion of elasticity.

$$
\begin{aligned}
\dot{W}_1 = \frac{1}{B^1_{33}} \Big\{ & L_2 \Big[Q_2 (Q_2 B^2_{33} - R_2 B^2_{23}) + P_2 (P_2 B^2_{33} - R_2 B^2_{13}) \\
& - B^2_{13} \dot{Q}_2 + B^2_{23} \dot{P}_2 \Big] + \dot{L}_2 \Big[2 (P_2 B^2_{23} - Q_2 B^2_{13}) \Big] + \ddot{L}_2 B^2_{33} \\
& + (R_3 B^3_{23} - Q_3 B^3_{33}) (U_3 - Q_3 L_3) + B^3_{13} (\dot{U}_3 - \dot{Q}_3 L_3) \\
& + (P_3 B^3_{33} - R_3 B^3_{13}) (V_3 + P_3 L_3) + B^3_{23} (\dot{V}_3 + \dot{P}_3 L_3) \\
& + (Q_3 B^3_{13} - P_3 B^3_{23}) (W_3) + B^3_{33} (\dot{W}_3) \\
& - (R_1 B^1_{23} - Q_1 B^1_{33}) (U_1 + Q_1 L_{C_M}) - B^1_{13} (\dot{U}_1 + \dot{Q}_1 L_{C_M} + Q_1 \dot{L}_{C_M}) \\
& - (P_1 B^1_{33} - R_1 B^1_{13}) (V_1 - P_1 L_{C_M}) - B^1_{23} (\dot{V}_1 - \dot{P}_1 L \quad - P_1 \dot{L}_{C_M}) \\
& - (Q_1 B^1_{13} - P_1 B^1_{23}) (W_1 + \ddot{L}_{C_M}) \Big\} - \ddot{L}_{C_M}
\end{aligned}
\tag{62}
$$

$$
\begin{aligned}
\dot{P}_2 = & -\frac{1}{B_{22}^2}\Big\{Q_2\,(Q_2B_{32}^2 - R_2B_{22}^2) + P_2(P_2B_{32}^2 - R_2B_{12}^2) \\
& - \dot{Q}_2B_{12}^2 + \frac{1}{L_2}\Big[\dot{L}_2\,(2\,(P_2B_{22}^2 - Q_2B_{12}^2)) - B_{32}^2\ddot{L}_2 \\
& + (R_3B_{22}^3 - Q_3B_{32}^3)\,(U_3 - Q_3L_3) + B_{12}^3\,(\dot{U}_3 - \dot{Q}_3L_3) \\
& + (P_3B_{32}^3 - R_3B_{12}^3)\,(V_3 + P_3L_3) + B_{22}^3(\dot{V}_3 + \dot{P}_3L_3) \\
& + (Q_3B_{12}^3 - P_3B_{22}^3)\,(W_3) + B_{32}^3\,(\dot{W}_3) \\
& - (R_1B_{22}^1 - Q_1B_{32}^1)\,(U_1 + Q_1L_{C_M}) - B_{12}^1\,(\dot{U}_1 + \dot{Q}_1L_{C_M} + Q_1\dot{L}_{C_M}) \\
& - (P_1B_{32}^1 - R_1B_{12}^1)\,(V_1 - P_1L_{C_M}) - B_{22}^1(\dot{V}_1 - \dot{P}_1L_{C_M} - P_1\dot{L}_{C_M}) \\
& - (Q_1B_{12}^1 - P_1B_{22}^1)\,(W_1 + \dot{L}_{C_M}) - B_{32}^1(\dot{W}_1 + \ddot{L}_{C_M})\Big]\Big\}
\end{aligned}
\tag{63}
$$

$$
\begin{aligned}
\dot{Q}_2 = & \frac{1}{B_{11}^2}\Big\{Q_2(Q_2B_{31}^2 - R_2B_{21}^2) + P_2(P_2B_{31}^2 - R_2B_{11}^2) + \dot{P}_2B_{21}^2 \\
& + \frac{1}{L_2}\Big[\dot{L}_2(2(P_2B_{21}^2 - Q_2B_{21}^2)) - B_{31}^2\ddot{L}_2 \\
& + (R_3B_{21}^3 - Q_3B_{31}^3)\,(U_3 - Q_3L_3) + B_{11}^3\,(\dot{U}_3 - \dot{Q}_3L_3) \\
& + (P_3B_{31}^3 - R_3B_{11}^3)\,(V_3 + P_3L_3) + B_{21}^3(\dot{V}_3 + \dot{P}_3L_3) \\
& + (Q_3B_{11}^3 - P_3B_{21}^3)\,(W_3) + B_{31}^3(\dot{W}_3) \\
& - (R_1B_{21}^1 - Q_1B_{31}^1)\,(U_1 + Q_1L_{C_M}) - B_{11}^1\,(\dot{U}_1 + \dot{Q}_1L_{C_M} + Q_1\dot{L}_{C_M}) \\
& - (P_1B_{31}^1 - R_1B_{11}^1)\,(V_1 - P_1L_{C_M}) - B_{21}^1\,(\dot{V}_1 - \dot{P}_1L_{C_M} - P_1\dot{L}_{C_M}) \\
& - (Q_1B_{11}^1 - P_1B_{21}^1)\,(W_1 + \dot{L}_{C_M}) - B_{31}^1\,(\dot{W}_1 + \ddot{L}_{C_M})
\end{aligned}
$$

DEVELOPMENT OF AN AERODYNAMIC FORCE AND MOMENT SYSTEM IN AN UNSTEADY AIRMASS

The application of aerodynamic forces and moments in the simulation program is described in this section along with the models describing the nonsteady air mass and their effect on the aerodynamic forces and moments.

Least squares polynomial curve fits to the aerodynamic coefficients data as given in References 9 and 10 provide a convenient method of representation of the normal, tangential, and moment coefficients as functions of the angle of attack for the parachute and SRB. The parachute force and moment system is shown in Figure 9 followed by the normal and tangent force and moment coefficients curve fits in Figures 10, 11, and 12, respectively.

The SRB force and moment system is illustrated in Figure 13 and the SRB normal and tangent force and moment coefficients curve fits in Figures 14, 15, and 16, respectively.

Wind and gust models. -- To determine water entry characteristics of the SRB, the effects of winds and gusts near the surface of the earth on the attitude of the descending SRB must be accounted for.

Wind and gust models to provide inputs to the recovery simulation as required by the contracting agency are described as adapted from Reference 7 and Reference 8, respectively.

Wind model: The recovery analy- - of the space shuttle Solid Rocket Booster (SRB) requires steady-state winds to be defined in the layer of air between sea level and 3281 ft (1 KM). The following is the recommended 5% risk steady-state wind profile of Reference 7.

$$
\begin{aligned}
V_{wind\ (h)} &= V_{wind\ (h_o)} \left(\frac{h}{582}\right)^{P} \quad 0 \le h \le 582 \text{ ft} \\
V_{wind\ (h)} &= V_{wind\ (h_o)} \quad 582 \le h \le 3281 \text{ ft} \\
V_{wind\ (h_o)} &= 69 \text{ fps} \\
h_o &= 3281 \text{ ft} \\
P &= 0.21
\end{aligned}
\tag{65}
$$

The steady-state wind profile is shown in Figure 15.

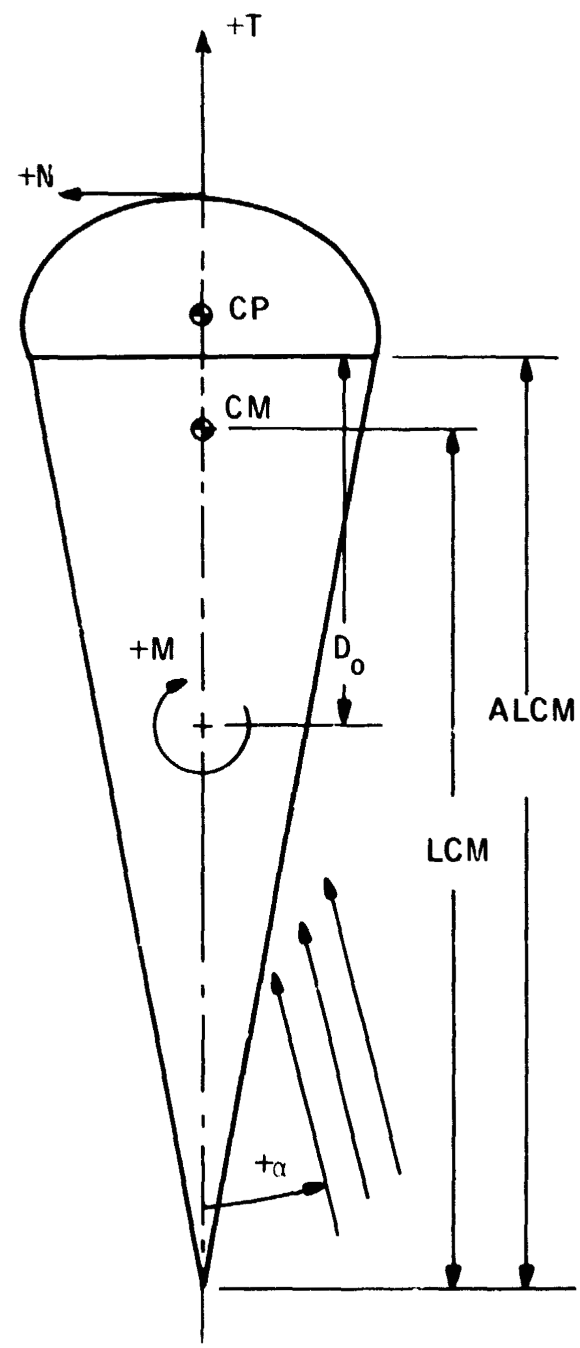

Figure 9. Parachute Force and Moment System

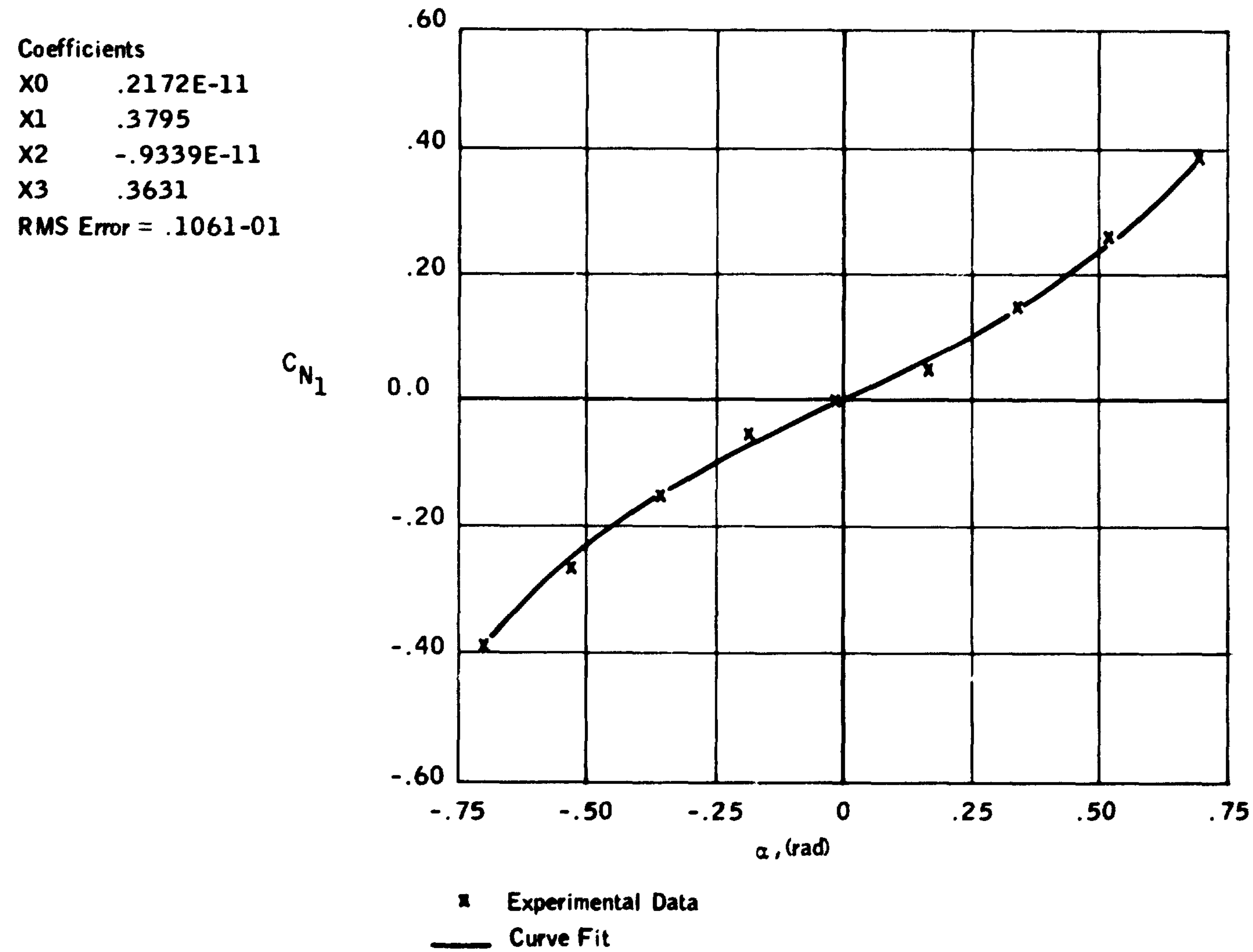

Figure 10. Polynomial Curve Fit to Normal Force Coefficients for a 20° Conical Ribbon Parachute

Coeffieients
X0 .5755
X1 -.1637E-10
X2 -.8091
X3 .3483E-10
X4 .4228
RMS Error = .2522E-02

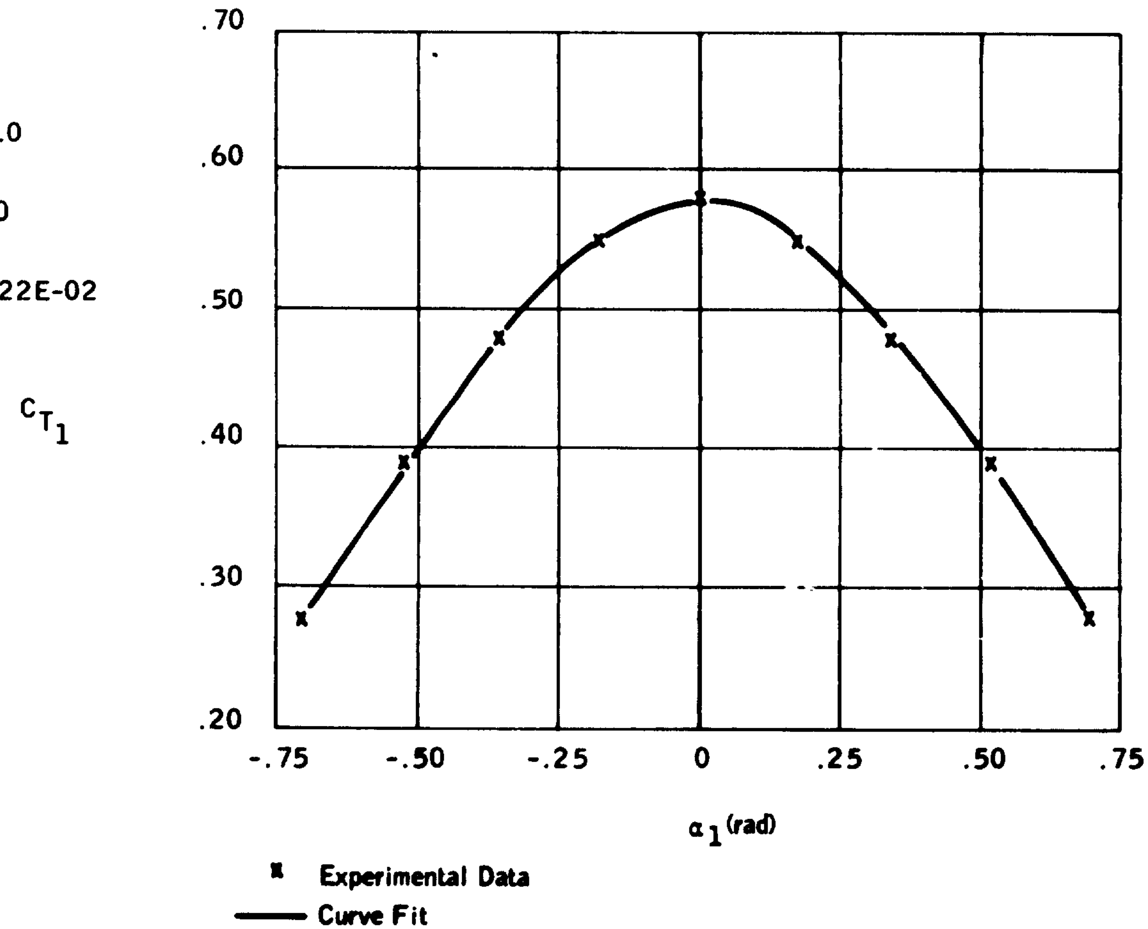

Figure 11. Polynomial Curve Fit to Tangential Force Coefficients for a 20° Conical Ribbon Parachute

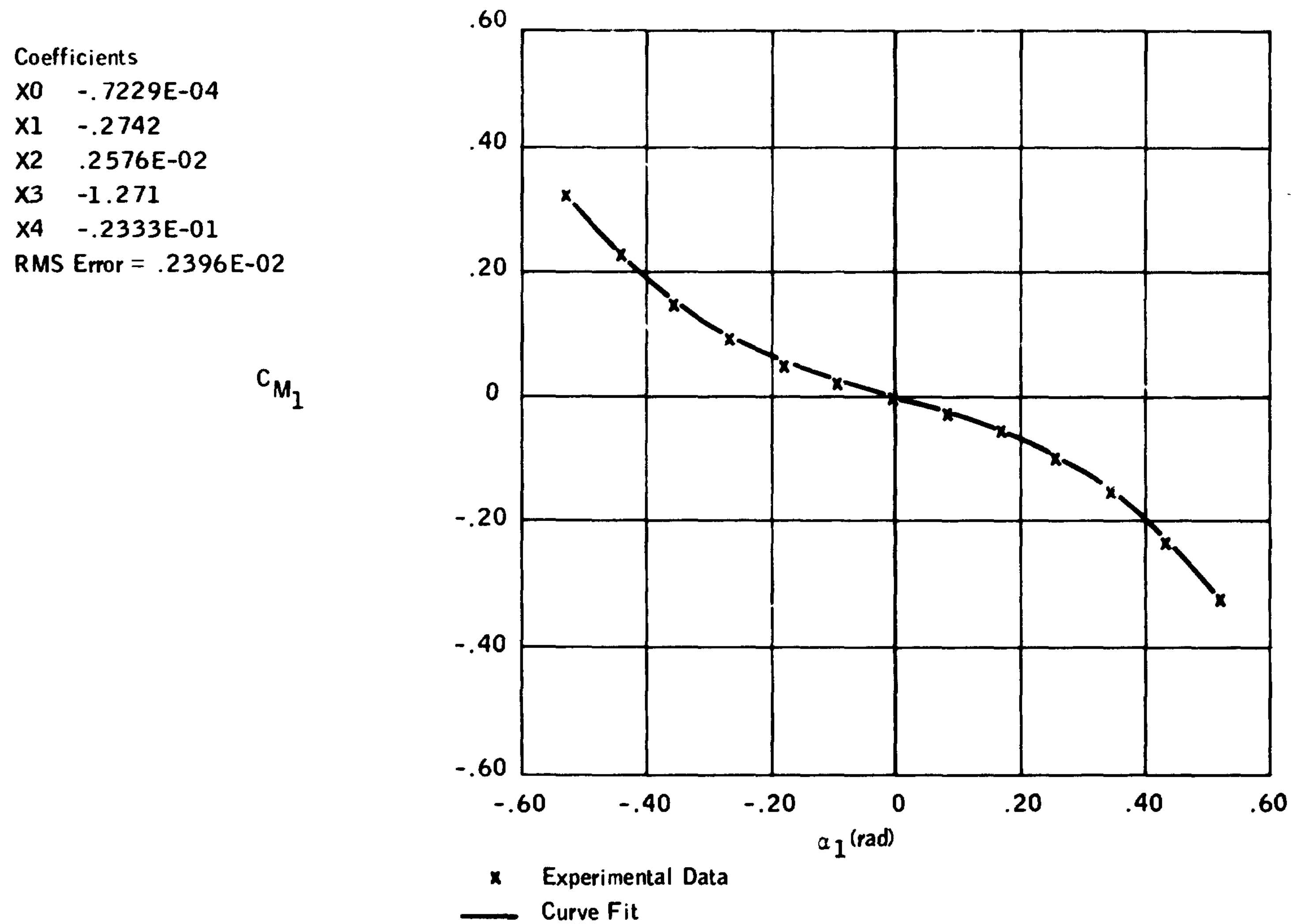

Figure 12. Polynomial Curve Fit to Moment Coefficients for a 70° Conical Ribbon Parachute

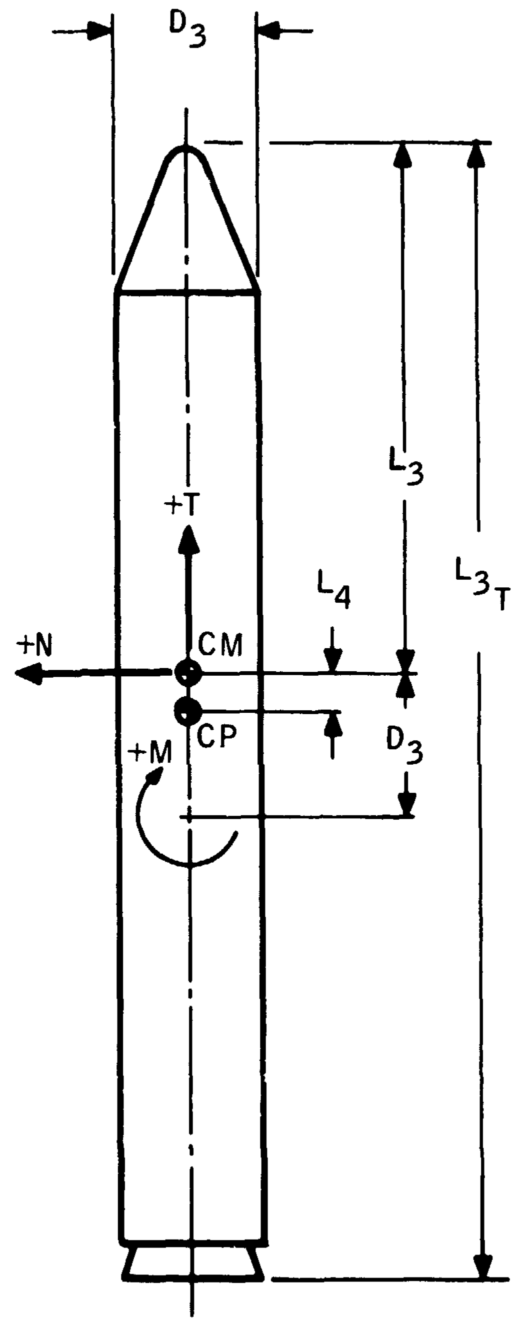

Figure 13. SRB Force and Moment System

Coefficients	
X0	.2355E-09
X1	3.645
X2	-.8473E-08
X3	15.20
X4	.4432E-07
X5	-12.60
X6	-.5784E-07

RMS Error = .5829E-01

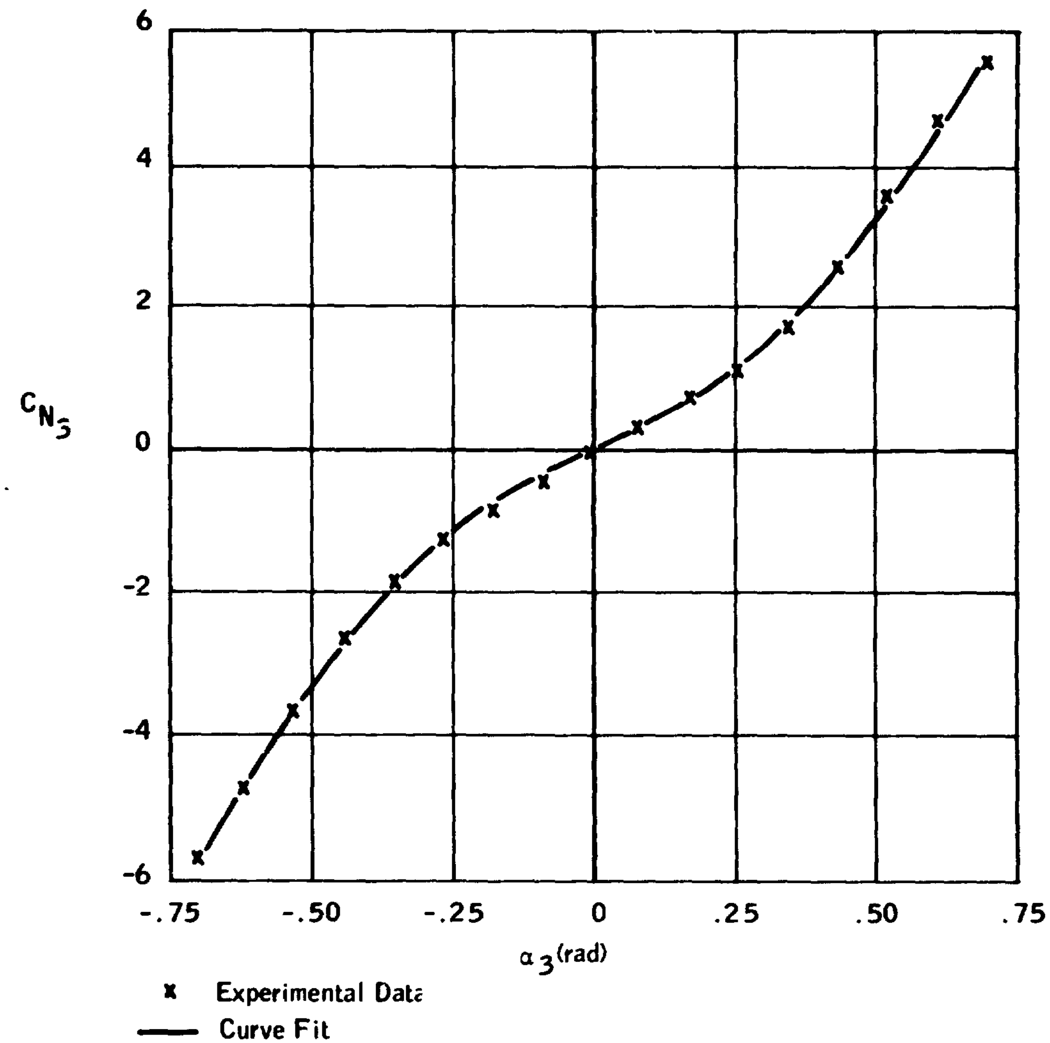

Figure 14. Polynomial Curve Fit to Normal Force Coefficients for the SRB

Coefficients	
X0	.6989
X1	.1915E-08
X2	12.56
X3	-.1682E-07
X4	-35.39
X5	2803E-07
X6	31.88

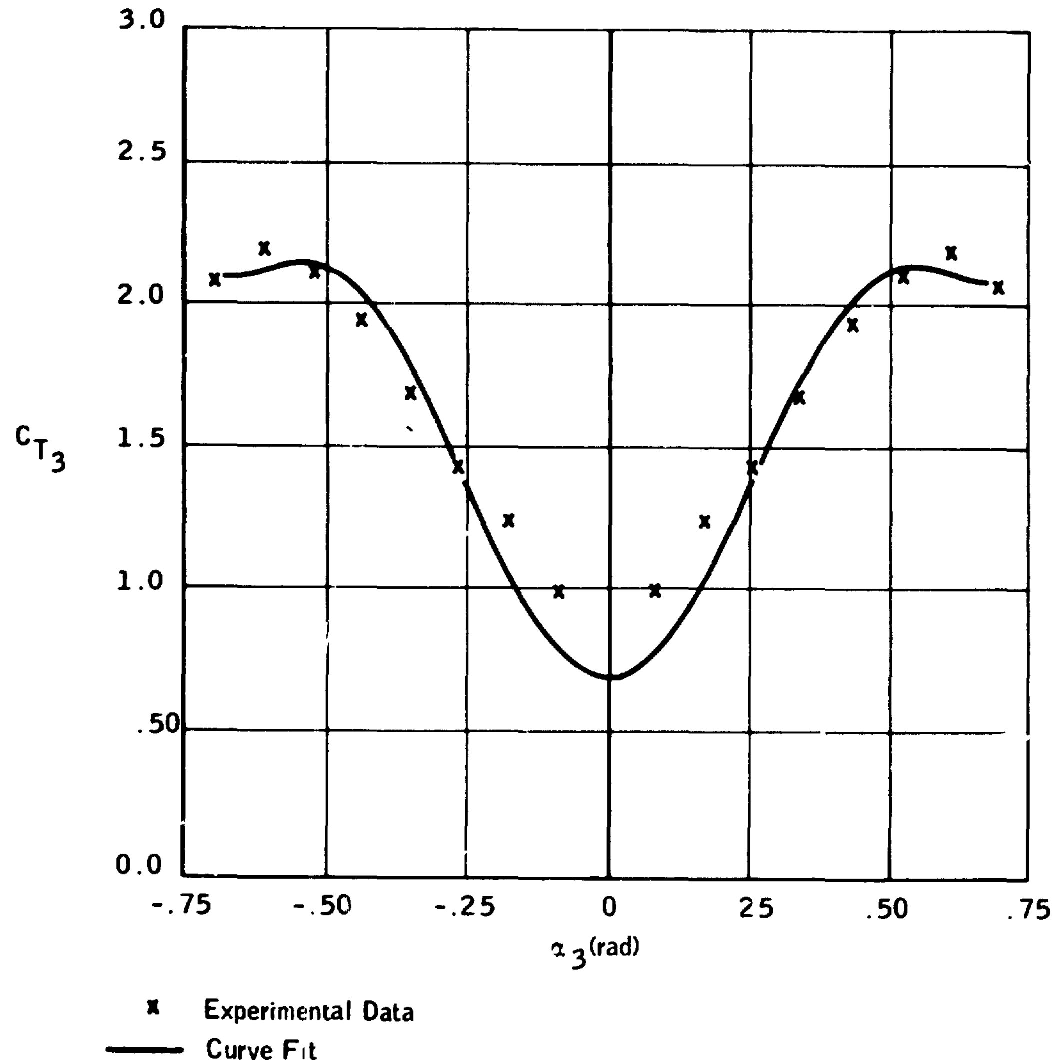

Figure 15. Polynomial Curve Fit to the Tangent Force Coefficients for the SRB

Coefficients
X0 -.1927
X1 -7.632
X2 -1.114
X3 -12.87
X4 33.24
X5 12.61
X6 -48.36
RMS Error = .1171

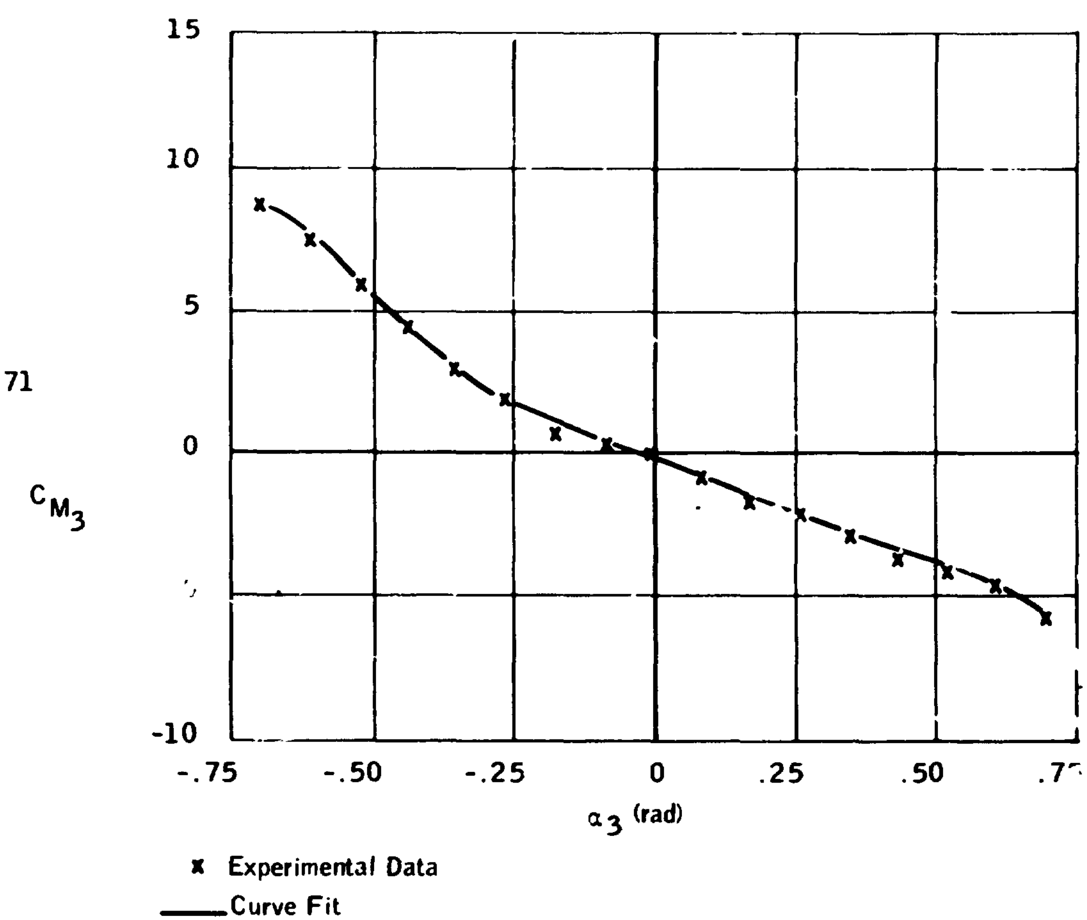

Figure 16. Polynomial Curve Fit to the Mom. 1t Coefficients of the SRB

Gust model: Associated with the steady-state wind profile (air mass velocity field) is a discrete gust environment. The gust amplitude represents a step velocity change in the air mass velocity field. The maximum gust amplitude envelope associated with the 5% risk steady-state wind profile as recommended by Reference 8 is as follows:

$$V_{gust} = 19.7 \text{ fps} \quad 0 \leq h \leq 980 \text{ ft}$$

$$V_{gust} = \frac{9.8}{2301}(h-980) + 19.7 \quad 980 \leq h \leq 3281 \text{ ft (66} \tag{66}$$

$$V_{gust} = 29.7 \text{ fps} \quad h > 3281 \text{ ft}$$

The gust envelope is superimposed on the steady-state wind profile in Figure 17.

Relative velocity vector: The aerodynamic forces and moments are functions of the angle of attack, the altitude, the nominal area, a reference length for the moments, and the velocity vector of the center of mass with respect to the wind.

The velocity field of the moving air mass can be written

$$\vec{V}_{wg} = \vec{V}_{wind} + \vec{V}_{gust}$$

where

$\vec{V}_{wg}$ is the velocity field vector

$\vec{V}_{wind}$ is the mean wind velocity field vector

$\vec{V}_{gust}$ is the gust velocity field vector

and all are, in general, altitude dependent.

The influence of the motion of the air on the body aerodynamics is accounted for by determining the velocity of the body with respect to the air to be used in developing the aerodynamic forces and moments. The relative motion of the center of pressure appears then as

$$\vec{V}_a = \vec{C} + \vec{\omega} \times \vec{L} - [B^i]\, \vec{V}_{wg} \tag{67}$$

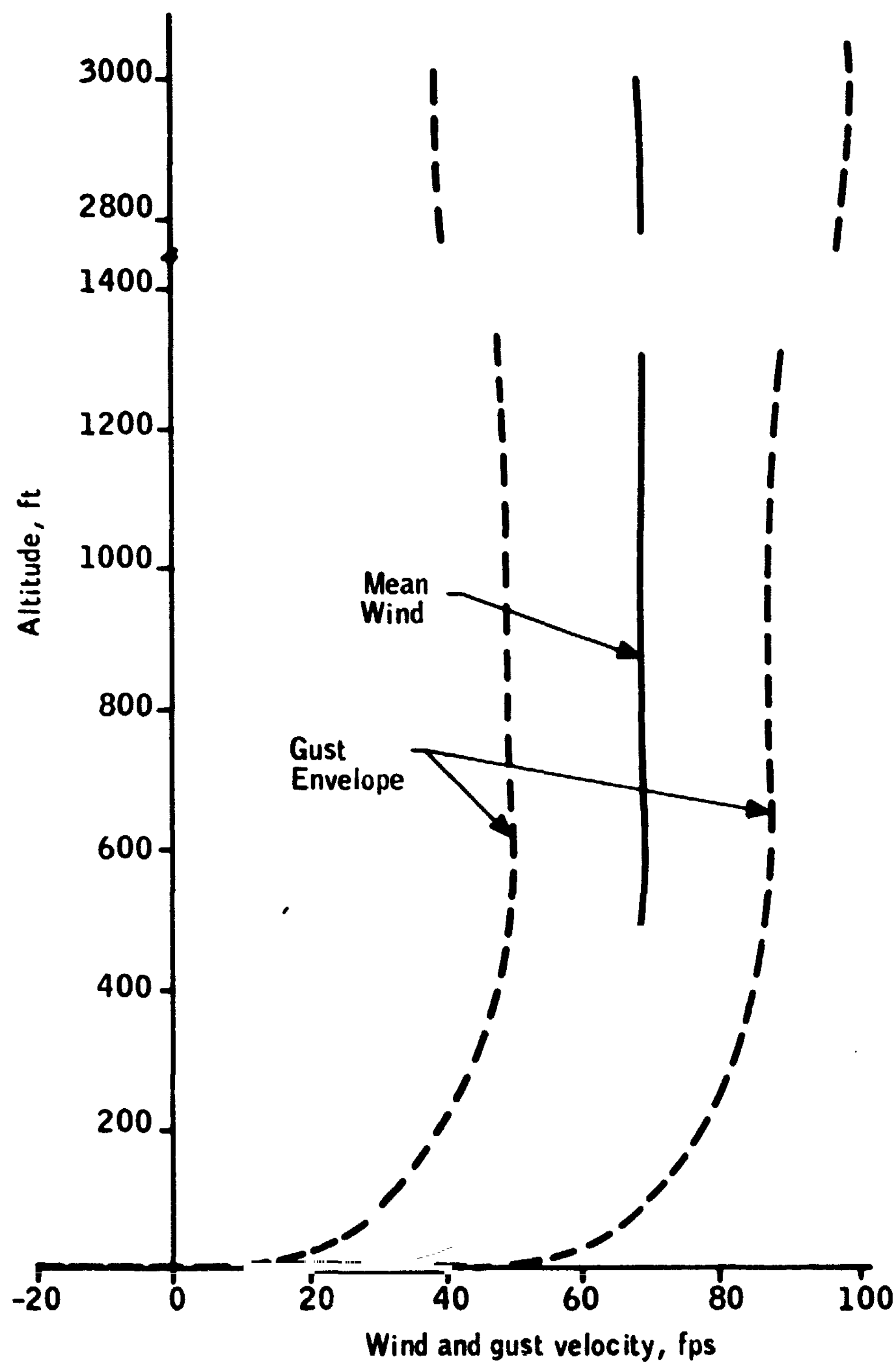

Figure 17. Mean Wind Profile and Gust Envelope (Refs. 7 and 8)

where

$\vec{C}$ is the velocity of the center of mass with respect to the earth in body coordinate directions

$\vec{\omega}$ is the angular velocity of the body

$\vec{L}$ is the vector from the body CM to the body CP

Written in matrix form, for body i

$$\begin{bmatrix} V_{a_{X_i}} \\ V_{a_{Y_i}} \\ V_{a_{Z_i}} \end{bmatrix} = \begin{bmatrix} U_i \\ V_i \\ W_i \end{bmatrix} \begin{bmatrix} 0 & -R_i & Q_i \\ R_i & 0 & -P_i \\ -Q_i & P_i & 0 \end{bmatrix} \begin{bmatrix} 0 \\ 0 \\ L \end{bmatrix}$$

$$- \begin{bmatrix} B^i_{11} & B^i_{12} & B^i_{13} \\ B^i_{21} & B^i_{22} & B^i_{23} \\ B^i_{31} & B^i_{32} & B^i_{33} \end{bmatrix} \begin{bmatrix} V_{WG_{XE}} \\ V_{WG_{YE}} \\ V_{WG_{ZE}} \end{bmatrix} \tag{68}$$

These are the velocity components used to determine the aerodynamic forces and moments.

Elsewhere in the dynamical equations, inertial velocities are used.

The angle of attack is given by

$$\alpha_i = \mathrm{Tan}^{-1} \left[\frac{\sqrt{V_{a_{X_i}}^{\;2} + V_{a_{Y_i}}^{\;2}}}{V_{a_{Z_i}}^{\;2}} \right] \tag{69}$$

The side slip angle is defined as

$$\beta_i = \mathrm{Tan}^{-1}\left[\frac{V_{a_{Y_i}}}{V_{a_{X_i}}}\right] \tag{70}$$

Aerodynamic Forces and Moments

The aerodynamic forces acting on the parachute can be written in the body fixed axes directions.

$$\begin{bmatrix} F_{1_X} \\ F_{1_Y} \\ F_{1_Z} \end{bmatrix} = \begin{bmatrix} C_{N_1} \ \mathrm{Cos}\,\beta_1 \\ C_{N_1} \ \mathrm{Sin}\,\beta_1 \\ C_{T_1} \end{bmatrix} \begin{bmatrix} q_1 S_{o_1} & 0 & 0 \\ 0 & q_1 S_{o_1} & 0 \\ 0 & 0 & -q_1 S_{o_1} \end{bmatrix} \tag{71}$$

Similarly for the SRB the aerodynamic force in the body fixed directions are

$$\begin{bmatrix} F_{3_X} \\ F_{3_Y} \\ F_{3_Z} \end{bmatrix} = \begin{bmatrix} C_{N_3} \ \mathrm{Cos}\,\beta_3 \\ C_{N_3} \ \mathrm{Sin}\,\beta_3 \\ C_{T_3} \end{bmatrix} \begin{bmatrix} q_3 S_{o_3} & 0 & 0 \\ 0 & q_3 S_{o_3} & 0 \\ 0 & 0 & -q_3 S_{o_3} \end{bmatrix} \tag{72}$$

In general aerodynamic moments are written in terms of a moment coefficient (C_M) and a reference length (MRP). The aerodynamic moments then about the X and Y body fixed axes whose origin is located at the MRP can be written.

$$\begin{bmatrix} M_{1_X} \\ M_{1_Y} \end{bmatrix} = \begin{bmatrix} C_M \ \mathrm{Sin}\,\beta_1 \\ C_M \ \mathrm{Cos}\,\beta_1 \end{bmatrix} \begin{bmatrix} -q_1 S_{o_1} \ \mathrm{MRP} & 0 \\ 0 & q_1 S_{o_1} \ \mathrm{MRP} \end{bmatrix} \tag{73}$$

$$q_i = \frac{1}{2} \rho V_{a_i}^{\,2}$$

The moment reference point length (MRP) for parachutes is generally one nominal diameter ahead of the skirt plane.

To write the aerodynamic moments about the body fixed axes system located at the body center of mass, new MRP lengths must be defined.

The normal force is experimentally measured at the vent of the parachute. The height of the canopy plus the moment reference length is given by

$$0.325\, D_o + D_o = 1.325\, D_o$$

The moment then is

$$N(1.325\, D_o) \quad , \quad \text{where N is the normal force}$$

The distance from the vent to the center of mass of the parachute is given by

$$0.325\, D_o + ALCM - LCM$$

The functional form then of the aerodynamic moments acting on the parachute written about the body fixed axes located at the parachute center of mass is

$$\begin{bmatrix} M_{1_X} \\ M_{1_Y} \end{bmatrix} = \begin{bmatrix} C_{M_1} \operatorname{Sin} \beta_1 \\ C_{M_1} \operatorname{Cos} \beta_1 \end{bmatrix} \cdot \begin{bmatrix} -q_1 S_{o_1} \dfrac{D_o(0.325\, D_o + ALCM - LCM)}{1.325\, D_o} & 0 \\ 0 & q_1 S_{o_1} \dfrac{D_o(0.325\, D_o + ALCM - LCM)}{1.325\, D_o} \end{bmatrix} \tag{74}$$

The SRB aerodynamic moment coefficients are defined by

$$C_{M_3} = \frac{N\,(L_3 + L_4)}{\frac{1}{2}\rho\, V_{a_3}{}^2\, S_3\, D_3} \quad , \quad \text{where N is the normal force}$$

The functional form of the aerodynamic moments acting on the SRB written about the body fixed axes located at the SRB center of mass due to aerodynamic normal forces acting at the center of pressure is

$$\begin{bmatrix} M_{3_x} \\ M_{3_y} \end{bmatrix} = \begin{bmatrix} C_{M_3} \operatorname{Sin} \beta_3 \\ C_{M_3} \operatorname{Cos} \beta_3 \end{bmatrix} \begin{bmatrix} -q_3 S_{o_3} \left(\frac{D_3 L_4}{L_3+L_4}\right) & 0 \\ 0 & q_3 S_{o_3} \frac{D_3 L_4}{(L_3+L_4)} \end{bmatrix} \tag{75}$$

LINEARIZATION OF THE EQUATIONS OF MOTION

Application of the root locus stability analysis techniques to the solution of the SRB recovery problem requires a linearized system of equations of motion. One method of linearization is to choose a reference state, say vertical descent, and define small disturbances about this state. After linearizing the aerodynamic coefficients with respect to small changes in angle of attack and making appropriate substitutions, the linearized state is obtained by neglecting terms of order 2 and higher. This is a cumbersome task and the result is applicable only to the particular reference state originally chosen.

A more general linearization method results from numerical techniques developed in Reference 11.

Linearization Technique

For a nonlinear system of equations implicit in time, the state can be represented as

$$\dot{\vec{x}} = f(\bar{x}, \dot{\bar{x}}) \tag{76}$$

where

$$\bar{x} = \bar{x}(t)$$

$$\dot{\bar{x}} = \frac{d}{dt}(\bar{x}(t))$$

$$t = \text{time}$$

We want to linearize the vector nonlinear differential equations represented by Equation (76) at a particular point in time t_o.

The methodology is to calculate the nonlinear solution of $\dot{\bar{x}}$ until $t = t_o$ and then use the nonlinear solution at t_o as the reference state about which the equations of motion are linearized.

Let $\vec{x}$ be the nonlinear solution of Equation (76) at time t_o and $\tilde{x}$ be the linearized solution at t_o:

$\bar{x}$ is known

$\tilde{x}$ is to be numerically derived

more explicitly

$$F_{\bar{x}}(\bar{x}, \dot{\bar{x}}) = \begin{bmatrix} \frac{\partial}{\partial x_1} f_1(\bar{x}, \dot{\bar{x}}), \ldots, \frac{\partial}{\partial x_n} f_1(\bar{x}, \dot{\bar{x}}) \\ \vdots \qquad\qquad \vdots \\ \frac{\partial}{\partial x_1} f_n(\bar{x}, \dot{\bar{x}}), \ldots, \frac{\partial}{\partial x_n} f_n(\bar{x}, \dot{\bar{x}}) \end{bmatrix} . \tag{77}$$

Here

$$f = \begin{bmatrix} f_1 \\ f_2 \\ f_3 \\ \vdots \\ f_n \end{bmatrix} \qquad \bar{x} = \begin{bmatrix} \bar{x}_1 \\ \bar{x}_2 \\ \cdot \\ \cdot \\ \cdot \\ \bar{x}_n \end{bmatrix}$$

for a system of n equations.

The matrix $F_x(x, \dot{x})$ represents the first partial derivatives of each state equation with respect to each state variable. The elements of $F_x(\bar{x}, \dot{\bar{x}})$ are determined by the central difference quotient

$$\frac{\partial f_i}{\partial \bar{x}_j} = \frac{f_i(\bar{x}_1, \bar{x}_2, \ldots, \bar{x}_j + \Delta\bar{x}_j, \ldots, \bar{x}_n) - f_i(\bar{x}_1, \bar{x}_2, \ldots, \bar{x}_j - \Delta\bar{x}_j, \ldots, \bar{x}_n)}{2\Delta\bar{x}_j} \tag{78}$$

where $\Delta\bar{x}_j$ is taken to be 1 percent of $\bar{x}_j$.

Further, let $\vec{\xi} = \tilde{x} - \bar{x}$ be the disturbance vector about $\bar{x}$. Differentiation yields

$$\dot{\vec{\xi}} = \dot{\tilde{x}} - \dot{\bar{x}} = f(\tilde{x}, \dot{\tilde{x}}) - f(\bar{x}, \dot{\bar{x}}). \tag{79}$$

Rearranging terms

$$\dot{\tilde{x}} = \dot{\bar{x}} - \dot{\vec{\xi}}$$

$$\dot{\vec{\xi}} = f(\bar{x} + \vec{\xi}, \dot{\bar{x}} + \dot{\vec{\xi}}) - f(\bar{x}, \dot{\bar{x}}).$$

The mean value theo:em of differential calculus allows

$$\dot{\vec{\xi}} = f(\bar{x} + \vec{\xi}, \dot{\bar{x}} + \dot{\xi}) \simeq F_{\bar{x}}(\bar{x}, \bar{x})\, \vec{\xi} \tag{80}$$

where

$$F_{\bar{x}}(\bar{x}, \dot{\bar{x}}) = \frac{\partial f(\bar{x}, \dot{\bar{x}})}{\partial \bar{x}}$$

and $\Delta\bar{x}_j$ is the disturbance of the element, $\bar{x}_j$, of $\bar{x}$.

Equation (80) can be solved using the matrix of partial derivatives (77). The solution, call it $\vec{y}$, is linear and the desired linearized state is found

$$\tilde{x} = \bar{x} + \bar{y}. \tag{81}$$

Eigenvalues

Manipulation of the coefficients matrix of Equation (80) results in an n^{th} degree characteristic polynomial whose n roots are the eigenvalues.

Actually the solution to Equation (80) is not found because only the eigenvalues are required. The matrix of system (80) is transformed to Upper Hessenberg form. Using a Q-R procedure with double iterations and a convergence check, the eigenvalues to Equation (80) are approximated.

The eigenvalues are of the form

$\sigma \pm j\omega$

where σ is the real part

ω is the damped frequency

j is $\sqrt{-1}$

STABILITY ANALYSIS TECHNIQUE

The Root locus technique plots the eigenvalues on a complex plane. The relative stability and transient performance of the system are directly related to the position of the eigenvalues. The root locus plot provides a tool for investigating the effect of parametric variations on system response and stability. The sensitivity to adjustments of a particular parameter can be examined and a systematic procedure can be followed to move the root locus to a desired position on the complex plane corresponding to required stability and response characteristics.

ANALYSIS OF THE SOLID ROCKET BOOSTER RECOVERY SYSTEM

To determine an entry envelope of orientations of the SRB as functions of initial conditions, elasticity dynamics, and nonsteady air mass conditions, a wide variety of simulations were made on the nominal descent configurations from an altitude of 6000 ft to water impact after approximately 74 seconds.

NOMINAL BASELINE CONFIGURATIONS

The drogue and main parachutes in combination with the SRB were illustrated in Figures 2 and 3, respectively. Their specific dimensions are listed in Table 1.

SINGLE PARACHUTE EQUIVALENCE TO THE CLUSTER

The cluster of parachutes is modeled by a single parachute having the physical dimensions of one of the parachutes in the cluster but the mass, inertia, and drag area characteristics of the entire cluster.

In program CHUTER, described in Appendix A, all of the parachute-related input data are for a single element of the cluster. The number of chutes in the cluster is also a data input. The conversion to the equivalent parachute is handled within the program.

NOMINAL SYSTEMS RESPONSE TO DISTURBANCES

Two principal modes of disturbance or initial conditions were used in examining the nominal systems response to initial conditions. For analytical purposes, the disturbances are induced in only one plane and thus the motions are in one plane only. A "pendulum" disturbance in which the parachute,

TABLE 1 - RECOVERY SYSTEM PARAMETERS

	Drogue/ SRB	Main/SRB (Equivalent)
Parachute		
D_{o_1}	48 ft	130 ft
S_{o_1}	1810 ft^2	39900 ft^2
L_s	96 ft	275 ft
L_1	100 ft	310 ft
M_c	11 slugs	69.9 slugs
M_L	9 slugs	81.6 slugs
Riser		
L_2	48 ft	67 ft
SRB		
D_{o_3}	11.8 ft	11.8 ft
S_{o_3}	110.0 ft^2	110.0 ft^2
L_3	81 ft	75 ft
L_{3_T}	157 ft	145 ft
M_3	5000 slugs	4750.0 slugs
I_{XX_3}	8.36 x 10^6	7.36 x 10^6
I_{YY_3}	8.36 x 10^6	7.36 x 10^6
I_{ZZ_3}	1.96 x 10^6	1.72 x 10^6

riser, and payload remain generally aligned while being tipped to some initial angle results in smaller angular excursions of the SRB with less damping in the transient phase of the response.

A "scissors" disturbance is one where the parachute and riser are markedly misaligned with the SRB. Response to this initial condition results in larger SRB angular excursions but with higher damping in the transient phase.

Several sets of each type of initial conditions were imposed on the SRB/Main parachute combination. To see the added effects of elasticity and wind, each set was first run without the elastic or nonsteady air mass options. The same cases were then run with the addition of elasticity only and rerun again with the nonsteady air mass option only.

For reference, a case with no initial disturbance was run without elasticity or wind, with wind only, and with elasticity only.

The cases specifically illustrated are listed in Table 2.

TABLE 2 - ILLUSTRATED NONLINEAR SIMULATION CASES

Configuration	Initial Displacement Type	θ1 (deg)	θ3 (deg)	Elastic	Winds and Gust	Nonlinear Response Figures	Root Locus Figures
SRB/Main	Pendulum	+20	+20	No	No	18, 19	41, 42
SRB/Main	Scissors	-20	+20	No	No	21, 22	43, 44
SRB/Drogue	See Fig. No. 24	---	---	No	No	25, 26	---
SRB/Main	Vertical	0	0	No	Yes	28, 29	45, 46
SRB/Main	Pendulum	-20	-20	No	Yes	30, 31	---
SRB/Main	Pendulum	+20	+20	No	Yes	33, 34	47, 48
SRB/Main	Scissors	+20	-20	No	Yes	35, 36	---
SRB/Main	Pendulum	+20	+20	Yes	No	37, 38	49, 50
SRB/Main	Scissors	-20	+20	Yes	No	39, 40	---

SRB/Main Parachute Response to Pendulum-Type Initial Displacements

Pendulum-type initial disturbances of up to 30 degrees were imposed on the SRB/Main parachute descent configuration. The responses were similar in nature so that only the angular response for a +20 deg pendulum-type disturbance is shown as Figure 18. In all pendulum-type initial disturbances with a steady air mass the parachute angular orientation over shoots by approximately 45% and the SRB angular orientation over shoots by approximately 55%. The response is typified by the shorter period oscillations of the SRB as it follows the orientation of the parachute. The relative motions of the parachute and SRB quickly become 180 deg out of phase, and the SRB motion induces perturbations on the long period parachute response. The angle of attack time history is depicted in Figure 19 and the trajectory is shown in Figure 20.

SRB/Main Parachute Response to Scissors-Type Initial Conditions

Scissors-type initial conditions of up to 60 deg misalignment were imposed on the SRB/Main parachute descent configurations. The responses for a scissors-type displacement with no wind or elasticity were similar so that the angular response for only one parachute initial angular displacement of -20 deg and a SRB initial angular disturbance of +20 deg is shown in (Figure 21). Scissors-type initial conditions produced responses typified by 180 deg out of phase oscillations of the parachute and SRB, with the parachute motion, again long period, driving the general motion of the SRB and the SRB inducing small perturbations on the otherwise smooth parachute response. As in the cases with pendulum displacements the parachute over shoots to approximately 55%. The greatly increased moments on the SRB cause overshoots of approximately 170%. The long-term result of a scissors displacement is larger SRB angular excursions through the entire descent. The angle of attack time history is shown in Figure 22 and the trajectory is shown as Figure 23.

SRB/Drogue Response to an Assumed Deployment Condition

The SRB, after leaving the space shuttle, is assumed to move along a trajectory with a large angle of attack near 90 deg. Additionally, the SRB may be spinning about an axis approximately parallel to the trajectory. The object of the drogue parachute is to stabilize the SRB; that is, reduce its angle of attack to sufficient conditions required for deployment of the main parachutes. If the SRB is spinning, the drogue parachute will also reduce the total angular velocity of the SRB.

The SRB/Drogue combination is simulated at an altitude of 20000 ft descending vertically at a rate of 580 fps. Its initial angle of attack is taken to be 80 deg and the SRB is assumed to be rotating at 40 deg/sec about the earth fixed Z axis. The drogue parachute, assumed to be previously deployed, is initially positioned at a 10 deg yaw angle. The initial conditions are illustrated in Figure 24.

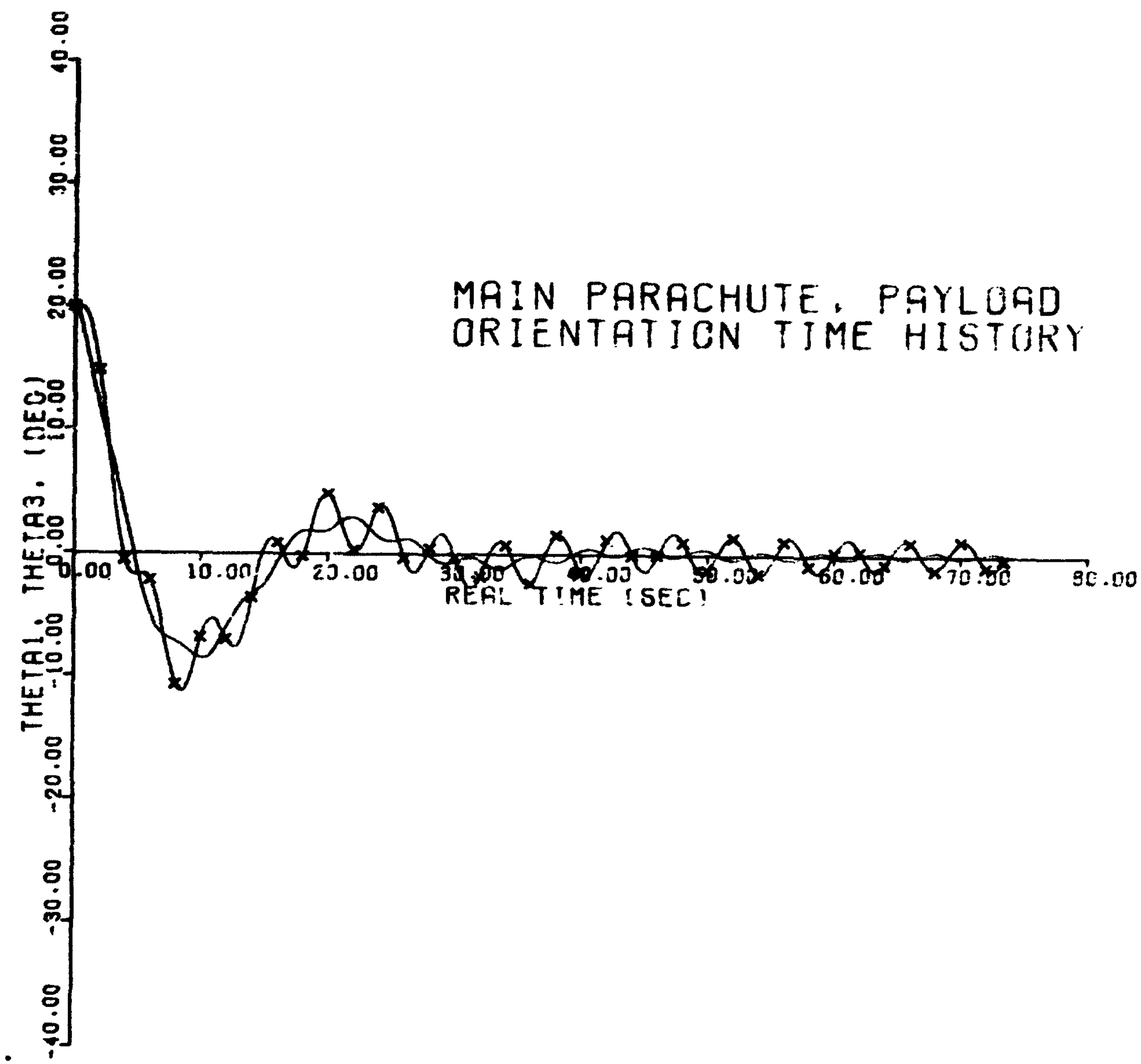

Figure 18. Main Parachute - SRB Response to a 20-deg Pendulum Disturbance (X-SRB, 2-sec Intervals)

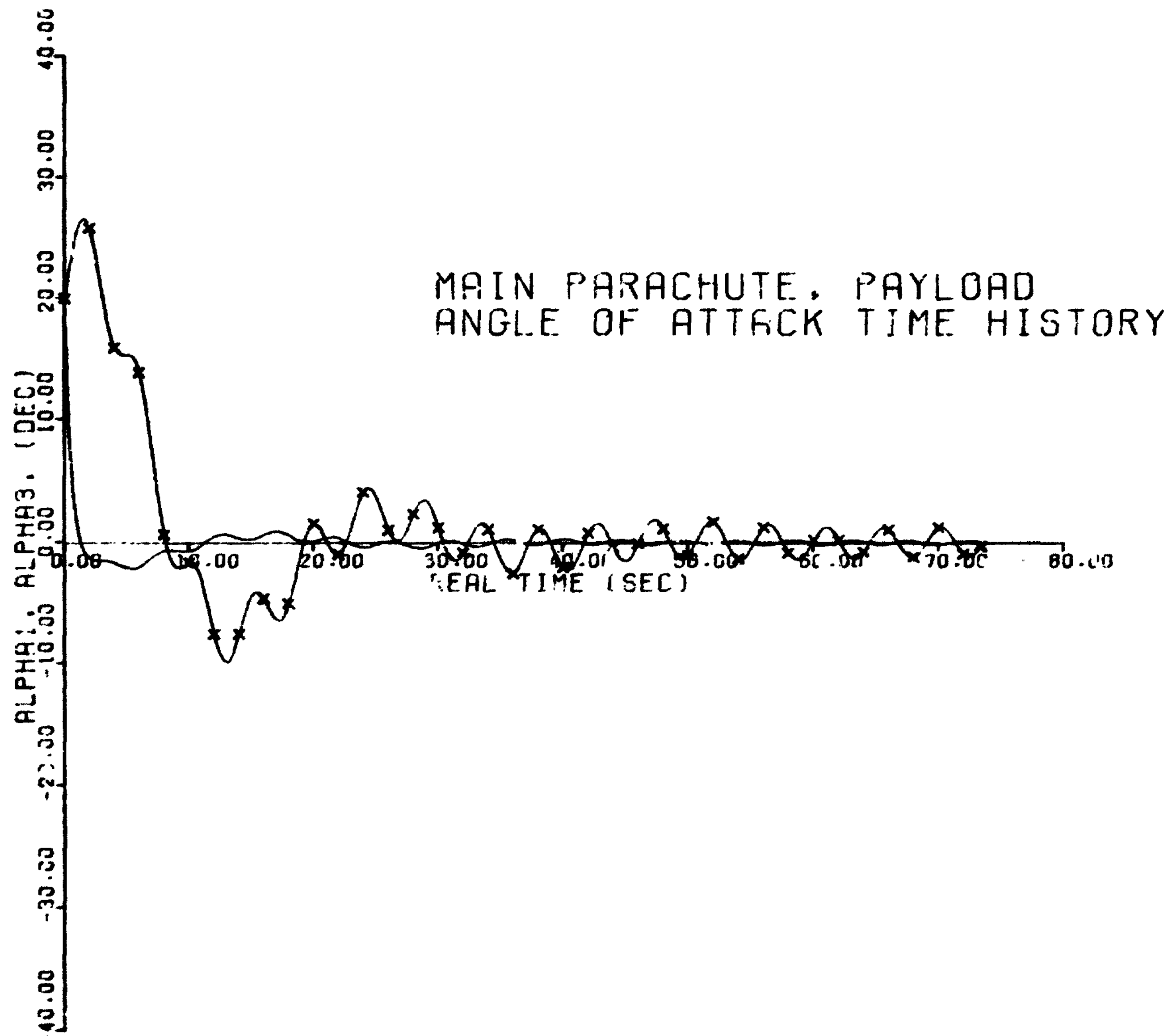

Figure 19. Main Parachute - SRB Angle of Attack Response to a 20-deg Pendulum Disturbance (X-SRB, 2-sec Intervals)

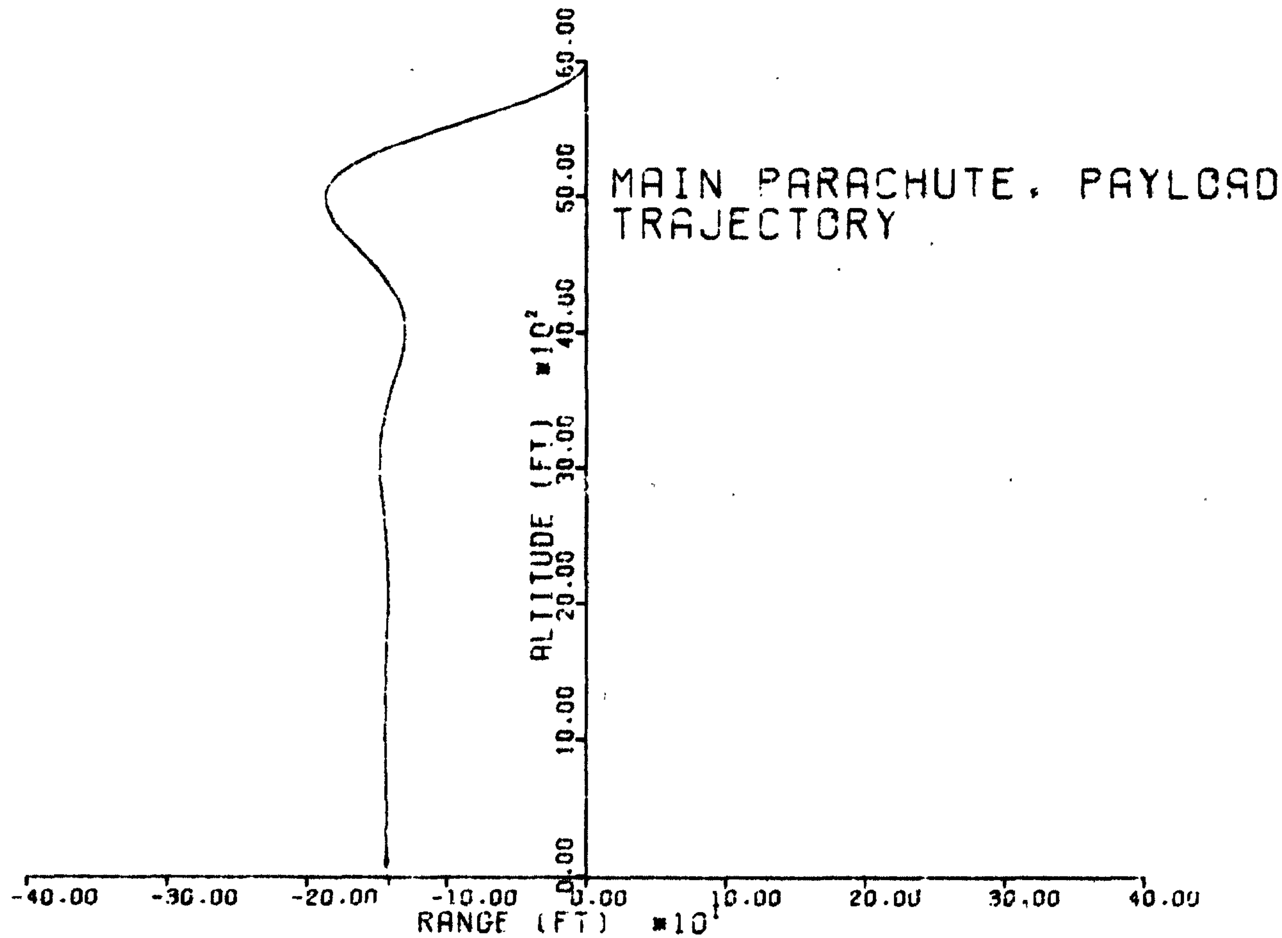

Figure 20. Recovery System Trajectory, Pendulum Initial Conditions

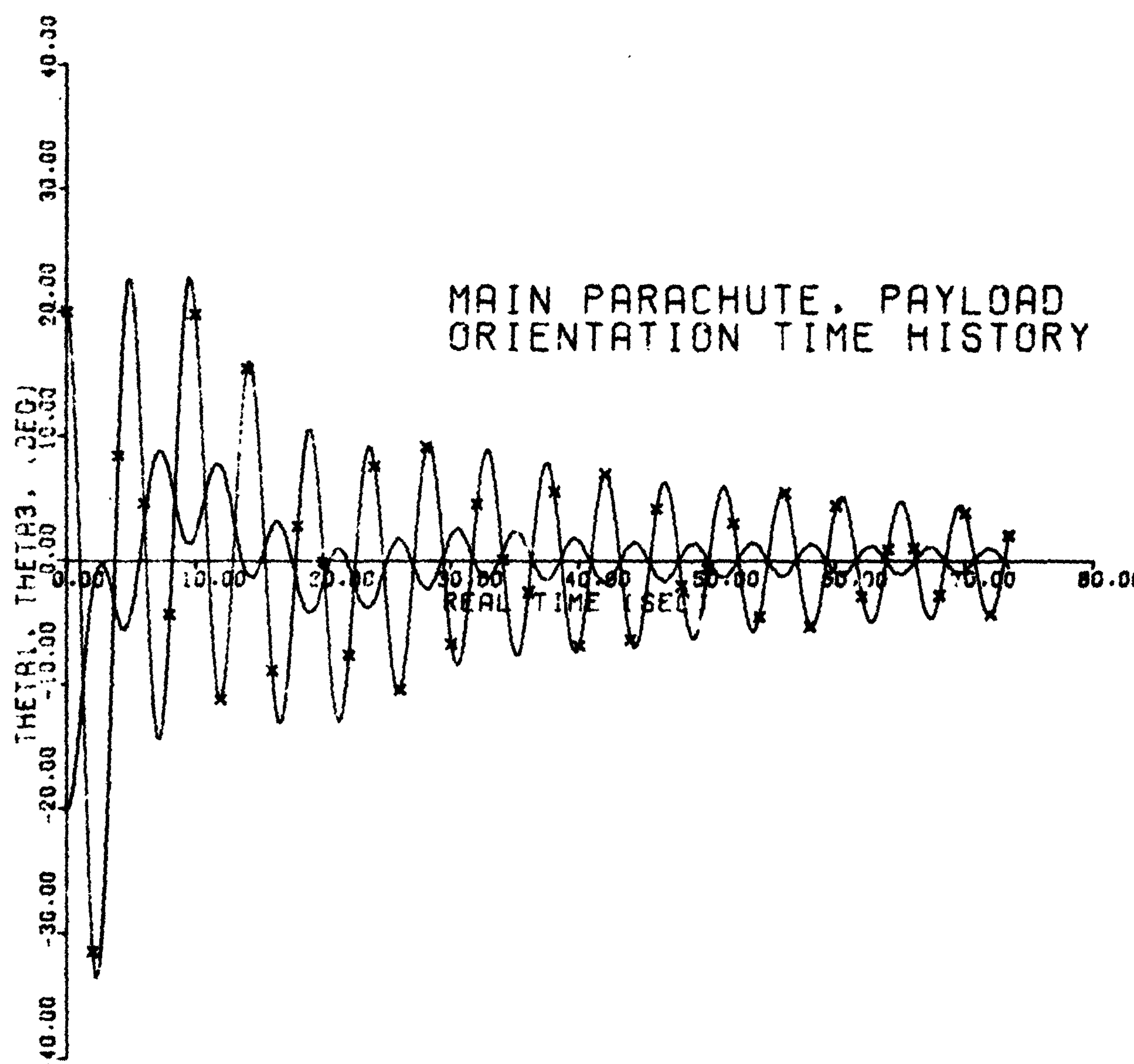

Figure 21. Main Parachute - SRB Response to a Scissors Displacement ($\theta 1 = -20$ deg, $\theta 3 = +20$ deg Initially) (X-SRB, 2-sec Intervals)

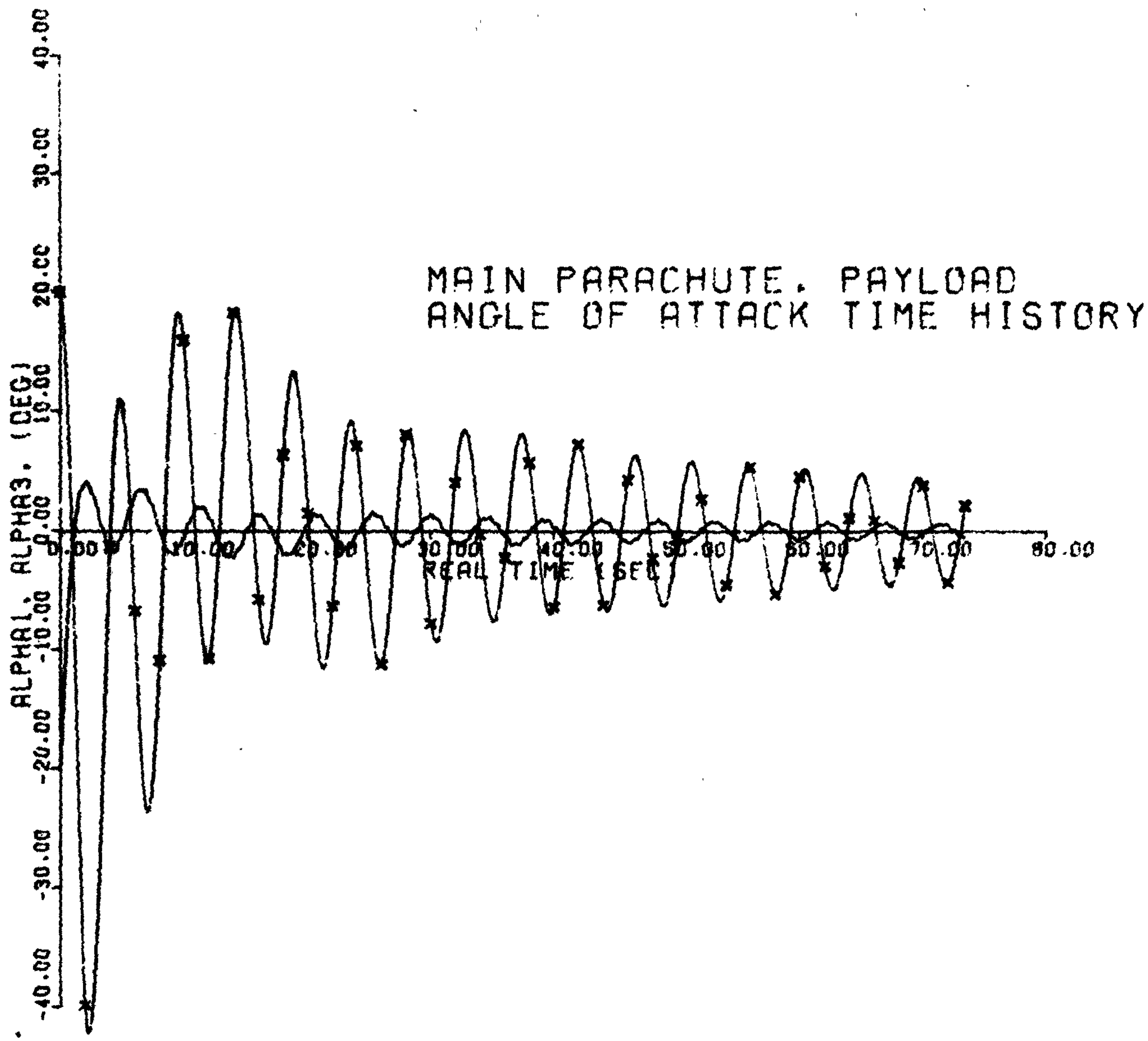

Figure 22. Main Parachute - SRB Angle of Attack Response to Scissors Displacement (θ 1 = -20 deg, θ 3 = +20 deg Initially) (X-SRB, 2 sec Intervals)

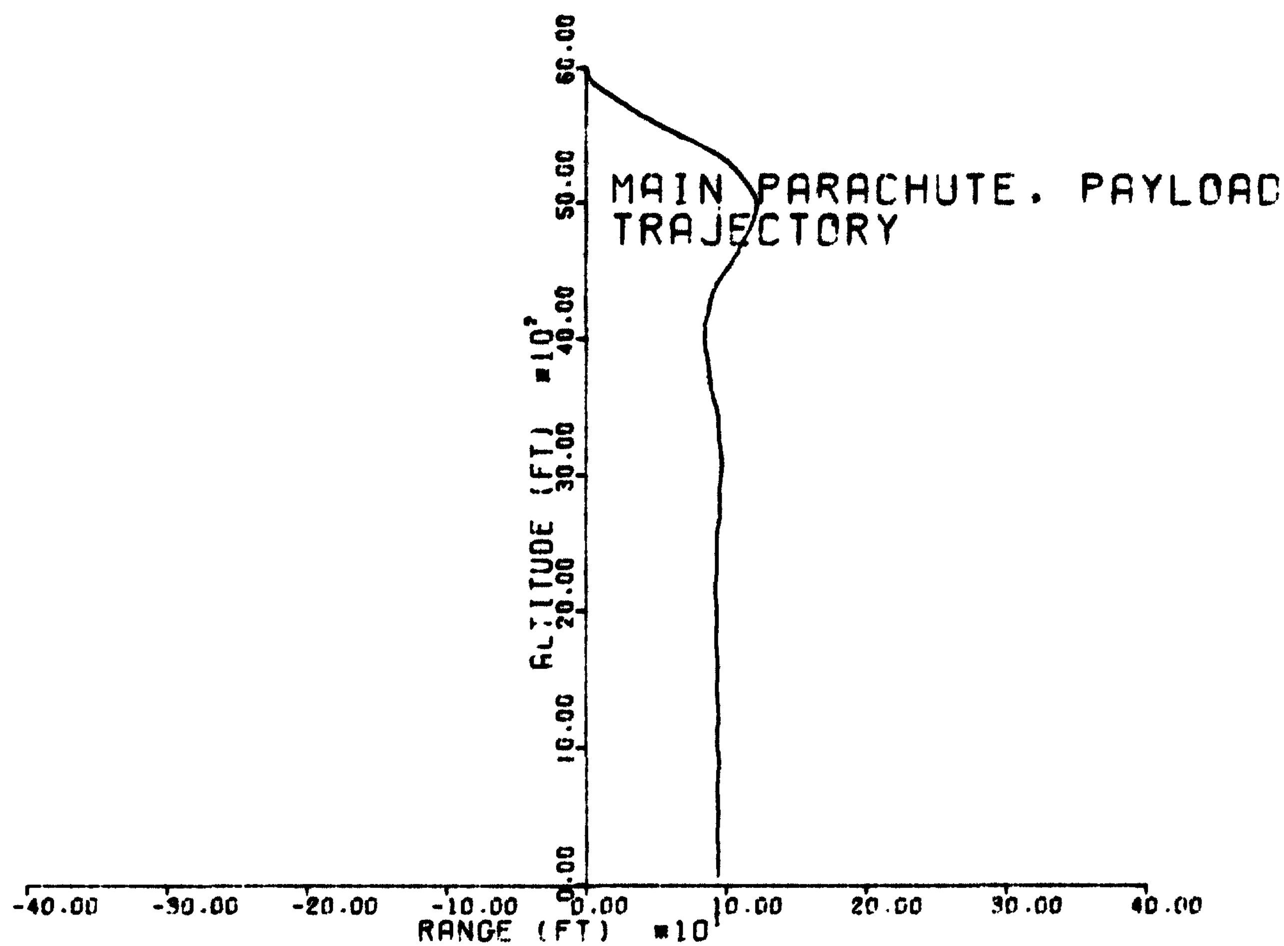

Figure 23. Recovery System Trajectory, Scissors Initial Conditions

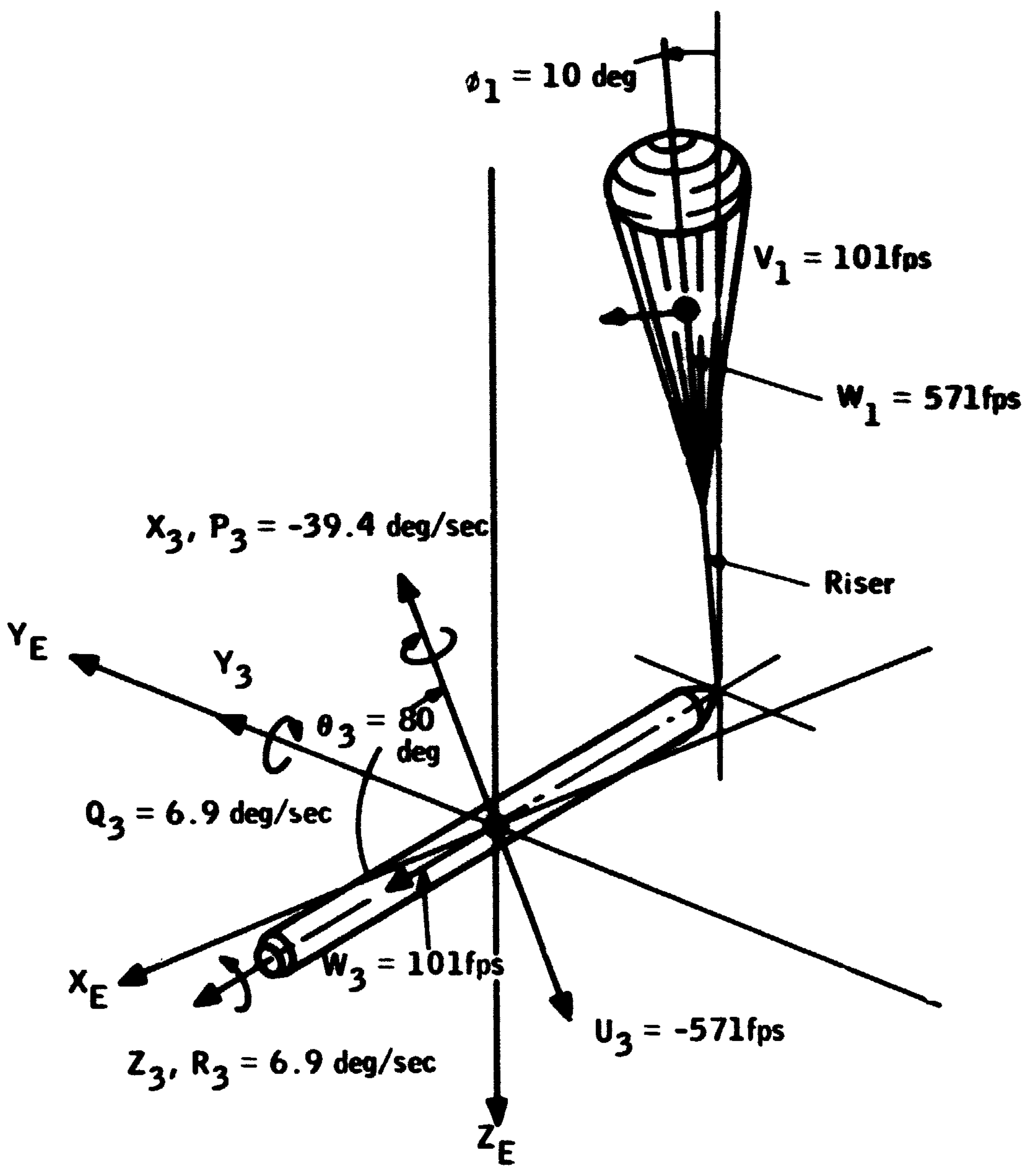

Figure 24. Initial Deployment Conditions for SRB/Drogue Combination

The coning angle is a combination of the Euler angles θ and ϕ

$$\text{cone angle} = \cos^{-1} (\cos \theta \cos \phi)$$

It is the angle between the vertical descent line and the axis of symmetry of the body. The reduction of the SRB cone angle by the action of the drogue parachute is shown in Figure 25. The angle of attack time histories of the parachute and SRB are shown in Figure 26.

Additional Effects Due to a Steady Wind and Gusts

The application of an air mass velocity profile (mean wind plus gusts) as shown in Figure 27 to the descending SRB/Main parachute configuration, which is previously undisturbed, causes a rapid increase in the downrange velocity of the entire system. Figure 28 shows the Euler angle, theta, time history of the parachute, and SRB whose initial conditions were vertical descent. For the same case Figure 29 shows the angle of attack time history. The initial large positive angle of attack produces large normal aerodynamic forces on the parachute. The parachute swings to a large negative orientation angle. The SRB, with a shorter period, being driven by the motion of the parachute, again follows. The parachute angle of attack quickly reduces to small angles while the SRB with far less aerodynamic pitch damping requires more time to stabilize and damp its angle of attack.

Pendulum Initial Conditions -- Since the parachute is the driving force in the motion of the recovery system, its orientation initially with respect to a nonsteady air mass dictates the system response. Figure 30 depicts the Euler angle theta, time history for the SRB/Main parachute recovery system tipped down wind at -20 deg. The SRB and parachute orientation angles respond quickly to gusts at 15 sec and 45 sec. The overall response in the nonsteady air mass is stable. The angle of attack time history for the down wind pendulum case is shown as Figure 31. The gust can easily be seen as large sudden changes in the angle of attack. The SRB angle of attack decreases near the ground as the air mass velocity field slows down in the boundary layer effect.

A trajectory typical of all cases run with nonsteady air mass is shown in Figure 32.

If the parachute and SRB in a pendulum displacement mode are tipped into the wind, the response, although similar to the pendulum displacement downwind, is more dramatic. The increased angular excursions for a case tipped +20 deg is seen in Figure 33. Similarly, while the characteristic shape of the angle of attack time history for pendulum initial conditions is evident, the increased amplitudes for the system tipped into the wind initially are evident in Figure 34.

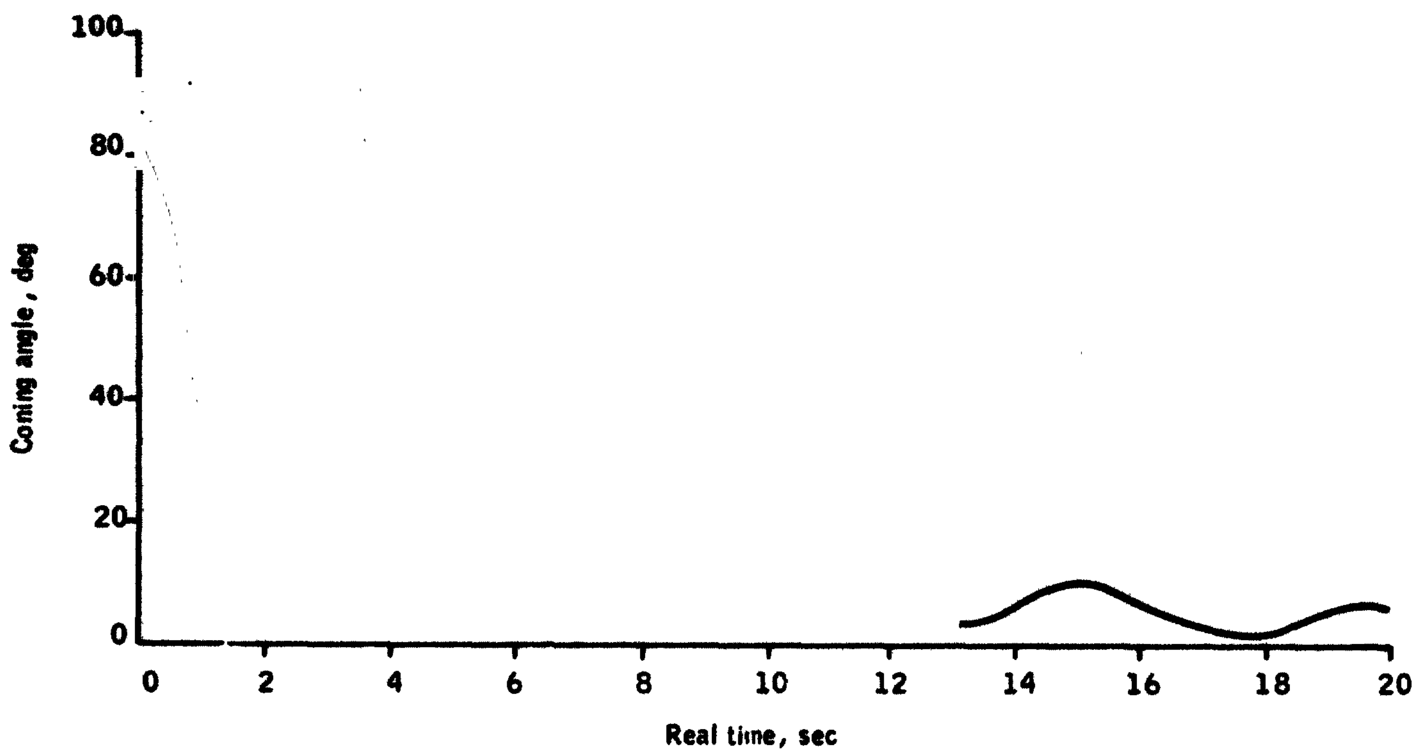

Figure 25. SRB Coning Angle as Reduced by the Action of the Drogue Parachute

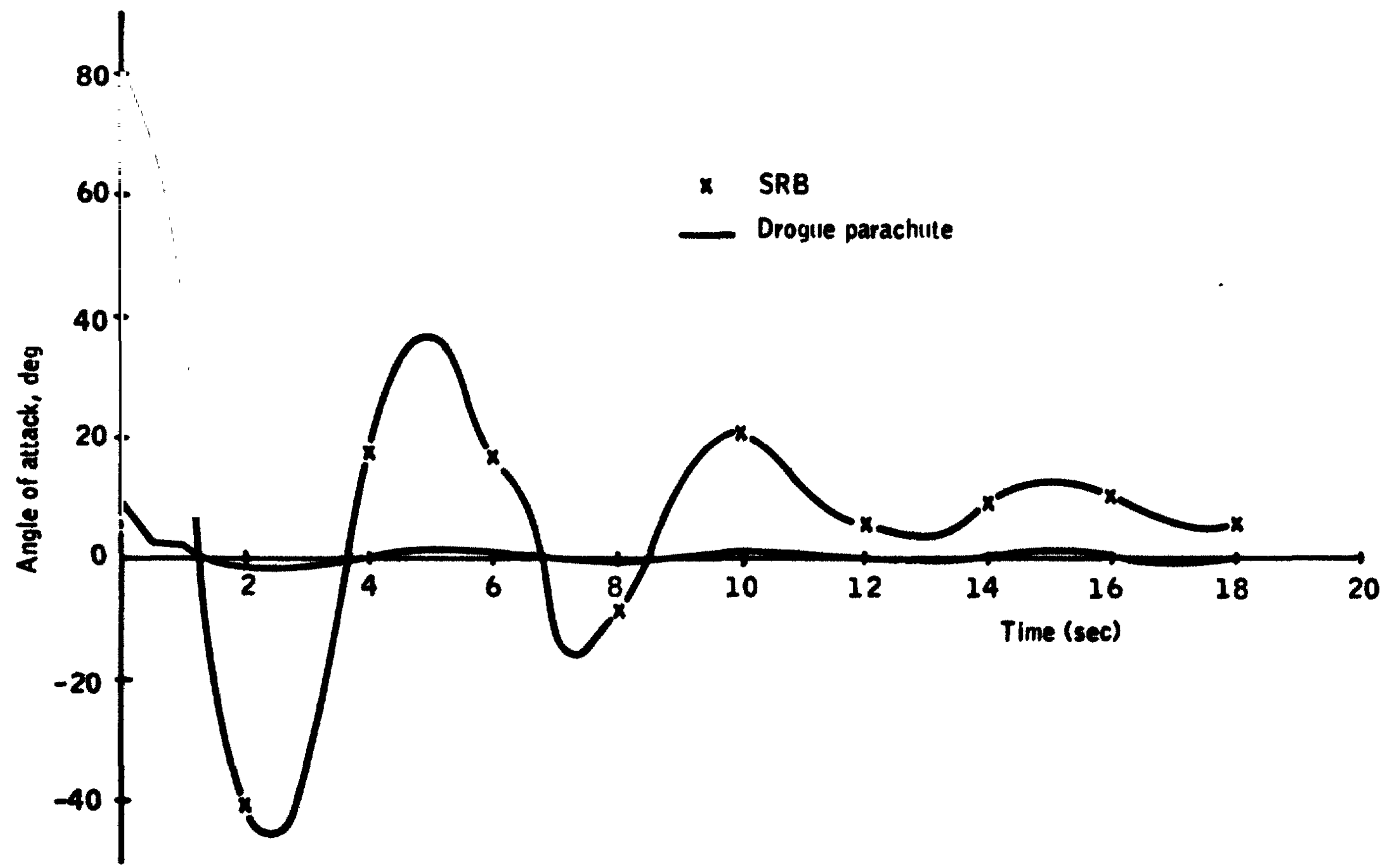

Figure 26. Drogue Parachute/SRB Angle of Attack Response to Initial Conditions Illustrated in Figure 24

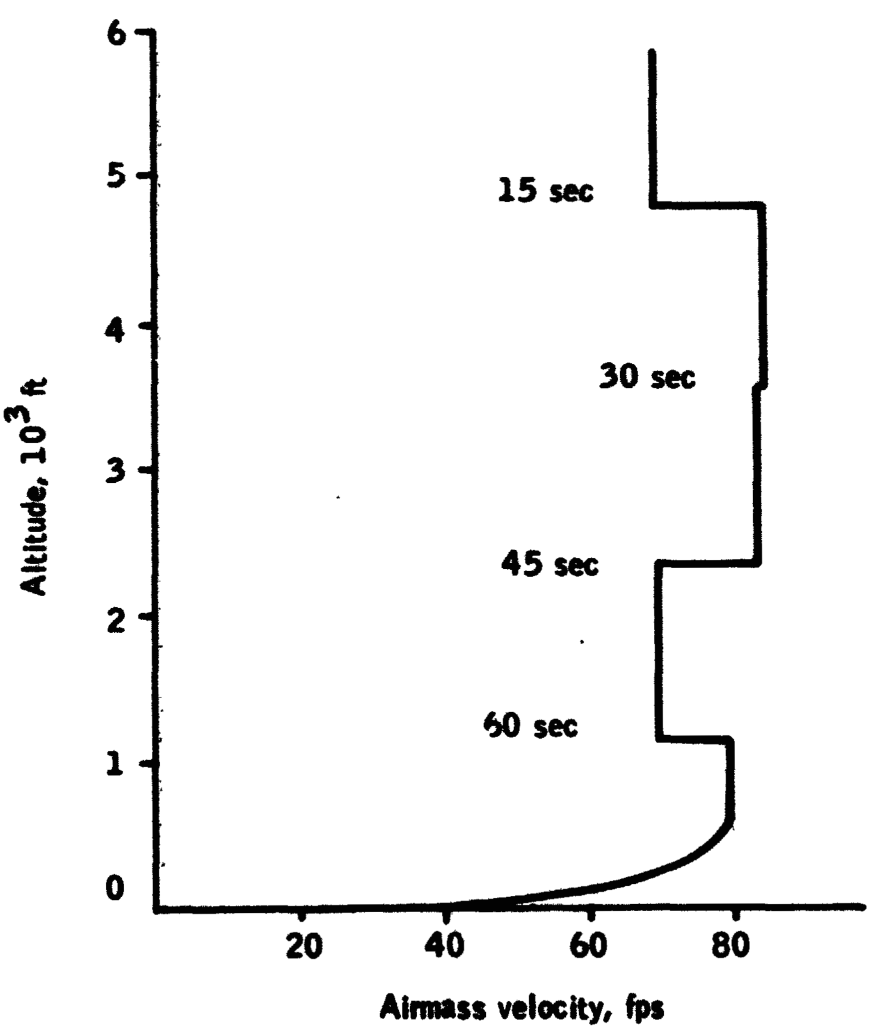

Figure 27. Airmass Velocity Profile

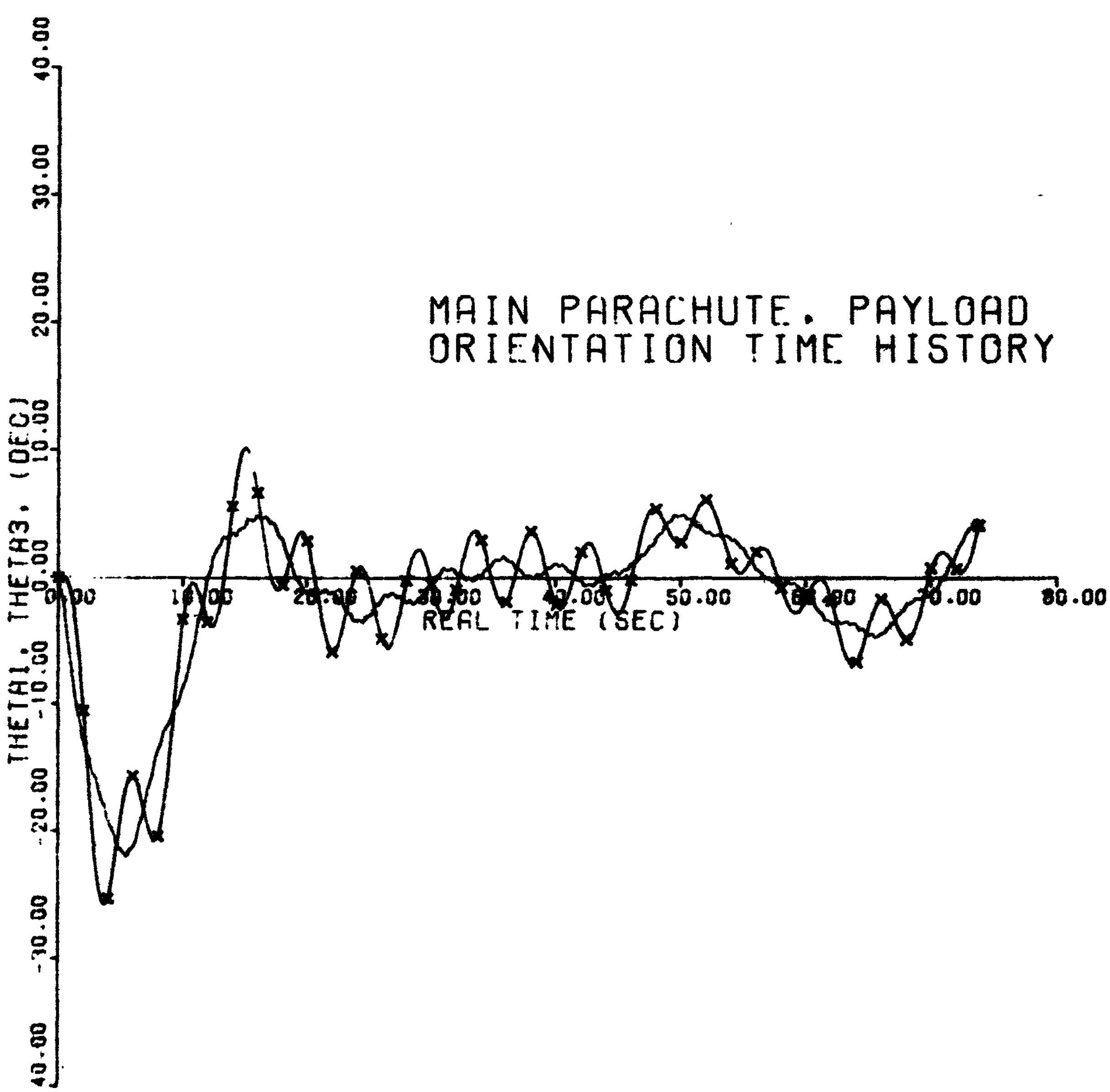

Figure 28. Main Parachute - SRB Response to Non Steady Air Mass; Vertical Descent Initial Conditions (X-SRB, 2-sec Intervals)

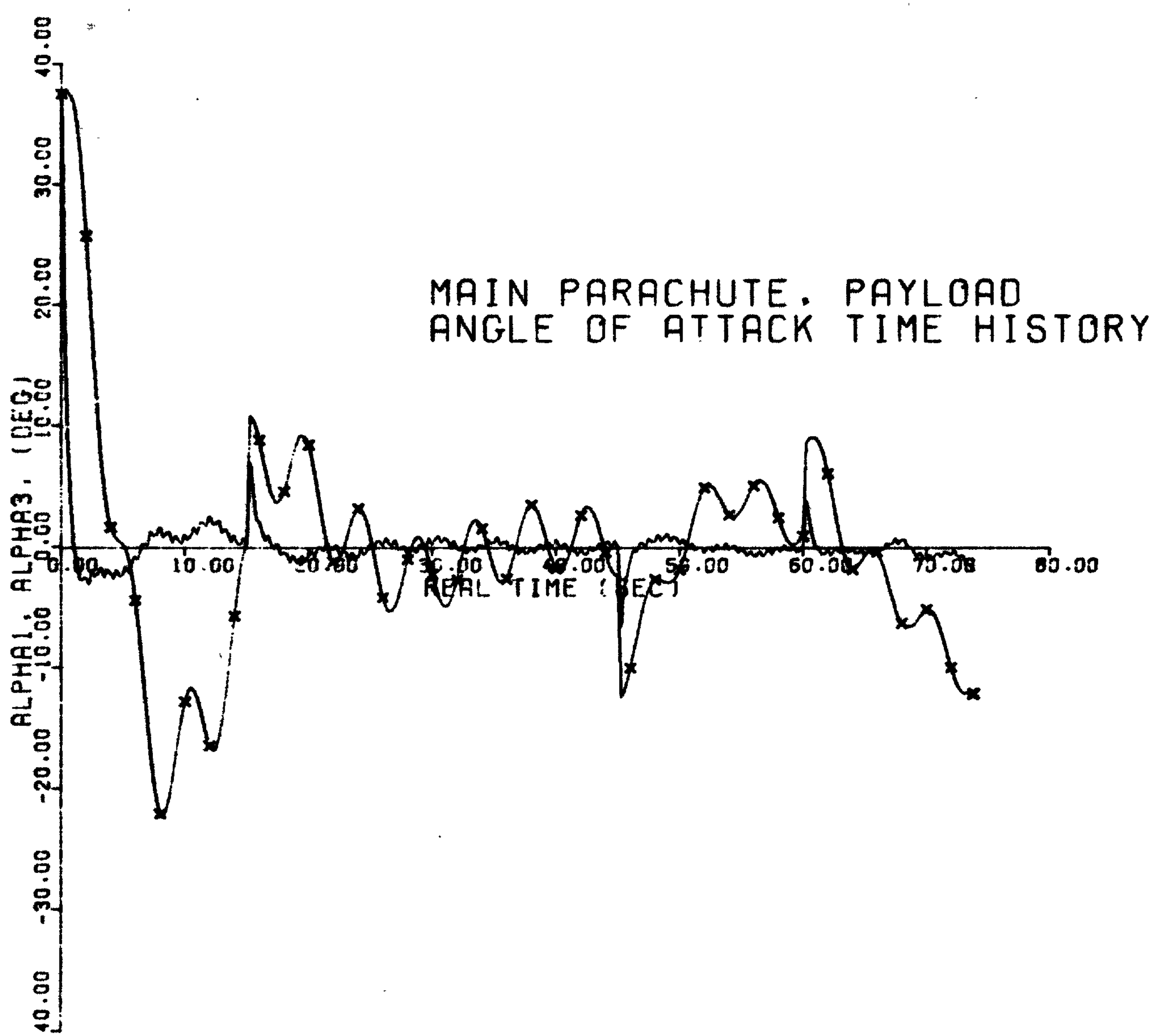

Figure 29. Main Parachute - SRB Angle of Attack Response to a Non Steady Air Mass (X-SRB, 2-sec Intervals)

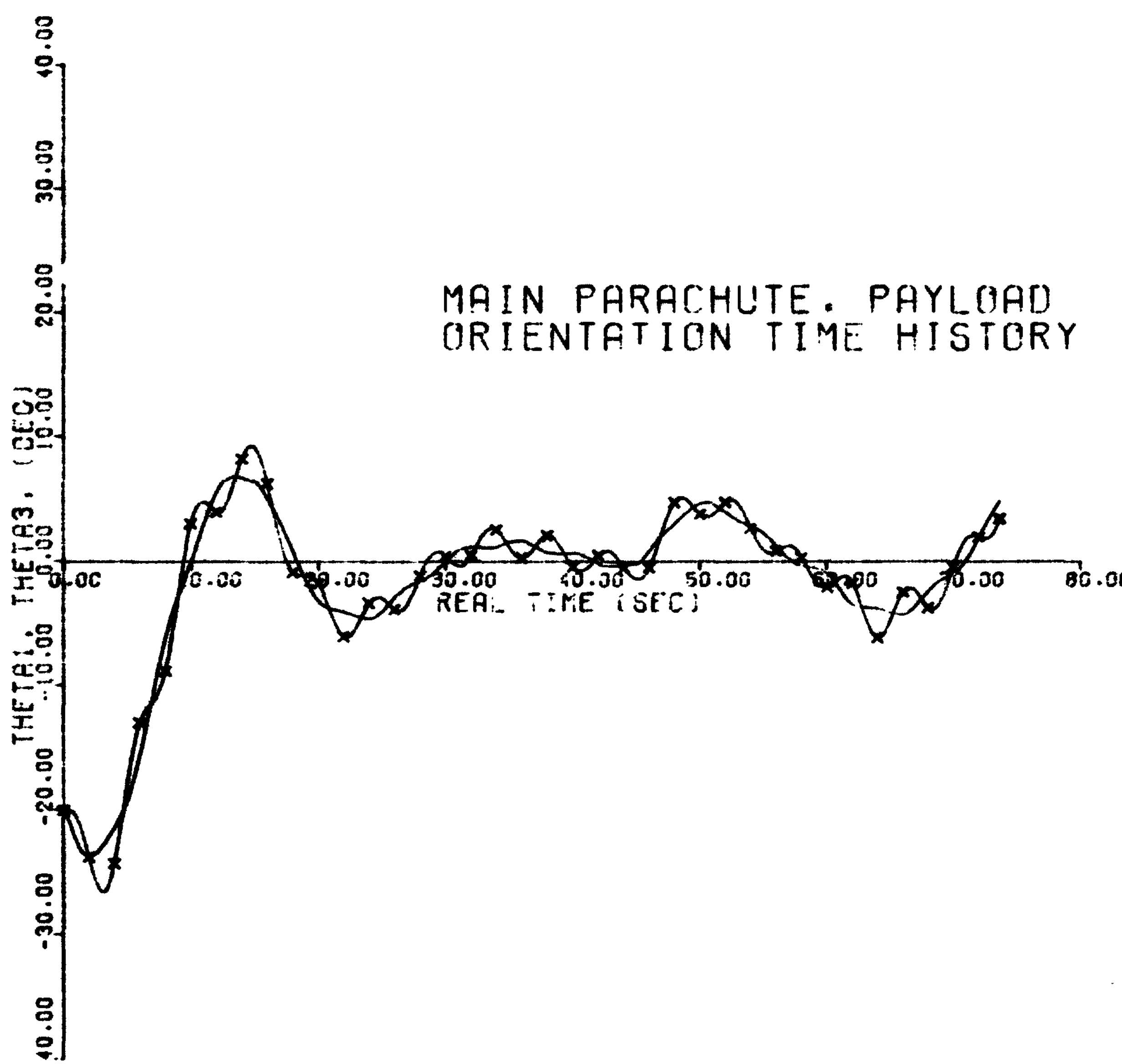

Figure 30. Main Parachute - SRB Response to a Downwind Pendulum Initial Condition in a Non Steady Air Mass (X-SRB, 2-sec Intervals)

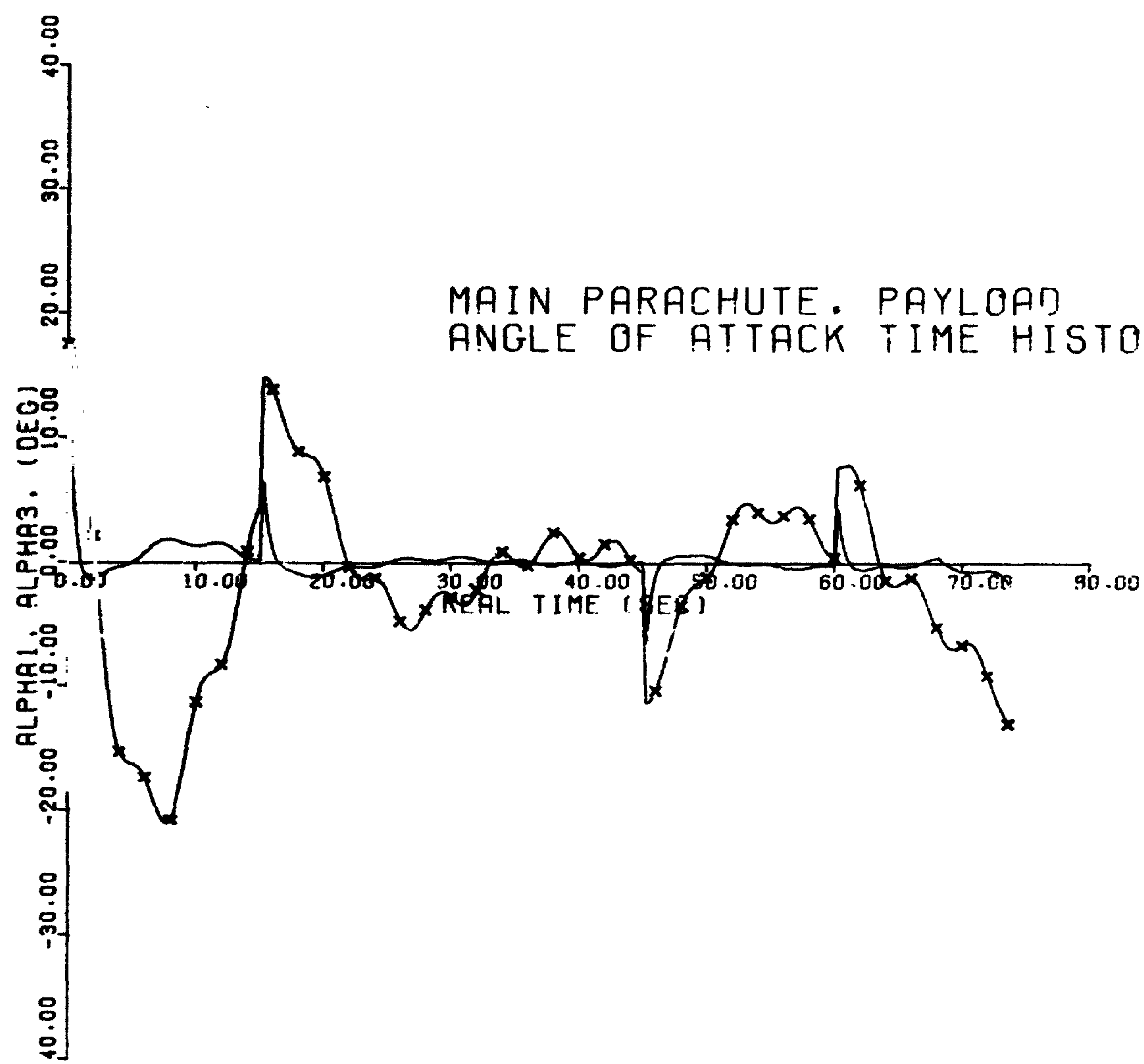

Figure 31. Main Parachute - SRB Angle of Attack Response to a Downwind Pendulum Initial Condition in a Non Steady Air Mass (X-SRB, 2-sec Intervals)

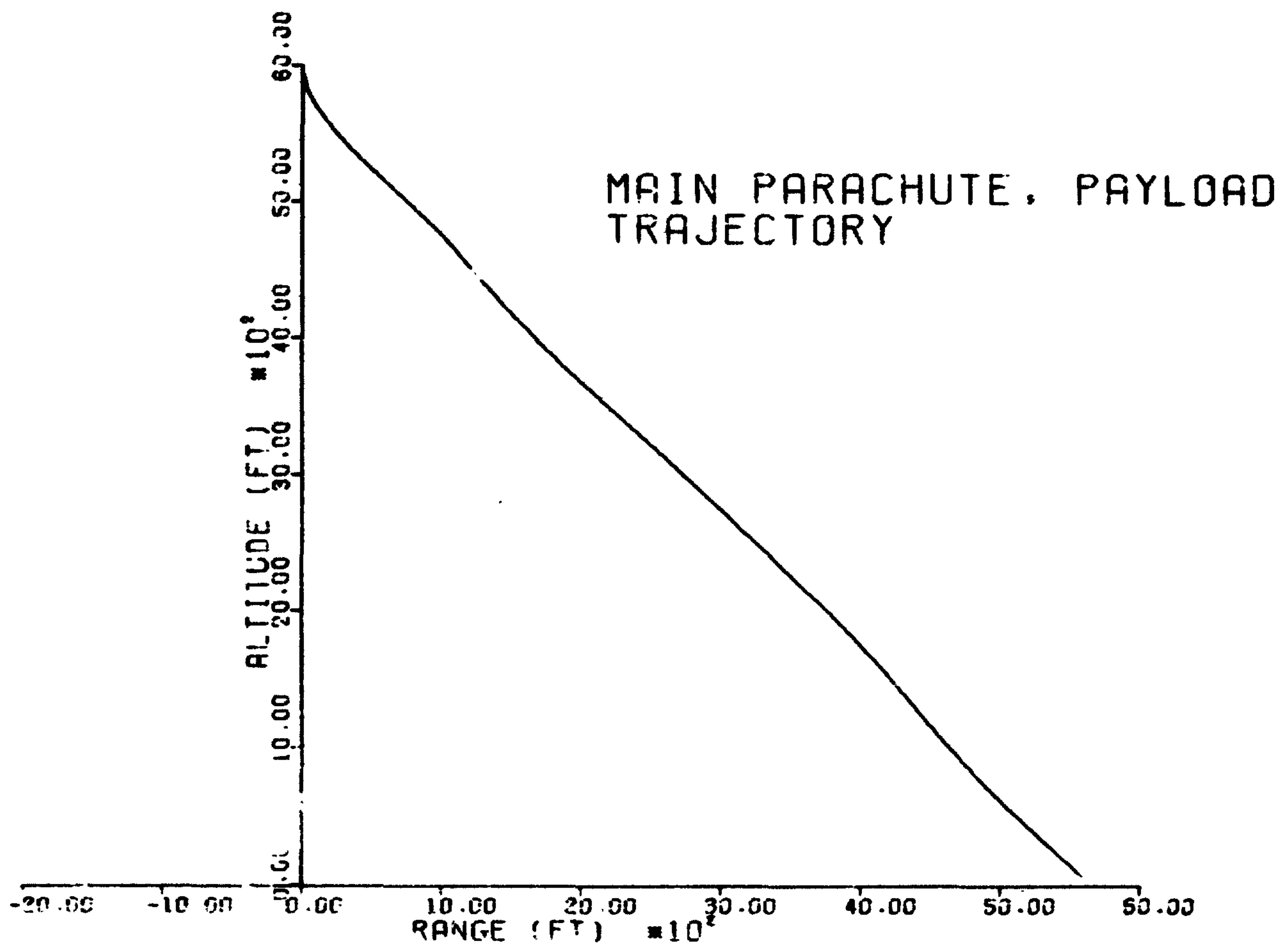

Figure 32. Recovery System Trajectory in a Non Steady Air Mass

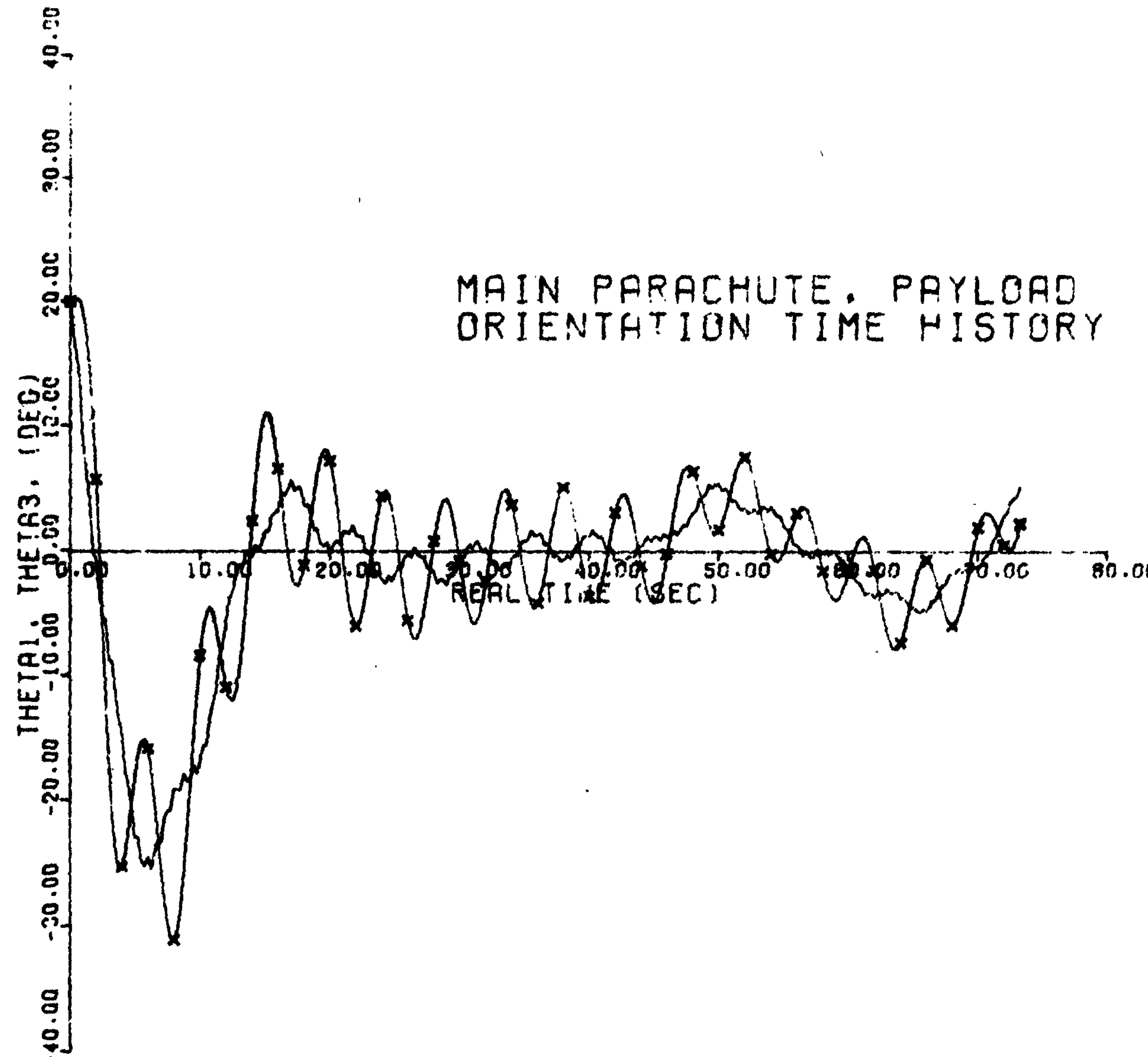

Figure 33. Main Parachute - SRB Response to an Upwind Pendulum Initial Condition in a Non Steady Air Mass (X-SRB, 2-sec Intervals)

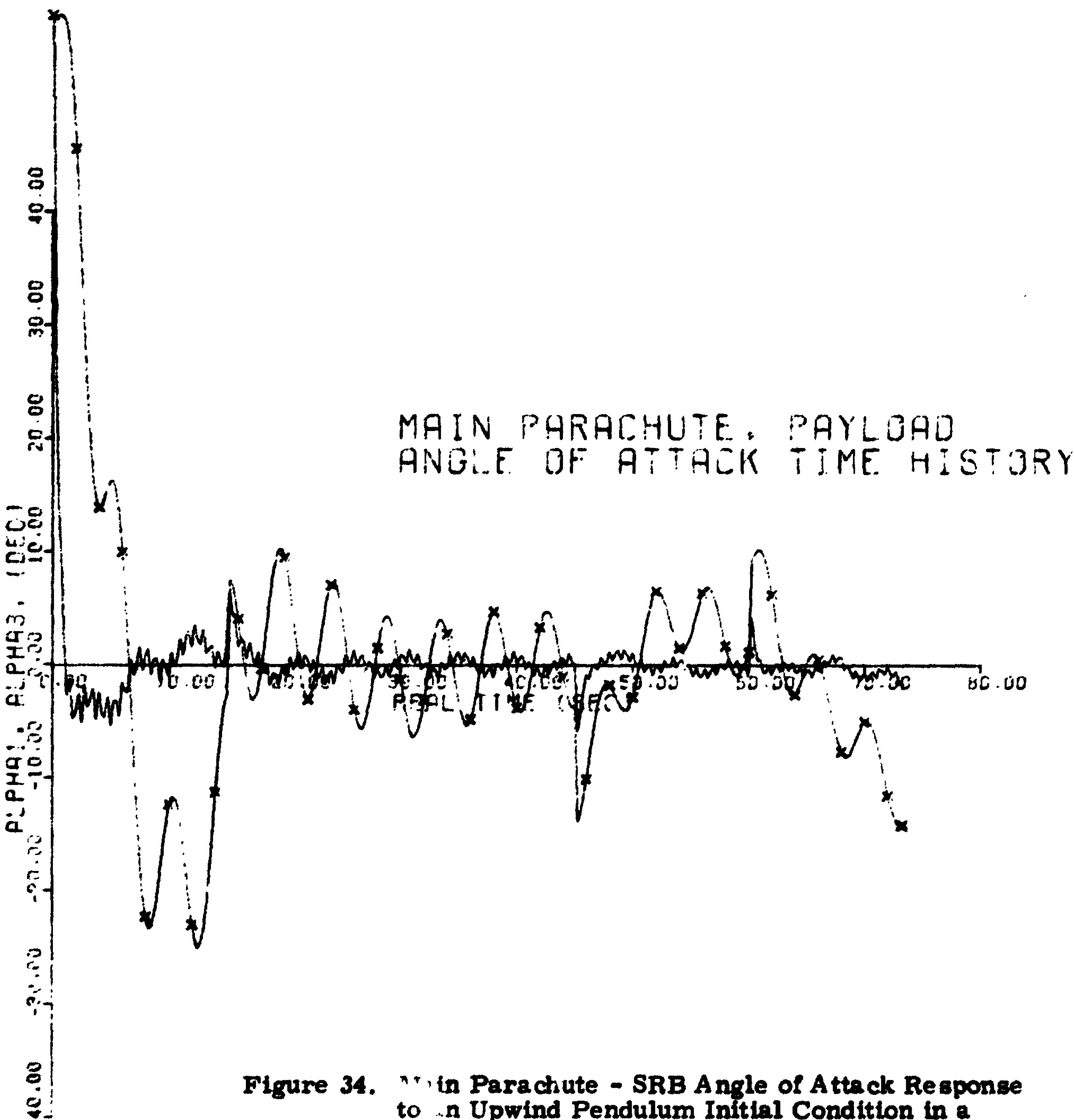

Figure 34. Main Parachute - SRB Angle of Attack Response to an Upwind Pendulum Initial Condition in a Non Steady Air Mass (X-SRB, 2-sec Intervals)

Scissors Initial Conditions -- As seen in Figure 21 the scissor mode initial conditions result in larger amplitude SRB oscillation. The application of an altitude-air mass velocity profile as in Figure 27 to scissors mode initial conditions of the SRB/Main parachute primarily causes a down wind drift approximately equal to the wind speed. During the initial transient period when the recovery system is accelerating down wind, large angular excursions of both the parachute and SRB are seen (Figure 35). The SRB angle of attack becomes quite large as seen in Figure 36. The stability of the system is evident at 15 and 45 sec as seen in the angular response (Figure 35) to gust inputs.

Additional Effects Due to Elasticity

The inclusion of the elastic suspension line model in the nonlinear simulation allows the geometry of the system to be dynamically variable. The change in suspension line lengths in particular changes the mass distribution of the parachute slightly; thus, through the change in moments of inertia a slight decrease in the period of the parachute is seen.

In the differentiated constraint [Equation (61)] which includes the elastic suspension system, the velocities and accelerations between the end points of the riser and the confluence point and center of mass location are required. The elastic elements flex at several frequencies depending on the frequencies of the parachute, riser, and SRB oscillations. To calculate the velocities and accelerations required, a numerical method was used to average the lengths over the high-frequency oscillations and then calculate the rates based on a frequency approximately one-half of the SRB natural frequency. This frequency was chosen since the riser force peaks at each local maximum misalignment of the parachute and SRB or at a frequency of one-half the SRB natural frequency.

No significant alteration of the non-elastic response characteristics of the SRB/Parachute combination was seen when the elastic model was employed. This is not unexpected since the variations in the suspension lines and riser lengths are quite small compared to their steady state lengths.

The Euler angle and angle of attack responses of the SRB/Main Parachute combination for pendulum and scissors initial conditions are shown in Figures 37-40.

LINEARIZATION OF THE NOMINAL DESCENT PHASE

The linearization techniques described in Section II were applied to a variety of cases to obtain Root Locus Plots. Using the frozen point spectrum analysis technique as described in Reference 11, the eigenvalue time histories for both pendulum and scissors type initial conditions are shown in Figures

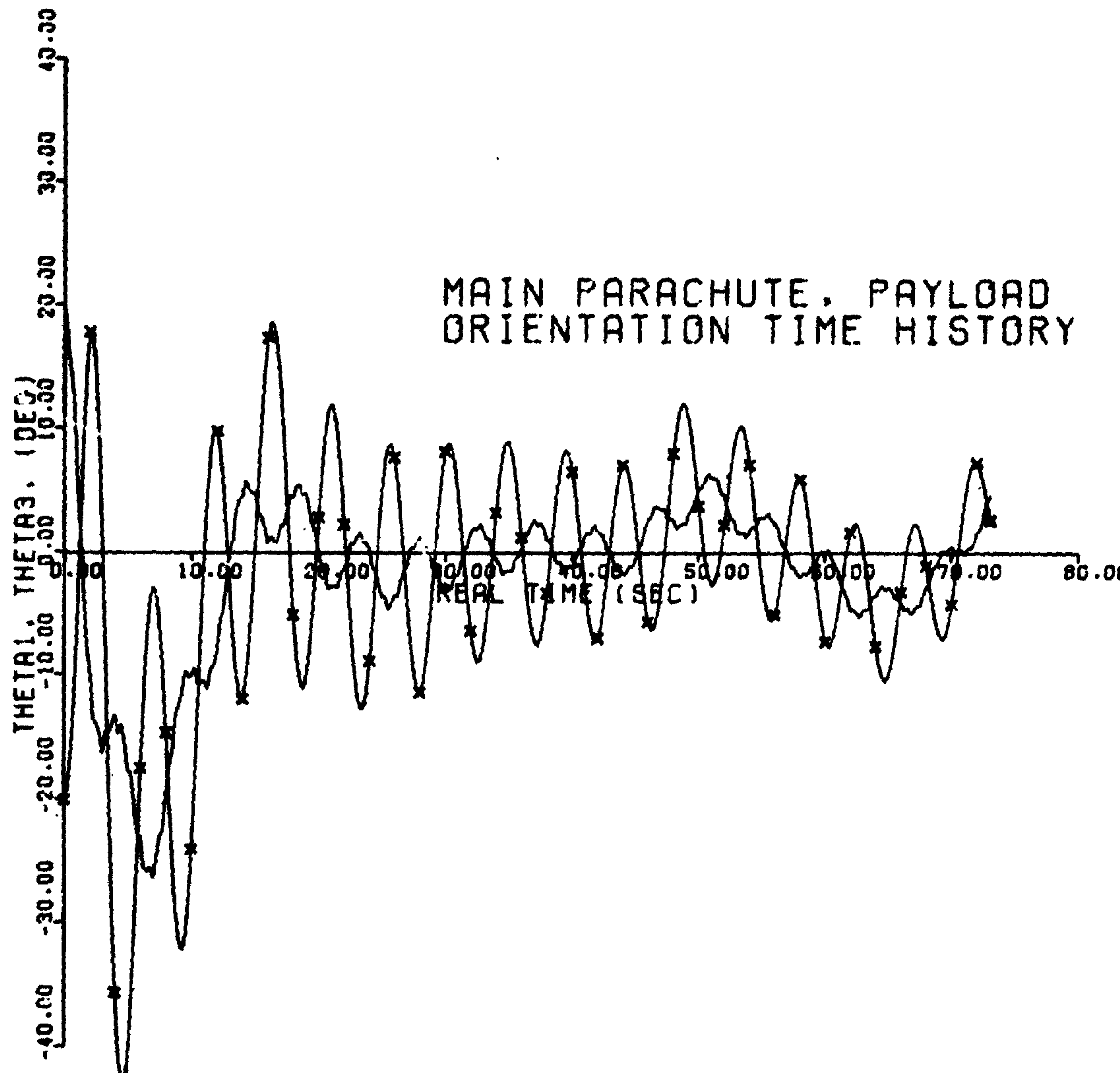

Figure 35. Main Parachute - SRB Response to Scissors Initial Conditions in a Non Steady Air Mass (X-SRB, 2-sec Intervals)

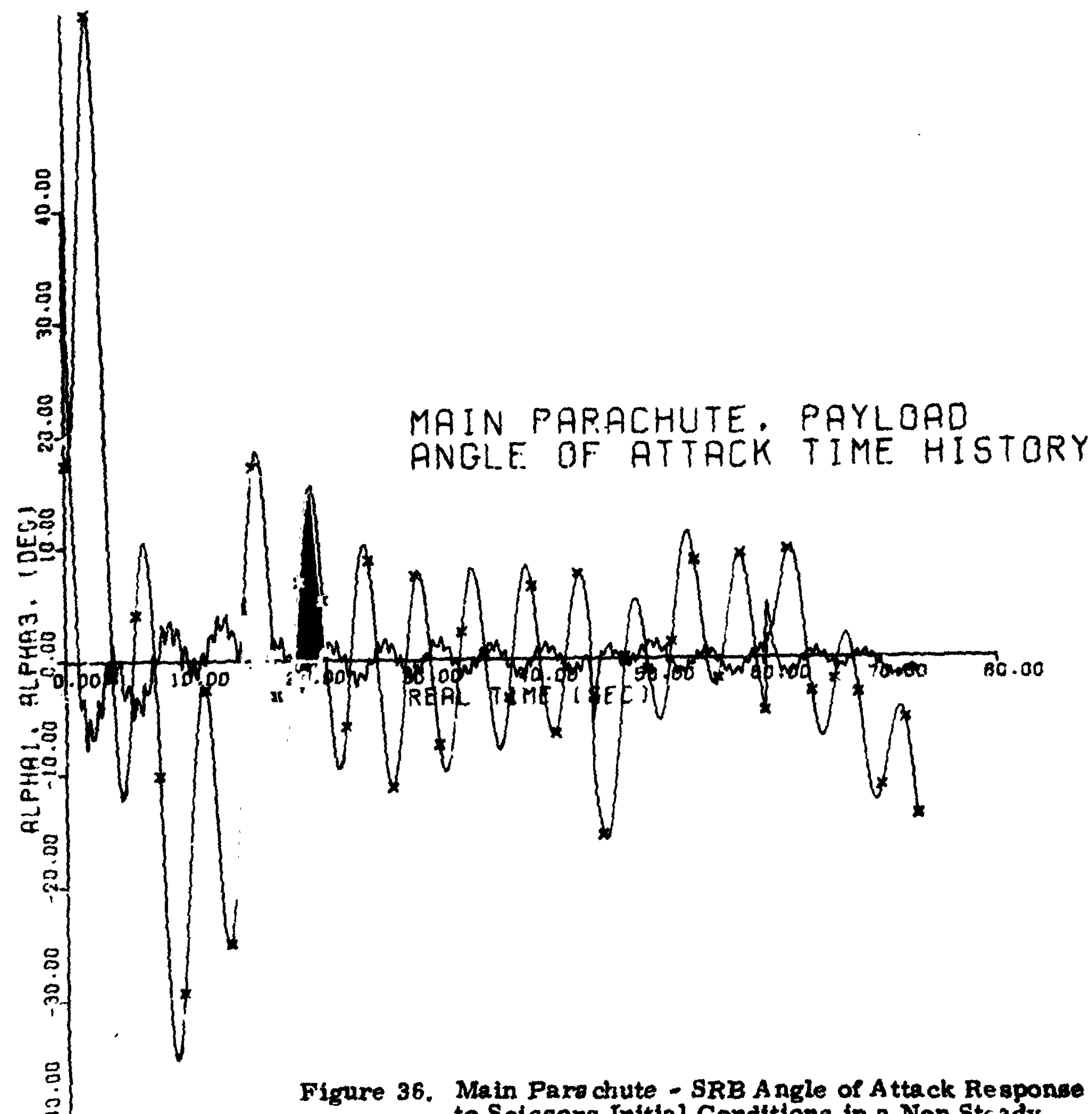

Figure 36. Main Parachute - SRB Angle of Attack Response to Scissors Initial Conditions in a Non Steady Air Mass (X-SRB, 2-sec Intervals)

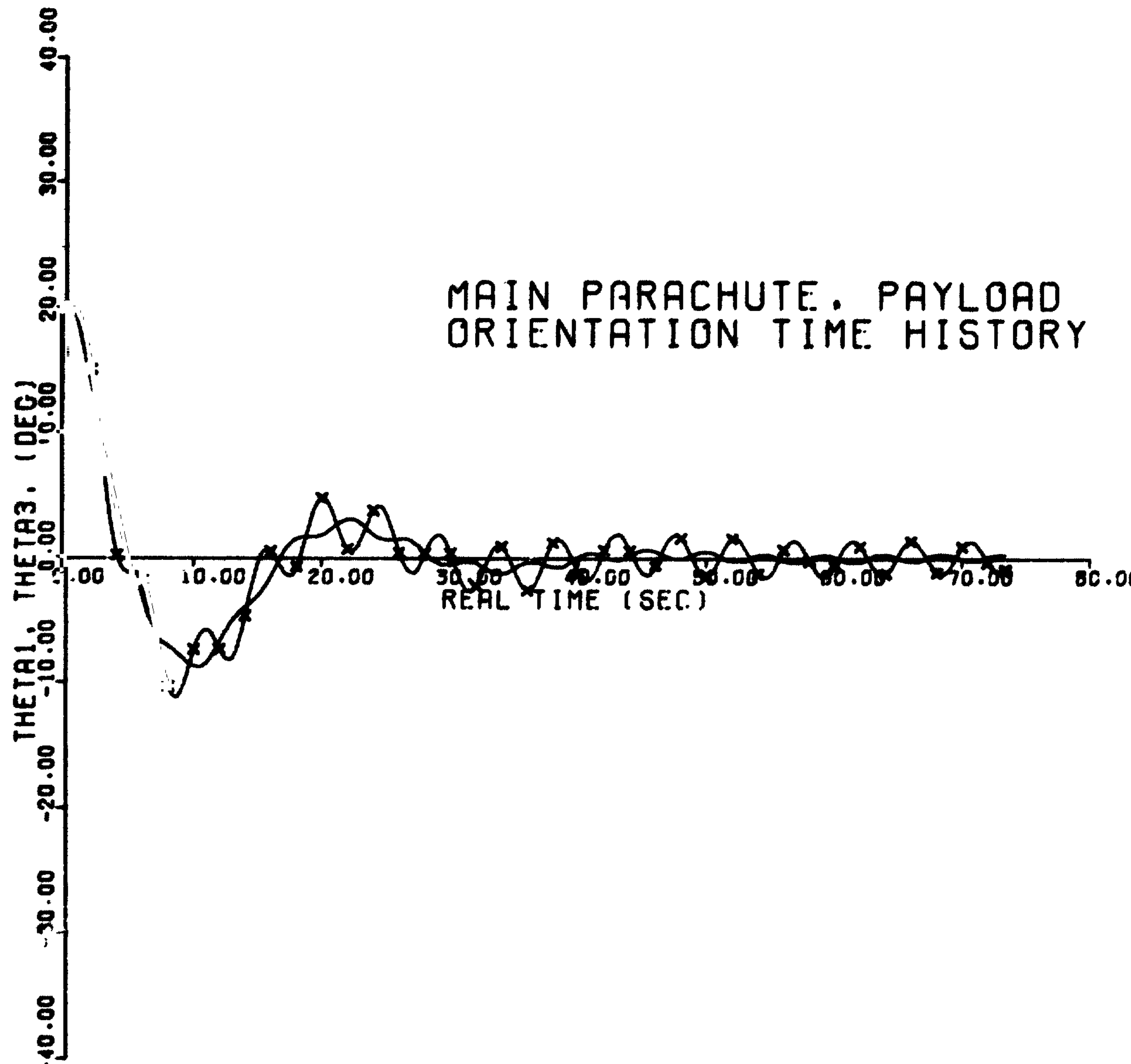

Figure 37. Main Parachute - SRB Response to a 20-deg Pendulum Initial Condition, Elastic Suspension System (X-SRB, 2-sec Intervals)

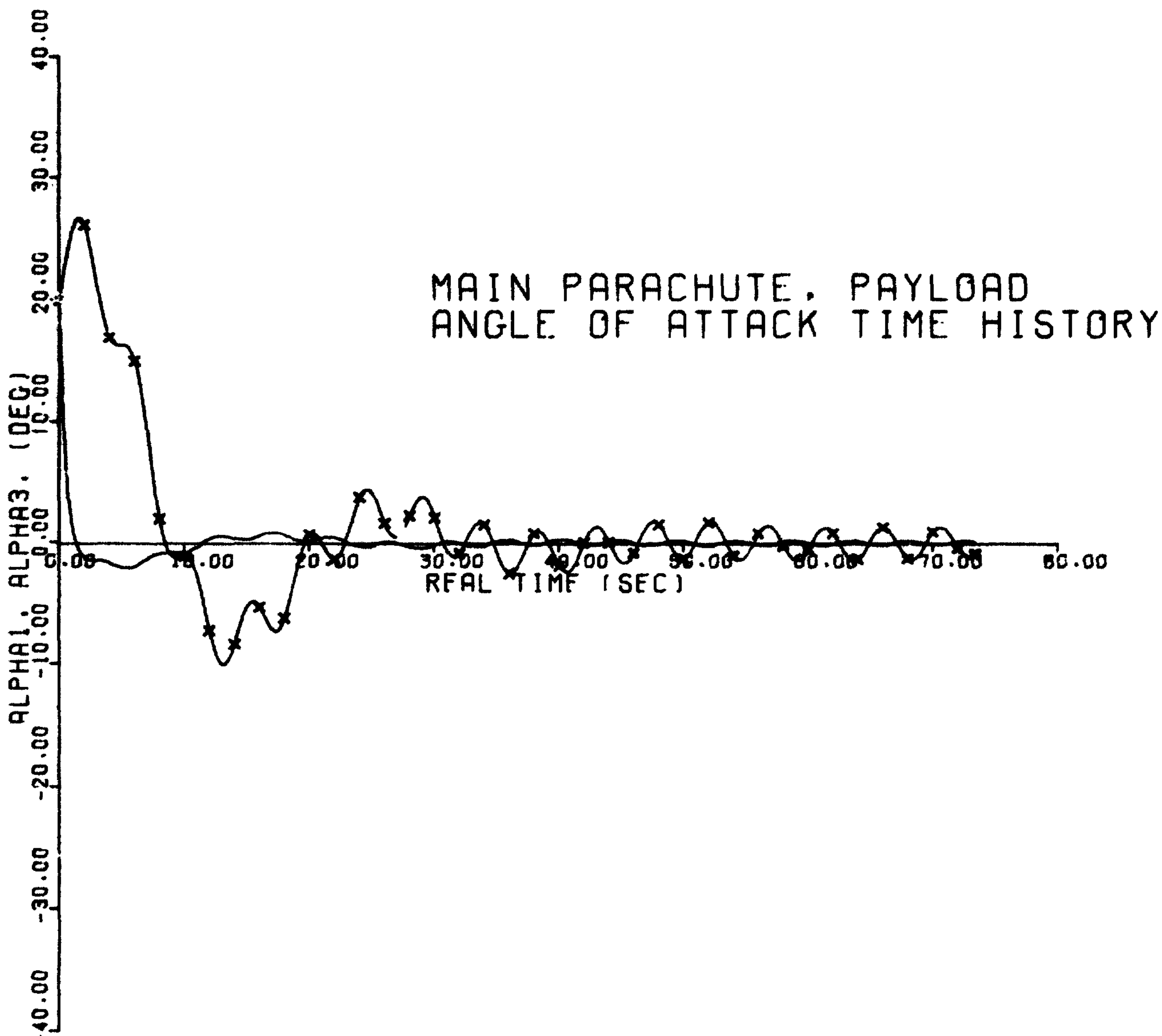

Figure 38. Main Parachute - SRB Angle of Attack Response to a 20-deg Pendulum Initial Condition, Elastic Suspension System (X-SRB, 2-sec Intervals)

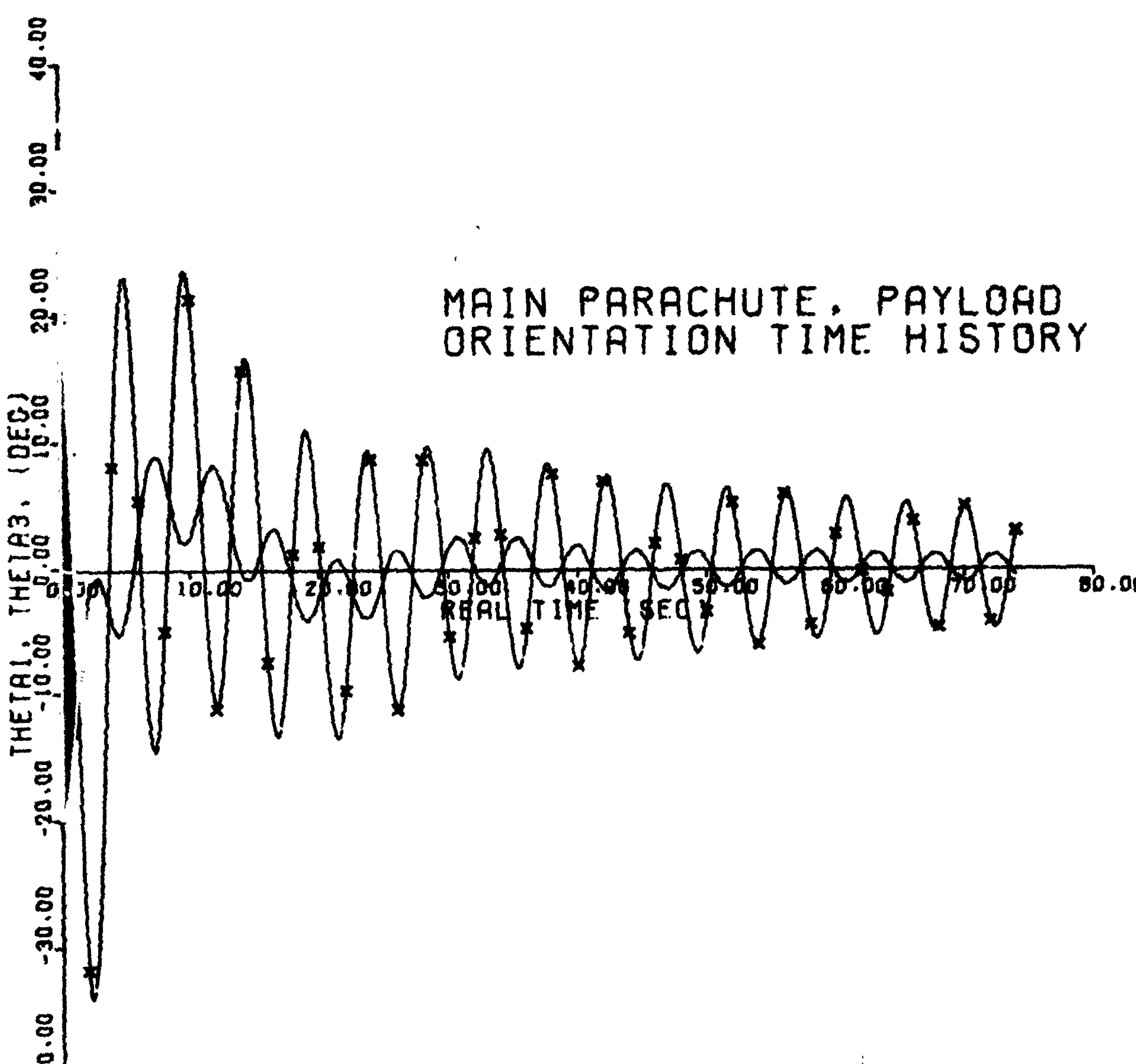

Figure 39. Main Parachute - SRB Response to Scissors Initial Conditions, Elastic Suspension System (θ 1 = -20 deg, θ 3 = +20 deg Initially) (X-SRB, 2-sec Intervals)

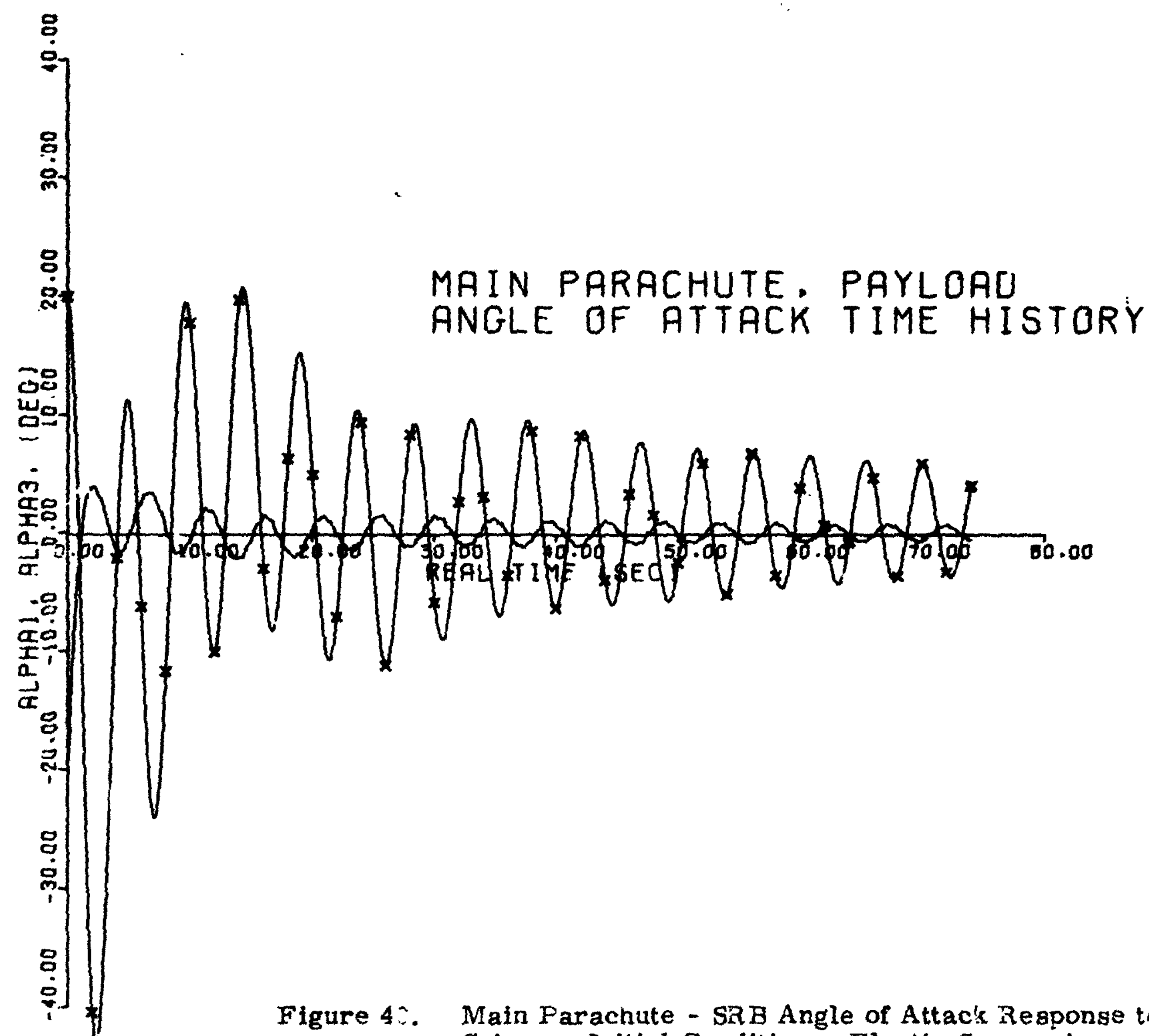

Figure 4[illegible]. Main Parachute - SRB Angle of Attack Response to Scissors Initial Conditions, Elastic Suspension System [θ_1 = - 20 deg, θ_3 = + 20 deg Initially (X-SRB, 2 sec Intervals)]

41 to 44. As expected, the eigenvalues describing the fundamental oscillatory modes cover a wider range for scissors initial conditions before settling to near the eigenvalue resulting from a vertical steady descent. The long period modes (parachute) are stable in all cases. The short period mode describing the riser is stable with very slight damping. The SRB short period mode, while unstable in the initial transient response to large scissors initial conditions, is after a short time stable and damped.

In viewing the eigenvalue time histories, it is important to recall some important features of the linearization technique used.

- The exact nonlinear state of the entire system is the reference state about which the linearization routine works.
- The roots to the characteristic polynomial (the eigenvalues) are determined from manipulation of the matrix of first partial derivatives which is found by applying small disturbances to each of the nonlinear state variables about the reference state.
- The resulting eigenvalues can each be related to a fundamental oscillatory mode of one of the state variables.
- The location of a single eigenvalue in the complex plane represents the local stability characteristics of the state variable it is associated with with respect to the exact nonlinear condition of that state variable from which the eigenvalue was calculated.
- The overall stability of the entire system is a function of the interaction of all the nonlinear motions.

Stability with Respect to Non-Steady Air Mass

Figures 45 to 48 show eigenvalue time histories for the SRB/Main configuration with no initial disturbance and a +20 deg pendulum disturbance. In a non steady air mass the stability of the response indicated by the eigenvalues is demonstrated through the transient response and the first gust at 15 sec.

Stability with Respect to Elasticity

The eigenvalue time histories for the principal oscillatory modes of the SRB/Main Parachute combination with elastic suspension system when a pendulum initial disturbance is applied are shown in Figures 49 and 50.

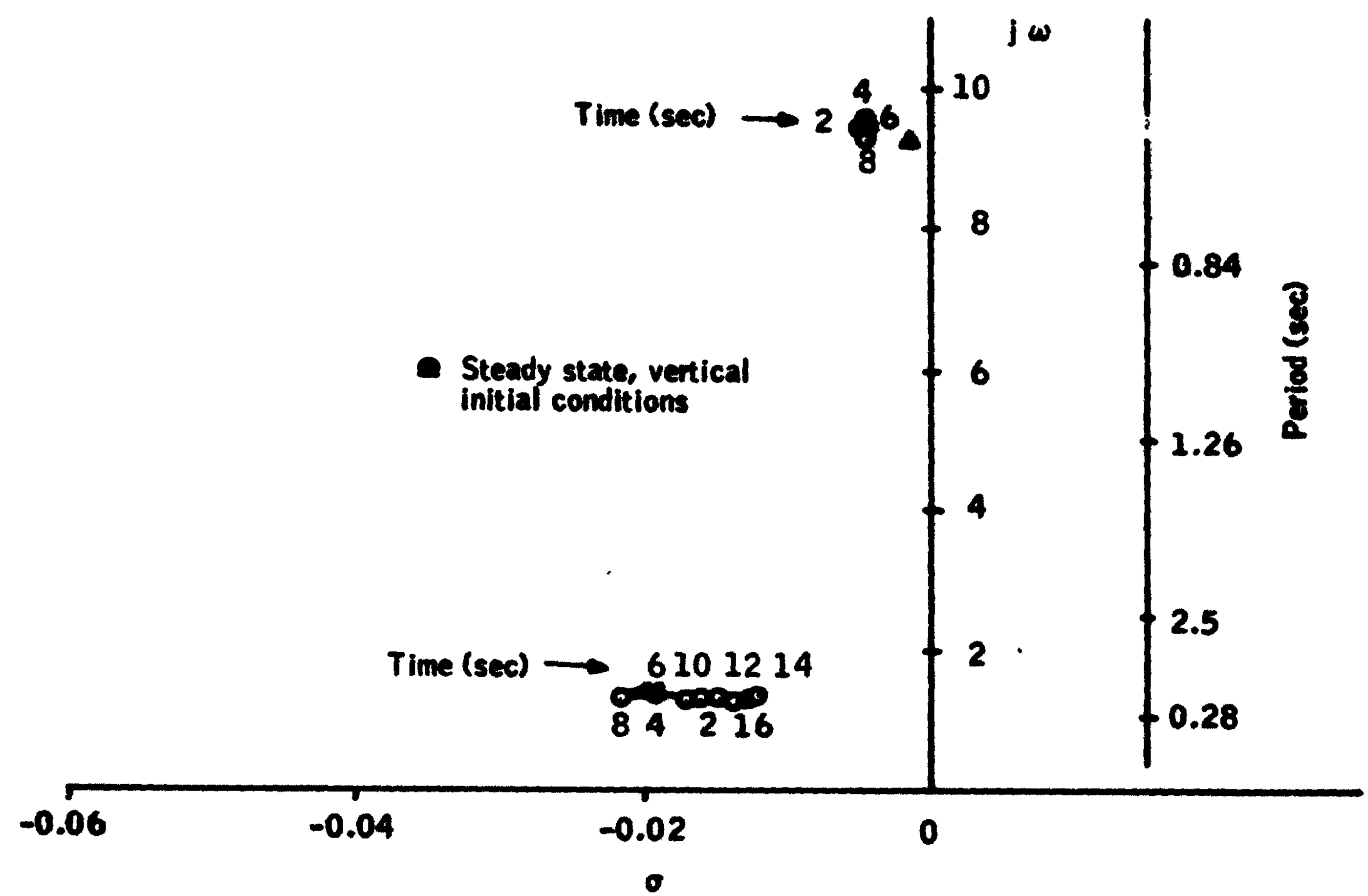

Figure 41. Short Period Eigenvalue Time Histories for the SRB/Main Parachute Configuration, Pendulum Initial Conditions, (θ_1 = +20 deg, θ_3 = +20 deg)

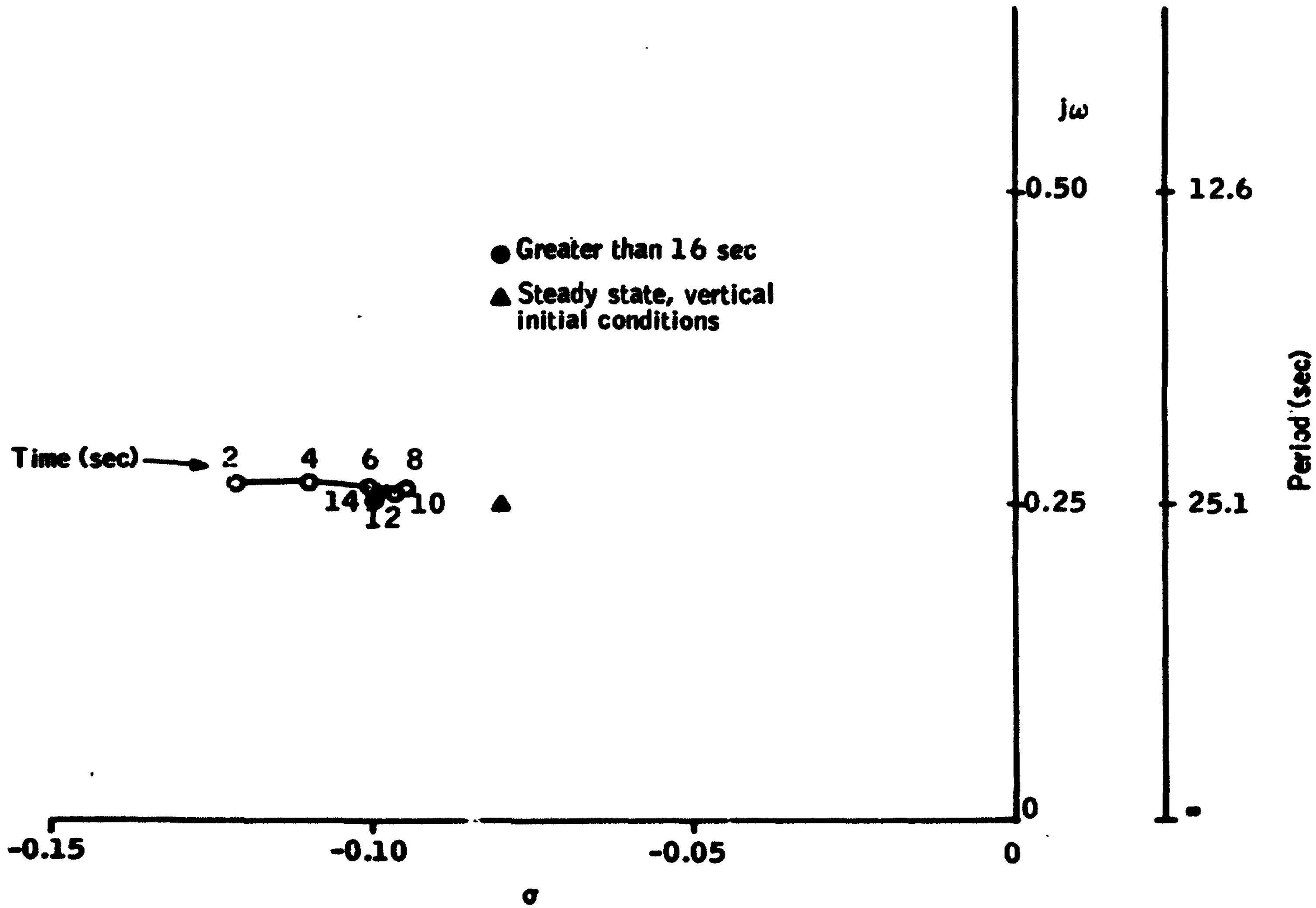

gure 42. Long Period Eigenvalue Time-History for the SRB/ Main Parachute Configuration, Pendulum Initial Conditions (θ_1 = 20 deg, θ_3 = 20 deg)

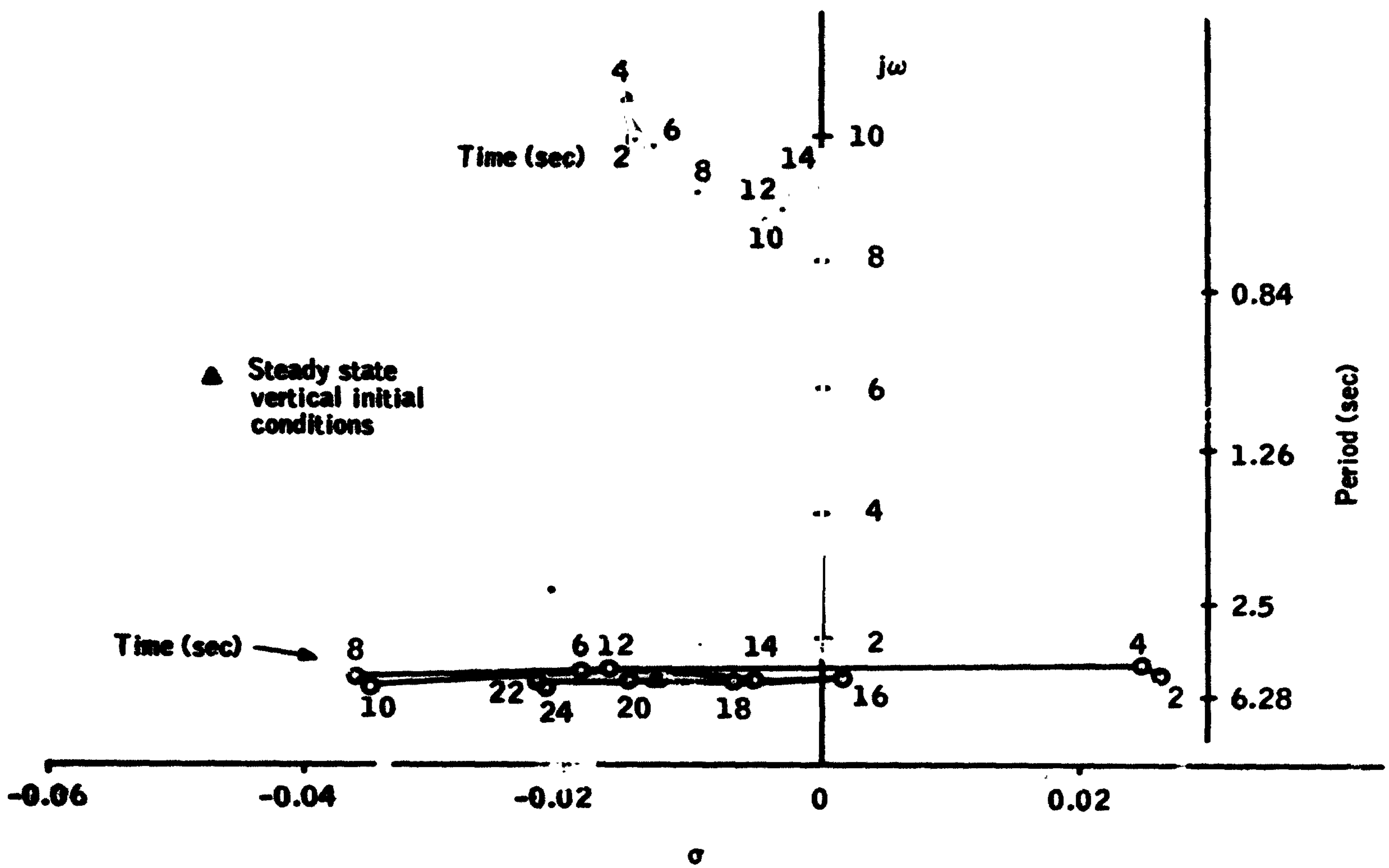

Figure 43. Short Period Eigenvalue, Time-Histories for the SRB/ Main Parachute Configuration, Scissors Initial Conditions (θ_1 = -20 deg, θ_3 = +20 deg)

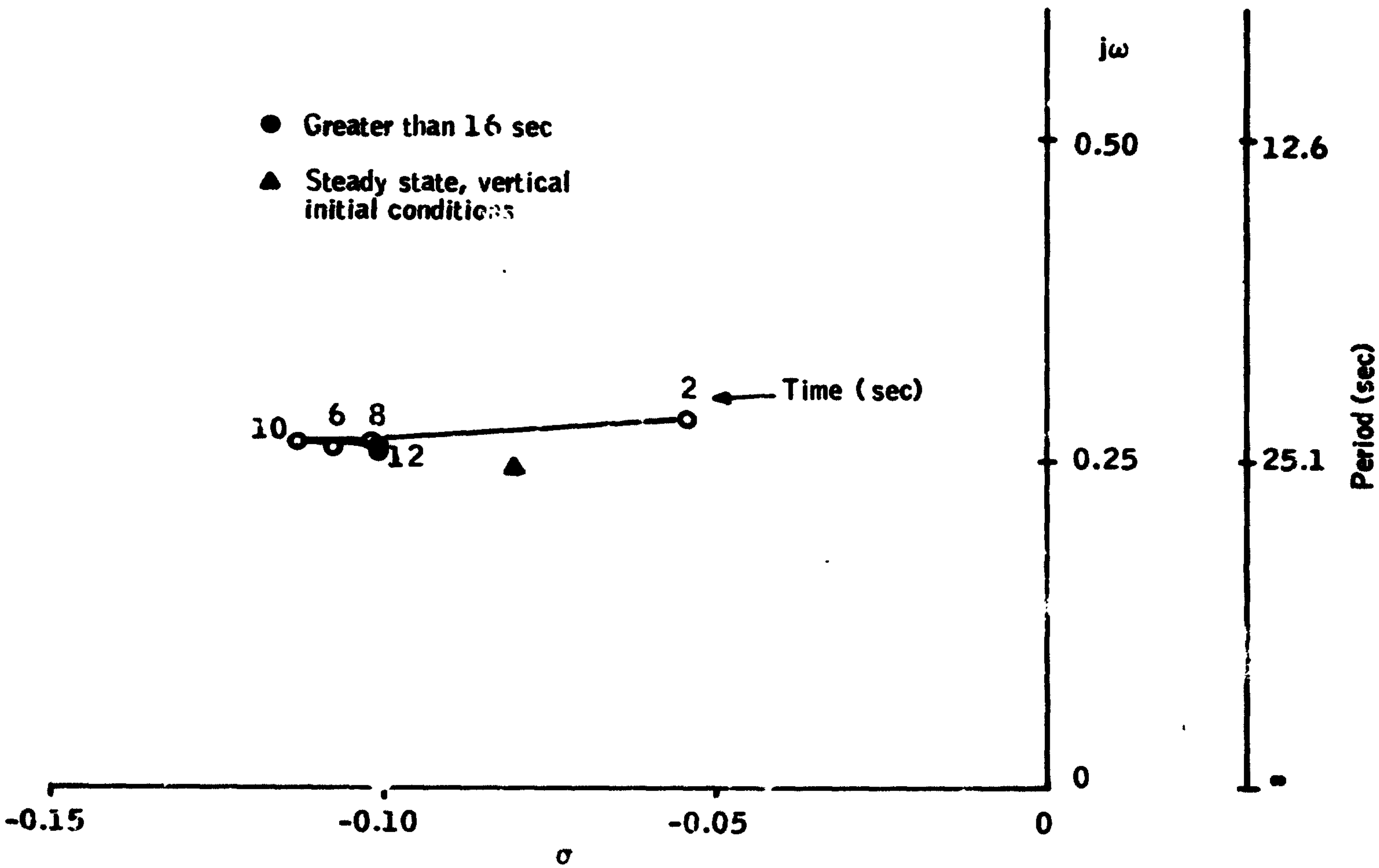

Figure 44. Long Period Eigenvalue Time History for the SRB/Main Parachute Configuration, Scissors Initial Conditions (θ_1 = -20 deg, θ_3 = +20 deg)

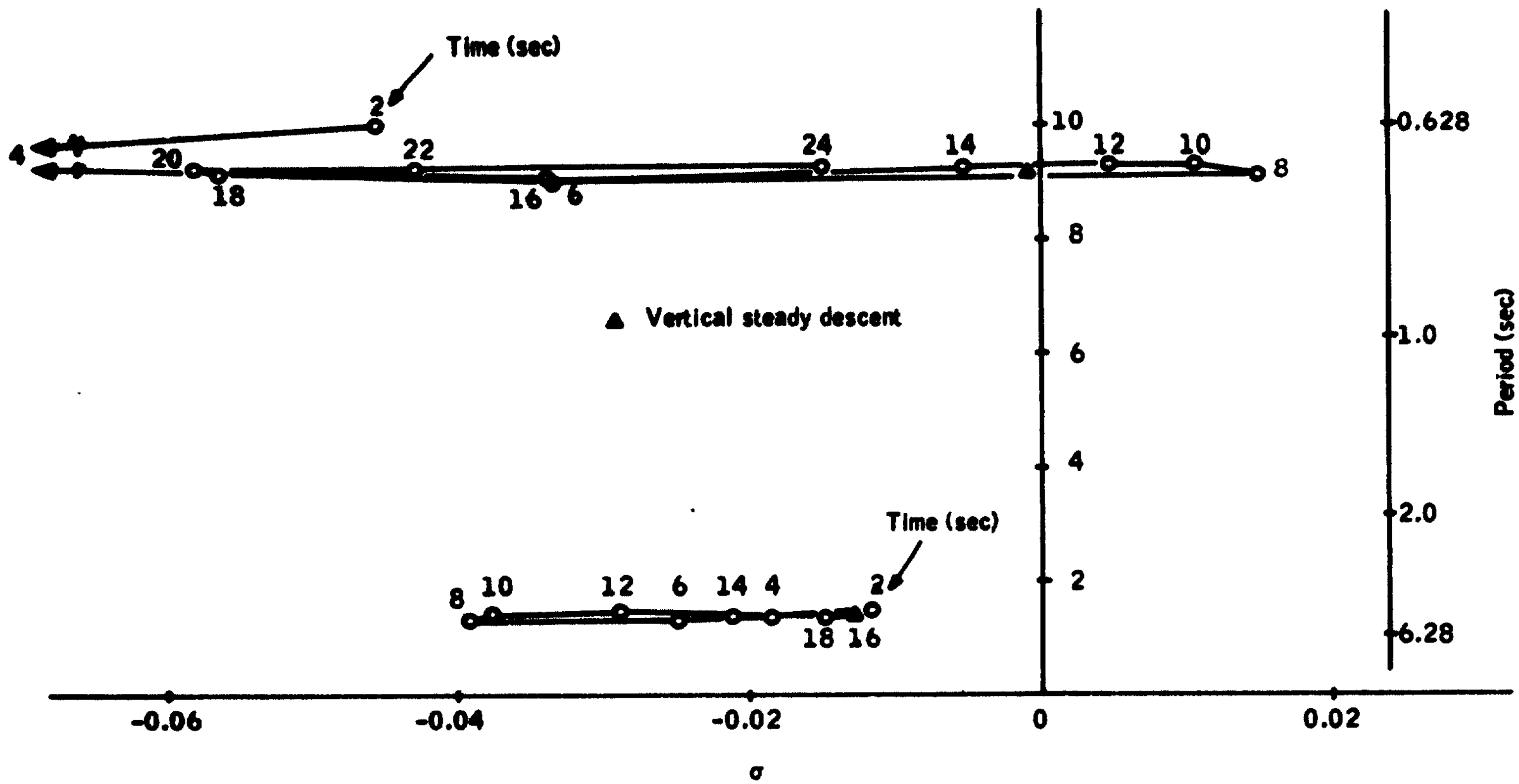

Figure 45. Short Period Eigenvalue Time Histories for the SRB/Main Parachute Configuration, Vertical Descent Initial Conditions, Non-Steady Air Mass

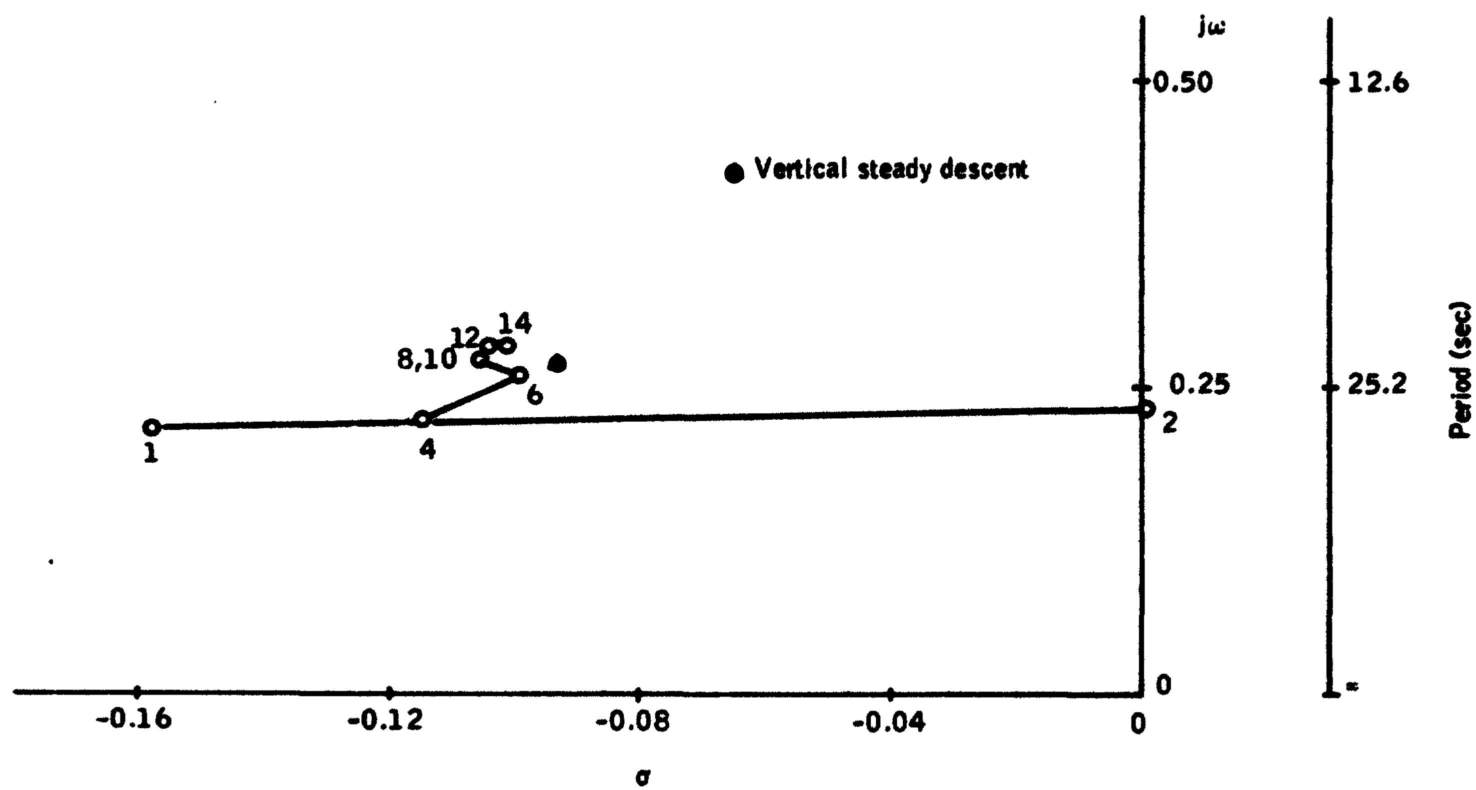

Figure 46. Long Period Eigenvalue Time History for the SRB/Main Parachute Configuration, Vertical Descent Initial Conditions, Non-Steady Airmass

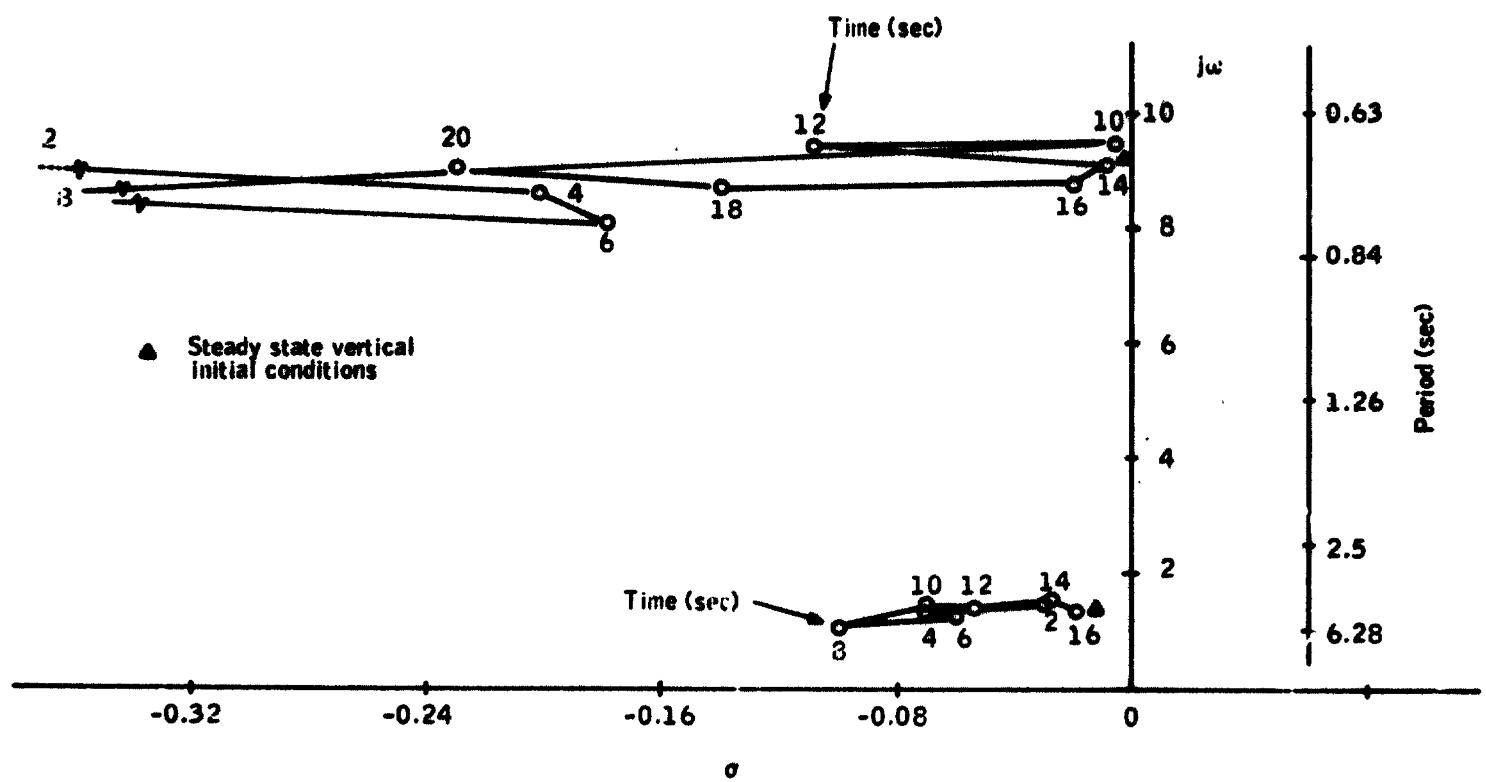

Figure 47. Short Period Eigenvalue Time Histories for the SRB/Main Parachute Configuration, Pendulum Initial Conditions, Non-Steady Airmass (θ_1 = 20 deg, θ_3 = 20 deg)

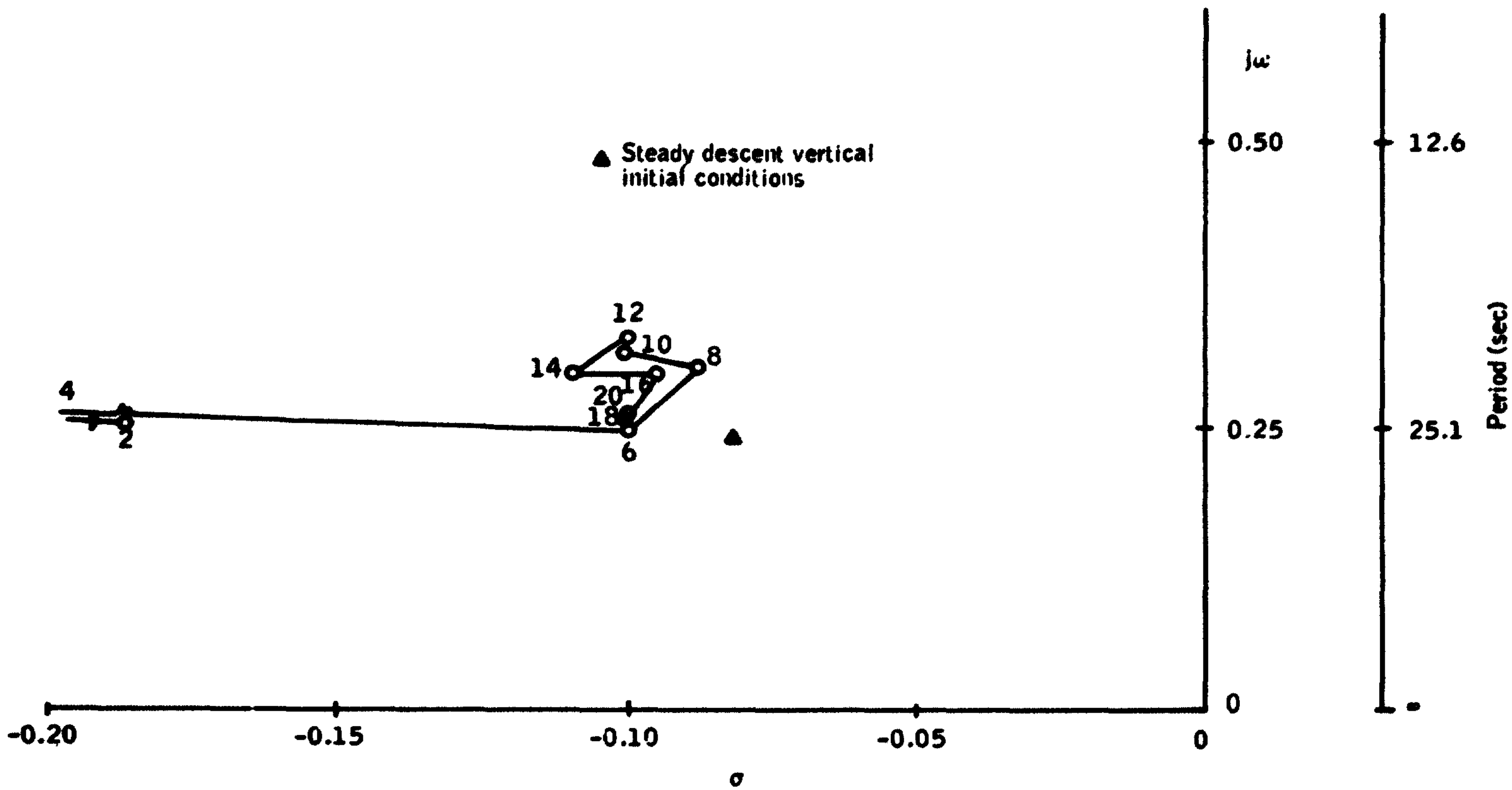

Figure 48. Long Period Eigenvalue Time History for the SRB/Main Parachute Configuration, Pendulum Initial Conditions Non-Steady Airmass (θ_1 = +20 deg, θ_3 = +20 deg)

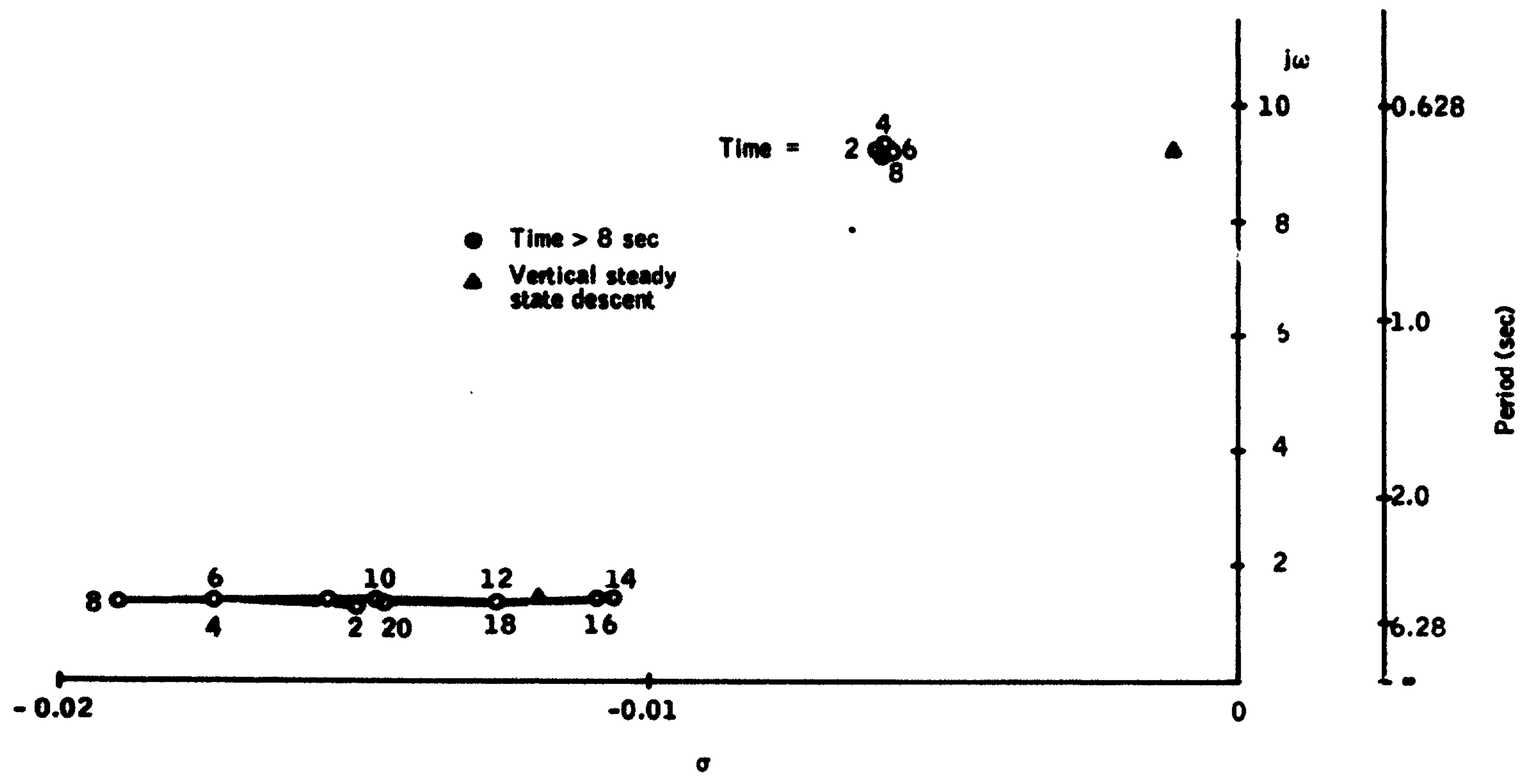

Figure 49. Short Period Eigenvalue Time Histories for the SRB/Main Parachute Combination, Pendulum Initial Conditions, Elastic Suspension System ($\theta_1 = \theta_3 = +20$ deg Initially)

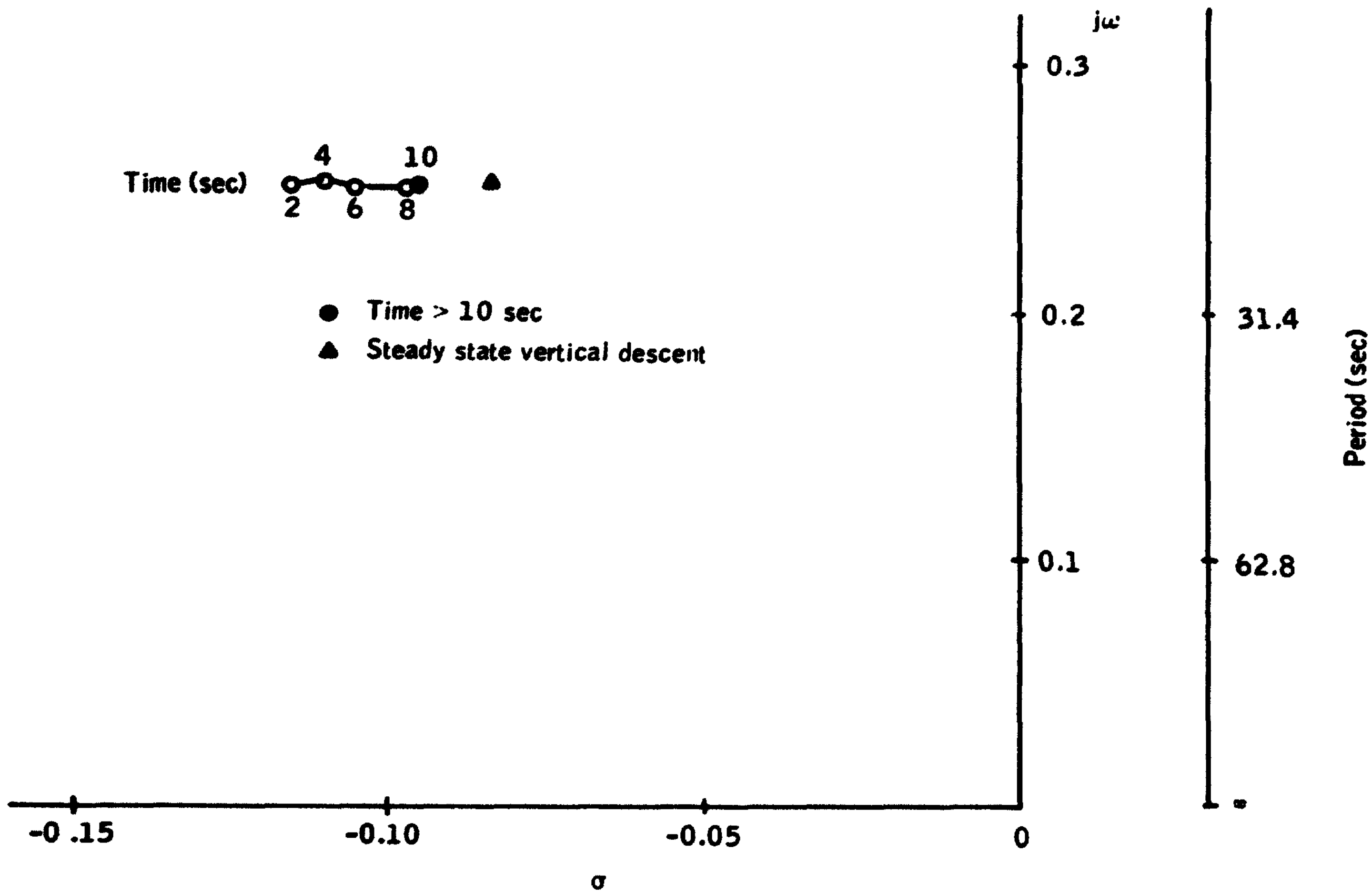

Figure 50. Long Period Eigenvalue Time History for the SRB/Main Combination, Pendulum Initial Conditions, Elastic Suspension System ($\theta_1 = \theta_3 = +20$ deg Initially)

When compared with Figures 41 and 42, no degradation of stability because of elasticity is seen.

LIMIT CYCLE RESPONSES

Throughout the investigations of this particular recovery system, special attention was paid to the possible occurrence of limit cycles. In no case treated has a limit cycle been observed or eigenvalues calculated which would indicate long-term undamped oscillatory motion of any component of the system.

CONCLUSIONS

In all cases tested on the nonlinear computer simulation program, the recovery configurations were stable. The cases tested represent the full range of expected disturbances. From the 6000-ft altitude at which the main parachutes are deployed, the recovery system would reach a vertical descent attitude if it were not for the wind. The response to the wind causes gliding down wind. The trajectory is determined by the vertical descent rate and the wind speed.

Although additional dynamics are induced by the elasticity of the suspension system, the overall response is not adversely affected. Large spring constants should be used to avoid sling-shot effects during transient periods of response.

RECOMMENDATIONS

The development of the present math model and computer simulation paves the way for useful extensions and generalizations of the analysis to provide a more complete and realistic representation of the entire recovery process including the Opening Dynamics phase.

INCORPORATION OF PARACHUTE OPENING DYNAMICS IN THE MATH MODEL

An important consideration in the overall dynamics of the parachute recovery process is the deployment and inflation of the parachute, the process referred to in the literature as Opening Dynamics.

An opening dynamics analysis would establish the most realistic initial conditions possible by including the inflation process of the deceleration system. The period in the descent phase between drogue stabilization of the SRB and fully inflated main parachutes sees the speed of the SRB drop dramatically. The dynamics of this period as described by an opening dynamics model would furnish more accurate initial conditions for the final descent and water impact. There are several Opening Dynamics theories which employ such concepts as dimension less parachute filling time, canopy volume as a function of filling time, drag areas and drag coefficient as functions of filling time, etc. Factors affecting the dynamics of the opening parachute are the canopy mass, suspension line mass, included and apparent masses, and moments of inertia both real and apparent of the inflating canopy. Experimental data have been collected and empirical models have been developed.

It appears, therefore, very desirable to add the parachute Opening Dynamics to the computer simulation model based on state of the art models and including snatch force and opening shock calculations for the inflating parachute through reefed stages to steady state.

RELAXATION OF GEOMETRIC CONSTRAINTS

By relaxing geometric axial symmetry constraints of the present math model, greater realism and additional flexibility would be obtained for use in stability and design analysis.

If one allows off-axis of symmetry attach points on the SRB and the confluence point, then individual suspension line stretch and stretch rates must be accounted for.

Another possible generalization would consider the parachute and/or the SRB to have a plane of symmetry instead of an axis of symmetry. Such a generalization increases the complexity of the analysis and permits the consideration of "gliding" decelerators and/or finned SRBs.

REFERENCES

1. Memo to S. K. Ibrahim from G. L. Watts received 10 September 1973.

2. Winder, Steve, "Parachute/SRB Low Altitude Wind Response," S&E-AERO-DD-4-73, August 8, 1973.

3. Wolf, Dean F., "The Dynamic Stability of a Nonrigid Parachute and Payload System," PhD Thesis, University of Rhode Island, 1968.

4. Reynolds, Donald T., "Optimization of Parachutes," MS Thesis, California State University at Northridge, 1973.

5. Poole, Lamont R., "Viscous Damping Characteristics of Dacron Parachute Suspension-Line Cord," Journal of Spacecraft, Vol. 10, No. 11, pp. 751-752, November 1973.

6. Chernowitz, G., ed., "Performance and Design Criteria for Deployable Aerodynamic Decelerators," ASD-TR-61-579, AF Flight Dynamics Laboratory, Wright-Patterson AFB, Ohio, December 1963.

7. Fichtl, George H., "Integrated Wind Profile for Shuttle SRB Water Entry Studies," S&E-AERO-YA-9-9-73, March 3, 1973.

8. Fichtl, George H., "Gust Environments for Space Shuttle SRB Water Entry Studies," S&E-AERO-YA-9-9-73, March 3, 1973.

9. Beeman, E.R., "SRM Entry Aerodynamics," Northrup Services, Inc., M9241-72-80, June 17, 1972

10. Bacchus, D., "Preliminary Parachute Characteristics for Use in SRB Recovery Studies," S&E-AERO-AA-72-83, NASA Marshall SFC, December 4, 1972.

11. Konar, A.F., "Development of Weapon Delivery Models and Analysis Programs," AFFDL-TR-71-123, Vol. 1, April, 1972.

12. D. McCracken and W. Dorn, <u>Numerical Methods and Fortran Programming</u>, John Wiley and Sons, New York, 1964.

APPENDIX A

DOCUMENTATION OF THE PARACHUTE DYNAMICS AND STABILITY ANALYSIS PROGRAMMING SYSTEM

Computer programs describing the descent dynamics and stability analysis of a parachute payload system are described.

The overall program is called CHUTER. The programs are developed in FORTRAN IV programming language. There are several running mode options. The basic running mode (no supplementary options employed) is simply a nonlinear dynamic simulation. Three supplementary options can be attached to the basic running mode.

- Elasticity. The use of the elastic option causes the riser and suspension lines to become dynamically elastic and the nonlinear simulation to reflect the influence of the additional dynamics.

- Non Steady Air Mass. The use of the non steady air mass option enables the subroutines describing wind and gust conditions to be imposed on the descending recovery system. The aerodynamic effects of the imposed non steady air mass are then accounted for.

- A third supplementary option enables the linearization subroutines to be incorporated in the analysis. Their use causes the nonlinear equations of motion to be linearized at intervals in time using as a reference state the exact nonlinear state at the particular time. Eigenvalues for the linearized equations of motion are determined.

OVERALL PROGRAM ORGANIZATION

The overall organization finds the main program directing and controlling the subsequent operation of the several subroutines as well as data input functions. The overall organization is diagrammed in Figure A1 showing the subroutines and available analysis options.

The principal variables describing the state of the system are contained in the "Y-array" and are passed through the various subroutines in the common block:

COMMON/AAB/Y(33).

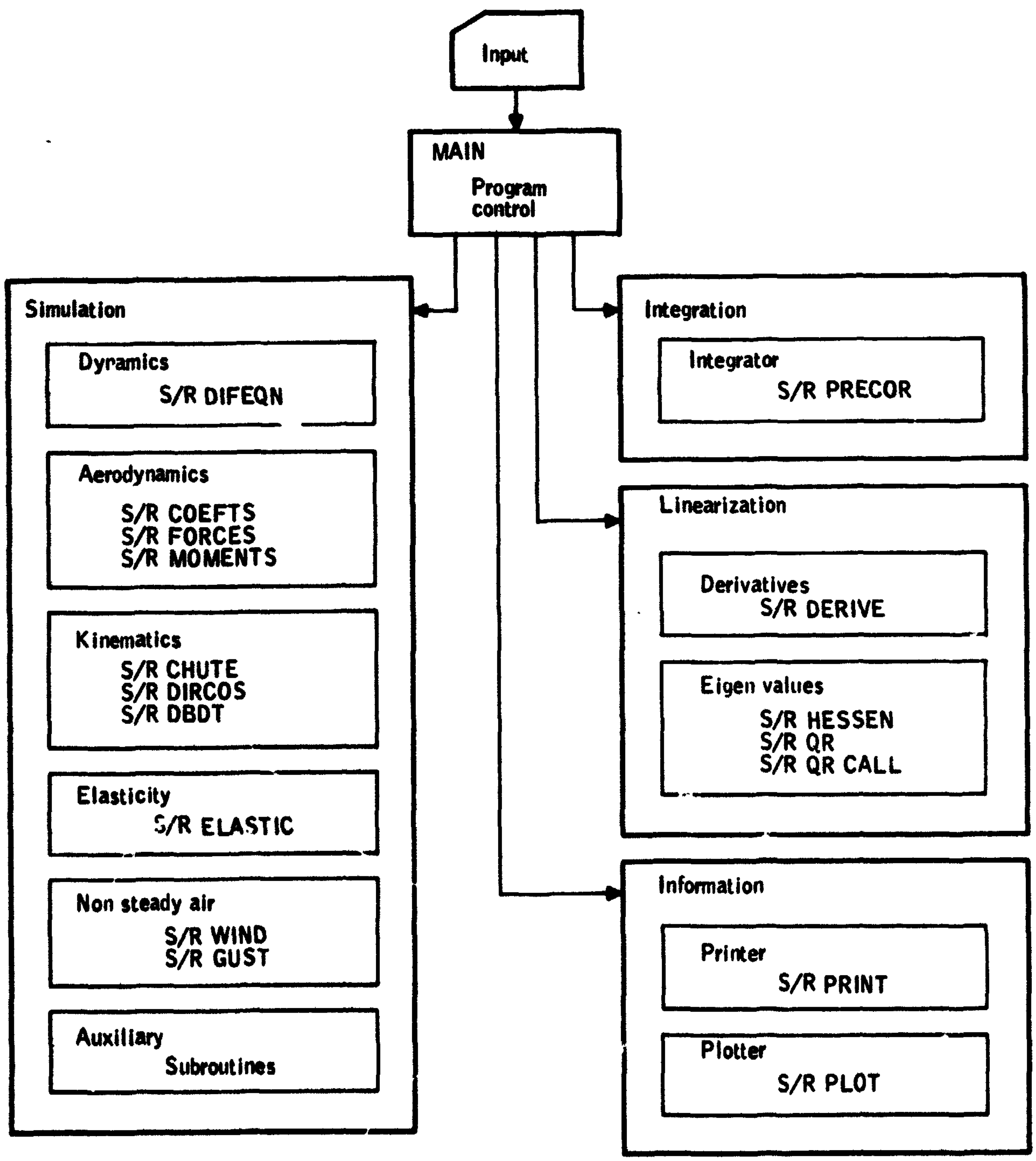

Figure A1. Overall Structure of Program CHUTER

The time rates of change of the state variables are contained in the "D-array" element having the same index and are passed through the various subroutines in the common block:

COMMON/AAC/D(30)

The principal variables are listed in Table A1. Nearly all other parameters and variables and constants which are required by more than one subroutine are passed through a series of common blocks containing related arguments.

CHUTER INPUT/OUTPUT

Input Description

An input card deck of 14 cards provides the required information for initialization and control. The input data deck is described in Table A2.

Output Description

There are two forms of information output from CHUTER. The line printer output provides detailed information on the nonlinear simulation at chosen time points along the trajectory, the interval being DTP. When the linearization option is employed, the eigenvalues of the linearized system are printed for the points along the trajectory at which the nonlinear system is linearized.

A plotting subroutine is included which charts information generated by the nonlinear simulation subroutines. Additional charts are drawn if the elastic or non steady air mass option is employed.

The line printer output during nonlinear simulation consists of groups of four lines each corresponding to the time printed at the left of the page. Each page is headed by column labels.

When the linearization routines are employed, the eigenvalues at the selected linearization points are stored until a single page can be printed with the eigenvalues for the previous five linearized points.

For each new run a run title page is printed listing the supplementary options employed, and a data deck reproduction is made for reference. An illustration is drawn on which the principal system initial geometric parameters are noted.

The line printer output continues through the maximum simulation time or water impact. The exact state at that point is printed.

TABLE A1 - DEFINITION OF PRINCIPAL VARIABLES

```
RUN VERSION 2.3 --PSR LEVEL 332--

      PROGRAM CHUTER(INPUT,OUTPUT,TAPE5=INPUT,TAPE6=OUTPUT,TAPE2)
C**********************************************************************C
C                                                                      C
C DEFINITIONS OF PRINCIPAL VARIABLES                                   C
C      Y(1)    = U1              Y(19)   = U2                          C
C      Y(2)    = V1              Y(20)   = V2                          C
C      Y(3)    = W1              Y(21)   = W2                          C
C      Y(4)    = P1              Y(22)   = P2                          C
C      Y(5)    = Q1              Y(23)   = Q2                          C
C      Y(6)    = R1              Y(24)   = R2                          C
C      Y(7)    = PHI1            Y(25)   = PHI2                        C
C      Y(8)    = THETA1          Y(26)   = THETA2                      C
C      Y(9)    = PSI1            Y(27)   = PSI2                        C
C      Y(10)   = U3              Y(28)   = SRB CG POSITION, EARTH X AXIS       C
C      Y(11)   = V3              Y(29)   = SRB CG POSITION, EARTH Y AXIS       C
C      Y(12)   = W3              Y(30)   = SRB CG POSITION, EARTH Z AXIS       C
C      Y(13)   = P3              Y(31)   = PARACHUTE CG POSITION, EARTH X AXIS C
C      Y(14)   = Q3              Y(32)   = PARACHUTE CG POSITION, EARTH Y AXIS C
C      Y(15)   = R3              Y(33)   = PARACHUTE CG POSITION, EARTH Z AXIS C
C      Y(16)   = PHI3                                                  C
C      Y(17)   = THETA3                                                C
C      Y(18)   = PSI3                                                  C
C                                                                      C
C**********************************************************************C
C ---- 1  PARACHUTE
C ---- 2  RISER
C ---- 3  PAYLOAD
```

TABLE A2 - TYPICAL DATA CARD INPUT DECK

```
0.000     1.000     1.000
100.000
0.000     0.000     0.000     0.000     10.000    0.000
0.000     0.000     0.000     0.000     10.000    0.000
67.000
-.274     .004      -1.271    -.023     0.000     0.000     0.000     0.000     0.000
.380      0.000     .363      .576      0.000     -.809     0.000     .429      0.000
130.000   268.000   275.000   120.000   23.300    27.200    200.00013300.000    3.000
-7.032    -1.114    -12.870   33.240    12.610    -48.360   0.000     0.000     0.000
.699      .191      12.560    0.000     -35.390   0.000     31.980    0.000     0.000
3.645     0.000     15.200    0.000     -12.600   0.000     0.000     0.000
.736E+07  .736E+07  .172E+06
11.800    75.000    145.000   0.000     4750.000  110.000
6000.000  30.000
```

TABLE A1 - TYPICAL DATA CARD INPUT DECK
(CONTINUED)

Data Description (All Data is Floating Point)

Card 1. Format (2F 8.0)

Variable	Units	Definition
Y (30)	ft	Initial altitude
HDOT	fps	Rate of Descent

Card 2 Format (6F 8.0)

Variable	Units	Definition
D3	ft	SRB Diameter
L3	ft	SRB CM Location
L3T	ft	SRB Total length
L4	ft	SRB CP Location
M3	Slugs	SRB Mass
S3	ft^2	SRB Cross Section Area

Card 3 Format (3E 10.3)

Variable	Units	Definition
IXX 3	slug ft^2	SRB Inertia about its X axis
IYY 3	slug ft^2	SRB Inertia about its Y axis
IZZ 3	slug ft^2	SRB Inertia about its Z axis

Card 4 Format (8F 8.0)

Variable	Units	Definition
BCN (Array)	---	Constants in the polynomial describing the normal force coefficient of the SRB

Card 5 Format (9F 8.0)

Variable	Units	Definition
BCT (Array)	---	Constants in the polynomial describing the tangent force coefficient of the SRB

TABLE A1 - TYPICAL DATA CARD INPUT DECK (CONTINUED)

Data Description

Card 6 Format (9F 8.0)

Variable	Units	Definition
BCM (Array)	---	Constants in the polynomial describing the moment coefficient of the SRB

Card 7 Format (9F 8.0)

Variable	Units	Description
DO	ft	Parachute nominal diameter
L1	ft	Length from confluence point to parachute CP
LS0	ft	Initial value of suspension line length
M	---	Number of suspension lines
MC	slugs	Mass of canopy
ML	slugs	Mass of lines
LCM	ft	Initial guess at parachute CM distance from confluence point
S1	ft^2	Nominal parachute area
CLUST	---	Number of chutes in cluster

Card 8 Format (9F 8.0)

Variable	Units	Description
ACN (Array)	---	Constants in the polynomial describing the parachute normal force coefficient
ACT (Array)	---	Constants in the polynomial describing the parachute tangent force coefficient

Card 9 Format (9F 8.0)

Variable	Units	Description
ACM (Array)	---	Constants in the polynomial describing the parachute moment coefficient

TABLE A1 - TYPICAL DATA CARD INPUT DECK (CONCLUDED)

Data Description

Card 10 (Format (1F 8.0)

Variable	Units	Description
L20	ft	Nominal riser length

Card 11 Format (6F 8.0)

Variables	Units	Description
Y (4)	deg/sec	Initial P1
Y (5)	deg/sec	Initial Q1
Y (6)	deg/sec	Initial R1
Y (7)	deg	Initial $\phi 1$
Y (8)	deg	Initial $\theta 1$
Y (9)	deg	Initial $\psi 1$

Card 12 Format (6F 8.0)

Variables	Units	Description
Y (13)	deg/sec	Initial P3
Y (14)	deg/sec	Initial Q3
Y (15)	deg/sec	Initial R3
Y (16)	deg	Initial $\phi 3$
Y (17)	deg	Initial $\theta 3$
Y (18)	deg	Initial $\psi 3$

Card 13 Format (1F 8.0)

Variable	Unit	Description
TMAX	Sec	Maximum time

Card 14 Format (3F 8.0)

Variable	Units	Description
YWIND	---	Wind option, 1-yes, 0-no
YELAST	---	Elastic option, 1-yes, 0-no
YLIN	---	Linearization option, 1-yes, 0-no

A typical page showing information on the nonlinear simulation is shown in Figure A2, and a page showing the eigenvalues at selected points is shown as Figure A3.

PROGRAM DESCRIPTION

Main Program

CHUTER is a series of subroutines whose operation is controlled by the MAIN program to provide nonlinear and linear analysis. The MAIN program is diagrammed in Figure A4 and a source listing is presented in Figure A5.

The MAIN program is broken down into three parts. The first is input and establishes constants and control variables. The second segment initializes the elastic variables, sets angles and angular rates to units of radians, sets the initial velocities in the body fixed coordinates, and establishes the direction cosines matrix corresponding to the initial conditions. Finally, the third segment is a high-frequency loop which runs the nonlinear simulation.

The high-frequency loop is initially entered with mode and time = 0, which causes the initial conditions to be output by subroutine PRINT. Successive passes through the loop increase the MODE to its nominal value of 4 or 5 depending on whether subroutine PRECOR is about to predict or about to correct.

Elasticity initial conditions (i.e., riser and parachute center of mass lengths) are updated through time = 0.25, at which point the numerical determination of elastic rates begins.

Time = 0.25 is an arbitrary but convenient time greater than time = 0 since at time = 0 the elastic elements are unstressed.

There are four normal exits from the high-frequency loop. After the print time interval DTP the loop is exited by a call to subroutine PRINT. The second normal exit occurs when a water impact occurs. This is sensed by comparing the altitude with length from the SRB center of mass to the engine end. The third normal exit occurs when the simulation time exceeds TMAX. The fourth normal exit occurs when a point in time is reached about which a linearized solution is to be found.

The subroutines used with CHUTER are listed in Table A3.

			PARACHUTE					SPR					
TIME	PSI1 THETA1 PHI1	U1 V1 W1	P1 Q1 R1	XF1 YF1 ZF1	C1 ALPHA1	PSI3 THETA3 PHI3	U3 V3 W3	P3 Q3 R3	XF3 YF3 ZF3	XE3DOT YE3DOT ZE3DOT	C3 ALPHA3	LCN L2	F2
57.75	0.000	69.009	0.000	4250.554	106.368	0.000	64.800	0.000	4249.175	64.768	101.667	292.156	152649.135
	-.882	0.000	-.312	0.000		-.075	0.000	-3.103	0.000	0.000		67.000	
	0.000	78.159	0.000	-1750.512	-.026	0.000	78.327	0.000	-1316.366	78.356	3.229		
	VWIND	69.000	VGUST	.071									
58.00	0.000	69.276	0.000	4267.767	106.286	0.000	65.928	0.000	4265.377	64.826	101.660	292.156	153682.608
	-.354	0.000	-.869	0.000		-.816	0.000	-3.075	0.000	0.000		67.000	
	0.000	77.901	0.000	-1730.926	-.072	0.000	77.373	0.000	-1296.781	78.309	2.386		
	VWIND	69.000	VGUST	.071									
58.25	0.000	69.660	0.000	4284.993	106.462	0.000	66.862	0.000	4281.578	64.791	101.609	292.156	153652.528
	-.232	0.000	1.399	0.000		-1.515	0.000	-2.528	0.000	0.000		67.000	
	0.000	78.006	0.000	-1711.338	-.362	0.000	76.522	0.000	-1277.209	78.273	1.695		
	VWIND	69.000	VGUST	.071									
58.50	0.000	69.753	0.000	4302.225	106.019	0.000	67.734	0.000	4297.790	64.897	101.644	292.156	152601.890
	-.171	0.000	-1.179	0.000		-2.098	0.000	-2.137	0.000	0.000		67.000	
	0.000	77.986	0.000	-1691.769	.215	0.000	75.797	0.000	-1257.649	78.229	1.024		
	VWIND	69.000	VGUST	.071									
58.75	0.000	69.622	0.000	4319.355	106.090	0.000	68.335	0.000	4314.025	64.961	101.635	292.156	152528.728
	-.499	0.000	-.412	0.000		-2.539	0.000	-1.280	0.000	0.000		67.000	
	0.000	77.596	0.000	-1672.174	-.181	0.000	75.228	0.000	-1238.099	78.181	.528		
	VWIND	69.000	VGUST	.071									
59.00	0.000	69.288	0.000	4336.574	106.186	0.000	68.612	0.000	4330.258	64.949	101.620	292.156	153361.637
	-.350	0.000	.533	0.000		-2.729	0.000	-.318	0.000	0.000		67.000	
	0.000	77.749	0.000	-1652.617	-.237	0.000	74.966	0.000	-1218.557	78.155	.301		
	VWIND	69.000	VGUST	.071									
59.25	0.000	68.952	0.000	4353.712	103.650	0.000	68.767	0.000	4346.519	65.103	101.710	292.156	152856.566
	-.557	0.000	-1.998	0.000		-2.730	0.000	.324	0.000	0.000		67.000	
	0.000	77.361	0.000	-1633.072	.126	0.000	74.949	0.000	-1199.020	78.144	.168		
	VWIND	69.000	VGUST	.071									
59.50	0.000	69.765	0.000	4370.785	103.820	0.000	68.549	0.000	4362.805	65.154	101.725	292.156	152019.939
	-.898	0.000	-.068	0.000		-2.536	0.000	1.256	0.000	0.000		67.000	
	0.000	76.910	0.000	-1613.535	-.468	0.000	75.164	0.000	-1179.489	78.121	.297		
	VWIND	69.000	VGUST	.071									
59.75	0.000	69.322	0.000	4387.914	103.736	0.000	68.160	0.000	4379.107	65.263	101.772	292.156	152686.405
	-.821	0.000	-.402	0.000		-2.138	0.000	1.801	0.000	0.000		67.000	
	0.000	77.051	0.000	-1594.011	-.265	0.000	75.600	0.000	-1159.963	78.092	.597		
	VWIND	69.000	VGUST	.071									
60.00	0.000	69.389	0.000	4404.910	111.396	0.000	67.744	0.000	4395.458	65.480	101.898	292.156	153494.465
	-1.232	0.000	-2.116	0.000		-1.669	0.000	1.979	0.000	0.000		67.000	
	0.000	76.571	0.000	-1574.491	-.167	0.000	76.126	0.000	-1140.441	78.075	.904		
	VWIND	69.000	VGUST	.071									

Figure A2. Typical Nonlinear Simulation Output Page

EIGENVALUES

TIME = 56.00		TIME = 57.00		TIME = 58.00		TIME = 59.00		TIME = 60.00	
REAL	IMAGINARY	REAL	IMAGINARY	REAL	IMAGINARY	REAL	IMAGINARY	REAL	IMAGINARY
0.	0.	0.	0.	0.	0.	0.	0.	0.	0.
0.	0.	0.	0.	0.	0.	0.	0.	0.	0.
0.	0.	0.	0.	0.	0.	0.	0.	0.	0.
0.	0.	0.	0.	0.	0.	0.	0.	0.	0.
0.	0.	0.	0.	0.	0.	0.	0.	0.	0.
0.	0.	0.	0.	0.	0.	0.	0.	0.	0.
.2925E-09	0.	-.8674E-08	.2114E-07	.9986E-07	0.	.2778E-08	0.	.2300E-06	0.
-.1088E-04	0.	.3683E-03	0.	.4487E-09	0.	-.7672E-07	0.	-.4252E-08	0.
.5577E-03	0.	-.8356E-02	0.	-.2985E-03	0.	.1058E-03	0.	-.5281E-03	0.
-.1832E-01	0.	-.1077E+00	0.	-.7885E-02	0.	-.7924E-02	0.	-.8067E-02	0.
-.3096E-01	0.	-.3761E-01	.2594E+00	-.1588E+00	0.	-.1485E+00	0.	-.1219E+00	0.
-.7645E-01	.2483E+00	-.1214E-01	.1370E+01	-.1306E-01	.2648E+00	-.1621E-01	.2715E+00	-.3282E-01	.2517E+00
-.1201E-01	.1371E+01	-.1715E+01	0.	-.1126E-01	.1374E+01	-.1715E+01	0.	-.1192E-01	.1375E+01
-.1715E+01	0.	-.1354E-02	.3216E+01	-.1714E+01	0.	-.1136E-01	.1373E+01	-.1708E+01	0.
-.1669E-02	.9223E+01	0.	0.	-.1263E-02	.9239E+01	-.1174E-02	.9235E+01	-.1229E-02	.9267E+01
0.	0.	.6275E-06	0.	-.2983E-05	0.	0.	0.	0.	0.
.1536E-02	0.	-.7620E-03	.2914E-01	-.3339E-03	0.	.1871E-02	0.	.1544E-02	0.
-.1054E-02	.2168E-01	-.9667E-01	.2690E+00	-.5894E-03	.5369E-01	-.1662E-02	.5844E-02	-.7655E-03	.3444E-01
-.9733E-01	.2684E+00	-.7223E+00	0.	-.9533E-01	.2636E+00	-.9369E-01	.2721E+00	-.9734E-01	.2562E+00
-.7169E+00	0.	-.1339E-01	.1367E+01	-.7272E+00	0.	-.7327E+00	0.	-.7602E+00	0.
-.1661E-01	.1372E+01	-.1716E+01	0.	-.1301E-01	.1374E+01	-.1677E-01	.1371E+01	-.1176E-01	.1374E+01
-.1717E+01	0.	-.3262E-01	.3198E+01	-.1715E+01	0.	-.1716E+01	0.	-.1708E+01	0.
-.2673E-01	.9195E+01			-.3320E-01	.9232E+01	-.2758E-01	.9239E+01	-.1830E-01	.9256E+01

Figure A3. Typical Eigenvalue Output Page

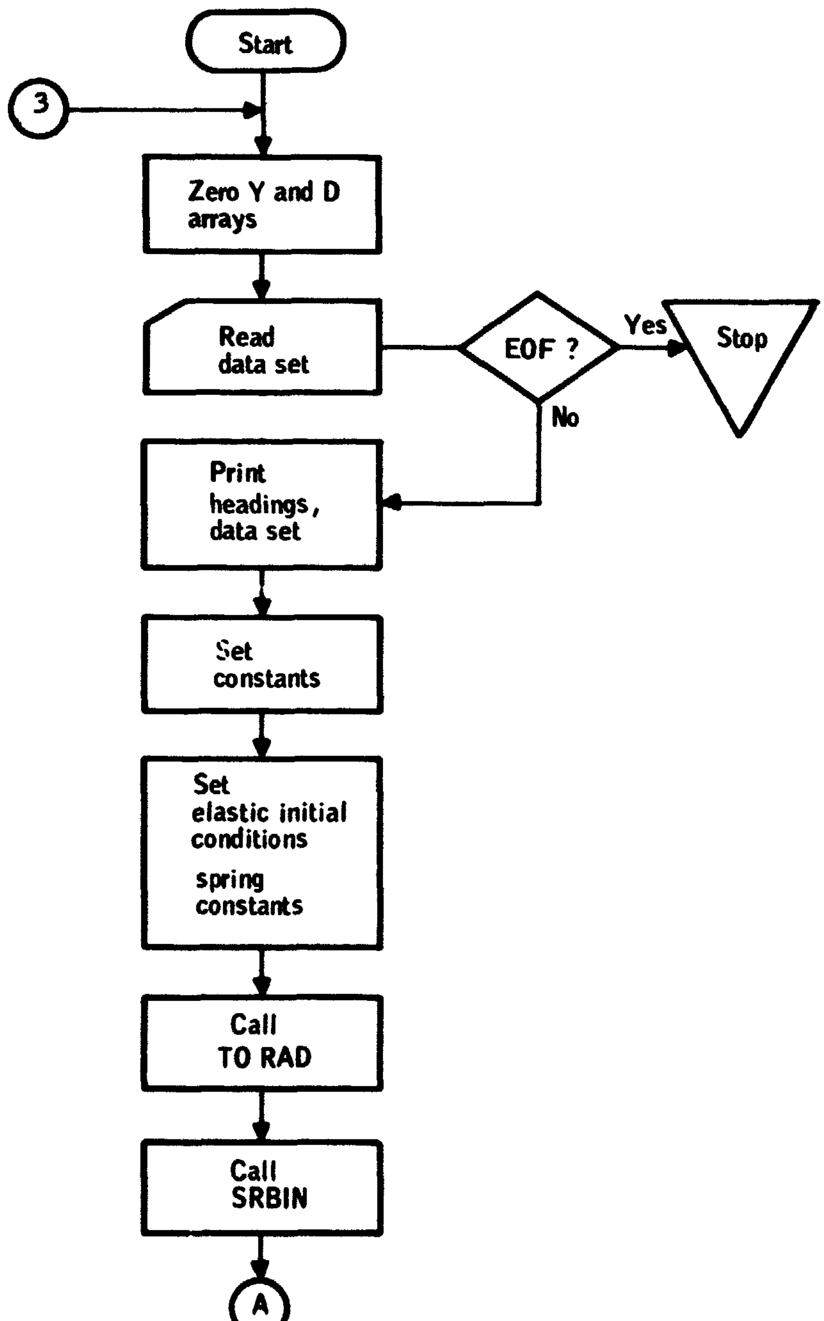

Figure A4. CHUTER Main Program Flow Diagram

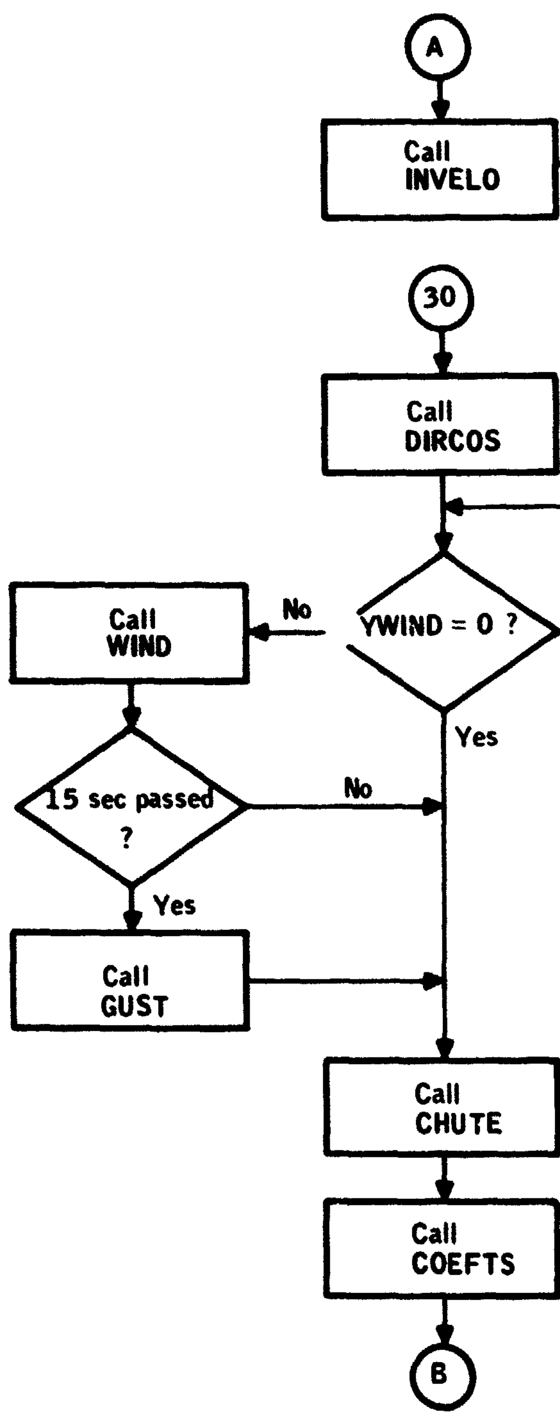

Figure A4. CHUTER Main Program Flow Diagram (Continued)

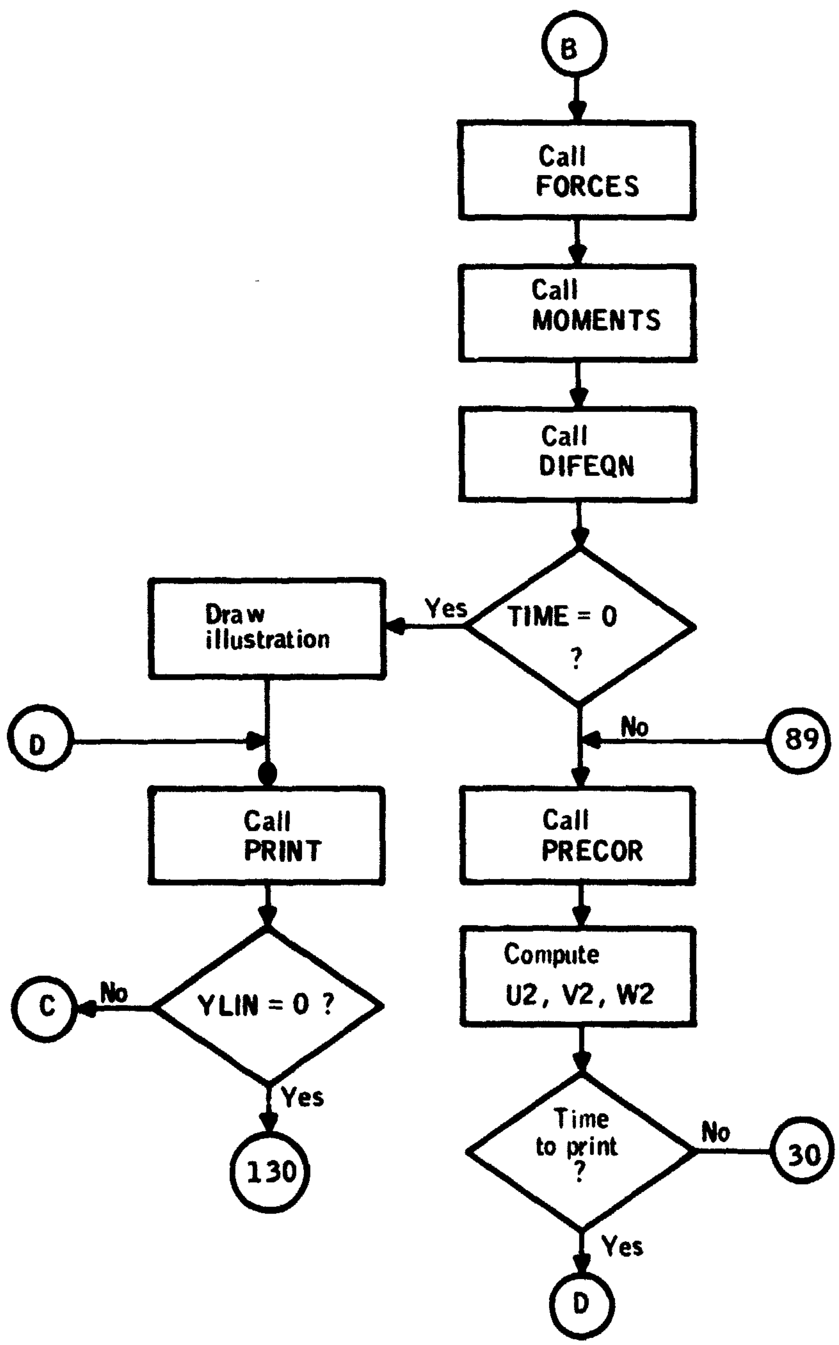

Figure A4. CHUTER Main Program Flow Diagram (Continued)

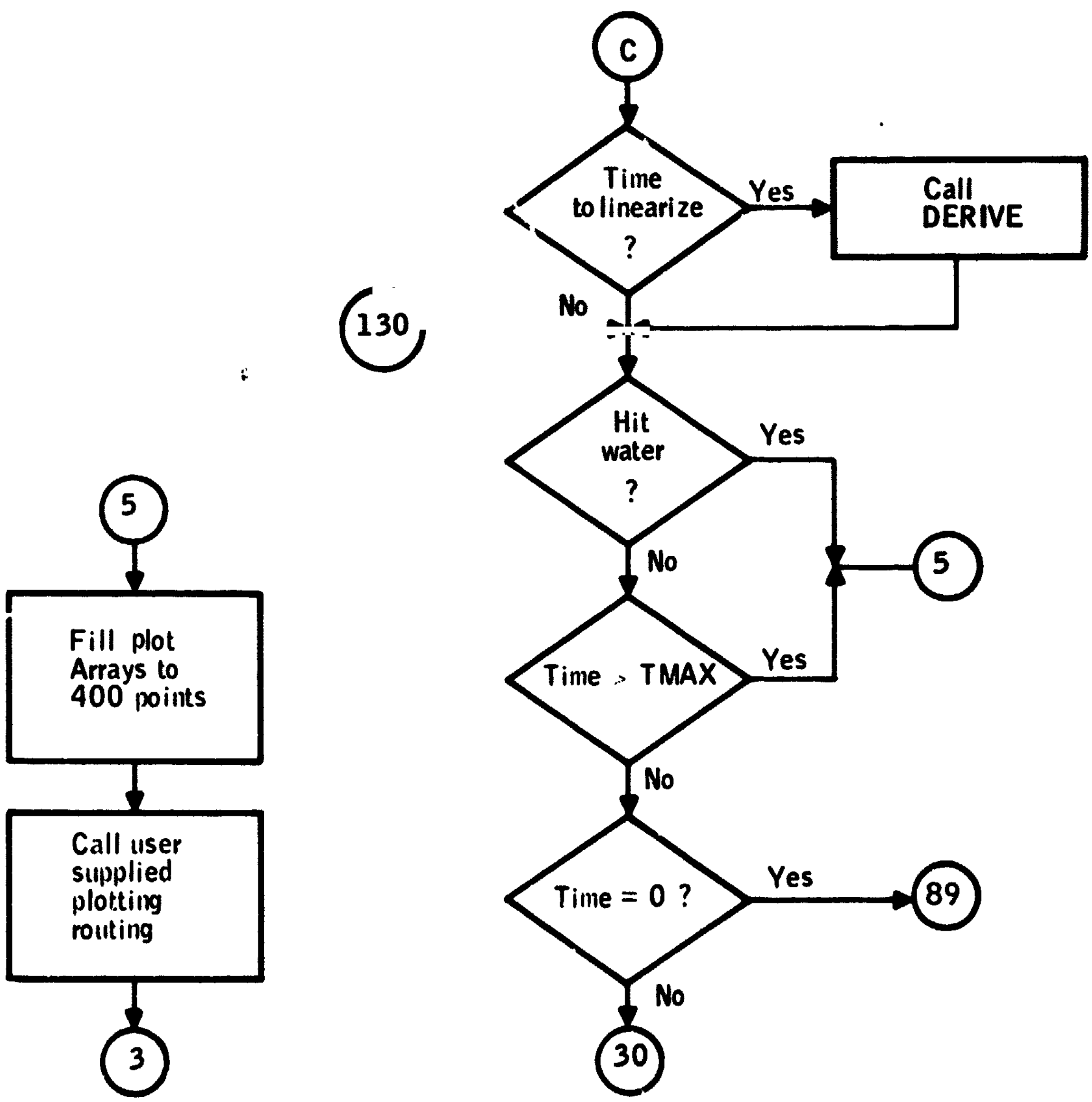

Figure A4. CHUTER Main Program Flow Diagram (Concluded)

```
      PROGRAM CHUTER(INPUT,OUTPUT,TAPE5=INPUT,TAPE6=OUTPUT,TAPE2)
C*****************************************************************************C
C                                                                             C
C DEFINITIONS OF PRINCIPAL VARIABLES                                          C
C       Y(1)   = U1             Y(19)  = U2                                   C
C       Y(2)   = V1             Y(20)  = V2                                   C
C       Y(3)   = W1             Y(21)  = W2                                   C
C       Y(4)   = P1             Y(22)  = P2                                   C
C       Y(5)   = Q1             Y(23)  = Q2                                   C
C       Y(6)   = R1             Y(24)  = R2                                   C
C       Y(7)   = PHI1           Y(25)  = PHI2                                 C
C       Y(8)   = THETA1         Y(26)  = THETA2                               C
C       Y(9)   = PSI1           Y(27)  = PSI2                                 C
C       Y(10)  = U3             Y(28)  = SRB CG POSITION, EARTH X AXIS        C
C       Y(11)  = V3             Y(29)  = SRB CG POSITION, EARTH Y AXIS        C
C       Y(12)  = W3             Y(30)  = SRB CG POSITION, EARTH Z AXIS        C
C       Y(13)  = P3             Y(31)  = PARACHUTE CG POSITION, EARTH X AXIS  C
C       Y(14)  = Q3             Y(32)  = PARACHUTE CG POSITION, EARTH Y AXIS  C
C       Y(15)  = R3             Y(33)  = PARACHUTE CG POSITION, EARTH Z AXIS  C
C       Y(16)  = PHI3                                                         C
C       Y(17)  = THETA3                                                       C
C       Y(18)  = PSI3                                                         C
C                                                                             C
C*****************************************************************************C
C ---- 1  PARACHUTE
C ---- 2  RISER
C ---- 3  PAYLOAD
C
C COMPLETE LIST OF ALL COMMON BLOCKS
      COMMON/AAA/ACT(9),ACN(9),ACM(9),BCT(9),BCN(9),BCM(9)
      COMMON/AAB/ Y(33)
      COMMON/AAC/D(30)
      COMMON/AAD/B(3,3,3),RS(6),T(3,6)
      COMMON/AAE/ AA(9),AB(9),AC(9)
      COMMON/AAF/CN1,CT1,CN3,CT3,ALPHA1,ALPHA3,BETA1,BETA3,GAMMA
      COMMON/AAFF/CM1,CM3,ALCM
      COMMON/AAG/L2,L2DOT,L2DDOT,LCM,LCMDOT,LCMDDT
      COMMON/AAH/C1,C3,F2,L3,RAD,L1,L4,CF1,CF3,S1,S3
      COMMON/AAHH/D3
      COMMON/AAJ/MODE
      COMMON/AAK/AL1,AL2,AL3,AL4
      COMMON/AAL/F1X,F1Y,F1Z,F3X,F3Y,F3Z
      COMMON/AAM/M1X,M1Y,M1Z,M3X,M3Y,M3Z
      COMMON/AAN/A6,A7,A8,A9,A10,A11,A12,A13,A14,A15,A16,A17,A18,A19,A20
      COMMON/AANN/A21
      COMMON/AAO/OLDTIME,YELAST,ETIME
      COMMON/AAP/YWIND,VWIND,VGUST,WIGU
      COMMON/AAQ/IXX1,IYY1,IZZ1,IXX3,IYY3,IZZ3
      COMMON/AAQQ/IXZ1,IYX1,IZY1,IXZ3,IYX3,IZY3
      COMMON/AAR/KLS,KR,MC,ML,M1,M1A,MP,DO,RO,RHO,L2O,LCMO,LSO,M,M3
      COMMON/AARR/LS,LCP
      COMMON/AAT/TIME
      COMMON/AAW/NOBS
      COMMON/PLTR/XX(402),THE1(402),THE3(402),AP1(402),AP3(402),ALT(402)
```

Figure A5. Main Program Source Listing

```
      1,RNG(402),FOR(402),RL(402),CL(402),WG(402)
       COMMON/XOROS/SUMMA1,SUMMA2,TOTAL,AVERA1,AVERA2,OVERA1,OVERA2,DT
       REAL IXXA1,IXXA3,IXX1,IXX10,IXX3,IXZ1,IXZ3
       REAL IYYA1,IYYA3,IYY1,IYY10,IYY3,IYX1,IYX3
       REAL IZZA1,IZZA3,IZZ1,IZZ10,IZZ3,IZY1,IZY3
       REAL KLS,KR,LCM,LCMDOT,LCMDDT,LCMO,LCP,LS,LSO,L1,L2,L2DOT,L2DDOT
       REAL L20,L3,L3T,L4,MC,ML,M1,M1A,M1X,M1Y,M1Z,M3X,M3Y,M3Z,MP,M3,M
       DT=1.0
       DT2=2.0*DT
     1 GOTO 3
     5 WRITE (6,450)
       DO 7 I=NOBS,400
       THE1(I) = THE1(NOBS)
       THE3(I) = THE3(NOBS)
       AP1  (I) = AP1  (NOBS)
       AP3  (I) = AP3  (NOBS)
       RNG  (I) = RNG  (NOBS)
       ALT  (I) = ALT  (NOBS)
       FOR  (I) = FOR  (NOBS)
       RL   (I) = RL   (NOBS)
       CL   (I) = CL   (NOBS)
     7 WG   (I) = WG   (NOBS)
       CALL PICTUR (YWIND,YELAST)
     3 CONTINUE
       SUMMA1= SUMMA2= TOTAL= 0.0
C ZERO Y AND D ARRAYS
       DO 10 I = 1,30
       D(I) = 0.0
    10 Y(I) = 0.0
C READ INITIAL ALTITUDE AND RATE OF DESCENT -- RECALL THAT THE + Z AXIS OF
C THE EARTH IS DIRECTED DOWNWARD SO THAT THE INITIAL ALTITUDE IS NEGATIVE
       READ (5,410) Y(30),HDOT
C READ SRB PHYSICAL DIMENSIONS
       READ (5,410)  D3,L3,L3T,L4,M3,S3
C READ SRB INERTIAL CHARACTERISTICS
       READ (5,420)  IXX3,IYY3,IZZ3
C READ SRB AERODYNAMIC CHARACTERISTICS
       READ (5,410) (BCN(I),I=1,8)
       READ (5,410) (BCT(I),I=1,9)
       READ(5,410)(BCM(I),I=1,9)
C READ PARACHUTE PHYSICAL DIMENSIONS
C CLUST IS THE NUMBER OF CHUTES IN THE CLUSTER
       READ (5,410) DO,L1,LSO,M,MC,ML,LCMO,S1,CLUST
C READ PARACHUTE AERODYNAMIC CHARACTERISTIC EQUATIONS COEFFICIENTS
       READ (5,410)  (ACN(I),I=1,3),(ACT(I),I=1,6)
       READ (5,410) (ACM(I) , I=1,7)
C READ SYSTEM CHARACTERISTICS
       READ (5,410) L20
C READ INITIAL CONDITIONS
       READ (5,410)  (Y(I),I=4,9)
       READ (5,410)  (Y(I),I=13,18)
C READ THE TIME AT WHICH THE ANALYSIS MUST STOP
       READ (5,410) TMAX
C READ WIND, ELASTICITY, AND LINEARIZATION OPTION CONTROLS -- 0 FOR NO AND 1 FOR
```

Figure A5. Main Program Source Listing (Continued)

```
C YES
      READ (5,410) YWIND,YELAST,YLIN
C DATA CARD LIST
      WRITE (6,550)
      WRITE (6,555)
      IF (YWIND.NE.0.0)WRITE (6,556)
      IF(YELAST.NE.0.0)WRITE (6,557)
      IF(YLIN  .NE.0.0)WRITE (6,558)
      IF(YLIN.EQ.0.0.AND.YELAST.EQ.0.0.AND.YWIND.EQ.0.0) WRITE (6,559)
      WRITE (6,560)
      WRITE (6,430) Y(30),HDOT
      WRITE (6,430) D3,L3,L3T,L4,M3,S3
      WRITE (6,440) IXX3,IYY3,IZZ3
      WRITE (6,430) (BCN(I),I=1,8)
      WRITE (6,430) (BCT(I),I=1,9)
      WRITE(6,430)(BCM(I),I=1,9)
      WRITE (6,430) DO,L1,LSO,M,MC,ML,LCMO,S1,CLUST
      WRITE (6,430) (ACN(I),I=1,3),(ACT(I),I=1,6)
      WRITE (6,430) (ACM(I) ,I=1,9)
      WRITE (6,430) L20
      WRITE (6,430) (Y(I),I=4,9)
      WRITE (5,430) (Y(I),I=13,18)
      WRITE (6,430) TMAX
      WRITE (6,430) YWIND,YELAST,YLIN
C CONSTANTS
      DT2 = 0.25
      ETIME  = 0.25
      G      = 32.17
      J      = 0
      LCM    = LCMO
      LCP    = 0.163*DO
      LS     = LSO
      L2     = L20
      MODE   = 0
      MC     = MC*CLUST
      ML     = ML*CLUST
      M1     = MC+ML
      N      = 30
      OLDTIME  = 0.25
      RAD    = 57.29578
      RC     = 1.0
      RO     = 0.36*DO
      S1     = S1*CLUST
      TIME   = 0.0
      VWIND = VGUST = 0.0
      WIGU   = 0.0
C ALIGN RISER WITH THE PARACHUTE AXIS OF SYMMETRY
      DO 15 I= 22,27
   15 Y(I)   = Y(I-18)
C ELASTICITY INITIAL CONDITIONS
      LCMDOT = 0.0
      LCMDDT = 0.0
      L2DOT  = 0.0
      L2DDOT   0.0
```

Figure A5. Main Program Source Listing (Continued)

```
      AL1     = L2
      AL2     = L2DOT
      AL3     = LCM
      AL4     = LCMDOT
C ELASTIC COEFFICIENTS
      IF (YELAST.GT.0.0) GOTO 13
      KR      = 1.0E20
      KLS     = 1.0E20
      GOTO 14
   13 CONTINUE
      KR      = M3*G*15./L20
      KLS     = M3*G*15./M/LS0
   14 CONTINUE
      CALL TORAD
      CALL SRBIN
      CALL INVELO (HDOT)
      GOTO 31
   30 CALL DIRCOS
   31 CONTINUE
C UPDATE L2,LCM
      IF(TIME.GT.0.25) GOTO 32
   33 AL1     = L2
      AL3     = LCM
   32 CONTINUE
C WIND CALLS
      IF (YWIND.EQ.0.0) GOTO 17
      CALL WIND
      IF (TIME .EQ. 0.0) GOTO 16
C GUST CALLS -- PERIOD = 15 SEC
      IF(TIME-WTIME-15.0) 17,16,16
   16 CALL GUST
      WTIME   = TIME
   17 CONTINUE
      WIGU    = VWIND + VGUST
      CALL CHUTE (CLUST)
      CALL COEFTS (RC)
      CALL FORCES
      CALL MOMENTS (RHO)
      CALL DIFFQN
      IF (TIME.NE.0.0) GOTO 89
C ILLUSTRATION
      WRITE (6,1000)CLUST,D1,S1,MC,LCP,RO,ML,LCM,LS,L2,D3,S3,L3T,L4,L3,
     1M3
      GOTO 120
   89 CALL PRECOR (N,D,H)
C U2,V2,W2
      DO 125 I = 1,3
  125 Y(18+I)= (Y(1)+Y(5)*LCM)*(B(1,1,I)* B(2,1,1)+B(1,2,I)*B(2,2,1)
     1         +B(1,3,I)*B(2,3,1))+(Y(2)-Y(4)*LCM)*(B(1,1,I)*B(2,2,1)
     1         +B(1,2,I)*B(2,2,2)+B(1,3,I)*B(2,3,2))+Y(3)*(B(1,1,I)
     1         *B(2,1,3)+B(1,2,I)*B(2,2,3)+B(1,3,I)*B(2,3,3))
      IF (Y(30) .GE. -75.0) GOTO 120
  110 IF (TIME-TPRINT-DTP)30 ,120,120
  120 CALL PRINT
```

Figure A5. Main Program Source Listing (Continued)

```
      TPRINT = TIME
      IF (YLIN.EQ.0.0) GOTO 130
      POLIS=ITRUK=TIME
      IF((POLIS.EQ.TIME).AND.(TIME.NE.0.0))CALL DERIVE(POLIS,RC,RHO,CLUS
     1T)
  130 CONTINUE
      IF(Y(30).GE.-75.0) GOTO 5
      IF (TIME .GE. TMAX) GOTO 5
      IF (TIME) 89,89,30
  410 FORMAT (10F8.0)
  420 FORMAT(3F10.3)
  430 FORMAT (10F9.3)
  440 FORMAT (3F12.3)
  450 FORMAT (20X,31HWATER IMPACT OR MAX TIME -- END)
  550 FORMAT (1H1)
  555 FORMAT(10X,41HPARACHUTE DYNAMICS AND STABILITY ANALYSIS,//,12X,
     126HNON LINEAR SIMULATION WITH,/)
  556 FORMAT (12X,19HNON STEADY AIR MASS,/)
  557 FORMAT (12X,34HELASTIC RISER AND SUSPENSION LINES,/)
  558 FORMAT (12X,42HNUMERICAL LINEARIZATION AT SELECTED POINTS,/)
  559 FORMAT(12X,10HNO OPTIONS,//)
  560 FORMAT (2X, 18HDATA CARDS AS READ,//)
 1000 FORMAT(1H1,37X,F2.0,14H CHUTE CLUSTER,7X,7HCCCCCCC,11X,4HD1 =,F7.1
     1,3H FT,/,57X,1HC,13X,1HC,7X,4HS1 =,F7.1,6H SQ FT,/,55X,1HC,17X,
     21HC,/,54X,1HC,19X,1HC,4X,4HMC =,F7.1,6H SLUGS,/,53X,1HC,21X,1HC,/,
     352X,1HC,7X,5HCP  O,11X,7HC LCP =,F7.1,3H FT ,/,51X,1HC,25X,1HC,/,
     451X,1HC,25X,1HC,/,52X,25HCCCCCCCCCCCCCCCCCCCCCCCCC,/,52X,1HL,23X,7
     5HL  RO =,F7.1,3H FT,//,53X,1HL,21X,1HL,/,79X,4HML =,F7.1,6H SLUGS,
     6/,54X,1HL,19X,1HL,/,60X,5HCM  O,14X,4HLCM=,F7.1,3H FT,/,55X,1HL,
     717X,1HL,//,56X,1HL,15X,1HL,//,57X,1HL,13X,5HL LS=,F7.1,3H FT,//,
     858X,1HL,11X,1HL,//,59X,1HL,9X,1HL,//,60X,1HL,7X,1HL,//,61X,1HL,
     95X,1HL,//,62X,1HL,3X,1HL,//,63X,3HL L,//,38X,5HRISER,21X,8HR    L2
     1=,F7.1,3H FT,/,8(64X,1HR,/),38X,20HSOLID ROCKET BOOSTER,6X,1HR,9X,
     14HD3 =,F7.1,3H FT,/,63X,3HR R,8X,4HS3 =,F7.1,6H SQ FT,/,62X,
     25HR   R,/,62X,5HR   R,7X,4HL3T=,F7.1,3H FT,/,3(62X,5HR   R,/),
     358X,9HCP  B O B,7X,4HL4 =,F7.1,3H FT,/,62X,5HR   R,/,58X,
     49HCM  B O B,7X,4HL3 =,F7.1,3H FT,/,62X,5HR   R,/,62X,5HR   R,7X,
     54HM3 =,F7.1,6H SLUGS,/,5(62X,5HR   R,/),62X,5HRRRRR,/)
      END
```

Figure A5. Main Program Source Listing (Concluded)

TABLE A3 -- BASIC SUBROUTINES USED IN PROGRAM CHUTER

Subroutine	Description	Diagram Figure No.	Listing Figure No.	Symbols Table No.
DIFEQN	Differential Equations of Motion	A6	A7	A4
CHUTE	Parachute Geometry, Inertia	A8	A9	A5
COEFTS	Parachute and Payload Aerodynamic Coefficients	A10	A11	A6
FORCES	Aerodynamic Forces	A12	A13	A7
MOMENTS	External Moments	A14	A15	A8
DIRCOS	Direction Cosines	A16	A17	A9
DBDT	Direction Cosines Rates	A18	A19	A10
PRECOR	Predictor-Corrector Integrator	A20	A29	A11
WIND	Mean Wind Profile	A22	A23	A12
GUST	Gust Envelope	A24	A25	A13
ELASTIC	Elastic Rates	A26	A27	A14
PRINT	Output	A28	A29	A15
CONST	Constants	A30	A30	--
INVELO	Initialize Velocities	A32	A33	--

Basic Subroutines

The basic subroutines are those which describe the aerodynamics, the dynamics, or the kinematics of the nonlinear simulation, the nonsteady and mass models, and techniques used in the linearization of the equations of motion. All the other subroutines are manipulatory in nature and hence are termed auxiliary subroutines.

Subroutine DIFEQN -- Subroutine DIFEQN implements the system of differential equations [Equations (16) to (39), (52) to (69)]. The time derivatives of each of the state variables and the riser force are calculated. Moments about the body fixed axes for the parachute and SRB are updated due to the change in riser force. During the Runge-Kutta initialization steps and the predictor step of subroutine PRECOR, the section of DIFEQN containing the equations coupled by the riser constraint is looped through four times to ensure that the influence of the coupled terms is uniform. Subroutine DIFEQN is diagramed in Figure A6 and a source listing is presented in Figure A7. Table A4 presents a list of symbols for DIFEQN.

Subroutine CHUTE -- Subroutine CHUTE computes the geometric and initial characteristics of the parachute as a function of time. Also calculated is the air density as a function of altitude.

The parameter CLUST, passed in calls to CHUTE, represents the number of chutes in the cluster. As all the input data were for a single chute, the mass and inertia are multiplied by CLUST to form the mass and inertial characteristics of the single chute equivalence to the cluster.

The parachute center of mass location is calculated as a function of the canopy mass, the suspension line mass, and the mass of the air included in the canopy.

Finally, when the elasticity option is employed, the ELASTIC subroutine is called to compute the rates of change of the lengths of the elastic elements.

Subroutine CHUTE is diagramed in Figure A8 and principal variables are defined in Table A5. A listing of CHUTE is given in Figure A9.

Subroutine COEFTS -- Aerodynamic coefficients are calculated for the normal and tangential forces and the moments on the parachute and payload.

The coefficients for normal force and moments are calculated as a function of the angle of attack, α, using the polynomial form.

$$C_1 \alpha + C_2 \alpha^2 + C_3 \alpha^3 + \ldots\ldots + C_8 \alpha^8 + C_9 \alpha^9$$

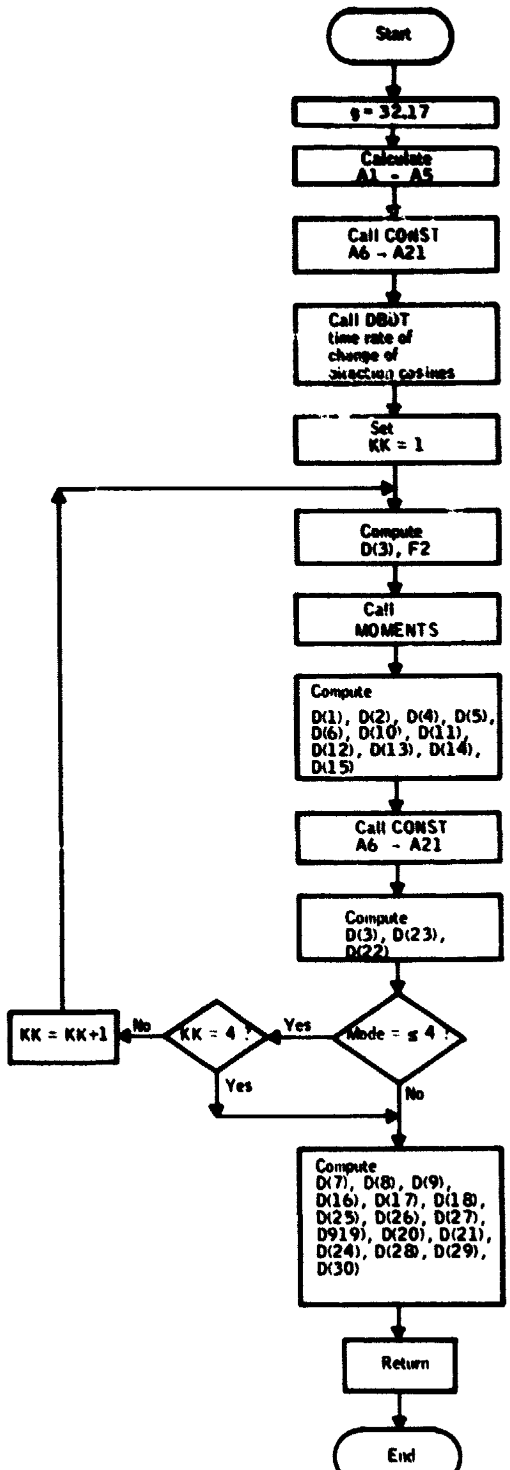

Figure A6. Subroutine DIFEQN Flow Diagram

```
      SUBROUTINE DIFEQN
C   SUBROUTINE DIFEQN CONTAINS THE SYSTEM OF NONLINEAR DIFFERENTIAL EQUATIONS    C
C   IT RETURNS THE SLOPES OF THE FUNCTIONS FOR THE TIME AT WHICH IT IS CALLED    C
      COMMON/AAB/Y(33)
      COMMON/AAC/D(30)
      COMMON/AAD/B(3,3,3),BS(6),T(3,6)
      COMMON/AAE/ AA(9),AB(9),AC(9)
      COMMON/AAG/L2,L2DOT,L2DDOT,LCM,LCMDOT,LCMDDT
      COMMON/AAH/C1,C3,F2,L3,RAD,L1,L4,CF1,CF3,S1,S3
      COMMON/AAJ/MODE
      COMMON/AAL/F1X,F1Y,F1Z,F3X,F3Y,F3Z
      COMMON/AAM/M1X,M1Y,M1Z,M3X,M3Y,M3Z
      COMMON/AAN/A6,A7,A8,A9,A10,A11,A12,A13,A14,A15,A16,A17,A18,A19,A20
      COMMON/AANN/A21
      COMMON/AAQ/IXX1,IYY1,IZZ1,IXX3,IYY3,IZZ3
      COMMON/AAQQ/IXZ1,IYX1,IZY1,IXZ3,IYX3,IZY3
      COMMON/AAR/KLS,KR,MC,ML,M1,M1A,MP,DO,RO,RHO,L2O,LCMO,LSO,M,M3
      COMMON/AARR/LS,LCP
      REAL          IXX1,IYY1,IZZ1,IXX3,IYY3,IZZ3
      REAL          IXZ1,IYX1,IZY1,IXZ3,IYX3,IZY3
      REAL M1,M3,MP,L3,KLS,KR,MC,ML,M1A,L2DOT,L2DDOT,LCM,LCMDOT,LCMDDT
      REAL L1,L3T,L4,L2O,LCMO,LSO
      REAL L2,LCP,LS
      REAL M1X,M1Y,M1Z,M3X,M3Y,M3Z,M
C CONSTANTS IN THE DIFFERENTIAL EQUATIONS
      G       = 32.17
      A1      = Y(10)-Y(14)*L3
      A2      = Y(11)+Y(13)*L3
      A3      = Y(1)+Y(5)*LCM
      A4      = Y(2)-Y(4)*LCM
      A5      = Y(3)+LCMDOT
      CALL CONST
      CALL DBDT
      MIKE=1
      IF(MODE.LE.4) MIKE=4
      DO 80 KK=1,MIKE
C DW1/DT
      D(3)    = +(1./B(1,3,3))*((AA(3)*Y(23)+Y(22)*AB(3))*L2+L2DOT*2.0
     1          *AC(3)-L2*(B(2,1,3)*D(23)-B(2,2,3)*D(22))-B(2,3,3)*L2D
     2          DOT+AA(6)*A1+A6+AB(6)*A2+A7+AC(6)*Y(12)+A10-AA(9)*A3-A
     3          8-AB(9)*A4-A9-AC(9)*A5)-LCMDDT
C RISER FORCE
      F2      = (MP*(D(3)+Y(2)*Y(4)-Y(1)*Y(5))-F1Z-M1*B(1,3,3)*G)/BS(3)
      CALL MOMENTS (RHO)
C U1DOT
      D(1)    = (F1X+M1*B(1,1,3)*G+F2*BS(1))/MP-Y(3)*Y(5)+Y(2)*Y(6)
C V1DOT
      D(2)    = (F1Y+M1*B(1,2,3)*G+F2*BS(2))/MP-Y(1)*Y(6)+Y(3)*Y(4)
C P1DOT
      D(4)    = (M1X-IZY1*Y(5)*Y(6))/IXX1
C Q1DOT
      D(5)    = (M1Y-IXZ1*Y(6)*Y(4))/IYY1
C R1DOT
      D(6)    = (M1Z-IYX1*Y(4)*Y(5))/IZZ1
```

Figure A7. Subroutine DIFEQN Source Listing

```
C U3DOT
      D(10)  = (F3X+M3*B(3,1,3)*G-F2*BS(4))/M3-Y(12)*Y(14)+Y(11)*Y(15)
C V3DOT
      D(11)  = (F3Y+M3*B(3,2,3)*G-F2*BS(5))/M3-Y(10)*Y(15)+Y(12)*Y(13)
C W3DOT
      D(12)  = (F3Z+M3*B(3,3,3)*G-F2*BS(6))/M3-Y(11)*Y(13)+Y(10)*Y(14)
C P3DOT
      D(13)  = (M3X-IZY3*Y(14)*Y(15))/IXX3
C Q3DOT
      D(14)  = (M3Y-IXZ3*Y(15)*Y(13))/IYY3
C R3DOT
      D(15)  = (M3Z-IYX3*Y(13)*Y(14))/IZZ3
      CALL CONST
C DW1/DT
      D(3)   = +(1./B(1,3,3))*((AA(3)*Y(23)+Y(22)*AB(3))*L2+L2DOT*2.0
     1         *AC(3)-L2*(B(2,1,3)*D(23)-B(2,2,3)*D(22))-B(2,3,3)*L2D
     2         DOT+AA(6)*A1+A6+AB(6)*A2+A7+AC(6)*Y(12)+A10-AA(9)*A3-A
     3         8-AB(9)*A4-A9-AC(9)*A5)-LCMDOT
C DP2/DT
      D(22)  = -(1./B(2,2,2))*(Y(23)*AA(2)+Y(22)*AB(2)-D(23)*B(2,1,2)
     1         +(1./L2)*(L2DOT*2.0*AC(2) -B(2,3,2)*L2DDOT+AA(5)*A1+A1
     2         1+AB(5)*A2+A12+AC(5)*Y(12)+A13-AA(8)*A3-A14-AB(8)*A4-A
     3         15-AC(8)*A5-A21*B(1,3,2)))
C DQ2/DT
      D(23)  = +(1./B(2,1,1))*(Y(23)*AA(1)+Y(22)*AB(1)+D(22)*B(2,2,1)
     1         +(1./L2)*(L2DOT*(2.0*(AC(1)))-B(2,3,1)*L2DDOT+AA(4)*A1
     2         +A16+AB(4)*A2+A17+AC(4)*Y(12)+A18-AA(7)*A3-A19-AB(7)*
     3         A4-A20-AC(7)*A5-A21*B(1,3,1)))
   80 CONTINUE
C PHI1DOT
      D(7)   = Y(4) +(Y(5) *SIN(Y(7)) +Y(6) *COS(Y(7)) )*TAN(Y(8))
C PHI3DOT
      D(16)  = Y(13)+(Y(14)*SIN(Y(16))+Y(15)*COS(Y(16)))*TAN(Y(17))
C PHI2DOT
      D(25)  = Y(22)+(Y(23)*SIN(Y(25))+Y(24)*COS(Y(25)))*TAN(Y(26))
C THETA1DOT
      D(8)   = Y(5) *COS(Y(7)) -Y(6) *SIN(Y(7))
C THETA3DOT
      D(17)  = Y(14)*COS(Y(16))-Y(15)*SIN(Y(16))
C THETA2DOT
      D(26)  = Y(23)*COS(Y(25))-Y(24)*SIN(Y(25))
C PSI1DOT
      D(9)   = (Y(5) *SIN(Y(7)) +Y(6) *COS(Y(7))) *SEC(Y(8))
C PSI3DOT
      D(18)  = (Y(14)*SIN(Y(16))+Y(15)*COS(Y(16)))*SEC(Y(17))
C PSI2DOT
      D(27)  = (Y(23)*SIN(Y(25))+Y(24)*COS(Y(25)))*SEC(Y(26))
C U2DOT  IS D(19) , V2DOT IS D(20) ,  AND W2DOT IS D(21) ALL UNUSED
      D(19)  = 0.0
      D(20)  = 0.0
      D(21)  = 0.0
C R2DOT
      D(24)  = 0.0
C X3EDOT
      D(28)  = +(Y(10)*B(3,1,1)+Y(11)*B(3,2,1)+Y(12)*B(3,3,1))
C Y3EDOT
      D(29)  = +(Y(10)*B(3,1,2)+Y(11)*B(3,2,2)+Y(12)*B(3,3,2))
C Z3EDOT
      D(30)  = +(Y(10)*B(3,1,3)+Y(11)*B(3,2,3)+Y(12)*B(3,3,3))
      RETURN
      END
```

Figure A7. Subroutine DIFEQN Source Listing (Concluded)

TABLE A4 – LIST OF SYMBOLS FOR SUBROUTINE DIFEQN

Quantity	Mnemonic	Units	Description
$\dot{U}_1$	D(1)	ft/sec^2	Parachute CM linear accelerations in XYZ body fixed axes directions
$\dot{V}_1$	D(2)	ft/sec^2	
$\dot{W}_1$	D(3)	ft/sec^2	
$\dot{P}_1$	D(4)	rad/sec^2	Parachute angular accelerations around XYZ body fixed axes
$\dot{Q}_1$	D(5)	rad/sec^2	
$\dot{R}_1$	D(6)	rad/sec^2	
$\dot{\phi}_1$	D(7)	rad/sec	Parachute reference frame Euler angular rates
$\dot{\theta}_1$	D(8)	rad/sec	
$\dot{\Psi}_1$	D(9)	rad/sec	
$\dot{U}_3$	D(10)	ft/sec^2	SRB CM linear acceleration in XYZ body fixed axes
$\dot{V}_3$	D(11)	ft/sec^2	
$\dot{W}_3$	D(12)	ft/sec^2	
$\dot{P}_3$	D(13)	rad/sec^2	SRB angular accelerations around XYZ body fixed axes
$\dot{Q}_3$	D(14)	rad/sec^2	
$\dot{R}_3$	D(15)	rad/sec^2	
$\dot{\phi}_3$	D(16)	rad/sec	SRB reference frame Euler angle rates
$\dot{\theta}_3$	D(17)	rad/sec	
$\dot{\Psi}_3$	D(18)	rad/sec	
$\dot{P}_2$	D(22)	rad/sec^2	Riser angular accelerations about XY body fixed axes
$\dot{Q}_2$	D(23)	rad/sec^2	

TABLE A4 - LIST OF SYMBOLS FOR SUBROUTINE DIFEQN (CONCLUDED)

Quantity	Mnemonic	Units	Description
$\dot{\phi}_2$	D(25)	rad/sec	Riser reference frame Euler angle rates
$\dot{\theta}_2$	D(26)	rad/sec	
$\dot{\Psi}_2$	D(27)	rad/sec	
$\dot{X}_{E_3}$	D(28)	ft/sec	Down range, cross range, and altitude rates of change of the SRB center of mass
$\dot{Y}_{E_3}$	D(29)	ft/sec	
$\dot{Z}_{E_3}$	D(30)	ft/sec	
F_2	F2	lbs	Riser force

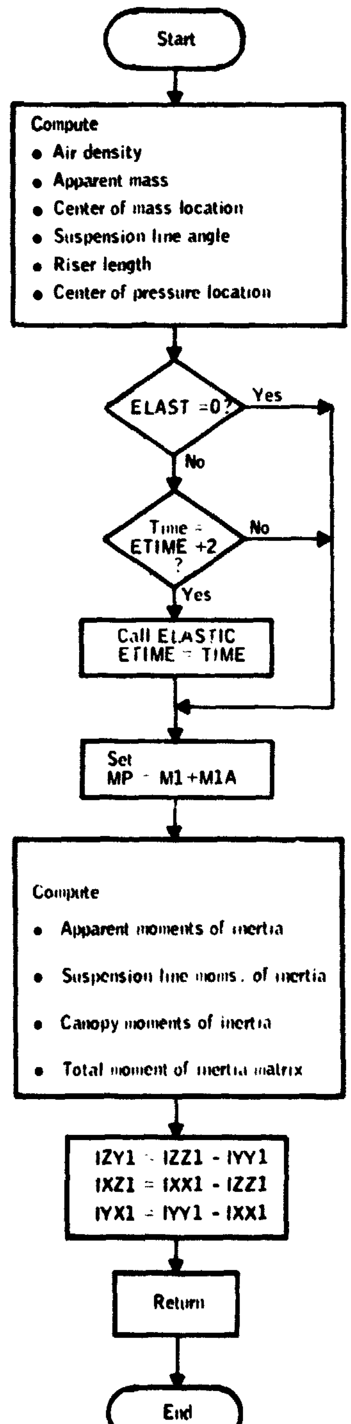

Figure A8. Subroutine CHUTE Flow Diagram

```
      SUBROUTINE CHUTE (CLUST)
C  SUBROUTINE CHUTE CALCULATES THE PARACHUTE GEOMETRY DEPENDENT VARIABLES      C
      COMMON/AAT/TIME
      COMMON/AAO/DLOTIME,YELAST,ETIME
      COMMON/AAB/ Y(33)
      COMMON/AAF/CN1,CT1,CN3,CT3,ALPHA1,ALPHA3,BETA1,BETA3,GAMMA
      COMMON/AAFF/CM1,CM3,ALCM
      COMMON/AAG/L2,L2DOT,L2DDOT,LCM,LCMDOT,LCMDDT
      COMMON/AAH/C1,C3,F2,L3,RAD,L1,L4,CF1,CF3,S1,S2
      COMMON/AAO/IXX1,IYY1,IZZ1,IXX3,IYY3,IZZ3
      COMMON/AAOO/IXZ1,IYX1,IZY1,IXZ3,IYX3,IZY3
      COMMON/AAR/KLS,KR,MC,ML,M1,M1A,MP,DO,RO,RHO,L2O,LCMO,LSO,M,M3
      COMMON/AARR/LS,LCP
      COMMON/XOROS/SUMMA1,SUMMA2,TOTAL,AVERA1,AVERA2,OVERA1,OVERA2,DT
      REAL IXXA1,IXXA3,IXX1,IXX1O,IXX3,IXZ1,IXZ3
      REAL IYYA1,IYYA3,IYY1,IYY1O,IYY3,IYX1,IYX3
      REAL IZZA1,IZZA3,IZZ1,IZZ1O,IZZ3,IZY1,IZY3
      REAL KLS,KR,LCM,LCMDOT,LCMDDT,LCMO,LCP,LS,LSO,L1,L2,L2DOT,L2DDOT
      REAL L2O,L3,L3T,L4,MC,ML,M1,M1A,M,MP,M3
C CLUST IS THE NUMBER OF CHUTES IN THE CLUSTER
C **CLUSTER REPRESENTATION** THE CLUSTER OF PARACHUTES IS MODELED AS A SINGLE
C EQUIVELANT PARACHUTE HAVING THE SAME GEOMETRIC CHARACTERISTIC AS A SINGLE
C ELEMENT OF THE CLUSTER BUT HAVING THE MASS, INERTIA, AND DRAG AREA OF THE
C ENTIRE CLUSTER)   IN THE INPUT DATA ALL THE  PHYSICAL QUANTITIES FOR THE
C PARACHUTE SHOULD BE FOR THE SINGLE ELEMENT.  THE CHANGE TO THE EQUIVELANCE
C IS HANDLED BY THE PROGRAM AS REQUIRED.    THE NUMBER OF PARACHUTES IN THE
C CLUSTER IS GIVEN BY THE VARIABLE *CLUST*.
      RHONOT = 0.00238
      RHO    = RHONOT*(EXP(-Y(30)/31600.))
C APPARENT MASS
      M1A    = RHO*0.782*(0.36*DO)**3
      M1A    = M1A*CLUST
C LENGTH FROM CONFLUENCE POINT TO THE PLANE OF THE SKIRT
      ALCM   = SQRT(LS*LS-RO*RO)
C INCLUDED CANOPY MASS
      CAPMAS  = 0.00817*DO**3
C PARACHUTE CENTER OF MASS LOCATION
      LCM    = (ALCM*ML/2.0+(ALCM+LCP)*CAPMAS*CLUST+(ALCM+LCP)*MC)/
     1(CAPMAS*CLUST+MC+ML)
C SUSPENSION LINE ANGLE
      GAMMA  = ATAN(RO/ALCM)
C SUSPENSION LINE LENGTH
      LS     = LSO+(F2-0.05*LCMDOT)/(M*COS(GAMMA)*KLS)
C RISER LENGTH
      L2     = L2O+(F2-0.05*L2DOT)/KR
      SUMMA1= SUMMA1+L2
C DISTANCE FROM THE CONFLUENCE POINT TO THE CENTER OF PRESSURE
      L1     = ALCM + LCP
C  ELASTICITY CALLS
      IF (YELAST.EQ.0.0) GOTO 35
C ELASTIC RATES ARE CALCULATED AT ONE SECOND INTERVALS
      IF((TIME-ETIME-1.0).LT.0.0) GOTO 35
      IF(TIME.GT.DT2) GO TO 10
      L2= OVERA1= SUMMA1/TOTAL

      LCM= OVERA2= SUMMA2/TOTAL
      GO TO 30
   10 AVERA1= SUMMA1/TOTAL
      AVERA2= SUMMA2/TOTAL
      CALL ELASTIC
   30 SUMMA1= SUMMA2= TOTAL= 0.0
      ETIME= TIME
   35 CONTINUE
      SUMMA2= SUMMA2+LCM
      TOTAL =TOTAL+1.0
C INERTIAL CHARACTERISTICS, PARACHUTE
      MP     = M1+M1A
C APPARENT MOMENTS OF INERTIA WRT CM LOCATION
      IXXA1  = 0.042*RHO*(0.36*DO)**5+M1A*(L1-LCM)*(L1-LCM)/CLUST
      IXXA1  = IXXA1*CLUST
      IYYA1  = IXXA1
      IZZA1  = 0.063*RHO*(0.36*DO)**5
      IZZA1  = IZZA1*CLUST
C SUSPENSION LINE MOMENTS OF INERTIA ABOUT A POINT ALCM/2 AHEAD OF THE
C CONFLUENCY POINT
      XSL    = (ML*LS*LS*(COS(GAMMA))**2)/12.0
      ZSL    = (ML*LS*LS*(SIN(GAMMA))**2)/ 12.0
C CANOPY MOMENTS OF INERTIA ABOUT A POINT ALCM AHEAD OF THE CONFLUENCE POINT
      XC     = 0.32833*MC*DO*DO
      ZC     = 0.375*MC*DO*DO
C TOTAL REAL MOMENTS OF INERTIA WRT THE CM LOCATION
      IXX1O  = XSL+ML*(LCM-ALCM/2.0)**2+XC+MC*(ALCM-LCM)**2
      IYY1O  = IXX1O
      IZZ1O  = ZSL+ZC
C TOTAL MOMENTS OF INERTIA OF THE PARACHUTE WRT THE CM LOCATION
      IXX1   = IXX1O+IXXA1
      IYY1   = IYY1O+IYYA1
      IZZ1   = IZZ1O+IZZA1
C **NOTE** THE APPARENT AND REAL INERTIAL PROPERTIES OF
C           THE PARACHUTE HAVE BEEN COMBINED AT THIS POINT
      IZY1   = IZZ1-IYY1
      IXZ1   = IXX1-IZZ1
      IYX1   = IYY1-IXX1
      RETURN
```

Figure A9. Subroutine CHUTE Source Listing

TABLE A5 - LIST OF SYMBOLS FOR SUBROUTINE CHUTE

Quantity	Mnemonic	Units	Description
ALCM	ALCM	ft	Length, confluence point to plane of skirt
MI	CAPMAS	slugs	Included mass
γ	GAMMA	rad	Suspension line angle
IXX_{A1}	IXXA1		Apparent mass tensor
IYY_{A1}	IYYA1		Diagonal Elements
IZZ_{A1}	IZZA1		
IXX*	IXX10		Total parachute
IYY*	IYY10		Inertia Matrix
IZZ*	IZZ10		Diagonal Elements
L_{C_M}	LCM	ft	Length, confluence point to plane of skirt
L_{C_P}	LCP	ft	Length, plane of skirt to center of pressure
L_S	LS	ft	Suspension line length
L1	L1	ft	LCM + LCP
L2	L2	ft	Riser length
L3	L3	ft	SRB Center of Mass Location from nose
L4	L4	ft	SRB Center of pressure location from center of mass
N	M	---	Number of suspension lines
m_C	MC	slugs	Canopy mass
m_L	ML	slugs	Suspension lines mass
m_P	MP	slugs	$m_1 + m_{1a}$
m_1	M1	slugs	$m_c + m_L$
m_{1a}	M1A	slugs	Apparent mass
m_3	M3	slugs	SRB mass

TABLE A5 - LIST OF SYMBOLS FOR SUBROUTINE CHUTE (CONCLUDED)

Quantity	Mnemonic	Units	Description
ρ	RHO	slugs/ft^3	Air density
R_o	RO	ft	Skirt diameter
S_{o_1}	S1	ft^2	Nominal area of parachute
S_{o_3}	S3	ft^2	Nominal area SRB
	XC	slug ft^2	Canopy moments of inertia
	ZC	slug ft^2	
	XSL	slug ft^2	Suspension lines moments of inertia
	ZSL	slug ft^2	

Coefficients for the tangent force are calculated as function of the angle of attack, α, using the polynomial form

$$C_1 \alpha + C_2 \alpha^2 + C3 \alpha^3 + \ldots\ldots + C_8 \alpha^8 + C_9 \alpha^9$$

Specifically for the parachute the normal force coefficient polynomial is of order three, the tangent force coefficient polynomial is of order five, and the moment coefficient polynomial is of order eight.

The SRB normal force coefficient polynomial is of order eight, the tangent force coefficient polynomial is of order five, and the moment coefficient polynomial is of order nine.

Angle of Attack -- The angle of attack is defined as the angle between the body axis of symmetry and the relative velocity vector.

$$\alpha_i = \mathrm{Tan}^{-1} \sqrt{\frac{Va_{Xi}{}^2 + Va_{Yi}{}^2}{Va_{Zi}}}$$

Sideslip Angle -- The side slip angle is defined for this problem to be the angle between the body fixed X axis and the projection of the relative velocity vector on the body fixed X-Y plane. Thus,

$$\beta_i = \mathrm{Tan}^{-1} \frac{Va_{Yi}}{Va_{Xi}}$$

Subroutine COEFTS is diagrammed in Figure A10 and listed in Figure A11. Principal variables are listed in Table A6.

Subroutine FORCES, Subroutine MOMENTS -- The subroutines FORCES and MOMENTS calculate the aerodynamic forces and total external (aero-dynamic and constraint) moments on the parachute and the payload. The dynamic pressure at the center of pressure of each body is calculated.

Subroutine FORCES is diagrammed in Figure A12 and listed in Figure A13, and its principal variables are listed in Table A7.

Subroutine MOMENTS is diagrammed in Figure A14 and listed in Figure A15, and its principal variables listed in Table A8.

Subroutine DIRCOS, Subroutine DBDT -- Subroutines DIRCOS and Subroutine DBDT calculate and manipulate the matrices of direction cosines describing the orientations of the reference frame, parachute, riser, and payload with respect to the earth. DIRCOS calculates the immediate direction cosines matrices as functions of the Euler angles at each integration step.

For resolution of the riser force (the constraint force) into the parachute and payload reference frames directions, direction cosines matrices are formed describing the orientations of [illegible] fixed axis system with respect to the parachute and the payload body fixed axes systems.

Subroutine DIRCOS is diagrammed in Figure A16 and listed in Figure A17, and its principal variables defined in Table A9.

Subroutines DBDT is diagrammed in Figure A18 and listed in Figure A19, and its principal variables defined in Table A10.

Subroutine PRECOR -- Subroutine PRECOR integrates the equations of motion using a Runge Kutta initialization and a predictor-corrector integration algorithm (Ref. 12).

The Runge Kutta method establishes values for the state vector at time zero and at time equal to one integration step size. Using these two initial points the state vector is updated in the predictor mode (mode = 5) and time is increased one integration step size. The corrector mode (mode = 6) refines the prediction made when mode = 5. Completion of the corrections returns control to the main program for calculation of everything associated with the newly calculated state vector.

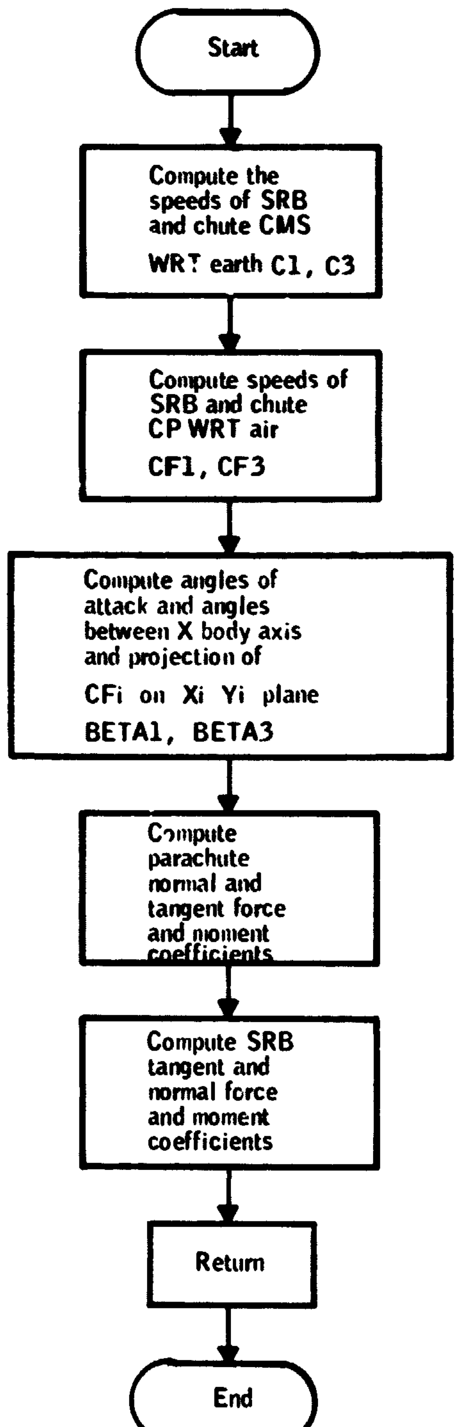

Figure A10. Subroutine COEFTS Flow Diagram

```
      SUBROUTINE COEFTS (BC)
C  SUBROUTINE COEFTS CALCULATES THE AERODYNAMIC COEFFICIENTS OF THE PARA-   C
C  CHUTE AND THE SRB AS FUNCTIONS OF ALTITUDE,VELOCITY, AND ANGLE OF ATTACK  C
      COMMON/AAA/ACT(9),ACN(9),ACM(9),BCT(9),BCN(9),BCM(9)
      COMMON/AAB/ Y(33)
      COMMON/AAD/B(3,3,3),BS(6),T(3,6)
      COMMON/AAF/CN1,CT1,CN3,CT3,ALPHA1,ALPHA3,BETA1,BETA3,GAMMA
      COMMON/AAFF/CM1,CM3,ALCM
      COMMON/AAG/L2,L2DOT,L2DDOT,LCM,LCMDOT,LCMDDT
      COMMON/AAH/C1,C3,F2,L3,RAD,L1,L4,CF1,CF3,S1,S3
      COMMON/AAP/YWIND,VWIND,VGUST,WIGU
      REAL L1,L3,L4
      REAL L2,L2DOT,L2DDOT,LCM,LCMDOT,LCMDDT
C VELOCITIES SQUARED OF THE CGS OF BODIES 1 AND 3
C INERTIAL VELOCITIES SQUARED OF THE CM'S OF BODIES 1 AND 3
      C1      = Y(1)*Y(1)+Y(2)*Y(2)+Y(3)*Y(3)
      C3      = Y(10)*Y(10)+Y(11)*Y(11)+Y(12)*Y(12)
C VELOCITIES SQUARED AT THE CP'S OF BODIES 1 AND 3 WRT THE AIR MASS
      CF1     = (Y(1)-Y(5)*(L1-LCM)-WIGU*B(1,1,1))**2+(Y(2)+Y(4)*(L1-LCM)
     1          -WIGU*B(1,2,1))**2+(Y(3)-WIGU*B(1,3,1))**2
      CF3     = (Y(10)+Y(14)*L4-WIGU*B(3,1,1))**2+(Y(11)-Y(13)*L4-WIGU*B(
     1          3,2,1))**2+(Y(12)-WIGU*B(3,3,1))**2
C NORMAL COMPONENTS OF VELOCITY AT THE CP OF BODIES 1 AND 3
C WITH RESPECT TO THE AIR MASS
      CNORF1 = SQRT(ABS(CF1-(Y(3)-WIGU*B(1,3,1))**2))
      CNORF3 = SQRT(ABS(CF3-(Y(12)-WIGU*B(3,3,1))**2))
C ANGLES OF ATTACK
      ALPHA1 = ATAN(CNORF1/(Y(3)-WIGU*B(1,3,1)+1.0E-14))
      IF (Y(1)-Y(5)*(L1-LCM )-WIGU*B(1,1,1).GT. 0.0) ALPHA1 = -ALPHA1
      ALPHA3 = ATAN(CNORF3/(Y(12)-WIGU*B(3,3,1)+1.0E-14))
      IF (Y(10)+Y(14)*L4-WIGU*B(3,1,1).GT.0.0) ALPHA3 = -ALPHA3
C ANGLE BETWEEN THE X AXIS AND THE PROJECTION OF C ON THE X-Y PLANE,
C BODIES 1 AND 3
      BETA1   = ATAN((Y(2)+Y(4)*(L1-LCM)-WIGU*B(1,2,1))/(Y(1)-Y(5)*(L1-LC
     1M)-WIGU*B(1,1,1)+1.0E-14))
      BETA3   = ATAN((Y(11)-Y(13)*L4-WIGU*B(3,2,1))/(Y(10)+Y(14)*L4-WIGU*
     1B(3,1,1)+1.0E-14))
C PARACHUTE NORMAL FORCE COEFFICIENT
      CN1     = ACN(1)*ALPHA1+ACN(2)*ALPHA1**2+ACN(3)*ALPHA1**3
C SRB NORMAL FORCE COEFFICIENT
      CN3     = BCN(1)*ALPHA3+BCN(2)*ALPHA3**2+BCN(3)*ALPHA3**3
     1        +BCN(4)*ALPHA3**4+BCN(5)*ALPHA3**5+BCN(6)*ALPHA3**6
     2        +BCN(7)*ALPHA3**7+BCN(8)*ALPHA3**8
C PARACHUTE TANGENT FORCE COEFFICIENT
      CT1     = ACT(1)+ACT(2)*ALPHA1+ACT(3)*ALPHA1**2+ACT(4)*ALPHA1**3
     1          +ACT(5)*ALPHA1**4+ACT(6)*ALPHA1**5
C SRB TANGENT FORCE COEFFICIENT
      CT3     = BCT(1)+BCT(2)*ALPHA3+BCT(3)*ALPHA3**2+BCT(4)*ALPHA3**3
     1          +BCT(5)*ALPHA3**4+BCT(6)*ALPHA3**5
     2        +BCT(7)*ALPHA3**6+BCT(8)*ALPHA3**7+BCT(9)*ALPHA3**8
      CM1     = ACM(1)*ALPHA1
      CM3     = BCM(1)*ALPHA3
      DO 10 I=2,9
C PARACHUTE MOMENT COEFFICIENT

      CM1     = CM1+ACM(I)*ALPHA1**I
C PAYLOAD  MOMENT COEFFICIENT
   10 CM3     = CM3+BCM(I)*ALPHA3**I
      RETURN
      END
```

Figure A11. Subroutine COEFTS Source Listing

TABLE A6 - LIST OF SYMBOLS FOR SUBROUTINE COEFTS

Quantity	Mnemonic	Units	Description	
	ACM	---	Constants in polynomials	
	ACN	---	for parachute aerodynamic	
	ACT	---	coefficient	
α_1	ALPHA 1	rad	Parachute angle of attack	
α_3	ALPHA 3	rad	SRB angle of attack	
	BCM	---	Constants in polynomials	
	BCN	---	for SRB aerodynamic	
	BCT	---	coefficients	
β_1	BETA 1	rad	Parachute sideslip angle	
β_3	BETA 3	rad	SRB sideslip angle	
Va_1^2	CF1	(ft/sec^2)	Velocities squared of the CP's WRT	parachute
Va_3^2	CF3	(ft/sec^2)	the moving air mass	SRB
C_{M_1}	CM1	---	Moment coefficients	parachute
C_{M_3}	CM3	---		SRB
C_{N_1}	CN1	---	Normal force coefficients	parachute
C_{N_3}	CN3	---		SRB
C_{T_1}	CT1	---	Tangent force coefficients	parachute
C_{T_3}	CT3	---		SRB
C_1	C1	$(ft/sec)^2$	Inertial velocities	parachute
C_3	C3	$(ft/sec)^2$	Squared	SRB

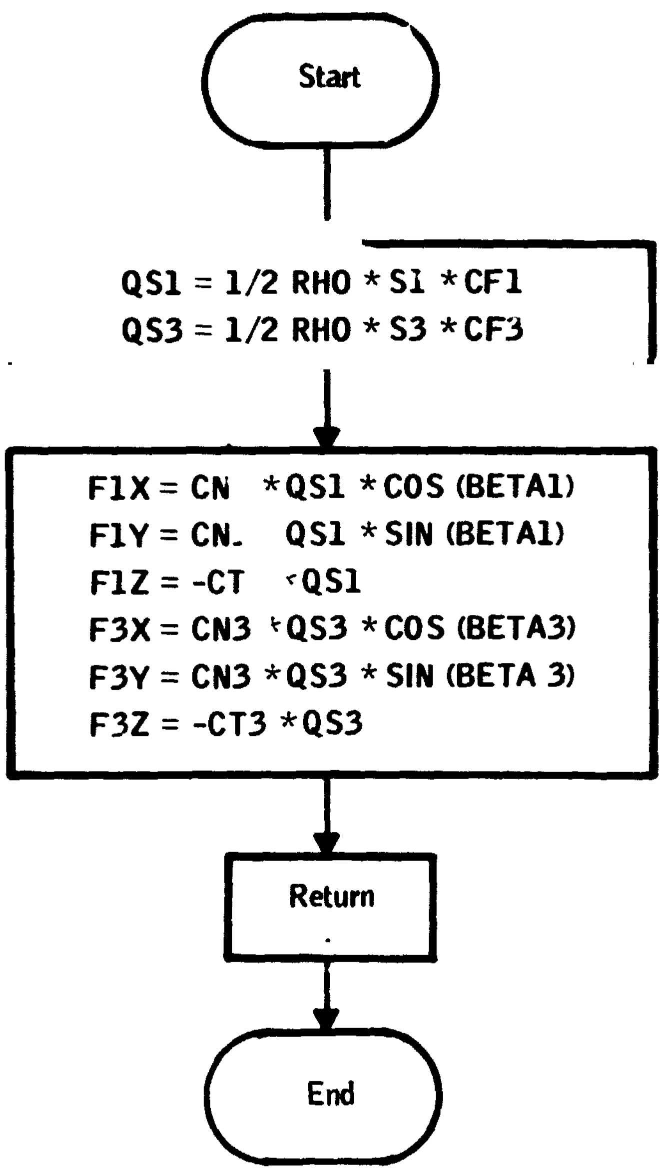

Figure A12. Subroutine FORCES Flow Diagram

```
      SUBROUTINE FORCES
C SUBROUTINE FORCES CALCULATES THE AERODYNAMIC FORCES ON THE PARACHUTE AND SRB C
C AS FUNCTIONS OF THE VELOCITY OF THE CP RELATIVE TO THE AIR AND THE ANGLE OF  C
C ATTACK                                                                        C
      COMMON/AAF/CN1,CT1,CN3,CT3,ALPHA1,ALPHA3,BETA1,BETA3,GAMMA
      COMMON/AAH/C1,C3,F2,L3,RAD,L1,L4,CF1,CF3,S1,S3
      COMMON/AAL/F1X,F1Y,F1Z,F3X,F3Y,F3Z
      COMMON/AAR/KLS,KR,MC,ML,M1,M1A,MP,DO,RO,RHO,L2O,LCMO,LSO,M,M3
      REAL L1,L3,L4
      REAL KLS,KR,MC,ML,M1,M1A,MP,L2O,LCMO,LSO,M,M3
C DYNAMIC PRESSURE, BODIES 1 AND 3
      QS1    = 0.5*CF1*S1*RHO
      QS3    = 0.5*CF3*S3*RHO
C AERODYNAMIC FORCES IN X, Y, AND Z BODY FIXED AXIS DIRECTIONS, BODIES 1 AND 3
      F1X    = +CN1*QS1*COS(BETA1)
      F1Y    = +CN1*QS1*SIN(BETA1)
      F1Z    = -CT1*QS1
      F3X    = +CN3*QS3*COS(BETA3)
      F3Y    = +CN3*QS3*SIN(BETA3)
      F3Z    = -CT3*QS3
      RETURN
      END
```

Figure A13. Subroutine FORCES Source Listing

TABLE A7 - LIST OF SYMBOLS FOR SUBROUTINE FORCES

Quantity	Mnemonic	Units	Description
F_{1X}	F1X	lb	parachute aerodynamic
F_{1Y}	F1Y	lb	forces in XYZ
F_{1Z}	F1Z	lb	body fixed axes directions
F_{3X}	F3X	lb	SRB aerodynamic forces
F_{3Y}	F3Y	lb	in XYZ body fixed
F_{3Z}	F3Z	lb	directions
$q_1 S_{o_1}$	QS1	lb/ft^2	$\frac{1}{2} \rho V_{a1}^2 S_{o_1}$
$q_3 S_{o_3}$	QS3	lb/ft^2	$\frac{1}{2} \rho V_{a3}^2 S_{o_3}$

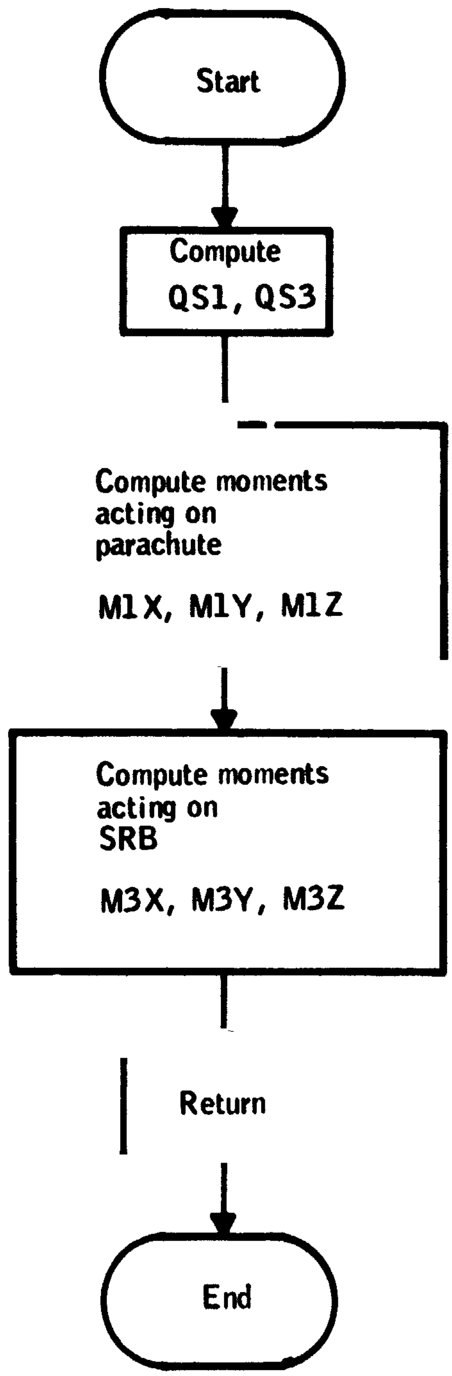

Figure A14. Subroutine Moments Flow Diagram

```
      SUBROUTINE MOMENTS (ROW)
      COMMON/AAF/CN1,CT1,CN3,CT3,ALPHA1,ALPHA3,BETA1,BETA3,GAMMA
C SUBROUTINE MOMENTS CALCULATES THE MOMENTS ABOUT THE CM OF THE PARACHUT AND SRB
C AS RESULTING FROM THE EXTERNAL FORCES ACTING ON THE BODIES                   C
      COMMON/AAD/P(3,3,3),RS(5),T(3,6)
      COMMON/AAFF/CM1,CM3,ALCM
      COMMON/AAG/L2,L2DOT,L2DDOT,LCM,LCMDOT,LCMDDT
      COMMON/AAH/C1,C3,F2,L3,RAD,L1,L4,CF1,CF3,S1,S3
      COMMON/AAHH/D3
      COMMON/AAI/F1X,F1Y,F1Z,F3X,F3Y,F3Z
      COMMON/AAJ/M1X,M1Y,M1Z,M3X,M3Y,M3Z
      COMMON/AAR/KLS,KR,MC,ML,M1,M1A,MP,DO,RO,RHO,L20,LCMO,LSO,M,M3
      REAL KLS,KR,MC,ML,M1,M1A,MP,L20,LCMO,LSO,M,M3
       REAL L1,L3,L3T,L4,LCM,M1X,M1Y,M1Z,M3X,M3Y,M3Z
      REAL L2,L2DOT,L2DDOT,LCMDOT,LCMDDT
C EXTERNAL MOMENTS SUMMED ABOUT THE CG  FOR BODIES 1 AND 3
      RHO = ROW
      QS1    = 0.5*CF1*S1*RHO
      QS3    = 0.5*CF3*S3*RHO
      M1X    = -CM1*QS1*DO*((0.325*DO+ALCM-LCM)/(1.326*DO))*SIN(BETA1)-
     1F2*RS(2)*LCM
      M1Y    =  CM1*QS1*DO*((0.325*DO+ALCM-LCM)/(1.326*DO))*COS(BETA1)+
     1F2*RS(1)*LCM
      M1Z    = 0.0
      M3X    = -CM3*QS3*(D3*L4/(L3+L4))*COS(BETA3)-F2*RS(5)*L3
      M3Y    =  CM3*QS3*(D3*L4/(L3+L4))*SIN(BETA3)+F2*RS(4)*L3
      M3Z    = 0.0
      RETURN
      END
```

Figure A15. Subroutine Moments Source Listing

TABLE A8 - LIST OF SYMBOLS FOR SUBROUTINE MOMENTS

Quantity	Mnemonic	Units	Description
M_{1X}	M1X	ft-lb	total external moments
M_{1Y}	M1Y	ft-lb	about XYZ parachute
M_{1Z}	M1Z	ft-lb	body fixed axes
M_{3X}	M3X	ft-lb	total external moments
M_{3Y}	M3Y	ft-lb	about XYZ SRB
M_{3Z}	M3Z	ft-lb	body fixed axes

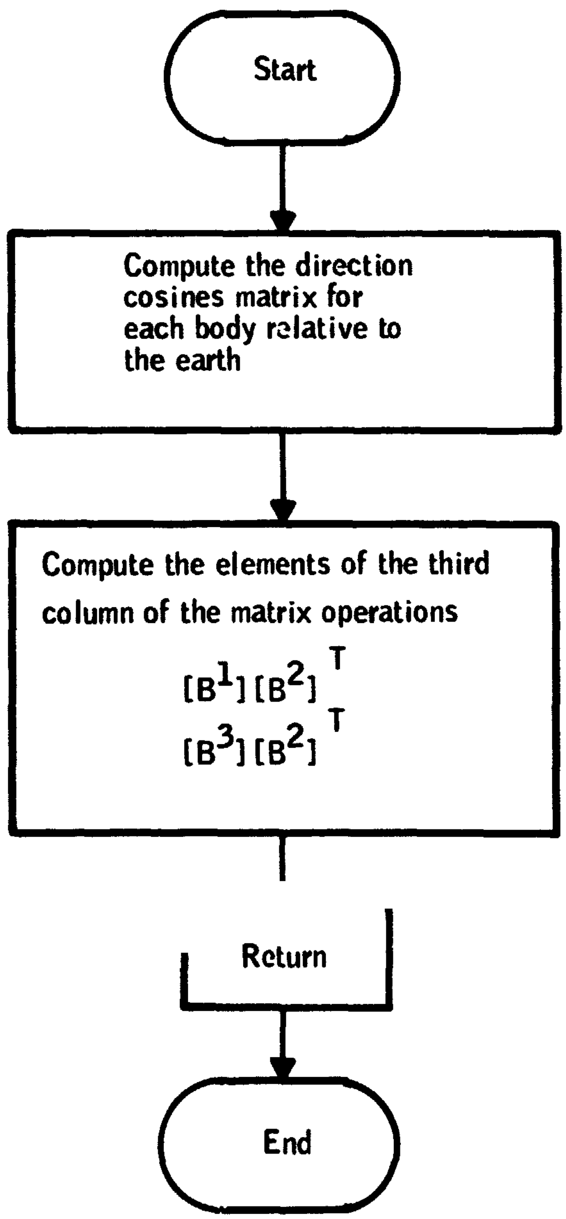

Figure A16. Subroutine DIRCOS Flow Diagram

```
      SUBROUTINE DIRCOS
C*************************************************************************C
C SUBROUTINE DIRCOS (DIRECTION COSINES) FORMS THE IMMEDIATE DIRECTION     C
C COSINES MATRICES FOR THE PARACHUTE, THE RISERS, AND THE PAYLOAD AND     C
C FORMS THE RELATIONS NEEDED TO RESOLVE THE FORCE IN THE RISER  INTO THE BODY C
C FIXED COORDINATE SYSTEMS OF THE PARACHUTE AND THE PAYLOAD               C
C THE DIRECTION COSINE MATICES ARE NOTED AS FOLLOWS ... B(I,J,K) WHERE I IS C
C THE PARTICULAR REFERENCE FRAME,  J  IS THE ROW NUMBER, AND  K  IS THE   C
C COLUMN NUMBER FOR THE ELEMENTS IN THE 3X3 MATRIX.                       C
C                                                                         C
C*************************************************************************C
      COMMON/AAB/ Y(33)
      COMMON/AAD/B(3,3,3),BS(6),T(3,6)
      K        = 1
      DO 20 IJ = 1,5,2
      I = IJ
      IF (IJ .EQ.5) I = 2
      K        = K+6
      DO 10  J = 2,6,2
      T(I,J-1) = SIN(Y(K))
      T(I,J)   = COS(Y(K))
   10 K        = K+1
   20 CONTINUE
      DO 30 IJ = 1,5,2
      I = IJ
      IF (IJ .EQ.5) I = 2
      B(I,1,1) = T(I,6)*T(I,4)
      B(I,1,2) = T(I,5)*T(I,4)
      B(I,1,3) =-T(I,3)
      B(I,2,1) = T(I,1)*T(I,3)*T(I,6)-T(I,2)*T(I,5)
      B(I,2,2) = T(I,5)*T(I,3)*T(I,1)+T(I,6)*T(I,2)
      B(I,2,3) = T(I,4)*T(I,1)
      B(I,3,1) = T(I,6)*T(I,3)*T(I,2)+T(I,5)*T(I,1)
      B(I,3,2) = T(I,2)*T(I,3)*T(I,5)-T(I,1)*T(I,6)
   30 B(I,3,3) = T(I,4)*T(I,2)
      K        = 1
      DO 40  I = 1,3,2
      DO 40  J = 1,3
      BS(K)    = B(I,J,1)*B(2,3,1)+B(I,J,2)*B(2,3,2)+B(I,J,3)*B(2,3,3)
   40 K        = K+1
      RETURN
      END
```

Figure A17. Subroutine DIRCOS Source Listing

TABLE A9 - LIST OF SYMBOLS FOR SUBROUTINE DIRCOS

Quantity	Mnemonic	Units	Description
B^j_{ik}	B(J, I, K)	---	Direction cosine matrix elements i, k = 1, 2, 3 j = 1 parachute j = 2 riser j = 3 SRB used for rotating a vector in Earth coordinates to one in j coordinate system
B_{S1}	BS(1)	---	proportion of F_2 projected
B_{S2}	BS(2)	---	on X, Y, Z parachute
B_{S3}	BS(3)	---	body-fixed axes
B_{S4}	BS(4)	---	proportion of F_2 projected
B_{S5}	BS(5)	---	on X, Y, Z SRB body
B_{S6}	BS(6)	---	fixed axes

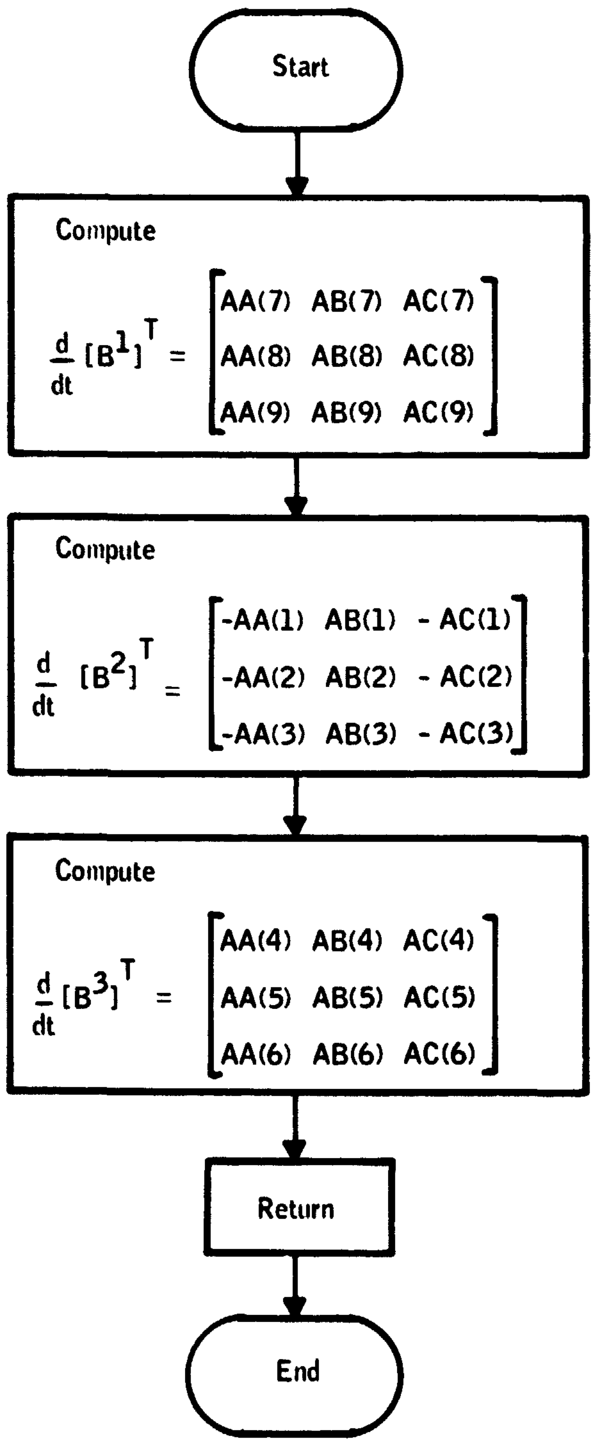

Figure A18. Subroutine DBDT Flow Diagram

```
      SUBROUTINE DBDT
C SUBROUTINE DBDT CALCULATES THE TIME RATE OF CHANGE OF THE DIRECTION COSINES  C
C MATRIX FOR USE IN THE DIFFERENTIAL EQUATIONS OF MOTION                         C
      COMMON/AAB/ Y(33)
      COMMON/AAD/B(3,3,3),BS(6),T(3,6)
      COMMON/AAF/ AA(9),AB(9),AC(9)
C CONSTANTS IN THE DIFFERENTIAL EQUATIONS
      DO 40 I= 1,3
      AA(I)   = Y(23)*B(2,3,I)-Y(24)*B(2,2,I)
      AA(I+3)= Y(15)*B(3,2,I)-Y(14)*B(3,3,I)
      AA(I+6)= Y(6) *B(1,2,I)-Y(5) *B(1,3,I)
      AB(I)   = Y(22)*B(2,3,I)-Y(24)*B(2,1,I)
      AB(I+3)= Y(13)*B(3,3,I)-Y(15)*B(3,1,I)
      AB(I+6)= Y(4) *B(1,3,I)-Y(6) *B(1,1,I)
      AC(I)   = Y(22)*B(2,2,I)-Y(23)*B(2,1,I)
      AC(I+3)= Y(14)*B(3,1,I)-Y(13)*B(3,2,I)
   40 AC(I+6)= Y(5) *B(1,1,I)-Y 4) *B(1,2,I)
      RETURN
      END
```

Figure A19. Subroutine DBDT Source Listing

TABLE A10 - LIST OF SYMBOLS FOR SUBROUTINE DBDT

Quantity	Mnemonic	Units	Description
- -	AA (array)	---	Array containing elements of the first columns of the time derivatives matrices of bodies 1, 2, and 3
---	AB (array)	---	Second column elements
---	AC (array)	---	Third column elements

Subroutine PRECOR is diagrammed in Figure A20 and listed in Figure A21, and its principal variables are listed in Table A11.

Subroutine WIND -- Subroutine WIND calculates at each integration step the value of the 5% risk wind speed profile as a function of the altitude. The wind velocity vector is assumed to be aligned with the earth-fixed reference frame X axis.

Subroutine WIND is diagrammed in Figure A22 and listed in Figure A23, and its principal variables are listed in Table A12.

Subroutine GUST -- Subroutine GUST computes a step change in the air mass velocity vector according to a 5% risk gust envelope related to the 5% risk wind profile. The step changes are calculated at a frequency of four per minute of simulation time and are both sign and magnitude modified by a random function.

Subroutine GUST is diagrammed in Figure A24 and listed in Figure A25, and its principal variables are listed in Table A13.

Subroutine ELASTIC -- When the elasticity option is employed, subroutine ELASTIC is called at two-second intervals to determine the first and second time derivatives of the lengths of the elastic elements, the riser, and the suspension lines. The method employs a central difference method on an averaged length.

Subroutine ELASTIC is diagrammed in Figure A26 and listed in Figure A27, and its principal variables are listed in Table A16.

Subroutine PRINT -- Subroutine PRINT controls the line printer operation and loads plotting storage arrays. Ten groups of data are printed on each page. This is adjusted by changing the line output counter (LOC). When the number of groups printed equals LOC, a heading is printed at the top of the next page and the LOC is set to zero.

Corresponding to each output group, the values for altitude, range, angles of attack, pitch angles (θi), riser force, riser length, center of parachute mass, and the air mass velocity are loaded into arrays for use in plotting.

Subroutine PRINT is diagrammed in Figure A28 and listed in Figure A29. Its principal variables are listed in Table A15.

Subroutine CONST --Subroutine CONST calculates a group of variable combinations used in the differential equations subroutine DIFEQN that result from the method of coupling of the parachute and payload. Generally, these are the accelerations of the confluence point and attach point in components parallel to the earth fixed axis system.

Subroutine CONST is diagrammed in Figure A30 and listed in Figure A31.

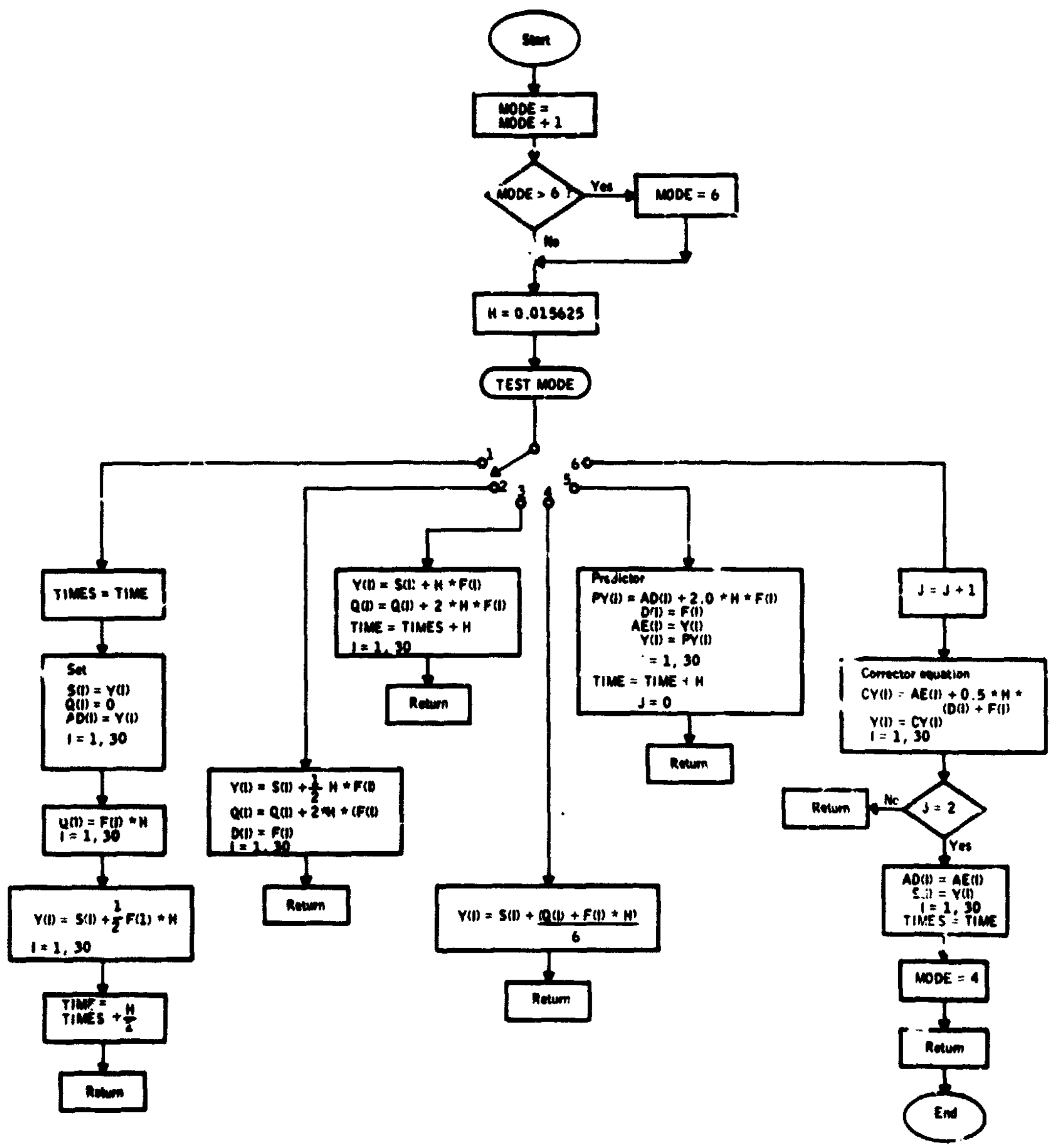

Figure A20. Subroutine PRECOR Source Listing

```
      SUBROUTINE PRECOR (N,F,H)
C***********************************************************************************C
C                                                                                   C
C SUBROUTINE PRECOR (PREDICTOR - CORRECTOR) INTEGRATES THE SYSTEM OF                C
C DIFFERENTIAL EQUATIONS.  ITS FEATURES INCLUDE A RUNGA-KUTTA INITIALIZATION.       C
C                                                                                   C
C***********************************************************************************C
      COMMON/AAB/ Y(33)
      COMMON/AAJ/MODE
      COMMON/AAT/TIME
      DIMENSION D(33),AD(33),AE(33),F(33),PY(33),CY(33),Q(33),S(33)
      MODE   = MODE + 1
      IF (MODE .GT. 6) MODE = 6
    2 CONTINUE
      H      =  .015625
      IF (TIME.LT.15.) H = 0.0078125
      IF (TIME.GE.25.0) H = 0.03125
      GOTO (3,4,8,9,16,19), MODE
    3 TIMES    = TIME
      DO 5 I = 1,N
      S(I)    = Y(I)
      Q(I)    = 0.0
      AD(I)   = Y(I)
      D(I)    = F(I)*H
    5 Y(I)    = S(I) + 0.5*H*F(I)
      TIME    = TIMES +0.5*H
      GOTO 13
    4 DO 50 I =1,N
      Y(I)    = S(I)+0.5*H*F(I)
      Q(I)    = Q(I)+2.0*H*F(I)
   50 D(I)    = F(I)
      GOTO 13
    8 DO 60 I=1,N
      Y(I)    = S(I)+H*F(I)
   60 Q(I)    = Q(I)+2.0*H*F(I)
      TIME    = TIMES + H
      GOTO13
    9 DO 70 I=1,N
   70 Y(I)    = S(I)+(Q(I)+F(I)*H)/6.0
   13 K       = 1
      RETURN
   16 DO 17 I= 1,N
C PREDICTOR EQUATION
      PY(I)   = AD(I)+2.0*H*F(I)
      D(I)    = F(I)
      AE(I)   = Y(I)
   17 Y(I)    = PY(I)
      TIME    = TIME+H
      J       = 0
   18 K       = 1
      RETURN
   19 J       = J+1
      DO 20 I= 1,N
C CORRECTOR EQUATION
      CY(I)   = AE(I)+0.5*H*(D(I)+F(I))
   20 Y(I)    = CY(I)
      IF (J.EQ.2) GOTO 32
      RETURN
   32 DO 100 I =1,N
      AD(I)   = AE(I)
  100 S(I)    = Y(I)
      TIMES   = TIME
      MODE    = 4
      RETURN
      END
```

Figure A21. Subroutine PRECOR Source Listing

TABLE A11 - LIST OF SYMBOLS FOR SUBROUTINE PRECOR

Quantity	Mnemonic	Units	Description
---	AD(I)	---	$Y(J)\|_{t-H}$
---	AE(I)	---	$Y(I)\|_{t}$
---	CY(I)	---	corrected value $Y(I)\|_{t+H}$
---	D(I)	---	$\frac{d}{dt} Y(J)\|_{t}$
---	F(I)	---	$\frac{d}{dt} Y^{(I)}\|_{t+H}$
Δt	H	sec	stepsize
---	MODE	---	MODE = 4, Runge Kutta initialization MODE = 5, Predict MODE = 6 correct
---	N	---	number of equations
---	PY(J)	---	predicted value $Y(I)\|_{t+H}$
t	TIME	sec	time
---	Y(I)	---	state vector

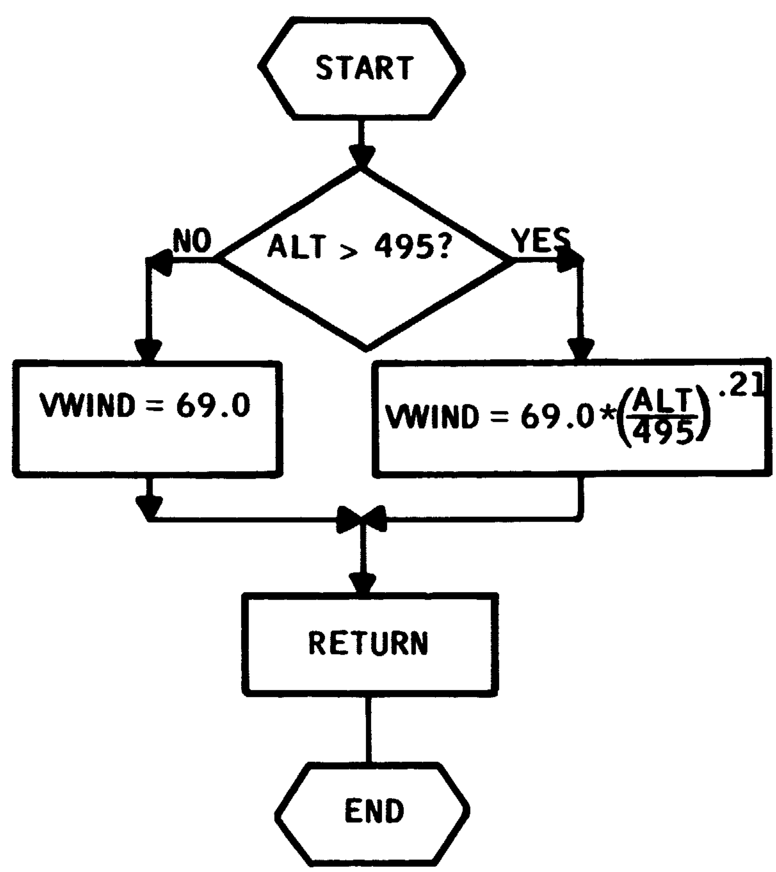

Figure A22. Subroutine WIND Flow Diagram

```
      SUBROUTINE WIND
C SUBROUTINE WIND CALCULATES A WIND INPUT TO THE VELOCITY OF THE AIR MASS      C
      COMMON/AAB/ Y(33)
      COMMON/AAP/YWIND,VWIND,VGUST,WIGU
      IF (Y(30).LT.-495.0) GOTO 10
      VWIND  = 69.0*(-Y(30)/495.0)**0.21
      GOTO 20
   10 VWIND  = 69.0
   20 CONTINUE
      RETURN
      END
```

Figure A23. Subroutine WIND Source Listing

TABLE A12 - LIST OF SYMBOLS FOR SUBROUTINE WIND

Quantity	Mnemonic	Units	Description
V_{wind}	VWIND	ft/sec	mean wind speed

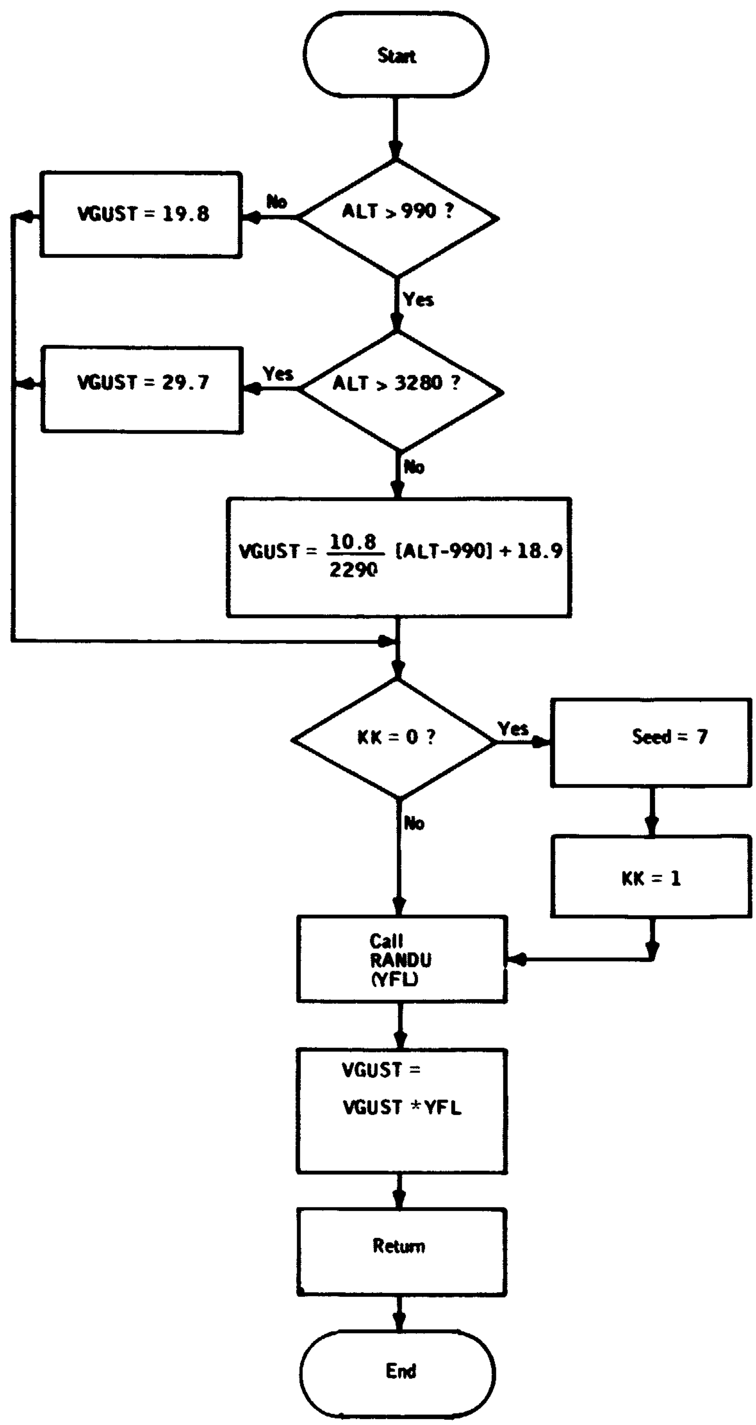

Figure A24. Subroutine GUST Flow Diagram

```
      SUBROUTINE GUST
C SUBROUTINE GUST CALCULATES A GUST INPUT TO THE VELOCITY OF THE UNSTEADY AAR C
C MASS AS A FUNCTION OF ALTITUDE AND A RANDOM MAGNITUDE MODIFIER               C
      COMMON/AAR/ Y(33)
      COMMON/AAP/YWIND,VWIND,VGUST,WIGU
   20 IF(Y(30).LT.-990.0) GOTO 30
      VGUST  = 19.8
      GOTO 50
   30 IF(Y(30).LT.-3280.0)GOTO 40
      VGUST  = 10.8/2290.0*(-Y(30)-990.0)+18.9
      GOTO 50
   40 VGUST  = 29.7
   50 IF(KK.EQ.0) SEED = 7.0
      KK     = 1
      CALL RANDU (YFL,SEED)
C YFL IS IN THE RANGE -1.0 TO +1.0
      VGUST  = YFL*VGUST
      RETURN
      END
```

Figure A25. Subroutine GUST Source Listing

TABLE A13 - LIST OF SYMBOLS FOR SUBROUTINE GUST

Quantity	Mnemonic	Units	Description
V_{GUST}	VGUST	ft/sec	gust velocity
---	YFL	---	random modifier in range $-1 \le YFL \le 1$

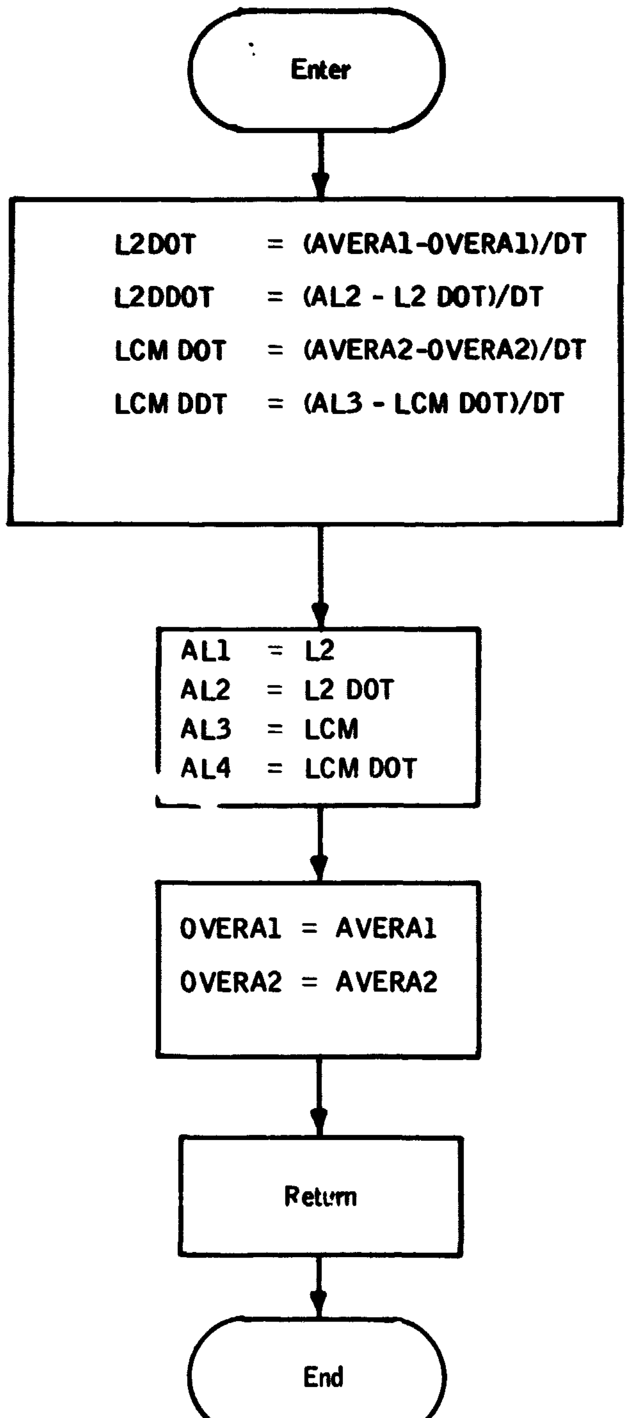

Figure A26. Subroutine ELASTIC Flow Diagram

```
      SUBROUTINE ELASTIC
C SUBROUTINE ELASTIC CALCULATES THE TIME RATE OF CHANGE OF THE LENGTH OF TH    C
C ELASTIC RISERS AND SUSPENSION LINES AS WELL AS THE TIME RATE OF CHANGE OF    C
C THE RELATIVE VELOCITIES OF EACH END OF THE ELASTIC ELEMENTS                  C
      COMMON/AAG/L2,L2DOT,L2DDOT,LCM,LCMDOT,LCMDDT
      COMMON/AAK/AL1,AL2,AL3,AL4
      COMMON/AAO/OLDTIME,YELAST,ETIME
      COMMON/AAT/TIME
      COMMON/XOROS/SUMMA1,SUMMA2,TOTAL,AVERA1,AVERA2,OVERA1,OVERA2,DT
      REAL L2,L2DOT,L2DDOT,LCM,LCMDOT,LCMDDT
C ELASTICITY CALCULATIONS
      L2DOT= (AVERA1-OVERA1)/DT
      LCMDOT= (AVERA2-OVERA2)/DT
      L2DDOT= (AL2-L2DOT)/DT
      LCMDDOT= (AL4-LCMDOT)/DT
      AL1    = L2
      AL2    = L2DOT
      AL3    = LCM
      AL4    = LCMDOT
      OVERA1= AVERA1
      OVERA2= AVERA2
      RETURN
      END
```

Figure A27. Subroutine ELASTIC Source Listing

TABLE A14 - LIST OF SYMBOLS FOR SUBROUTINE ELASTIC

Quantity	Mnemonic	Units	Description
---	AL1	ft	Last calculated value L_2
---	AL2	ft/sec	Last calculated value $\dot{L}_2$
---	AL3	ft	Last calculated value L_{C_M}
---	AL4	ft/sec	Last calculated value $\dot{L}_{C_M}$
---	AVERA1	ft	Average value of L_2 during interval from t - DT to t - DT/2
---	AVERA2	ft	Average value of L_{C_M} during interval from t - DT/2 to t
$2\Delta t$	DT	sec	Averaging interval
L_{C_M}	LCM	ft	Length from confluence point to parachute center of mass
$\dot{L}_{C_M}$	LCMDOT	ft/sec	$\frac{d}{dt} L_{C_M}$ at t - DT/2
L_2	L2	ft	Length of riser
$\dot{L}_2$	L2DOT	ft/sec	$\frac{d}{dt} L_{C_M}$ at t - DT/2
---	OVERA1	ft	Average value of L_2 during the interval from t - DT to DT/2
---	OVERA2	ft	Average value of L_{C_M} during the interval from t - DT to t - DT/2
t	TIME	sec	time

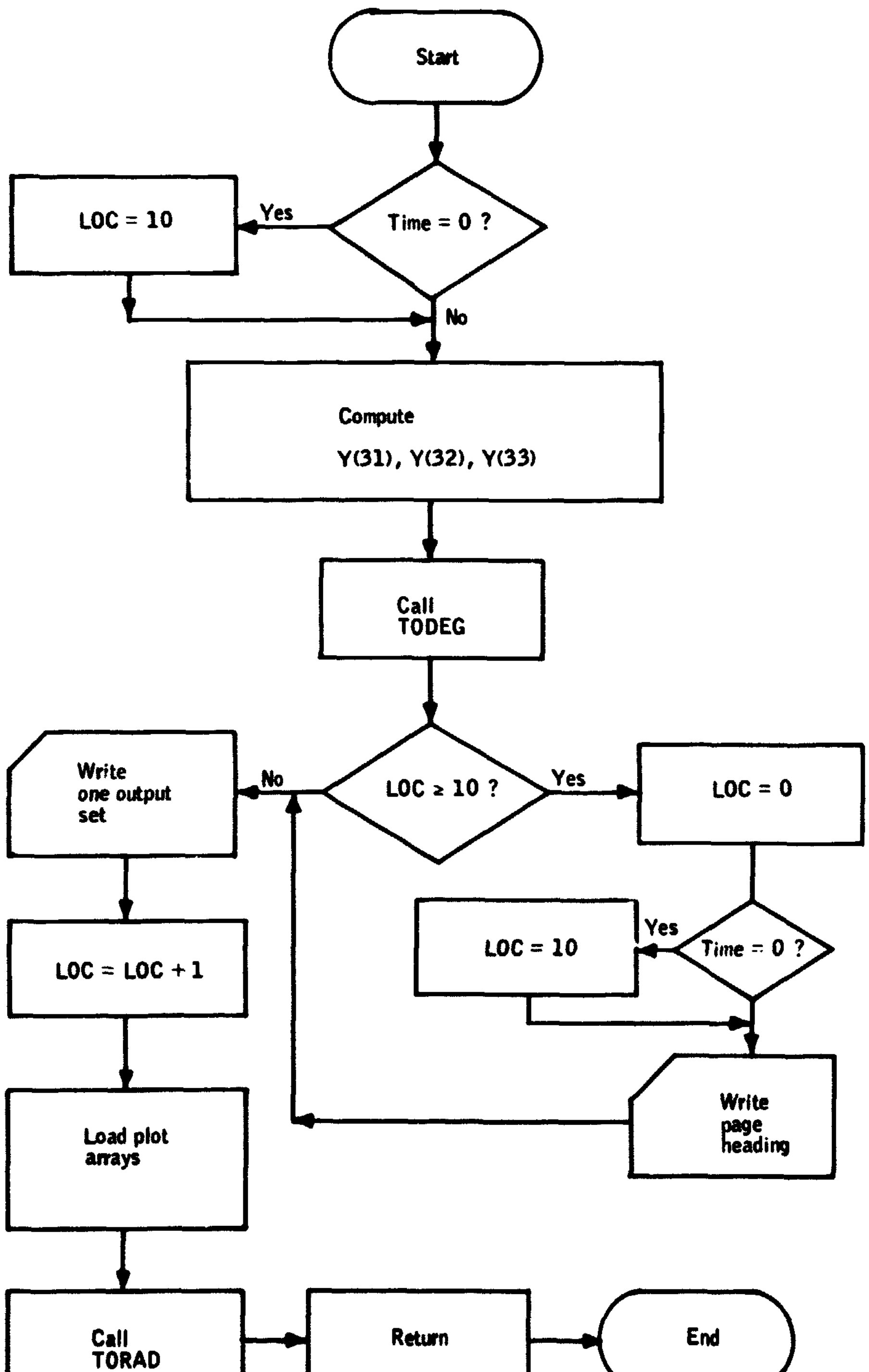

Figure A28. Subroutine PRINT Flow Diagram

```
      SUBROUTINE PRINT
C SUBROUTINE PRINT HANDLES ALL THE PRINT OUTPUT FUNCTINS OF THE PROGRAM
      COMMON/AAB/ Y(33)
      COMMON/AAC/D(30)
      COMMON/AAD/B(3,3,3),BS(6),T(3,6)
      COMMON/AAF/CN1,CT1,CN3,CT3,ALPHA1,ALPHA3,BETA1,BETA3,GAMMA
      COMMON/AAG/L2,L2DOT,L2DDOT,LCM,LCMDOT,LCMDDT
      COMMON/AAH/C1,C3,F2,L3,RAD,L1,L4,CF1,CF3,S1,S3
      COMMON/AAP/YWIND,VWIND,VGUST,WIGU
      COMMON/AAT/TIME
      COMMON/AAW/NOBS
      COMMON/PLTR/XX(402),THE1(402),THE3(402),AP1(402),AP3(402),ALT(402)
     1,RNG(402),FOR(402),RL(402),CL(402),WG(402)
      REAL L2,LCM,L3,L1,L4
      REAL L2DOT,L2DDOT,LCMDOT,LCMDDT
      IF (TIME.EQ.0.0) LOC = 10
      Y(31)  = -B(1,3,1)*LCM-B(2,3,1)*L2-B(3,3,1)*L3+Y(28)
      Y(33)  = -B(1,3,3)*LCM-B(2,3,3)*L2-B(3,3,3)*L3+Y(30)
      Y(32)  = -B(1,3,2)*LCM-B(2,3,2)*L2-B(3,3,2)*L3 +Y(29)
      CALL TODEG
      E1     = SQRT(C1)
      E3     = SQRT(C3)
      ALP1   = ALPHA1*RAD
      ALPHA3 = ALPHA3*RAD
      IF (LOC .EQ. 10) GOTO 300
      GOTO 330
  300 LOC    = 0
      IF (TIME.EQ.0.0) LOC = 10
      WRITE (6,550)
  550 FORMAT (1H1)
  320 WRITE (6,500)
      XX(NOBS) = TIME
      THE1(NOBS) = Y(8)
      THE3(NOBS) = Y(17)
      AP1 (NOBS) = ALP1
      AP3 (NOBS) = ALPHA3
      ALT (NOBS) = -Y(30)
      RNG (NOBS) = Y(28)
      FOR (NOBS) = F2
      RL  (NOBS) = L2
      CL  (NOBS) = LCM
      WG  (NOBS) = WIGU
  135 CONTINUE
      CALL TORAD
      ALP1   = ALP1/RAD
      ALPHA3 = ALPHA3/RAD
  400 FORMAT(10X,5HVWIND,F8.3, 5X,5HVGUST,F8.3,/)
  500 FORMAT (23X,9HPARACHUTE,43X,3HSRB/2X,4HTIME,4X,4HPSI1,
     16X,2HU1,7X,2HP1,7X,3HXE1,6X,2HC1,7X,4HPSI3,5X,2HU3,7X,2HP3
     2,7X,3HXE3,5X,6HXE3DOT,4X,2HC3,7X,3HLCM,6X,2HF2/9X,6HTHETA1
     3,5X,2HV1,7X,2HQ1,7X,3HYE1,14X,6HTHETA3,4X,2HV3,7X,2HQ3,7X,
     43HYE3,5X,6HYE3DOT,13X,2HL2/10X,4HPHI1,6X,2HW1,7X,2HR1,7X,3HZE1,
     54X,6HALPHA1,5X,4HPHI3,5X,2HW3,7X,2HR3,7X,3HZE3,5X,6HZE3DOT,
     63X,6HALPHA3,/)
  510 FORMAT(F7.2,12F9.3,F12.3/7X,4F9.3,9X,5F9.3,9X,F9.3/7X,11F9.3)
      RETURN
      END
  330 WRITE (6,510)     TIME,Y(9),Y(1),Y(4),Y(31),  E1,Y(18),Y(10),Y(13),
     1Y(28),D(28),E3,LCM,F2,Y(8),Y(2),Y(5),Y(32),       Y(17),Y(11),Y(14),
     2Y(29),D(29),L2,       Y(7),Y(3),Y(6),Y(33),ALP1,Y(16),Y(12),Y(15),
     3Y(30),D(30),ALPHA3
      WRITE (6,400) VWIND,VGUST
      LOC    = LOC+1
C LOAD PLOT ARRAYS
C UP TO 400 POINTS PER CURVE
      IF(NOBS.GE.400) GOTO 135
      NOBS     = NOBS+1
```

Figure A29. Subroutine PRINT Source Listing

TABLE A15 - LIST OF SYMBOLS FOR SUBROUTINE PRINT

Quantity	Mnemonic	Units	Description
α_1	ALP1	deg	parachute angle of attack
h	ALT	ft	plotting storage array, altitude
α_1	AP1	deg	plotting storage array parachute angle of attack
α_3	AP3	deg	plotting storage array SRB angle of attack
L_{C_M}	CL	ft	plotting storage array, L_{C_M}
$\sqrt{C_1}$	E1	ft/sec	speed, parachute center of mass
$\sqrt{C_3}$	E3	ft/sec	speed, SRB center of mass
F_2	FOR	lb	plotting storage array, riser force
---	LOC	---	line output count
---	NOBS	---	number of points in each curve
L_2	RL	ft	plotting storage array, riser length
XE_3	RNG	ft	plotting storage array, range
θ_1	THE1	deg	plotting storage array, θ_1
θ_3	THE3	deg	plotting storage array, θ_3
---	WG = WIGU	ft/sec	air mass velocity vector
t	XX	sec	plotting storage array, time

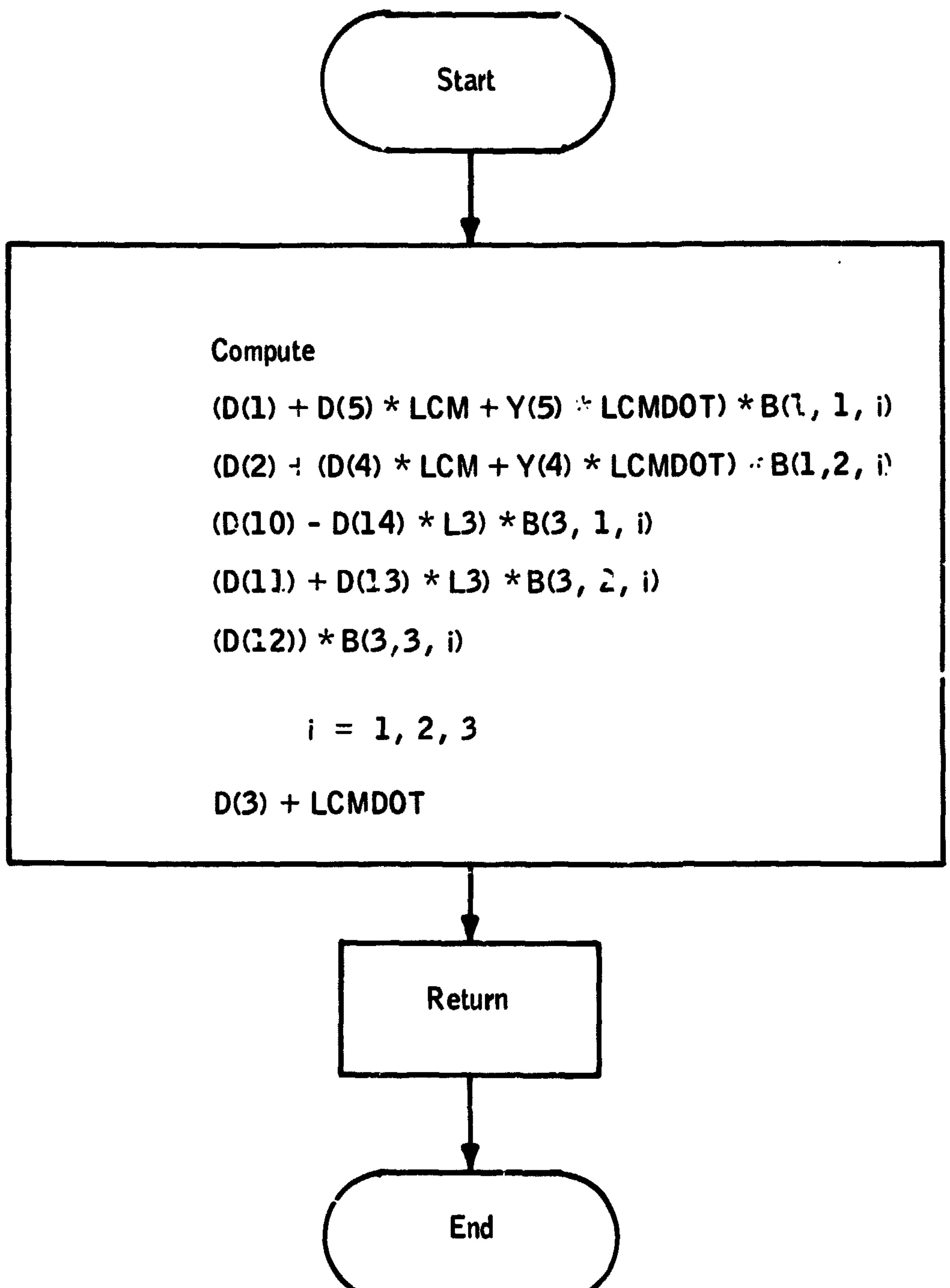

Figure A30. Subroutine CONST Flow Diagram

```
      SUBROUTINE CONST
C SUBROUTINE CONST CALCULATES CONSTANTS USED IN THE DIFFERENTIAL EQUATIONS     C
      COMMON/AAG/L2,L2DOT,L2DDOT,LCM,LCMDOT,LCMDDT
      COMMON/AAH/C1,C3,F2,L3,RAD,L1,L4,CF1,CF3,S1,S3
      COMMON/AAB/Y(33)
      COMMON/AAC/D(30)
      COMMON/AAD/B(3,3,3),BS(6),T(3,6)
      COMMON/AAN/A6,A7,A8,A9,A10,A11,A12,A13,A14,A15,A16,A17,A18,A19,A20
      COMMON/AANN/A21
      REAL L2,L2DOT,L2DDOT,L1,L4
      REAL L3,LCM,LCMDOT,LCMDDT
      A6      = (D(10)-D(14)*L3)*(B(3,1,3))
      A7      = (D(11)+D(13)*L3)*B(3,2,3)
      A8      = (D(1)+D(5)*LCM+Y(5)*LCMDOT)*B(1,1,3)
      A9      = (D(2)-D(4)*LCM-Y(4)*LCMDOT)*B(1,2,3)
      A10     = (D(12)*B(3,3,3))
      A11     = (D(10)-D(14)*L3)*B(3,1,2)
      A12     = (D(11)+D(13)*L3)*B(3,2,2)
      A13     = D(12)*B(3,3,2)
      A14     = (D(1)+D(5)*LCM+Y(5)*LCMDOT)*B(1,1,2)
      A15     = (D(2)-D(4)*LCM-Y(4)*LCMDOT)*B(1,2,2)
      A16     = (D(10)-D(14)*L3)*B(3,1,1)
      A17     = (D(11)+D(13)*L3)*B(3,2,1)
      A18     = D(12)*B(3,3,1)
      A19     = (D(1)+D(5)*LCM+Y(5)*LCMDOT)*B(1,1,1)
      A20     = (D(2)-D(4)*LCM-Y(4)*LCMDOT)*B(1,2,1)
      A21     = D(3)+LCMDDT
      RETURN
      END
```

Figure A31. Subroutine CONST Source Listing

Subroutine INVELO -- Subroutine INVELO initializes the inertial components of velocity in the body fixed axis systems at time zero for the initial orientations and vertical rate of descent as read in the input data deck.

Subroutine INVELO is diagrammed in Figure A32 and listed in Figure A33.

Auxiliary Subroutines

Auxiliary trigonometric functions SEC provided. SEC is listed as Figure A34.

Subroutine SRBIN calculates the SRB inertial differences as used in Equation (8A). Subroutine SRBIN is listed as Figure A35.

Subroutine TORAD converts angles and angular velocities to radians and radians per second. Subroutine TORAD is listed as Figure A36.

Subroutine TODEG converts angles and angular velocities to degrees and degrees per second. Subroutine TODEG is listed as Figure A37.

Subroutine RANDU calculates a random number in the range -1 to +1. Subroutine RANDU is listed as Figure A38.

Linearization Subroutines

Five subroutines make up the package to linearize and find the eigenvalues for a set of nonlinear differential equations.

Subroutine DERIVE calculates the first partial derivative matrix. Subroutine DERIVE is listed as Figure A39.

Subroutine EIGEN is called from subroutine DERIVE and performs the control, storage, and output functions for the eigenvalue calculation process. Subroutine EIGEN is listed in Figure A40.

Subroutine HESSEN is called from subroutine EIGEN and manipulates the matrix of first partial derivatives into the upper Hessenberg form. Subroutine HESSEN is listed in Figure A41.

Subroutine QRCALL is called from subroutine EIGEN and hence calls subroutine QR. QRCALL is a double iterative eigenvalue approximation method using a quotient reduction scheme provided by QR. Subroutine QRCALL is listed as Figure A42, and subroutine QR is listed as Figure A43.

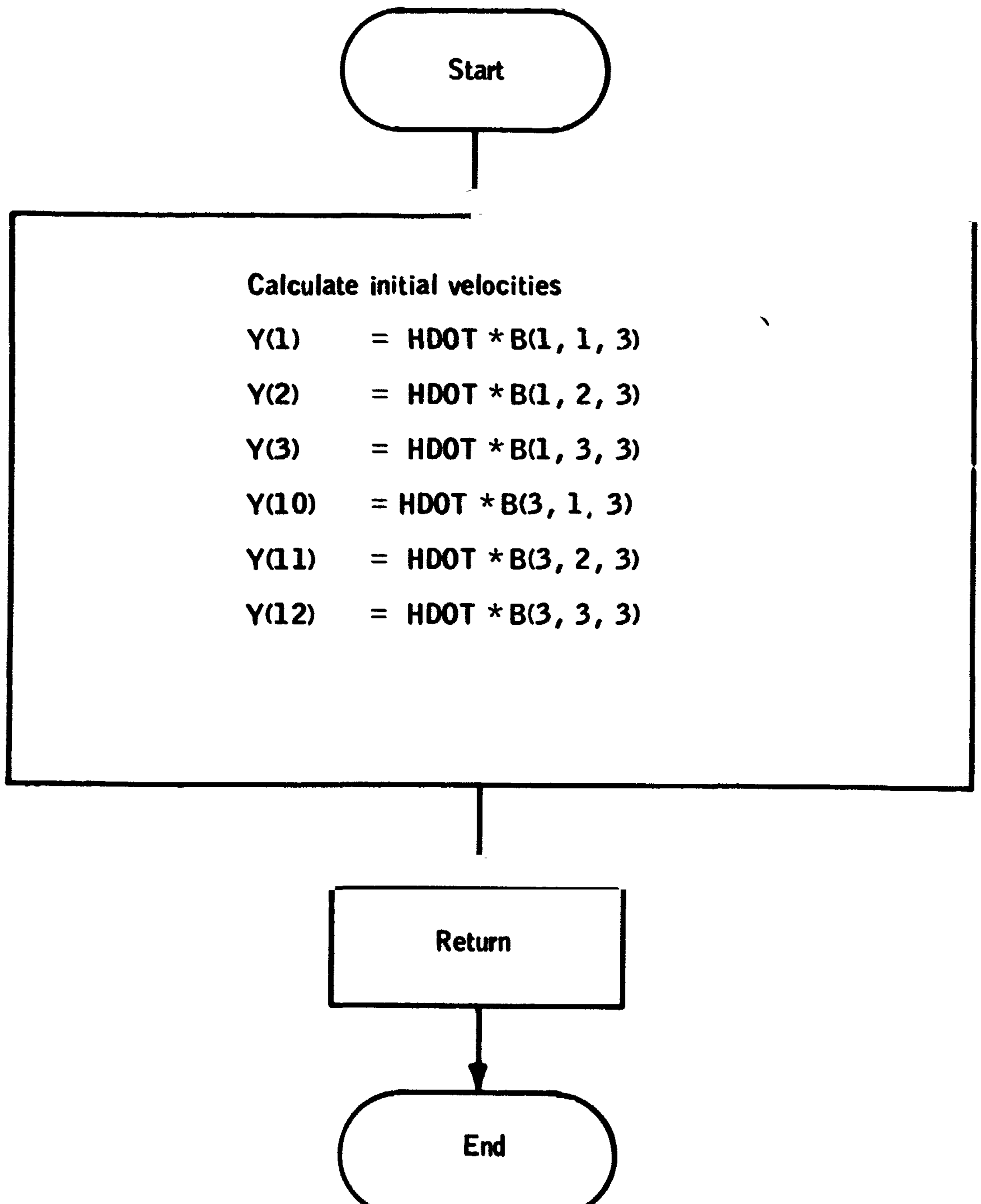

Figure A32. Subroutine INVELO Flow Diagram

```
      SUBROUTINE INVELO (HDOT)
C SUBROUTINE INVELO CALCULATES THE INITIAL VELOCITIES OF THE CHUTE AND SRB
      COMMON/AAB/ Y(33)
      COMMON/AAD/B(3,3,3),BS(6),T(3,6)
      CALL DIRCOS
C INITIAL INERTIAL VELOCITIES
C U1 = Y(1)        V1 = Y(2)        W1 = Y(3)
C U3 = Y(10)       V3 = Y(11)       W3 = Y(12)
      DO 30 I=1,3
      Y(I)   = HDOT*B(1,I,3)
      Y(I+9) = HDOT*B(3,I,3)
   30 CONTINUE
      RETURN
      END
```

Figure A33. Subroutine INVELO Source Listing

```
      REAL FUNCTION SEC (X)
      SEC     = 1.0/(COS(X)+1.0E-14)
      RETURN
      END
```

Figure A34. Function SEC Source Listing

```
      SUBROUTINE SRBIN
C SUBROUTINE SRBIN CALCULATES THE INERTIAL CHARACTERISTICS OF THE SRB
      COMMON/AAO/IXX1,IYY1,IZZ1,IXX3,IYY3,IZZ3
      COMMON/AAOO/IXZ1,IYX1,IZY1,IXZ3,IYX3,IZY3
      REAL         IXX1,IYY1,IZZ1,IXX3,IYY3,IZZ3
      REAL         IXZ1,IYX1,IZY1,IXZ3,IYX3,IZY3
C INERTIAL CHARACTERISTICS, SRB
      IZY3    = IZZ3-IYY3
      IYX3    = IYY3-IXX3
      IXZ3    = IXX3-IZZ3
      RETURN
      END
```

Figure A35. Subroutine SRBIN Source Listing

```
      SUBROUTINE TORAD
C SUBROUTINE TORAD CONVERTS ANGLES AND ANGULAR VELOCITIES TO RADIANS
      COMMON/AAP/Y(33)
      COMMON/AAH/C1,C3,F2,L3,RAD,L1,L4,CF1,CF3,S1,S3
      REAL L1,L3,L4
      DO 20 I= 7,9
C EULER ANGLES IN RADIANS
      Y(I)    = Y(I)/RAD
      Y(I+9)  = Y(I+9)/RAD
      Y(I+18)= Y(I+18)/RAD
C ANGULAR VELOCITIES IN RADIANS PER SEC
      L       = I-3
      Y(L)    = Y(L)/RAD
      Y(L+9)  = Y(L+9)/RAD
   20 Y(L+18)= Y(L+18)/RAD
      RETURN
      END
```

Figure A36. Subroutine TORAD Source Listing

```
      SUBROUTINE TODEG
C SUBROUTINE TODEG CONVERTS ANGLES AND ANGULAR VELOCITIES TO DEGREES
      COMMON/AAB/Y(33)
      COMMON/AAH/C1,C3,F2,L3,RAD,L1,L4,CF1,CF3,S1,S3
      REAL L1,L3,L4
C EULER ANGLES IN DEGREES
      DO 200 I = 7,9
      Y(I)    = Y(I)*RAD
      Y(I+9)  = Y(I+9)*RAD
      Y(I+18)= Y(I+18)*RAD
C ANGULAR VELOCITIES IN DEGREES PER SEC
      L       = I-3
      Y(L)    = Y(L)*RAD
      Y(L+9)  = Y(L+9)*RAD
  200 Y(L+18)= Y(L+18)*RAD
      RETURN
      END
```

Figure A37. Subroutine TODEG Source Listing

```
      SUBROUTINE RANDU(YFL,SEED)
      SEED=AMOD(131075.*SEED,34359738368.)
      YFL=SEED*.291038304567E-10
      RETURN
      END
```

Figure A38. Subroutine RANDU Source Listing

```
      SUBROUTINE DERIVE (POLIS,RC,RHO,CLUST)
      COMMON/AAB/Y(33)
      COMMON/AAC/D(30)
      COMMON/AAJ/MODE
      DIMENSION DY(30), D1(30), F(30,30)
      DIMENSION YOLD(30),DOLD(30)
      ISAVE=MODE
      NE=30
      DO 20 I=1,NE
      YOLD(I)=Y(I)
      DOLD(I)=D(I)
      IF(Y(I).EQ.0.0)GO TO 10
      DY(I) = .01*Y(I)
      GO TO 15
   10 DY(I) = .01
   15 CONTINUE
   20 CONTINUE
      MODE = 4
      SIGN = 1.
      DO 70 J=1,NE
   25 SIGN = -SIGN
      PERT = SIGN * DY(J)
      Y(J) = Y(J) + PERT
      CALL DIRCOS
      CALL CHUTE (CLUST)
      CALL COEFTS(RC)
      CALL FORCES
      CALL MOMENTS (RHO)
      CALL DIFEQN
      Y(J) = Y(J) - PERT
      IF(SIGN.EQ.1.) GO TO 45
      DO 35 I=1,NE
      D1(I) = D(I)
   35 D(I)=DOLD(I)
      GO TO 25
   45 DO 60 I = 1,NE
      DIFFR= D(I) - D1(I)
      IF(DIFFR.NE.0.0) GO TO 50
      F(I,J) = 0.0
      GO TO 55
   50 F(I,J) = DIFFR/(2.*DY(J))
   55 CONTINUE
   60 CONTINUE
      DO 65 I = 1,NE
   65 D(I) = DOLD(I)
   70 CONTINUE
      CALL EIGEN(F,NE,POLIS)
      DO 75 I = 1,NE
      D(I)=DOLD(I)
   75 Y(I) = YOLD(I)
      MODE=ISAVE
      RETURN
      END
```

Figure A39. Subroutine DERIVE Source Listing

```
      SUBROUTINE EIGEN(A,N,CHRONOS)
      DIMENSION A(30,30),R(80),STORE(240),TIME(5),MM(5)
      DIMENSION IVAR(10)
      ILOW=60*LIMIT
      LIMIT=LIMIT+1
      TIME(LIMIT)=CHRONOS
      CALL HESSEN(N,A,N)
      CALL QRCAL1(N,A,R,M,N)
      MM(LIMIT)=M
      M=M+M
      IF(LIMIT.EQ.5) GO TO 15
      DO 10 K=1,M
   10 STORE(ILOW+K)=R(K)
      RETURN
   15 MTOP=0
      DO 20 I=1,5
      IF(MM(I).GT.MTOP) MTOP=MM(I)
   20 CONTINUE
      WRITE(6,100)
      WRITE(6,105)(TIME(I),I=1,5)
      WRITE(6,110)
      IVAR(1)=10H(/3X,F10.4
      IVAR(10)=10H,3X,F10.4)
      DO 11 I=2,9
   11 IVAR(I)=10H,3X,F10.4
      DO 30 K=1,MTOP
      II=2*K
      I=II-1
      JJ=60+II
      J=JJ-1
      LL=120+II
      L=LL-1
      NN=180+II
      N1=NN-1
      IF(K.LE.MM(1))GO TO 35
      STORE(I)=STORE(II)=10H
      IVAR(1)=10H(/,3X,A10
      IVAR(2)=10H,3X,A10
   35 IF(K.LE.MM(2))GO TO 40
      STORE(J)=STORE(JJ)=10H
      IVAR(3)=IVAR(4)=10H,3X,A10
   40 IF(K.LE.MM(3))GO TO 45
      STORE(L)=STORE(LL)=10H
      IVAR(5)=IVAR(6)=10H,3X,A10
   45 IF(K.LE.MM(4))GO TO 50
      STORE(N1)=STORE(NN)=10H
      IVAR(7)=IVAR(8)=10H,3X,A10
   50 IF(K.LE.MM(5))GO TO 55
      R(I)=R(II)=10H
      IVAR(9)=10H,3X,A10
      IVAR(10)=10H    ,3X,A10)
   55 CONTINUE
   30 PRINT IVAR,STORE(I),STORE(II),STORE(J),STORE(JJ),STORE(L),
     1           STORE(LL),STORE(N1),STORE(NN),R(I),R(II)
```

Figure A40. Subroutine EIGEN Source Listing

```
      LIMIT=0
      RETURN
  100 FORMAT(1H1,59X,11HEIGENVALUES)
  105 FORMAT(//,8X,5(6HTIME =,F6.2,13X))
  110 FORMAT(/,3X,5(4HREAL,9X,9HIMAGINARY,4X))
      END
```

Figure A40. Subroutine EIGEN Source Listing (Concluded)

```
      SUBROUTINE HESSEN(N,A,D)                                          HESS1001
      DIMENSION A(1)                                                    HESS1002
      INTEGER P,PM,PX,D                                                 HESS1003
      IF(N.LE.2)    RETURN                                              HESS1004
      ID=D+1                                                            HESS1005
      NN=(N-1)*ID+1                                                     HESS1006
      KX=NN-ID-ID+1                                                     HESS1007
      PX=N                                                              HESS1008
      PM=1                                                              HESS1009
      DO 71 K = 2,KX,ID
      NK=PX                                                             HESS1011
      PM=PM+D                                                           HESS1012
      PX=PX+D                                                           HESS1013
      JP=PM                                                             HESS1014
      R=0.                                                              HESS1015
      J=K                                                               HESS1016
      JC=JP                                                             HESS1017
      JK=J                                                              HESS1018
   30 T=ABS(A(J))                                                       HESS1019
      IF(T.LE.R) GO TO 35                                               HESS1020
      JC=JP                                                             HESS1021
      JK=J                                                              HESS1022
      R=T                                                               HESS1023
   35 IF(J.GE.NK) GO TO 37                                              HESS1024
      J=J+1                                                             HESS1025
      JP=JP+D                                                           HESS1026
      GO TO 30                                                          HESS1027
   37 IF(JK.EQ.K) GO TO 44                                              HESS1028
      J=JC                                                              HESS1029
      DO 38 P=PM,PX                                                     HESS1030
      T=A(P)                                                            HESS1031
      A(P)=A(J)                                                         HESS1032
      A(J)=T                                                            HESS1033
   38 J=J+1                                                             HESS1034
      P=JK                                                              HESS1035
      DO 39 J=K,NN,D                                                    HESS1036
      T=A(J)                                                            HESS1037
      A(J)=A(P)                                                         HESS1038
      A(P)=T                                                            HESS1039
   39 P=P+D                                                             HESS1040
   44 IF(A(K).EQ.0.) GO TO 70                                           HESS1041
      JC=PM+D                                                           HESS1042
      JK=K+1                                                            HESS1043
      T=1./A(K)                                                         HESS1044
   45 R=A(JK)                                                           HESS1045
      IF(R.EQ.0.) GO TO 65                                              HESS1046
      R=R*T                                                             HESS1047
      KM=K+D                                                            HESS1048
      JKD = JK+D                                                        HESS1049
      DO 50  JM=JKD,NN,D                                                HESS1050
      AJM=A(JM)-R*A(KM)                                                 HESS1051
      IF(ABS(AJM).LE.(.1E-9*ABS(A(JM)))) AJM=0.                         HESS1052
      A(JM)=AJM                                                         HESS1053
   50 KM=KM+D                                                           HESS1054
```

Figure A41. Subroutine HESSEN Source Listing

```
      J=JC                                                              HESS1055
      DO 60 P=PM,PX                                                     HESS1056
      AP=A(P)+B*A(J)                                                    HESS1057
      IF(ABS(AP).LE.(.1E-9*ABS(A(P)))) AP=0.                            HESS1058
      A(P)=AP                                                           HESS1059
   60 J=J+1                                                             HESS1060
   65 JK=JK+1                                                           HESS1061
      JC=JC+D                                                           HESS1062
      IF(JK.LE.NK) GO TO 65                                             HESS1063
   70 CONTINUE                                                          HESS1064
    71 CONTINUE
      RETURN                                                            HESS1065
      END                                                               HESS1066
```

Figure A41. Subroutine HESSEN Source Listing (Concluded)

```
      SUBROUTINE QRCALL(P,A,R,M,NIN)                                    QRCA1001
      DIMENSION A(1),R(1)                                               QRCA1002
      INTEGER P                                                         QRCA1003
      N = NIN                                                           QRCA1004
      ANM = 1.                                                          QRCA1005
      ACT = .1E-7                                                       QRCA1006
      ACE = .1E-10                                                      QRCA1007
      ITER = 0                                                          QRCA1008
      M = 0                                                             QRCA1009
      NP   = P+1                                                        QRCA1010
      NN   = N+(N-1)*P                                                  QRCA1011
      NM   = NN-NP                                                      QRCA1012
      NL   = NM-NP                                                      QRCA1013
      IF(N.EQ.1)    GO TO 16                                            QRCA1014
      IF(N.LE.0)    RETURN                                              QRCA1015
      IF(N.EQ.2)    GO TO 25                                            QRCA1016
 15   DELTA = ACT*ABS(A(NN))                                            QRCA1017
      DELTA = AMAX1(DELTA,ACE)                                          QRCA1018
      ACC   = ABS(A(NM+1))                                              QRCA1019
      IF(ACC.EQ.0.)    GO TO 16                                         QRCA1020
      IF(ACC.GT.DELTA)    GO TO 25                                      QRCA1021
      IF(ITER.GT.25)    GO TO 16                                        QRCA1022
      IF(ANM.GT.ACT)     GO TO 25                                       QRCA1023
 16   M = M+2                                                           QRCA1024
      X = A(NN)                                                         QRCA1025
      IF(ABS(X).LE..1E-5)     X=0.                                      QRCA1026
      R(M-1)=X                                                          QRCA1027
      R(M) = 0.                                                         QRCA1028
 17   K = NIN-N+1                                                       QRCA1029
      IF(R(M).EQ.0.) GO TO 19                                           QRCA1030
      X = SQRT(R(M)*R(M)+R(M-1)*R(M-1))                                 QRCA1031
      X = - R(M-1)/X
      GO TO 21                                                          QRCA1035
 19   CONTINUE
 21   ITER = 0                                                          QRCA1038
      ACT = .1E-7                                                       QRCA1039
      N = N-1                                                           QRCA1040
      NN = NM                                                           QRCA1041
      NM = NL                                                           QRCA1042
      NL = NL-NP                                                        QRCA1043
      IF(N.GT.2)    GO TO 15                                            QRCA1044
      IF(N.EQ.2)    GO TO 25                                            QRCA1045
      IF(N.EQ.1)    GO TO 16                                            QRCA1046
      M=M/2                                                             QRCA1047
      RETURN                                                            QRCA1048
 25   B    = .5*(A(NM)+A(NN))                                           QRCA1049
      DAN  = ABS(A(NN)-A(NM))                                           QRCA1050
      SAN  = ABS(A(NN))+ABS(A(NM))                                      QRCA1051
      IF(DAN.LE.ACT*SAN)   DAN=0.                                       QRCA1052
      DAN=DAN*DAN*.25                                                   QRCA1053
      C    = A(NM+1)*A(NN-1)                                            QRCA1054
      T=DAN+C                                                           QRCA1055
      IF((ABS(T).LE.ACT*DAN).OR.(ABS(T).LE.ACT*B*B))  T=0.              QRCA1056
      C = SQRT(ABS(T))                                                  QRCA1058
```

Figure A42. Subroutine QRCALL Source Listing

```
      IF(N.NE.2)    GO TO 50                                          QRCA1059
26    IF(T.GE.0.)    GO TO 30                                         QRCA1060
      M = M+2                                                         QRCA1061
      R(M-1) = B                                                      QRCA1062
      R(M) = C                                                        QRCA1063
27    N = N-1                                                         QRCA1064
      NN = NM                                                         QRCA1065
      NM = NL                                                         QRCA1066
      NL = NL-NP                                                      QRCA1067
      GO TO 17                                                        QRCA1068
30    M = M+2                                                         QRCA1069
      R(M-1) = B+C                                                    QRCA1070
      R(M) = 0.                                                       QRCA1071
      K = NTN-N+1                                                     QRCA1072
      M = M+2                                                         QRCA1074
      R(M-1) = B-C                                                    QRCA1075
      R(M) = 0.                                                       QRCA1076
      GO TO 27                                                        QRCA1077
50    IF(T.GE.0.)    GO TO 60                                         QRCA1078
      R(M+5) = B                                                      QRCA1079
      R(M+6) = C                                                      QRCA1080
      R(M+7) = B                                                      QRCA1081
      R(M+8) = -C                                                     QRCA1082
      GO TO 70                                                        QRCA1083
60    X = B+C                                                         QRCA1084
      Y = B-C                                                         QRCA1085
      R(M+6) = 0.                                                     QRCA1086
      R(M+8) = 0.                                                     QRCA1087
      R(M+5) = X                                                      QRCA1088
      R(M+7) = Y                                                      QRCA1089
      IF(ABS(X).GT.ABS(Y))    GO TO 70                                QRCA1090
      R(M+5) = Y                                                      QRCA1091
      R(M+7) = X                                                      QRCA1092
70    IF(ITER.LE.0)    GO TO 130                                      QRCA1093
      X = ABS(R(M+5)-R(M+1))+ABS(R(M+6)-R(M+2))                       QRCA1094
      ACC = ABS(R(M+5))              +ABS(R(M+6))                     QRCA1095
      IF(ACC.GT.1.)    X=X/ACC                                        QRCA1096
      Y = ABS(R(M+7)-R(M+3))+ABS(R(M+8)-R(M+4))                       QRCA1097
      ACC = ABS(R(M+7))              +ABS(R(M+8))                     QRCA1098
      IF(ACC.GT.1.)    Y=Y/ACC                                        QRCA1099
      ACC = ABS(A(NL+1))                                              QRCA1100
      DELTA = AMAX1(DELTA,(ACT*ABS(A(NM))))                           QRCA1101
      IF(ACC.GT.DELTA)    GO TO 80                                    QRCA1102
      IF(ITER.GT.4 )    GO TO 26                                      QRCA1103
      IF((X.LE.ACT).AND.(Y.LE.ACT))    GO TO 26                       QRCA1104
80    IF(ITER.GT.200)    GO TO 200                                    QRCA1105
      IF((X.GT..5  ).AND.(Y.GT..5  ))    GO TO 130                    QRCA1106
      K = M+5                                                         QRCA1107
      IF(Y.GT..5  )    GO TO 120                                      QRCA1108
      IF(X.GT..5  )    GO TO 110                                      QRCA1109
      RHO = R(M+5)*R(M+7)-R(M+6)*R(M+8)                               QRCA1110
      SIGMA = R(M+5)+R(M+7)                                           QRCA1111
100   CONTINUE                                                        QRCA1112
      ANN = A(NN)                                                     QRCA1113
```

Figure A42. Subroutine QRCALL Source Listing (Continued)

```
      IF(ITER.LE.15) GO TO 102
      IF(RHO.NE.0.)  GO TO 102
      IF(SIGMA.NE.0.)  GO TO 102
      RHO = .0001
      SIGMA  = .02
102   CALL QR(N,A,RHO,SIGMA,R,DELTA)
      B = ABS(A(NN))
      ANN = ABS(ANN-A(NN))
      IF(B.GT.ACT)   ANN = ANN/B
      ITER = ITER+1
      IF(ITER.EQ.25)   ACT=.1E-5
      DO 105 I=1,4
      K = M+I
105   R(K) = R(K+4)
      GO TO 15
110   K = M+7
120   RHO = R(K)*R(K)
      SIGMA = R(K)+R(K)
      GO TO 100
130   RHO = 0.
      SIGMA = 0.
      GO TO 100
200   CONTINUE
      WRITE(6,210)   MIN
210   FORMAT(/4H ALL  ,I3,24H EIGENVALUES NOT FOUND            /)
      M=0
      RETURN
      END
```

Figure A42. Subroutine QRCALL Source Listing (Concluded)

```
      SUBROUTINE QR   (N,A,RHO,SIGMA,D,DELTA)
      DIMENSION A(1)
      REAL KAPPA
      INTEGER P,Q,D
      EQUIVALENCE (P,D)
      ID = D+1
      N0 = ID*(N-1)+1
      N1 = N0-ID
      N2 = N1-ID
      N3 = N2-ID
      IF(N.GT.3) GO TO 5
      IF(N.LE.2) RETURN
2     Q = 1
      GO TO 35
5     I = N3+1
7     IF(ABS(A(I)).LE.DELTA) GO TO 10
      IF(I.LE.2) GO TO 2
      I = I-ID
      GO TO 7
10    Q = I+D
      A(I) = 0.
35    I = P
      IQ = Q
      I0 = I-D
      I1 = I+D
      I2 = I1+D
      G1 = A(I)*(A(I)-SIGMA)+A(I1)*A(I+1)+RHO
      G2 = A(I+1)*(A(I)+A(I1+1)-SIGMA)
      G3 = A(I+1)*A(I1+2)
      A(I+2) = 0.
      GO TO 45
40    G1 = A(I0)
      G2 = A(I0+1)
      G3 = 0.
      I0 = I0+D
      IF(I.LE.N2) G3 = A(I0+2)
45    KAPPA = SQRT(G1*G1+G2*G2+G3*G3)
      IF(G1.LT.0.) KAPPA = -KAPPA
      IF(KAPPA.NE.0.) GO TO 47
      ALPHA = 2.
      P1 = 0.
      P2 = 0.
      GO TO 48
47    ALPHA = 1.+G1/KAPPA
      P1 = 1./(G1+KAPPA)
      P2 = P1*G3
      P1 = P1*G2
48    IF(I.EQ.Q) GO TO 49
      A(I0) = -A(I0)
      IF(I.NE.P) A(I0) = -KAPPA
49    J = I-D
50    J = J+D
      IF(J.GE.N0) GO TO 51
      ETA = A(J)+P1*A(J+1)
```

Figure A43. Subrou   QR Source Listing

```
      IF(I.LE.N2) ETA = ETA+P2*A(J+2)
      ETA = ALPHA*ETA
      A(J) = A(J)-ETA
      A(J+1) = A(J+1)-P1*ETA
      IF(I.LE.N2) A(J+2) = A(J+2)-P2*ETA
      GO TO 50
51    J = I0-1
      JINX = MIN0(I+2,N1+1)
60    J = J+1
      K = J+D
      ETA = A(J)+P1*A(K)
      L = K+D
      IF(I.LE.N2) ETA = ETA+P2*A(L)
      ETA = ETA*ALPHA
      A(J) = A(J)-ETA
      A(K) = A(K)-P1*ETA
      IF(I [illegible] N2) A(L) = A(L)-P2*ETA
      IF(J. [illegible] NX) GO TO 60
      IF(I. [illegible] .N2) GO TO 65
      ETA = ALPHA*P2*A(I2+3)
      A(I+3) = -ETA
      A(I1+3) = -P1*ETA
      A(I2+3) = A(I2+3)-P2*ETA
65    IF(I.GE.N1) RETURN
      I0 = I +1
      I = I1+1
      I1 = I2+1
      I2 = I2+ID
      GO TO 40
      END
```

Figure A43. Subroutine QR Source Listing (Concluded)